



Szkoła Główna Gospodarstwa Wiejskiego
w Warszawie

Instytut Nauk o Żywieniu Człowieka

mgr inż. Alicja Kizildag

Białka roślinne w mikrokapsułkowaniu olejków eterycznych z wykorzystaniem koacerwacji złożonej

Plant proteins in microencapsulation of essential oils using complex
coacervation

Rozprawa doktorska
Doctoral thesis

Rozprawa doktorska wykonana pod kierunkiem
prof. dr. hab. Marcina Andrzeja Kurka
Katedra Techniki i Projektowania Żywności
Instytut Nauk o Żywieniu Człowieka
Szkoła Główna Gospodarstwa Wiejskiego w Warszawie

Warszawa, 2024

Oświadczenie promotora rozprawy doktorskiej

Oświadczam, że niniejsza rozprawa została przygotowana pod moim kierunkiem i stwierdzam, że spełnia warunki do przedstawienia jej w postępowaniu o nadanie stopnia naukowego doktora.

Data 10.10.24.....

Czytelny podpis promotora [Podpis].....

Oświadczenie autora rozprawy doktorskiej

Świadoma odpowiedzialności prawnej, w tym odpowiedzialności karnej za złożenie fałszywego oświadczenia, oświadczam, że niniejsza rozprawa doktorska została napisana przez mnie samodzielnie i nie zawiera treści uzyskanych w sposób niezgodny z obowiązującymi przepisami prawa, w szczególności z ustawą z dnia 4 lutego 1994 r. o prawie autorskim i prawach pokrewnych (tj. z dnia 28 października 2022 r., Dz.U. z 2022 r. poz. 2509 ze zm.)

Oświadczam, że przedstawiona rozprawa nie była wcześniej podstawą żadnej procedury związanej z uzyskaniem stopnia naukowego doktora.

Oświadczam ponadto, że niniejsza wersja rozprawy jest identyczna z załączoną wersją elektroniczną.

Przyjmuję do wiadomości, że rozprawa doktorska poddana zostanie procedurze antyplagiatowej.

Data 10/10/2024.....

Czytelny podpis autora rozprawy [Podpis].....

Podziękowania

Pragnę serdecznie podziękować Profesorowi Marcinowi Kurkowi za jego cierpliwość, wyrozumiałość oraz nieocenione wsparcie merytoryczne na każdym etapie realizacji tej pracy.

Szczególne wyrazy wdzięczności kieruję do Profesor Justyny Franc-Dąbrowskiej za wsparcie w trudnych chwilach, bez którego ta praca nie mogłaby powstać.

Dziękuję również całemu zespołowi Katedry Techniki i Projektowania Żywności za okazaną pomoc, życzliwość i niezliczone uśmiechy, które towarzyszyły naszej współpracy.

Streszczenie

Białka roślinne w mikrokapsułkowaniu olejków eterycznych z wykorzystaniem koacerwacji złożonej

Celem badań była ocena możliwości zastosowania koacerwacji złożonej z użyciem białek roślinnych jako metody kapsułkowania olejków eterycznych oraz analiza właściwości fizykochemicznych proszków otrzymanych poprzez liofilizację płynnych koacerwatów. Ponadto, badanie obejmowało porównanie koacerwatów z białek roślinnych z modelowym układem koacerwacji złożonej, który wykorzystuje żelatynę i gumę arabską, w celu oceny ich efektywności i właściwości użytkowych.

Do koacerwacji złożonej stosowano żelatynę, białko z grochu, białko z bobu oraz białko owsiane, a jako polisacharydy użyto gumy arabskiej i polisacharydów z nasion chia. Olejki eteryczne, takie jak olejek z jałowca i olejek z czarnego pieprzu, były rozpuszczane w olejach roślinnych (sojowym, z pestek winogron, rzepakowym) w celu zminimalizowania ich ewaporacji podczas procesu tworzenia koacerwatów. Dodatkowo, zbadano wpływ emulgatora Tween 80 (polisorbate 80, mieszanina polioksyetylenowych pochodnych sorbitanu i kwasu oleinowego) na proces koacerwacji oraz na właściwości fizykochemiczne proszków uzyskanych po liofilizacji koacerwatów.

W ramach badań przeprowadzono szereg analiz, w tym pomiar wydajności procesu koacerwacji, wydajności procesu liofilizacji oraz wydajności mikrokapsułkowania. Oceniono także barwę, rozkład wielkości cząsteczek, a także przeprowadzono analizę mikroskopową SEM, analizę termiczną oraz FT-IR. Dodatkowo, oceniono rozpuszczalność w wodzie, gęstość nasypową i utrzoną, sypkość proszków za pomocą indeksu Cara i Hauser Ratio, a także początkową zawartość wody w proszkach i ich higroskopijność.

Na podstawie otrzymanych wyników badań stwierdzono, że białka roślinne mogą być stosowane do koacerwacji złożonej zapewniając porównywalne lub lepsze rezultaty w zakresie efektywności mikrokapsułkowania olejków eterycznych jak i stabilności termicznej otrzymywanych mikrokapsułek w porównaniu do żelatyny.

Słowa kluczowe: olejki eteryczne, koacerwacja złożona, białka roślinne, polisacharydy

Abstract

Plant proteins in microencapsulation of essential oils using complex coacervation

The aim of this research was to evaluate the potential application of complex coacervation using plant proteins as a method for encapsulating essential oils and to analyze the physicochemical properties of powders obtained through the lyophilization of the resulting liquid coacervates. Additionally, the study compared complex coacervates made from plant proteins with the traditional model of complex coacervation involving gelatin and gum Arabic to assess their efficiency and practical properties.

The study utilized gelatin, pea protein, fava bean protein, and oat protein, and as polysaccharides, gum Arabic and chia seed polysaccharides were used. Essential oils, such as juniper oil and black pepper oil, were dissolved in vegetable oils (soybean, grapeseed, and rapeseed) to minimize their evaporation during the coacervation process. Additionally, the impact of the emulsifier Tween 80 on the coacervation process and the physicochemical properties of the powders obtained after lyophilization of the coacervates were investigated.

Several analyses were conducted, including measurements of the efficiency of the coacervation process, the lyophilization process, and the microencapsulation efficiency. Furthermore, color, particle size distribution, and microscopic analysis using SEM were evaluated, along with thermal analysis and FT-IR analyses. The water solubility, bulk and tapped density, and powder flowability (using the Carr Index and Hausner Ratio) were also assessed, as well as the initial water content and hygroscopicity of the powders.

Based on the obtained research results, it was concluded that plant proteins can be used in complex coacervation, providing comparable or better results in terms of the efficiency of essential oil microencapsulation and the thermal stability of the resulting microcapsules compared to gelatin.

Key words: essential oils, complex coacervation, plant proteins, polysaccharides

Spis treści

Streszczenie	7
Abstract.....	8
Wykaz skrótów i oznaczeń wraz z jednostkami	11
Wykaz publikacji stanowiących rozprawę doktorską.....	12
Wstęp.....	13
Trend czystej etykiety a przemysł spożywczy	13
Syntetyczne konserwanty i dodatki do żywności	13
Olejki eteryczne – chemiczna złożoność i działanie.....	14
Olejki eteryczne z jałowca i czarnego pieprzu	16
Wyzwania i rozwiązania w stosowaniu EO w żywności	17
Wybór metody do mikrokapsułkowania olejków eterycznych.....	18
Koacerwacja złożona	19
Zastosowanie i ograniczenia materiałów ściennych w koacerwacji złożonej dla przemysłu spożywczego	20
Żelatyna i guma arabska.....	20
Białka mleka.....	21
Białka sojowe	22
Białka roślinne.....	22
Polisacharydy	23
Polisacharydy z nasion chia	23
Hipotezy badawcze, cel pracy oraz zakres badań.....	25
Materiał i metodyka badań	26
Skład mikrokapsułek	26
Przygotowanie mikrokapsułek.....	26
Wydajność koacerwacji, straty przy liofilizacji i efektywność kapsułkowania.....	27
Gęstość nasypowa, gęstość utrżona, indeks Carra i wskaźnik Hausnera	28
Pomiar barwy	29
Rozpuszczalność w wodzie, zawartość wody i higroskopijność	29
Rozkład wielkości cząstek	30
Skaningowa Mikroskopia Elektronowa (SEM).....	30
FT-IR.....	31
Skaningowa kalorymetria różnicowa (DSC)	31
Ultraszybka chromatografia gazowa (e-nos)	31
Analiza statystyczna	32

Projekt eksperymentu (DOE)	32
Optymalizacja procesu wytwarzania mikrokapsulek	32
Omówienie głównych wyników	34
Wykorzystanie klasycznego modelu koacerwacji złożonej pomiędzy żelatyną a gumą arabską do mikrokapsułkowania olejków eterycznych	34
Wykorzystanie koacerwacji złożonej pomiędzy białkami roślinnymi a gumą arabską do mikrokapsułkowania olejków eterycznych.	41
Wykorzystanie białka owsianego	41
Wykorzystanie białka grochowego	46
Wykorzystanie koacerwacji złożonej pomiędzy białkiem bobowym a polisacharydami wyizolowanymi z nasion chia do mikrokapsułkowania olejków eterycznych.....	50
Wnioski	56
Bibliografia	57
Pozostały dorobek naukowy	63
Publikacje stanowiące rozprawę doktorską wraz z oświadczeniami współautorów	65

Wykaz skrótów i oznaczeń wraz z jednostkami

G – żelatyna

GA – guma arabska

FB – białko bobowe

CHP – polisacharydy z nasion chia

OP – białko owsiane

EO – olejek eteryczny

EE – efektywność kapsułkowania, [%]

CY – wydajność koacerwacji, [%]

SY – wydajność mikroksułkowania (eng. solid yield), [%]

MR – proporcja mieszania materiałów ściennych [m/m]

T – emulgator Tween 80, polisorbat 80,
mieszanina polioksyetylenowych pochodnych sorbitanu i kwasu oleinowego

T_{on} – temperatura rozpoczęcia się reakcji endotermicznej, [°C]

T_{max} – temperatura szczytowa reakcji endotermicznej, [°C]

T_{end} – temperatura końcowa reakcji endotermicznej, [°C]

ΔH – entalpia towarzysząca reakcji endotermicznej, [mJ]

DSC – skaningowa kalorymetria różnicowa

FT-IR – spektroskopia w podczerwieni z transformacją Fouriera

Wykaz publikacji stanowiących rozprawę doktorską

1. Napiórkowska A, Kurek M. Coacervation as a Novel Method of Microencapsulation of Essential Oils—A Review. *Molecules*. 2022; 27(16):5142. <https://doi.org/10.3390/molecules27165142> (140 pkt. MNiSW, IF 4,6)
2. Napiórkowska A, Szpicer A, Wojtasik-Kalinowska I, Perez MDT, González HD, Kurek MA. Microencapsulation of Juniper and Black Pepper Essential Oil Using the Coacervation Method and Its Properties after Freeze-Drying. *Foods*. 2023; 12(23):4345. <https://doi.org/10.3390/foods12234345> (140 pkt. MNiSW, IF 5,2)
3. Napiórkowska, A., Szpicer, A., Górską-Horzyczak, E., & Kurek, M.. Understanding emulsifier influence on complex coacervation: Essential oils encapsulation perspective. *Journal of Food Science*. 2024, 89(8). <https://doi.org/10.1111/1750-3841.17220> (70 pkt. MNiSW, IF 3,9)
4. Napiórkowska A, Aktaş A, Szpicer A, Górską-Horzyczak E, Kurek MA. Optimization of oat protein and gum Arabic microcapsules containing juniper essential oil using Response Surface Methodology, *Food and Bioproducts Processing*, 2024, 145,203-216 <https://doi.org/10.1016/j.fbp.2024.04.001>. (140 pkt. MNiSW, IF 4,6)
5. Napiórkowska A, Szpicer A, Górską-Horzyczak E, Kurek MA. Microencapsulation of Essential Oils Using Faba Bean Protein and Chia Seed Polysaccharides via Complex Coacervation Method. *Molecules*. 2024; 29(9):2019. <https://doi.org/10.3390/molecules29092019> (140 pkt. MNiSW, IF 4,6)

Łączna punktacja Ministerstwa Nauki i Szkolnictwa Wyższego według wykazu czasopism punktowanych wynosi 630.

Łączny Impact Factor (IF) według Journal Citation Reports wynosi 22,9

Wstęp

Trend czystej etykiety a przemysł spożywczy

Rosnące zainteresowanie konsumentów żywnością o wysokiej wartości odżywczej, dłuższym terminie przydatności do spożycia i korzyściach zdrowotnych jest widoczne z roku na rok. Konsumenty są coraz bardziej świadomi metod produkcji żywności oraz jej składu. Pewne metody produkcji są postrzegane jako mniej „naturalne”, a niektóre składniki jako „niezdrowe” i „sztuczne”. Trend ten, określany jako „czysta etykieta”, skłania przemysł spożywczy do redukcji lub eliminacji konserwantów i syntetycznych dodatków na rzecz naturalnych substancji bioaktywnych pochodzenia roślinnego (Asioli i wsp. 2017). Jednak wiele z tych substancji charakteryzuje się dużą niestabilnością – są podatne na utlenianie, które nasila się pod wpływem światła, podwyższonej temperatury, wody i zmian pH. W związku z tym branża spożywcza jest zainteresowana technologiami, które stabilizują te substancje, aby zachować ich właściwości podczas przetwarzania i przechowywania oraz ułatwić ich dozowanie (Kunicka-Styczyńska, 2016; Falleh i wsp. 2019; Patrignani i wsp. 2020).

Syntetyczne konserwanty i dodatki do żywności

Konserwanty są używane do zapobiegania lub hamowania niekorzystnych zmian w żywności, takich jak mikrobiologiczne (wzrost bakterii lub grzybów), chemiczne (utlenianie, brunatnienie nieenzymatyczne) i biochemiczne (inaktywacja niektórych enzymów, metabolitów i składników niezbędnych do rozwoju mikroorganizmów). Z kolei dodatki do żywności to substancje dodawane do produktów spożywczych w celu modyfikacji lub poprawy ich walorów sensorycznych (Falleh i wsp. 2019; Rogozińska i Wichrowska 2011; Maruyama i wsp. 2020). Niestety coraz więcej dowodów wskazuje na to, że spożywanie sztucznych dodatków i konserwantów może prowadzić do alergii, zatruc pokarmowych czy rozwoju nowotworów (Gyawali, 2014; Voltolini i wsp. 2014; Aminzare i wsp. 2016; Laranjo i wsp. 2017; Xiaoqing i wsp., 2021).

Siarczyny (m.in. dwutlenek siarki i siarczyny sodu) są najbardziej znanymi dodatkami wywołującymi reakcje alergiczne. Tradycyjnie stosuje się je do konserwowania produktów owocowo-warzywnych. Ponadto, długoletnią praktyką winiarską jest dodatek SO₂, który zapobiega utlenianiu i brązowieniu wina (Grogan 2015). Związki te znacznie zmniejszają wchłanianie witaminy B₁, co prowadzi do reakcji alergicznych. Karmin i czerwień koszenilowa to inne znane dodatki wywołujące alergię. Te czerwone pigmenty pochodzą z ciał samic *Dactylopius coccus*, owadów żyjących na kaktusach koszenili (Ameryka Środkowa

i Południowa, Europa Południowa i Indie). Są szeroko stosowane jako barwniki w przetworzonej żywności i napojach, występują m.in. w burgerach, kiełbasach, czerwonych alkoholach, napojach bezalkoholowych, słodyczach i jogurtach owocowych (Gyawali 2014; Voltolini i wsp. 2014; Aminzare i wsp. 2016; Laranjo i wsp. 2017).

Stosowanie przeciwutleniaczy, takich jak BHT (butylowany hydroksytoluen), BHA (butylowany hydroksyanizol) i TBHQ (terc-butylohydrochinon), staje się coraz mniej popularne ze względu na obawy dotyczące ich wpływu na zdrowie człowieka. Substancje te są stosowane do utrwalania olejów roślinnych, zwierzęcych, wędlin oraz innych produktów zawierających tłuszcze. Choć te substancje skutecznie przeciwdziałają reakcjom utleniania, w organizmie człowieka wywierają działanie kancerogenne i cytotoksyczne (Xiaoqing i wsp., 2021).

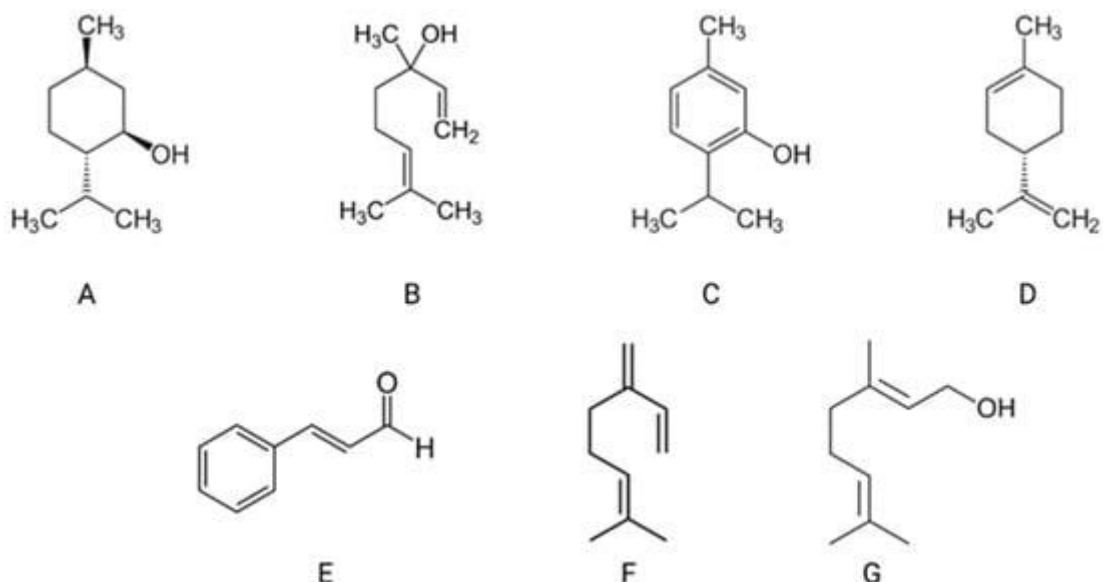
Aby sprostać wymaganiom konsumentów, producenci żywności intensywnie pracują nad eliminacją powszechnie stosowanych dodatków i konserwantów. Coraz więcej badaczy opracowuje także metody wykorzystania naturalnych substancji jako ich zamienników. Naturalne związki mają ogromny potencjał wydłużania okresu przydatności do spożycia żywności dzięki swoim właściwościom przeciwdrobnoustrojowym oraz dodatkowym korzyściom zdrowotnym, wynikającym z ich bioaktywnych właściwości przeciwutleniających (Grogan 2015; Gyawali 2014; Aminzare i wsp. 2016; Laranjo i wsp. 2017).

Spośród substancji pochodzenia roślinnego olejki eteryczne wyróżniają się tym, że łączą wszystkie te pożądane właściwości. Dzięki ich przeciwdrobnoustrojowym, przeciwutleniającym oraz prozdrowotnym działaniom, olejki eteryczne mają potencjał aby znaleźć szerokie zastosowanie w branży spożywczej (Hashemi i wsp. 2015; Pateiro i wsp. 2018).

Olejki eteryczne – chemiczna złożoność i działanie

Olejki eteryczne (EO) są metabolitami wtórnymi syntetyzowanymi przez rośliny olejkodajne. EO to wieloskładnikowe, hydrofobowe mieszaniny zawierające do kilkuset lotnych związków (zwykle od 100 do 200 substancji chemicznych na olejek eteryczny) w różnych stężeniach. Głównymi składnikami chemicznymi są terpeny, aldehydy, ketony, fenole, alkohole i inne (Hyldgaard i wsp. 2012; Giacometti i wsp. 2018; Delshadi i wsp. 2020). Ta złożoność chemiczna nadaje im właściwości terapeutyczne i wyjaśnia, dlaczego różne olejki eteryczne mogą mieć podobne działanie (Kunicka-Styczyńska 2016; Falleh i wsp. 2019; Valderrama i wsp. 2018; Falleh i wsp. 2020). EO charakteryzują się obecnością dwóch

lub trzech głównych składników w stosunkowo wysokich stężeniach (20–70%), co determinuje ich właściwości biologiczne (Ryc. 1). Karwakrol i tymol stanowią odpowiednio 30% i 27% składu EO z oregano (*Origanum compactum* Benth.). EO z kolendry (*Coriandrum sativum* L.) zawiera w swoim składzie 65% linaloolu. Mentol (59%) i menton (19%) występują w EO z mięty pieprzowej (*Mentha piperita* L.) (Turek i Stintzing 2013; Veiga i wsp. 2019).



Ryc. 1: Przykłady głównych składników olejków eterycznych: mentol (A), linalol (B), tymol (C), limonen (D), geraniol (E), aldehyd cynamonowy (F), mircen (G) (Napiórkowska i Kurek 2022)

Olejki eteryczne wykazują różnorodne właściwości farmakologiczne, takie jak działanie przeciwzapalne, przeciwskurczowe, uspokajające, przeciwbólowe oraz wspomagające trawienie. Ich bogaty i zróżnicowany skład chemiczny sprawia, że spożywanie jednego olejku eterycznego może przynosić wiele korzyści. Na przykład, olejek eteryczny z rozmarynu wspomaga trawienie, zwiększa apetyt i redukuje wzdęcia. Ponadto, olejki eteryczne mają dobrze udokumentowane działanie przeciwdrobnoustrojowe przeciwko bakteriom, drożdżom i pleśniom (Kunicka-Styczyńska 2016; Falleh i wsp. 2019; Patrignani i wsp. 2020). Ze względu na złożony skład, jeden olejek eteryczny może skutecznie hamować rozwój wielu mikroorganizmów. Przykładem jest olejek rozmarynowy, który hamuje rozwój bakterii Gram-dodatnich (*Enterococcus* spp.), Gram-ujemnych (*Salmonella* spp.), drożdży (*Candida* spp.) oraz pleśni (*Penicillium* spp.) (Singletary 2016; Valková i wsp. 2021; Stojanović-Radić i wsp. 2022).

Do tej pory przeprowadzono wiele badań nad wykorzystaniem EO potwierdzających ich zdolność do przedłużania trwałości różnego rodzaju produktów spożywczych. Podejmowano próby wykorzystania olejków eterycznych także do przedłużenia trwałości takich produktów jak sałata rzymska, sałata lodowa, szpinak dojrzały i szpinak młody (*Origanum vulgare* L.) (Moore-Neibel i wsp. 2013), przekąski na bazie mięsa i owoców morza (*Rosamary officinalis* L., *Coriander sativum* L., *Laurus nobilis* L., *Allium sativum* L., *Thymus vulgaris*, L.) (Kocatepe i wsp. 2019; Lages i wsp. 2021; Snoussi i wsp. 2022), soki (*Citrus sinensis* L.) (Bento i wsp. 2020), mleko, jogurty i inne przetwory mleczne (*Origanum vulgare* L., *Artemisia dracunculus* L.) (Shah i wsp. 2013; Bedoya-Serna i wsp. 2018; Zedan i wsp. 2021) czy czekoladki (*Cinnamomum burmannii* Blume) (Muhammad i wsp. 2018). Badania sugerują także, że olejki eteryczne, takie jak te z moringi olejodajnej (*Moringa oleifera* Lam.), wykazują silniejsze działanie wychwytyjące rodniki tlenowe w porównaniu z powszechnie stosowanymi syntetycznymi przeciwutleniaczami, takimi jak trolox, kwas askorbinowy, BHT czy BHA (Hussein i wsp. 2014). W rezultacie, olejki eteryczne mogą stanowić atrakcyjną alternatywę dla tradycyjnych środków konserwujących żywność (źródło).

Olejki eteryczne z jałowca i czarnego pieprzu

Jałowiec i czarny pieprz to przyprawy o długiej historii, cenione na całym świecie za swoje wyjątkowe walory smakowe i aromatyczne. Jałowiec, o charakterystycznym, żywicznym smaku, jest często wykorzystywany do aromatyzowania mięs, zwłaszcza dziczyzny, oraz do produkcji ginów. Czarny pieprz, nazywany „królem przypraw,” jest jedną z najpowszechniej używanych przypraw na całym świecie, docenianą za swój ostry, pikantny smak, który dodaje głębi i intensywności wielu potrawom (Sarma i wsp. 2014). Obie rośliny stanowią także surowce farmaceutyczne.

Jałowiec pospolity (*Juniperus communis* L.), a dokładnie szyszkojadody jałowca pospolitego zawierają olejek eteryczny, w którego skład wchodzi głównie α -pinen, limonen i mircen (Hojjati i wsp. 2019; Ghorbanzadeh i wsp. 2021). To właśnie olejek eteryczny odpowiedzialny jest za działanie poprawiające trawienie (na drodze zwiększania wydzielania żółci i soków żołądkowych) oraz działanie przeciwdrobnoustrojowe i antyoksydacyjne (Amalraj i wsp. 2020).

Czarny pieprz (*Piper nigrum* L.) to surowiec olejkodajny, którego olejek eteryczny składa się głównie z α i β -pinenu, sabinenu, limonenu i β -kariofylenu (Nikolić i wsp. 2015; Zheliakov

i wsp. 2018; Dosoky i wsp. 2019) wykazuje działanie pobudzające wydzielanie enzymów proteolitycznych i kwasu solnego, a także ogranicza powstawanie amin i siarkowodoru w jelicie grubym, co sprawia że ma on właściwości poprawiające trawienie i zapobiegające wzdęciom. Jak każdy olejek eteryczny, posiada on także silne działanie przeciwdrobnoustrojowe i antyoksydacyjne (Amalraj i wsp. 2020). x

W porównaniu do bardziej popularnych olejków, takich jak lawendowy, pomarańczowy czy cytrynowy, olejki z jałowca i czarnego pieprzu oferują unikatowe właściwości i nie są tak dobrze przebadane w kontekście ich mikrokapsułkowania. Z uwagi na ich powszechne stosowanie i akceptację konsumentów wydają się być one dobrym wyborem do prowadzenia dalszych badań na temat ich mikrokapsułkowania metodą koacerwacji złożonej. Może to przyczynić się do ich jeszcze szerszego zastosowania zarówno w przemyśle spożywczym, jak i farmaceutycznym.

Wyzwania i rozwiązania w stosowaniu EO w żywności

Olejki eteryczne charakteryzuje intensywny aromat i smak co może prowadzić do niepożądanych zmian organoleptycznych produktów spożywczych. EO są również wrażliwe na wpływ środowiska, takiego jak światło, tlen, zmiana pH i podwyższona temperatura. Dodatkowo, ze względu na ich lipofilowy charakter, charakteryzują się niską rozpuszczalnością w wodzie oraz niską biodostępnością (Bakry i wsp. 2016; Delshadi i wsp. 2020). Te problemy można rozwiązać za pomocą mikrokapsułkowania, które jest skuteczną metodą zachowania jakości wrażliwych substancji.

Mikrokapsułkowanie polega na powlekanii substancji aktywnej (substancji rdzenia) otoczką (materiałem ściennym) najczęściej wykonanej z gum, białek, lipidów lub polimerów syntetycznych, które zazwyczaj są nierozpuszczalne i niereagujące z materiałem rdzenia (Bakry i wsp. 2016; Devi i wsp. 2017; Arenas-Jal i wsp. 2020). Materiał ściany jest zwykle наносzony w postaci cieczy (roztworu, zawiesiny lub materiału stopionego), aby umożliwić oblewanie materiału rdzenia. Średnia wielkość mikrokapsulek wynosi 100–500 μm (Mohammadalinejad i Kurek 2021). Proces ten może ułatwić aplikację EO w żywności poprzez przekształcenie cieczy w fazę stałą, zapewniając precyzyjne dozowanie, poprawiając stabilność i maskując ich smak i/lub zapach. Dodatkowo izolując EO od środowiska, mikrokapsułkowanie może ochronić EO przed światłem, tlenem, drastycznymi zmianami temperatury oraz pH. Ułatwianie dystrybucji EO w obszarach żywności, w których rozwijają się mikroorganizmy (faza wodna)

i minimalizowanie średnicy ich cząstek może również przyczynić się do poprawy ich właściwości przeciwdrobnoustrojowych. Mniejszy rozmiar cząsteczek sprzyja migracji i przyłączaniu się do ścian komórkowych bakterii (Delshadi i wsp. 2020; Almas i wsp. 2021).

Powszechnie stosowanymi technikami mikrokapsułkowania są emulgacja, suszenie rozpyłowe i sublimacyjne, polimeryzacja *in situ*, wytłaczanie, powlekanie w złożu fluidalnym i technologia płynu nadkrytycznego oraz koacerwacja prosta i złożona (Bakry i wsp. 2016; Arenas-Jal i wsp. 2020). Jednakże do mikrokapsułkowania EO najczęściej stosuje się suszenie rozpyłowe.

Wybór metody do mikrokapsułkowania olejków eterycznych

Mikrokapsułkowanie metodą suszenia rozpyłowego jest najstarszym (stosowanym od lat 30. XX wieku) i najpowszechniejszym procesem stosowanym w mikrokapsułkowaniu w przemyśle spożywczym w celu zachowania właściwości fizykochemicznych związków lotnych, takich jak olejki eteryczne. Metoda ta jest najczęściej stosowana w przemyśle spożywczym ze względu na niskie koszty produkcji, produkcję na dużą skalę w trybie ciągłym, różnorodność matryc kapsułkujących oraz odpowiednią retencję i stabilność związków lotnych (Veiga i wsp. 2019; Bakry i wsp. 2016). Polega na rozpyleniu emulsji w ośrodku suszącym w stosunkowo wysokiej temperaturze, co pozwala na szybkie odparowanie wody i niemal natychmiastowe kapsułkowanie materiału rdzenia (Bakry i wsp. 2016; Arenas-Jal i wsp. 2020). Podczas tego procesu powstają kapsułki wielojądrowe, w których olejek eteryczny jest rozprowadzany zarówno wewnątrz, jak i na powierzchni mikrokapsułki, przez co substancje lotne mogą zostać utracone. Do utraty tej może dochodzić na trzech etapach procesu: podczas atomizacji, po utworzeniu kropli na powierzchni, kiedy stabilna membrana nie została jeszcze utworzona oraz, gdy woda wewnątrz kropli przekracza temperaturę wrzenia i powstałe w kropli bąbelki pękają, rozrywając powierzchnię i uwalniając lotne substancje (Rojas-Moreno i wsp. 2017).

Temperatura otoczenia ma zasadniczy wpływ na stabilność EO; z tego powodu EO mogą ulec degradacji podczas tego procesu. Degradacja olejków eterycznych pod wpływem ciepła jest zjawiskiem chemicznym i może zachodzić na drodze degradacji oksydacyjnej, rozerwania wiązania CC, eliminacji, hydrolizy i przegrupowania termicznego. Pod wpływem podwyższonej temperatury oraz ze względu na ich strukturalne powiązania w ramach tych samych grup chemicznych, składniki olejków eterycznych mogą łatwo wzajemnie przekształcać się w siebie, co może powodować zmiany ich smaku, zapachu oraz aktywności

przeciwdrobnoustrojowej (Turek i Stintzing 2013; Rojas-Moreno i wsp. 2017; Mahanta i wsp. 2021). Z tego powodu uzasadnione wydaje się stosowanie metod otrzymywania mikrokapsułkowanych olejków eterycznych, które nie wykorzystują wysokiej temperatury.

Liofilizacja, czyli suszenie sublimacyjne, jest interesującym procesem wykorzystującym niską temperaturę i obniżone ciśnienie. Podczas tego procesu zamrożona woda zawarta w próbce przechodzi bezpośrednio ze stanu stałego (lodowego) do stanu gazowego (pary wodnej) (Nowak i Jakubczyk, 2020). Liofilizacja znajduje szerokie zastosowanie w utrwalaniu wysokiej jakości produktów spożywczych oraz mikrokapsułkowaniu, w tym olejków eterycznych (Luo i in., 2019; Napiórkowska i in., 2023). Jednakże mikrokapsułki otrzymane tą metodą charakteryzują się wysoce porowatą strukturą (Nowak i Jakubczyk, 2020), co może negatywnie wpływać na zawartość olejków eterycznych, które, jako substancje lotne, łatwo ulegają parowaniu (Gardeli i in., 2010; Nedovic i in., 2011; Yaman i in., 2023).

Aby uniknąć podwyższonej temperatury oraz strat olejków eterycznych podczas suszenia sublimacyjnego, interesującym rozwiązaniem może być zastosowanie liofilizacji materiału już zmikrokapsułkowanego. Taki proces może pozwolić na lepszą ochronę lotnych substancji, minimalizując ich straty podczas suszenia. Interesującą metodą mogącą spełnić te wymagania może być koacerwacja złożona.

Koacerwacja złożona

Koacerwacja jest jedną z najstarszych stosowanych technik enkapsulacji. Jest to stosunkowo prosta metoda, którą można porównać do zmodyfikowanej techniki emulsyfikacji. Mechanizm tego procesu polega na oddzieleniu hydrokoloidu od roztworu pierwotnego, a następnie jego aglomeracji w oddzielną, ciekłą fazę, która nazywana jest "koacerwatem". Koacerwaty nazywane są "fazą ciągłą", podczas gdy druga faza nazywana jest "roztworem równowagi" (Pakzad i wsp. 2013; Devi i wsp. 2017). Proces koacerwacji można podzielić na cztery etapy: zawieszanie cząstek materiału rdzeniowego w fazie ciekłej, produkcja trójfazowego systemu, tj. wydzielanie drugiej fazy ciekłej (koacerwatu), odkładanie ciekłego polimeru wokół rdzenia, żelowanie i utwardzanie ściany mikrokapsułki (Napiórkowska i Kurek 2022).

Złożona koacerwacja jest procesem rozdziału faz spowodowanym interakcją dwóch lub więcej przeciwnie naładowanych koloidów (biopolimerów), zwykle białek i polisacharydów. W tej technice faza ciekła oddziela się od fazy bogatej w polimery (koacerwatu) (Devi i wsp. 2017).

Główną siłą napędową złożonej koacerwacji jest redukcja wolnej energii elektrostatycznej układu reakcyjnego wynikająca z interakcji między przeciwnie naładowanymi jonami (Timilsena i wsp. 2019). Proces ten zależy również od takich parametrów jak: pH (formowanie się koacerwatów zachodzi w wąskim zakresie pH poniżej punktu izoelektrycznego), siła jonowa, stosunek białka do polisacharydu, całkowite stężenie biopolimeru, rodzaj materiału rdzenia oraz stosunek materiału rdzenia do materiałów ściennych (Evans i wsp. 2013; Yang i wsp. 2015; Bakry i wsp. 2016; Rojas-Moreno i wsp. 2017). Szybkość mieszania odgrywa ważną rolę w kontrolowaniu wielkości powstających koacerwatów. Ponadto, różnica między ładunkami polimerów musi być wystarczająco duża, aby powodować interakcję, ale nie na tyle duża, aby powodować wytrącanie (Timilsena i wsp. 2019). Mikrokapsułki przygotowane w ten sposób są nierozpuszczalne w wodzie i odporne na ciepło, ale głównymi zaletami złożonej koacerwacji w porównaniu z innymi metodami mikrokapsułkowania są ogólnie wyższa wydajność enkapsulacji oraz możliwość zastosowania kontrolowanego uwalniania. Proces ten prowadzi do powstania okrągłej mikrokapsułki, w której rdzeń jest otoczony materiałem ściany chroniącym aktywny związek (Evans i wsp. 2013; Yang i wsp. 2015; Rojas-Moreno i wsp. 2017). Dodatkowo brak konieczności użycia podwyższonej temperatury stanowi kolejną zaletę tej metody w kontekście mikrokapsułkowania olejków eterycznych.

Zastosowanie i ograniczenia materiałów ściennych w koacerwacji złożonej dla przemysłu spożywczego

Żelatyna i guma arabska

Najczęściej stosowanym systemem w złożonej koacerwacji jest żelatyna (G)–guma arabska (AG) (Yang i wsp. 2015; Li i wsp. 2018; Shaddel i wsp. 2018; Ogilvie-Battersby i wsp. 2022). Podczas tego procesu dochodzi do elektrostatycznego przyciągania między dodatnimi ładunkami białka (NH_3^+) a ujemnymi ładunkami pochodzącymi od AG (COO^-) (Kontogiorgos 2019; Muhoza i wsp. 2022). Poddane oddziaływaniom elektrostatycznym substancje te tworzą warstwę koacerwatu, która twardnieje w procesie sieciowania żelatyny. Najczęściej jednak proces sieciowania indukowany jest w sposób chemiczny przez formaldehyd, glutaraldehyd, glyoksal lub epichlorohydrynę dzięki czemu w wyniku reakcji reszt aldehydowych środka sieciującego z grupami aminowymi białka wytwarzana jest nierozpuszczalna sieć. Nowo powstała sieć wzmacnia ścianę kapsułki, co ułatwia proces suszenia i zwiększa ich stabilność podczas przechowywania (Reis i wsp. 2022). Jest to jedno z głównych ograniczeń produkcji mikrokapsulek dla przemysłu spożywczego przy użyciu systemu (G)–(AG), ponieważ

stosowane środki sieciujące są uznawane za toksyczne dla organizmu ludzkiego (Pakzad i wsp. 2013; Muhoza i wsp. 2019; Timilsena i wsp. 2019). Ponadto, przygotowanie roztworów żelatyny i gumy arabskiej wymaga stosunkowo wysokiej temperatury (50–60°C) do ich całkowitego rozpuszczenia (Shaddel i wsp. 2018; Timilsena i wsp. 2019). W efekcie substancje wrażliwe na temperaturę oraz silnie lotne, takich jak olejki eteryczne, mogą ulec degradacji oraz ewaporacji. Kolejnym jest fakt, że najczęściej stosowana jest żelatyna wieprzowa, która jednak nie jest akceptowana przez pewną grupę konsumentów ze względu na ich preferencje religijne i dietetyczne (Timilsena i wsp. 2019). Ponadto, ze względu na rosnącą popularność diet wegetariańskich i wegańskich, przemysł spożywczy dąży obecnie do minimalizacji użycia składników pochodzenia zwierzęcego. Guma arabska mimo pochodzenia roślinnego nie cieszy się uznaniem wśród konsumentów z uwagi na klasyfikację jej jako dodatku do żywności i przypisanie jej symbolu E 414 (Paans 2013; Van Gunst i Roodenburg 2019). W związku z tym wydaje się być zasadnym poszukiwanie innych źródeł białek i polisacharydów, które mogłyby stanowić otoczkę w procesie mikrokapsułkowania olejków eterycznych.

Białka mleka

Białka mleka są szeroko stosowane w przemyśle spożywczym ze względu na ich amfifilowy charakter, który pozwala im adsorbować i rozprzestrzeniać się wokół matrycy olej/woda. Te białka są również popularne jako dodatki do żywności ze względu na ich właściwości odżywcze, funkcjonalne i aktywne (Liang i wsp. 2017; Vargas i wsp. 2021). Jak wspomniano wcześniej wydajność koacerwacji złożonej zależy między innymi od stężenia materiałów ściennych jak i ich wzajemnego stosunku. Zwiększenie stężenia białek mleka i stosunku biopolimerów prowadzi do wzrostu pH, przy którym zachodzi proces koacerwacji złożonej, co prowadzi do zwiększenia średniej wielkości formowanych mikrokapsulek. Zjawisko to można wyjaśnić zmniejszającą się siłą odpychania elektrostatycznego między białkami a polisacharydami (Muhoza i wsp. 2022). Stanowi to pewnego rodzaju ograniczenie w stosowaniu takiej kombinacji materiałów ściennych. Dodatkowo, podczas przygotowywania emulsji (ultradźwięki, temperatura, wysokie ciśnienie) może dochodzić do częściowej denaturacji i zmian konformacyjnych białek mleka. Negatywnie wpływa to na proces formowania koacerwatu. Kolejnymi ograniczeniami są fakt, że przemysł spożywczy stara się zredukować stosowanie produktów pochodzenia zwierzęcego, jak i silna alergenicność tych protein (Boné Calvo i wsp. 2021).

Białka sojowe

Z powodu opisanych powyżej trendów wśród konsumentów i ograniczeń związanych z używaniem żelatyny i białek mleka w procesie koacerwacji złożonej, białka pochodzenia roślinnego cieszą się rosnącym zainteresowaniem. Innym powodem jest to, że są one przyjazne dla środowiska, tanie, łatwo dostępne i mają interesujące właściwości funkcjonalne (Shishir i wsp. 2018). Wśród różnych białek roślinnych, białka sojowe są najczęściej badane i najczęściej stosowane w technice mikrokapsułkowania. Jest to spowodowane ich amfipatyczną naturą (hydrofilową i hydrofobową), dzięki czemu działają jako skuteczne emulgatory do tworzenia i stabilizowania emulsji olej-woda (Tang i wsp. 2017; Rios-Mera i wsp. 2019). Jednak równowaga hydrofilowości/hydrofobowości powierzchni białka wpływa również na rozpuszczalność białka, co jest kluczowe dla procesu koacerwacji złożonej. Białko sojowe charakteryzuje się niską rozpuszczalnością, ale można ją zwiększyć przez dodanie innego polimeru (np. polisacharydu) (Devi i wsp. 2017; Rojas-Moreno i wsp. 2017; Warnakulasuriya i Nickerson 2018).

Białka roślinne

W ostatnich latach białka roślinne takie jak białka grochu, ryżu, owsa, bobu, czy soczewicy zyskują na popularności. Ich zaletą jest hipoalergiczność, bezglutenowość, a także szeroka dostępność i niska cena. Produkcja białek roślinnych wymaga mniejszej ilości zasobów naturalnych, takich jak woda i ziemia w porównaniu do produkcji białek zwierzęcych. Dlatego też ich pozyskiwanie jest bardziej zrównoważone i mniej obciążające dla środowiska (Shishir i wsp. 2018; Carpentier i wsp. 2021). Żelatyna i białka mleka, dzięki swojej specyficznej strukturze, wykazują bardzo dobre właściwości żelujące i stabilizujące, co jest korzystne w tworzeniu stabilnych emulsji w procesie koacerwacji złożonej. Białka roślinne, choć posiadają dobre właściwości emulgujące i stabilizujące, mogą wymagać dostosowania procesów technologicznych, aby osiągnąć porównywalne rezultaty (Carpentier i wsp. 2022; Lan i wsp. 2020).

Powyższe sprawia, że białka roślinne zyskują w kontekście mikrokapsułkowania olejków eterycznych, chociaż nie są popularnie stosowane w koacerwacji złożonej olejków eterycznych. Niemniej jednak, dotychczas przeprowadzone badania wykazały, że są one w stanie tworzyć mikrokapsułki w tym procesie, zwiększając stabilność oksydacyjną i termiczną substancji rdzeniowych (Carpentier i wsp. 2022; Lan i wsp. 2020).

Polisacharydy

Tak jak wspomniano, guma arabska, która jest szeroko stosowana w procesie koacerwacji, mimo swojego naturalnego pochodzenia, może być negatywnie postrzegana przez niektórych konsumentów. Skłania to naukowców do próby zastąpienia gumy arabskiej polisacharydami pochodzącymi z surowców śluzowych, takich jak nasiona chia (*Salvia hispanica* L.), nasiona rzeżuchy (*Cardamine* L.), nasiona lnu (*Linum usitatissimum* L.), prawoślazu (*Althaea officinalis* L.), aloesu (*Aloe vera* L.) czy opuncji figowej (*Opuntia ficus-indica* L.) (Jannasari i wsp. 2019; Otálora i wsp. 2019; Hernandez-Nava i wsp. 2020b; Amani i wsp. 2022).

Polisacharydy z nasion chia

Chia (*Salvia hispanica* L.) była spożywana jako podstawowe pożywienie przez Majów i Azteków w Ameryce Centralnej i Północnej przez wieki. Po podboju hiszpańskim popadła w zapomnienie i obecnie przeżywa swój renesans. Można ją znaleźć w wielu różnych produktach, głównie śniadaniowych - chleb, bułki, musli, jogurty, gotowe kaszki czy smoothie. Nasiona chia mają unikalny profil żywieniowy, stąd wzrost ich popularności. Chia jest doskonałym źródłem kwasów tłuszczowych ω -3 i ω -6, białek o wysokiej wartości biologicznej, przeciwutleniaczy, witamin i minerałów. Ponadto, stwierdzono, że spożywanie nasion chia może zapobiegać stanom zapalnym i występowaniu chorób cywilizacyjnych (Capitani i wsp. 2013; Tamargo i wsp. 2018; Brütsch 2019; Bustamante i wsp. 2020).

Nasiona chia mają wyjątkową zdolność pochłaniania dużych ilości wody, co prowadzi do pęcznienia i tworzenia sieci hydrożelowej, znanej jako śluz nasion chia. Śluz ten, zawierający polisacharydy takie jak D-ksyloza, D-glukoza, β -D-ksylopiranoza, α -D-glukopiranoza i 4-O-metyl- α -D-glukopiranozylo-kwas uronowy (Goh i wsp. 2016; Bustamante i wsp. 2020), może być wykorzystywany w procesach emulgacji. Jest to produkt szczególnie obiecujący dla przemysłu spożywczego, ponieważ jest biodegradowalny i łatwostrawny (Brütsch 2019; Kassem i wsp. 2021). Spożywanie śluzu z nasion chia ma pozytywny wpływ na zdrowie, wspomagając pasaż jelitowy i poprawiając perystaltykę ponadto posiada on właściwości prebiotyczne (Manaf i wsp. 2018; Kassem i wsp. 2021).

W dotychczasowo przeprowadzonych badaniach wykazano, że śluz z nasion chia jest dobrym materiałem do maskowania smaku i zapachu enkapsulowanych substancji rdzeniowych jednocześnie nie wpływając na właściwości sensoryczne produktu, do którego takie

mikrokapsułki są dodawane. Ponadto, materiał ten jest skuteczny w ochronie substancji rdzeniowej przed utlenianiem (Timilsena i wsp. 2017; da Silva i wsp. 2018). Takie właściwości śluzu z nasion chia mogą okazać się użyteczne w mikrokapsułkowaniu olejków eterycznych.

Przemysł spożywczy stara się odchodzić od stosowania nienaturalnych dodatków w żywności. Obecnie coraz większą popularność zyskują substancje pochodzenia roślinnego, w tym olejki eteryczne. Pomimo udokumentowanych prozdrowotnych i przeciwbakteryjnych właściwości, stosowanie olejków eterycznych na większą skalę jest obecnie niemożliwe ze względu na ich bardzo intensywny smak i aromat, który negatywnie wpływa na akceptowalność produktów, w których się znajdują. Dodatkowo cechują się one dużą niestabilnością (wrażliwością na światło, tlen i temperaturę) oraz hydrofobowością, co uniemożliwia ich rozpuszczanie w fazie wodnej żywności, gdzie rozwijają się mikroorganizmy. Dlatego naukowcy poszukują rozwiązań, które pozwolą na zachowanie ich właściwości podczas przechowywania, jednocześnie maskując ich intensywny smak i zapach oraz zmniejszając ich hydrofobowość.

Wszystkie te ograniczenia mogą zostać rozwiązane przez mikrokapsułkowanie olejków eterycznych metodą koacerwacji złożonej. Jest to alternatywna metoda wobec najczęściej stosowanego suszenia rozpyłowego. Pozwala ona nie tylko na wyeliminowanie podwyższonej temperatury podczas procesu enkapsulacji, ale również na lepsze zamknięcie materiału rdzeniowego i jego ochronę przed środowiskiem zewnętrznym. Wykorzystanie białek pochodzenia roślinnego, które nie wywołują alergii, oraz polisacharydów z nasion chia o właściwościach poprawiających perystaltykę jelit, znacznie zwiększyłoby wartość odżywczą i prozdrowotny efekt produktu, do którego dodane byłyby tak przygotowane mikrokapsułki.

Hipotezy badawcze, cel pracy oraz zakres badań

W niniejszej pracy sformułowano następujące hipotezy badawcze:

1. Białka roślinne mogą stanowić alternatywę dla żelatyny w procesie koacerwacji złożonej.
2. Białka roślinne są równie skuteczne w mikrokapsułkowaniu olejków eterycznych, co żelatyna.
3. Zamiana gumy arabskiej na polisacharydy z nasion chia może zwiększyć efektywność kapsułkowania olejków eterycznych

Celem badań była ocena możliwości zastosowania koacerwacji złożonej z użyciem białek roślinnych jako metody kapsułkowania olejków eterycznych oraz analiza właściwości fizykochemicznych proszków otrzymanych poprzez liofilizację płynnych koacerwatów. Ponadto, badanie obejmowało porównanie koacerwatów z białek roślinnych z tradycyjnym modelem koacerwacji złożonej, który wykorzystuje żelatynę i gumę arabską, w celu oceny ich efektywności i właściwości użytkowych.

Praca swoim zakresem obejmowała wytworzenie koacerwatów zawierających olejki eteryczne z jałowca oraz czarnego pieprzu za pomocą koacerwacji złożonej, a następnie otrzymanie z nich mikrokapsułek za pomocą suszenia sublimacyjnego. Po otrzymaniu mikrokapsułek w formie proszku oceniano wydajność procesu koacerwacji, straty podczas liofilizacji oraz efektywność mikrokapsułkowania. Następnie oceniano ich barwę, gęstość nasypową oraz utrzęsioną, sypkość za pomocą indeksu Carra i wskaźnika Hausnera, morfologię, rozkład wielkości cząsteczek, rozpuszczalność w wodzie, zawartość wody, higroskopijność. Dodatkowo określano także wytrzymałość termiczną przy użyciu skaningowej kalorymetrii różnicowej (DSC), profil zapachowy za pomocą ultra-szybkiej chromatografii gazowej (tzw. e-nos) oraz strukturę chemiczną mikrokapsułek za pomocą spektroskopii w podczerwieni z transformacją Fouriera (FT-IR).

Materiał i metodyka badań

Skład mikrokapsulek

Materiały ściennie mikrokapsulek stanowiły żelatyna (Agnex, Białystok, Polska) oraz białka roślinne: owsiane (Helhetshalsa AB, Borghamn, Szwecja), grochowe (Hortimex, Konin, Polska) i bobowe (Hortimex, Konin, Polska) oraz guma arabska (Warchem, Warszawa, Polska) i polisacharydy wyizolowane z nasion chia (Agnex, Białystok, Polska). Materiał rdzenia stanowiły olejek eteryczny z jagód jałowca (*Juniperus communis* L.) (Ancient Wisdom, Sheffield, Wielka Brytania) i olejek eteryczny z pieprzu czarnego (*Piper nigrum* L.) (Ancient Wisdom, Sheffield, Wielka Brytania), które rozpuszczano w oleju: sojowym (Dary Natury, Koryciny, Polska), z pestek winogron (Basso Fedele e figli s.r.l., Avellino, Włochy), rzepakowym (Olvita, Marcinowice, Polska), oraz z zarodków pszennych (Zielony Klub, Kielce, Polska). Do przygotowania części mikrokapsulek zastosowano emulgator Tween 80 (Sigma Aldrich, Poznań, Polska).

Materiały stanowiące otoczkę mikrokapsulek mieszano ze sobą w różnym stosunku masowym: 1:1; 1:2 lub 2:1. Olejki eteryczne rozpuszczano w wyżej wymienionych olejach tak, aby po zmieszaniu stanowiły one maksymalnie 6% całego układu, a sam olejek eteryczny stanowił 3% całego układu.

Przygotowanie mikrokapsulek

Jako materiałów ściennych używano roztworów białek (żelatyny, owsianego, grochowego, bobowego) oraz polisacharydów (gumy arabskiej, z nasion chia). Przygotowane roztwory mieszano ze sobą w różnych stosunkach masowych (MR = 1:1, 1:2 oraz 2:1). Po zmieszaniu roztworów poddano je homogenizacji przy użyciu Ultra Turrax (IKA T18 basic, Niemcy) przez 5 minut przy 15 000 obr./min w temperaturze pokojowej. Podczas homogenizacji dodawano materiał rdzenia, który stanowiły olejki eteryczne (jałowcowy, z czarnego pieprzu) rozpuszczone w oleju roślinnym (sojowy, z pestek winogron, rzepakowy, z zarodków pszennych). Następnie przy użyciu 1M HCl zmieniano pH układu poniżej punktu izoelektrycznego charakterystycznego dla danego białka. Wszystkie emulsje były przechowywane w temperaturze 4°C przez 24 godziny, następnie przenoszone do szybkozmrzacza z temperaturą wewnątrz komory -20°C na kolejne 24 godziny, a następnie przenoszone do niskotemperaturowej zamrażarki z temperaturą -60°C na następne 24 godziny. Zamrożone próbki były liofilizowane przez 72 godziny w temperaturze kondensatora -80°C.

Po tym czasie liofilizaty przesiewano przez laboratoryjne sito o rozmiarze oczek 710 μm , a następnie pakowano próżniowo i przechowywano w temperaturze 4°C do dalszych analiz.

Wydajność koacerwacji, straty przy liofilizacji i efektywność kapsulkowania

Wydajność koacerwacji złożonej (CY), obliczano zgodnie z równaniem (Rojas-Moreno i wsp. 2018):

$$CY = \frac{CM}{SM} * 100\%$$

gdzie:

- CM – masa płynnego koacerwatu
- SM – masa całego układu

Straty podczas procesu liofilizacji (SY), obliczano zgodnie z równaniem (Rojas-Moreno i wsp. 2018):

$$SY = \frac{PM}{CM} * 100\%$$

gdzie:

- PM – masa proszku po liofilizacji

Wydajność enkapsulacji (EE) obliczano przez pomiar zawartości oleju powierzchniowego (S_o) i oleju całkowitego (T_o) w otrzymanych mikrokapsułkach (Hernandez-Nava i wsp. 2020a). Wszystkie pomiary wykonywano w trzykrotnych powtórzeniach.

S_o określano przez zważenie 1 g próbki i rozproszenie jej w 30 ml n-heksanu przy stałym mieszaniu (60 obr./min) przez 15 minut. Fazę olejową z n-heksanem filtrowano do wcześniej zważonej kolby okrągłodennej i odparowywano na wyparce rotacyjnej (R-100 Büchi, Szwajcaria). Następnie próbkę przechowywano w piecu w temperaturze 105°C przez 30 minut, aby upewnić się, że cały n-heksan wyparował. Po tym próbkę pozostawiono w eksykatorze do ostygnięcia. Kolbę okrągłodenną wazono, a S_o obliczano jako:

$$S_o = OM_1 - OM_2$$

gdzie:

- OM_1 – masa oleju po ekstrakcji i odparowaniu rozpuszczalnika
- OM_2 – teoretyczna masa oleju w próbce

T_O określano przez zważenie 1,5 g próbki i rozprowadzenie jej w 4 ml KCl. W następnym kroku do próbki dodawano 4 ml acetonu i 8 ml chloroformu. Przygotowaną próbkę stale mieszano (60 obr./min) przez 15 minut, a następnie odwirowywano (5000 obr./min, 5 minut). Górną warstwę zlewano, a dolną warstwę zawierającą chloroform i fazę olejową przesączano przez bibułę filtracyjną z bezwodnym siarczanem sodu do zważonej kolby okrągłodennej, tak że próbka testowa pozostawała w probówce Falcon. Następnie do pozostałości dodawano 4 ml podwójnie destylowanej wody, 4 ml acetonu i 8 ml chloroformu. Próbkę ponownie odwirowywano, górną warstwę zlewano, a dolną warstwę przesączano przez bibułę filtracyjną. Następnie rozpuszczalnik odparowywano na wyparce rotacyjnej (R-100 Büchi, Szwajcaria). Próbkę przechowywano w piecu w temperaturze 105°C przez 30 minut, aby wyparować nadmiar chloroformu, po czym próbkę pozostawiono w eksykatorze do ostygnięcia. Kolbę okrągłodenną ważono, a T_O obliczano jako:

$$T_O = OM_1 - OM_2$$

Mając wyniki dla S_O i T_O , EE obliczano zgodnie z formułą:

$$EE = \frac{T_O - S_O}{T_O} * 100\%$$

Gęstość nasypowa, gęstość utrzęsiona, indeks Carra i wskaźnik Hausnera

Gęstość nasypowa (ρ_{bulk}) była określana przez pomiar objętości zajmowanej przez znaną masę proszku w 10 ml cylindrze miarowym oraz pomiar masy cylindra przed i po dodaniu proszku (Hernandez-Nava i wsp. 2020b). Podobnie, gęstość utrzęsiona (ρ_{tap}) była określana w 10 ml cylindrze miarowym poprzez wielokrotne podnoszenie i opuszczanie cylindra pod własnym ciężarem na wysokość 14 ± 2 cm przez jedną minutę (jedno uderzenie na sekundę) (Akseli i wsp. 2019). Oznaczenia przeprowadzano w trzykrotnych powtórzeniach. Gęstości wyrażano w g/cm^3 .

Indeks Carra (CI) i współczynnik Hausnera (HR) są miarami tendencji proszku do kompresji. Oznaczenia przeprowadzono w trzykrotnych powtórzeniach. Wartości CI i HR obliczono według równań (Xin i wsp. 2022).

$$CI = \frac{\rho_{tap} - \rho_{bulk}}{\rho_{tap}} * 100\%$$

$$HR = \frac{\rho_{tap}}{\rho_{bulk}}$$

Pomiar barwy

Kolor mikrokapsulek oceniano za pomocą kolorymetru Minolta CR-400 (Konica Minolta Inc., Japonia). Pomiarów dokonywano w warunkach oświetlenia D65, z głowicą pomiarową o średnicy 8 mm, zgodnie z protokołem standardowym dla obserwatorów o kącie widzenia 2°. Zarejestrowane dane wyrażano zgodnie z systemem Międzynarodowej Komisji Oświetleniowej (Commission Internationale de L'Eclairage) w przestrzeni barwnej CIELab.

Analizowane i oceniane składowe barwy obejmowały L* (gdzie L = 0 oznacza idealną czerń, a L = 100 oznacza idealną biel), a*, gdzie (-a*) oznacza nasycenie barwy zielonej, a (+a*) oznacza nasycenie barwy czerwonej) oraz b*, gdzie (-b*) oznacza nasycenie barwy niebieskiej, a (+b) oznacza nasycenie barwy żółtej (Otálora i wsp., 2023). Oznaczenia przeprowadzono w trzykrotnych powtórzeniach bezpośrednio po procesie produkcji, aby zapewnić dokładność i spójność wyników. Zastosowano przystawkę do analizy barwy proszków.

Rozpuszczalność w wodzie, zawartość wody i higroskopijność

Aby ocenić rozpuszczalność mikrokapsulek, zastosowano metodę polegającą na rozproszeniu 0,5 g próbki w 50 ml podwójnie destylowanej wody. Następnie próbkę mieszano przez 30 minut przy 60 obr./min, a następnie poddawano wirowaniu przy 10 000 obr./min przez 5 minut. Po odwirowaniu, 25 ml supernatantu przenoszono na wyważoną wcześniej szalkę Petriego i suszono w temperaturze 105°C przez 6 godzin (suszarka Binder FP 115, Tuttlingen, Niemcy). Rozpuszczalność (%) obliczano jako procent wysuszonego supernatantu w odniesieniu do początkowo dodanej ilości proszku (de Melo Ramos i wsp., 2019). Oznaczenia przeprowadzono w trzech powtórzeniach.

Zawartość wody w uzyskanych mikrokapsułkach określano poprzez umieszczenie 0,2 g próbki na wyważonej wcześniej szalce Petriego. Szalkę z próbką suszono następnie w temperaturze 70°C przez 24 godziny (suszarka Binder FP 115, Tuttlingen, Niemcy). Po suszeniu próbki przenoszono do eksykatora, aby całkowicie ostygły przed ponownym zważeniem. Zawartość wilgoci obliczano na podstawie zaobserwowanej różnicy w wadze przed i po procesie suszenia (Tavares i Norena 2020). Oznaczenia przeprowadzono w trzech powtórzeniach.

Higroskopijność uzyskanych proszków określano poprzez umieszczenie 0,2 g próbki na wyważonej wcześniej szalce Petriego. Następnie szalkę przechowywano w eksykatorze zawierającym nasycony roztwór Na₂SO₄ przez tydzień. Higroskopijność wyrażano jako g wody wchłoniętej na 100 g próbki (%) (Tavares i Norena 2020). Oznaczenia przeprowadzono w trzech powtórzeniach.

Rozkład wielkości cząstek

Pomiar został przeprowadzony za pomocą aparatu Morphologi® G3SE (Malvern Instruments Ltd., Malvern, UK) wyposażonego w jednostkę dyspersyjną do próbek suchych. Rozkład wielkości cząstek obliczano jako względną objętość cząstek w paśmie, przedstawioną jako krzywe rozkładu wielkości (oprogramowanie Malvern Microsoft v.5.40, Malvern Instruments Ltd.). Badane parametry rozkładu wielkości cząstek obejmowały największą wielkość cząstek (D₉₀), średnią wielkość cząstek (D₅₀) i najmniejszą wielkość cząstek (D₁₀) (Pieczykolan i Kurek 2019). Rozkład wielkości cząstek (wskaźnik Span – SI) szacowano za pomocą następującego wzoru (Fernandes 2014):

$$SI = \frac{D_{90} - D_{10}}{D_{50}}$$

Skaningowa Mikroskopia Elektronowa (SEM)

Skaningowy mikroskop elektronowy (Jeol JSM6010LA, Japonia) został użyty do analizy morfologii powierzchni próbek. Każda próbka została przymocowana na taśmie węglowej samoprzylepnej i pokryta (około 15 nm) złotem. Obrazy elektronów wtórnych wykonano przy kilku powiększeniach i przy napięciu przyspieszającym 10 kV.

Spektroskopia w podczerwieni z transformacją Fouriera (FT-IR)

Spektra FT-IR rejestrowano bez przygotowania próbek na spektrometrze FTIR Nicolet™ iS™ 5 (Thermo Scientific, Waltham, MA, USA), z poziomym urządzeniem do osłabionej całkowitej refleksji i kryształem diamentowym, w oknie spektralnym od 4000 do 400 cm^{-1} (16 skanów), z rozdzielczością spektralną 2 cm^{-1} . Uzyskane spektra przetwarzano za pomocą programu OMNIC (Thermo Scientific, Waltham, MA, USA) (Napiórkowska i wsp. 2023).

Skaningowa kalorymetria różnicowa (DSC)

Właściwości termiczne próbek oceniano za pomocą skaningowej kalorymetrii różnicowej (DSC 1) z Mettler Toledo 820 (Schwerzenbach, Szwajcaria) w atmosferze azotu przy przepływie 100 cm^3/min . Urządzenie skalibrowano za pomocą czystego indu i cynku. Każda próbka ($5,0 \pm 0,1$ mg) została umieszczona w aluminiowym tygielku (ME-51119870) i przykryta pokrywką (ME-51119871) za pomocą Mettler Toledo Crucible Sealing Press. Skanowanie DSC przeprowadzono w zakresie od 10°C do 230°C z szybkością 10°C/min. Termogramy analizowano za pomocą oprogramowania STARe (wersja 9.30) w celu określenia temperatur początkowych (T_{on}), maksymalnych (T_{max}) i końcowych (T_{end}) oraz powierzchni pod pikami (ΔH) (Napiórkowska i wsp. 2023).

Ultraszybka chromatografia gazowa (e-nos)

Lotne związki w mikrokapsułkach identyfikowano za pomocą elektronicznego nosa Heracles II (Alpha M.O.S., Tuluza, Francja), który wykorzystuje ultraszybką chromatografię gazową z fazą nadpowierzchniową. System wyposażony jest w dwie metalowe kolumny o różnych polarnościach (niepolarną MXT-5 i lekko polarną MXT1701, średnica = 180 μm , długość = 10 m) oraz dwa detektory jonizacji płomieniowej (FID).

Do analizy używano 10% wodnych roztworów (0,25 g w 5 g) każdej próbki, które umieszczano w standardowych fiolkach do fazy nadpowierzchniowej, zamykanych silikonowymi korkami pokrytymi teflonem. Inkubacja odbywała się w temperaturze 35 °C przez 900 s przy prędkości mieszania 8,33 Hz. Gazem nośnym był wodór (przepływ 1 mL/min). Temperatura wstrzykiwacza wynosiła 200 °C, z objętością wstrzykiwaną 3500 μL i prędkością 125 mL/s. Analizy były zbierane w pułapce w temperaturze 15 °C i następnie dzielone oraz jednocześnie przekazywane do dwóch kolumn. Gaz nośny utrzymywano pod stałym ciśnieniem 80 kPa, z przepływem podziałowym 10 mL/min przy głowicach kolumn. Parametry pieca były

następujące: 60 °C przez 2 s, rampa 3 °C/s do 270 °C, utrzymanie przez 20 s, oraz FID1/FID2 przy 280 °C.

Związki lotne zidentyfikowane w próbkach były prezentowane w formie tabeli z indeksami Kovatsa oraz wykresu PCA. Wszystkie próbki analizowano w trzech powtórzeniach. Indeksy Kovatsa ustalono za pomocą standardów alkanowych (n-butan do n-heksadekan) (Restek) mierzonych w tych samych warunkach co próbki (Górska-Horczyzak i wsp. 2017; Wojtasik-Kalinowska i wsp. 2018).

Analiza statystyczna

Do analizy statystycznej wykorzystano program statystyczny STATISTICA w wersji 13.3. Aby ocenić, czy proporcja mieszania białka i polisacharydów oraz dodatek emulgatora miały statystycznie istotny wpływ na proces złożonej koacerwacji oraz na końcowe parametry otrzymanych proszków, przeprowadzono jednoczynnikową analizę wariancji (ANOVA) oraz test Fishera LSD ($p\text{-value} < 0,05$, $\alpha = 95\%$).

Projekt eksperymentu (DOE)

Rozważono kombinacje różnych wartości pH (A) i zawartości białka owsianego (B) jako zmienne niezależne, wykorzystując projekt frakcyjny z dwoma zmiennymi wejściowymi, jednym blokiem i dwunastoma próbkami. Jeden dodatkowy punkt centralny został dodany do każdego bloku za pomocą oprogramowania Design Expert w wersji 11 (Stat-Ease, Inc., USA), co doprowadziło do 13 prób. Zakres wartości pH wynosił 2-6, a zawartości białka 20-80%.

Optymalizacja procesu wytwarzania mikrokapsulek

Odpowiedzi uzyskane z testów analizowano za pomocą Centralnego Kompozytowego Projektu Rotacyjnego (Central Composite Rotational Design, CCRD) w celu zbadania wpływu zmiennych niezależnych – A i B. Do tej analizy wykorzystano oprogramowanie Design Expert w wersji 11 (Stat-Ease, Inc., USA). Zmiennymi zależnymi, czyli odpowiedziami, były cechy jakości koacerwatów, takie jak wydajność, efektywność enkapsulacji, gęstość, płynność, rozpuszczalność, higroskopijność, zawartość wilgoci i kolor. Dla każdej odpowiedzi przeprowadzono jednoczynnikową analizę wariancji (ANOVA, $p \leq 0.05$), wraz z oceną braku dopasowania i współczynników determinacji (R^2) w celu zapewnienia dokładności modelu.

Trójwymiarowe wykresy powierzchniowe tworzono za pomocą oprogramowania Design Expert w wersji 11 (Stat-Ease, Inc., USA).

Oprócz wyjaśniania zachowania zmiennych za pomocą wykresów powierzchniowych, modele ustanowione w niniejszym badaniu były wykorzystane do optymalizacji procesu z zastosowaniem funkcji pożądania. Metoda ta polega na przekształceniu każdej zmiennej odpowiedzi w funkcję pożądania (d_i) o wartościach w zakresie od 0 do 1. Celem jest identyfikacja poziomów czynników, które odpowiadają maksymalnym lub minimalnym wartościom zmiennych odpowiedzi, przy czym $d_i = 1$ przypisywane jest wartościom wysokim, a $d_i = 0$ wartościom niskim. Efektywność enkapsulacji oraz rozpuszczalność uznano za zmienne „maksymalnie pożądane”, natomiast wskaźnik polidispersyjności uznano za zmienną „minimalnie pożądaną”. Funkcja pożądania pełni rolę funkcji kary, kierując algorytm w stronę obszarów, w których można znaleźć pożądane wartości zmiennych odpowiedzi. Poziomy czynniki, które odpowiadają maksymalnym lub minimalnym wartościom zmiennych odpowiedzi, nazywane są „punktami optymalnymi” (Kurek et al., 2016).

Po przeprowadzeniu optymalizacji oraz produkcji zoptymalizowanych mikrokapsulek, wybrane parametry zostały zmierzone zgodnie z wcześniejszymi procedurami. Uzyskane wyniki poddano jednoczynnikowej analizie wariancji (ANOVA, $p \leq 0,05$) przy użyciu programu Statistica w wersji 13.3.

Omówienie głównych wyników

Poniżej przedstawiono omówienie najważniejszych wyników prac badawczych, które zostały opublikowane w ramach cyklu publikacji stanowiących rozprawę doktorską.

Pracę podzielono na następujące etapy:

1. Wykorzystanie klasycznego modelu złożonej koacerwacji pomiędzy żelatyną a gumą arabską do mikrokapsułkowania olejków eterycznych. Uzyskane wyniki miały stanowić punkt odniesienia do porównania w dalszych badaniach realizowanych w kolejnych pracach badawczych. Wyniki tych badań zaprezentowano w publikacji 2, tj. *Microencapsulation of juniper and black pepper essential oil using the coacervation method and its properties after freeze-drying*.
2. Wykorzystanie koacerwacji złożonej pomiędzy białkami roślinnymi (grochowe, owsiane) a gumą arabską do mikrokapsułkowania olejków eterycznych. Uzyskane wyniki miały na celu określenie jak zamiana żelatyny na białko pochodzenia roślinnego wpływa na proces koacerwacji oraz parametry otrzymanych mikrokapsulek. Wyniki tych badań zaprezentowano w publikacji 3 i 4, tj. *Understanding emulsifier influence on complex coacervation: Essential oils encapsulation perspective* oraz *Optimization of oat protein and gum Arabic microcapsules containing juniper essential oil using Response Surface Methodology*.
3. Wykorzystanie koacerwacji złożonej pomiędzy białkiem bobowym a polisacharydami wyizolowanymi z nasion chia do mikrokapsułkowania olejków eterycznych. Uzyskane wyniki miały na celu określenie czy i jak zamiana powszechnie stosowanej gumy arabskiej na inne polisacharydy wpływa na proces koacerwacji oraz parametry otrzymanych mikrokapsulek. Wyniki tych badań zaprezentowano w publikacji 5, tj. *Microencapsulation of essential oils using faba bean protein and chia seed polysaccharides via complex coacervation method*.

Wykorzystanie klasycznego modelu koacerwacji złożonej pomiędzy żelatyną a gumą arabską do mikrokapsułkowania olejków eterycznych

Celem pracy było zastosowanie klasycznego modelu koacerwacji złożonej pomiędzy żelatyną a gumą arabską do mikrokapsułkowania olejków eterycznych. Uzyskane wyniki miały pełnić funkcję porównawczą dla badań przeprowadzonych w kolejnych pracach.

Ważnym czynnikiem wpływającym na proces koacerwacji złożonej jest stosunek masy białka do polisacharydu - różne proporcje wpływają na intensywność interakcji i kompleksacji, ze względu na równowagę ładunków między polimerami (Klemmer i wsp. 2012; Yuan i wsp. 2018; Hernandez-Nava i wsp. 2020b). W pracy zastosowano trzy różne proporcje pomiędzy żelatyną a gumą arabską – 1:1; 1:2; 2:1. Analiza statystyczna wykazała, że na uzyskane wyniki miała wpływ proporcja mieszania G/GA, rodzaj olejku eterycznego oraz oleju użytego do jego rozpuszczenia oraz interakcje między nimi. Jednak największy wpływ na uzyskane wartości CY i SY miała MR; tuż za nią najbardziej wpływowy był olejek eteryczny (Tab. 1). MR miała silny pozytywny wpływ na CY, natomiast negatywny na SY. Podobnie było w przypadku oleju, choć wpływ tego czynnika był niewielki. Z drugiej strony, w przypadku olejku eterycznego, efekt był odwrotny - zawartość olejku eterycznego powodowała niewielki spadek CY i niewielki wzrost wartości SY. W tym badaniu zarówno wydajność koacerwacji, jak i wydajność mikrokapsułkowania były niskie i nie przekraczały 50%. Próbkę GJ3, GB3, SJ3 i SB3 miały najwyższą wartość CY i wykazywały istotne różnice ($p < 0,05$) w CY. Próbkę miały ten sam proporcja mieszania G/GA (2:1), a olejki eteryczne były rozpuszczone w różnych olejach. Pomimo najwyższej wartości CY, nie odzwierciedlało to najwyższej wartości SY. Te próbki miały najniższe wartości SY, podczas gdy najwyższe wartości SY uzyskano dla próbek SB2, GB2, GJ2 i SB1, które charakteryzowały się najniższymi wartościami CY.

Żelatyna składa się głównie z glicyny, proliny, hydroksyproliny, alaniny i lizyny (Rohman i wsp. 2020). Te aminokwasy dostarczają więc dodatnio naładowane jony NH^{3+} do procesu koacerwacji. Guma arabska posiada głównie ujemnie naładowane jony COO^- pochodzącymi z kwasu arabinowego (Atgie i wsp. 2019). Proces ten zależy od elektrostatycznego przyciągania między tymi przeciwnie naładowanymi jonami (Muhoza i wsp. 2020). Dla każdej mieszaniny białka i polisacharydu zawsze istnieje określony molarny stosunek, aby uzyskać maksymalną wydajność koacerwacji - gdy białko i polisacharyd mają dokładnie przeciwną gęstość ładunków prowadzącą do ich neutralizacji (Bakry i wsp. 2016; Warnakulasuriya i Nickerson 2018; Muhoza i wsp. 2020). Prawdopodobnie ten stan osiągnięto przy stosunku mieszania 2:1, gdzie stosunek żelatyny do gumy arabskiej był najwyższy, co skutkowało najwyższym CY. Żelatyna ma wysoką zdolność wiązania wody w swojej strukturze (Kavoosi i wsp. 2014; Sanchez i wsp. 2018). Niemniej jednak te polimery wiążą wodę słabym wiązaniem wodorowym, które rozpada się i uwalnia wodę podczas procesu liofilizacji, co skutkowało obniżeniem wartości SY (Lashkari i wsp. 2014).

Efektywność kapsułkowania to procent materiału rdzeniowego zamkniętego w cząstkach proszku; jest to bardzo ważny parametr dla olejków eterycznych, ponieważ są to związki lotne bardzo podatne na utratę podczas procesu suszenia. Analiza statystyczna wykazała, że wyniki zależały od interakcji między stosunkiem mieszania polimerów a olejem (Tab. 1). Rodzaj oleju miał wyraźny pozytywny wpływ na EE, powodując jej wzrost. Najwyższa wartość EE została uzyskana dla próbki SJ1 (64,09%). Wysoka efektywność enkapsulacji została również uzyskana dla próbek SB3 i GJ2 (odpowiednio 61,92 i 59,89) i wykazała istotne różnice ($p < 0,05$) w wartościach EE. Próbkami GB2, SB1 i SJ2 nie wykazały istotnych różnic ($p < 0,05$) w EE - wartości znajdowały się w środkowym zakresie uzyskanych wyników (53,4-55,25%). Jednak podobieństwa można znaleźć w próbkach SB1 i GB2, które zawierały ten sam olej i olejek eteryczny oraz w próbkach GB2 i SJ2, które charakteryzowała taka sama proporcja G:GA mieszania (1:2). Wpływ interakcji między stosunkiem mieszania a olejem na wartość EE jest wyraźnie widoczny w tych przypadkach. Próbkami GJ1 i GJ3 również znalazły się w tej samej grupie statystycznej (odpowiednio 49,30 i 49,65) i zawierały ten sam olejek eteryczny. Najniższą wartość EE uzyskano dla próbki GB1 (Tab. 1).

Tab. 1: Wydajność koacerwacji (CY), wydajność mikrokapsułkowania (SY), efektywność kapsułkowania (EE) [%]

	Próbka	CY	SY	EE
	GJ1	30.93±0.44 ^b	29.79±1.21 ^c	49.3 ±0.07 ^{abe}
	GB1	30.49±0.56 ^b	29.25±1.29 ^c	42.7 ±0.11 ^e
	GJ2	28.01±0.16 ^a	37.11±0.49 ^e	59.89 ±0.01 ^{cdf}
	GB2	29.45±0.08 ^d	36.23±0.08 ^{de}	55.25 ±0.01 ^{abcd}
	GJ3	39.22±0.16 ^g	21.32±0.25 ^a	49.65 ±0.02 ^{abe}
	GB3	41.64±0.15 ⁱ	23.01±0.36 ^b	47.21 ±0.04 ^{ae}
	SJ1	33.78±0.46 ^f	26.58±0.36 ^g	64.09 ±0.09 ^f
	SB1	23.95±0.16 ^c	35.44±0.47 ^d	54.14 ±0.05 ^{abcd}
	SJ2	31.91±0.12 ^e	33.8±0.02 ^h	53.4 ±0.04 ^{abcd}
	SB2	28.34±0.12 ^a	38.45±0.34 ⁱ	52.33 ±0.01 ^{abc}
	SJ3	46.58±0.19 ^j	22.02±0.18 ^{ab}	56.8 ±0.01 ^{bcdf}
	SB3	41.04±0.51 ^h	20.21±0.61 ^f	61.92 ±0.04 ^{df}
	S.E.M.	0.369	0.096	26.524
Efekt	Olej	**	NS	**

EO	**	**	NS
MR	**	**	NS
Olej x EO	**	**	NS
EO x MR	**	**	**
Olej x MR	**	**	NS
Olej x EO x MR	**	**	NS

GJ1, GJ2, GJ3 – próbki zawierające żelatynę i gumę arabską w proporcji odpowiednio 1:1; 1:2; 2:1, olej z pestek winogron oraz olejek eteryczny z jałowca; **GB1, GB2, GB3** – próbki zawierające żelatynę i gumę arabską w proporcji odpowiednio 1:1; 1:2; 2:1, olej z pestek winogron oraz olejek eteryczny z czarnego pieprzu; **SJ1, SJ2, SJ3** – próbki zawierające żelatynę i gumę arabską w proporcji odpowiednio 1:1; 1:2; 2:1, olej sojowy oraz olejek eteryczny z jałowca; **SB1, SB2, SB3** – próbki zawierające żelatynę i gumę arabską w proporcji odpowiednio 1:1; 1:2; 2:1, olej sojowy oraz olejek eteryczny z czarnego pieprzu.

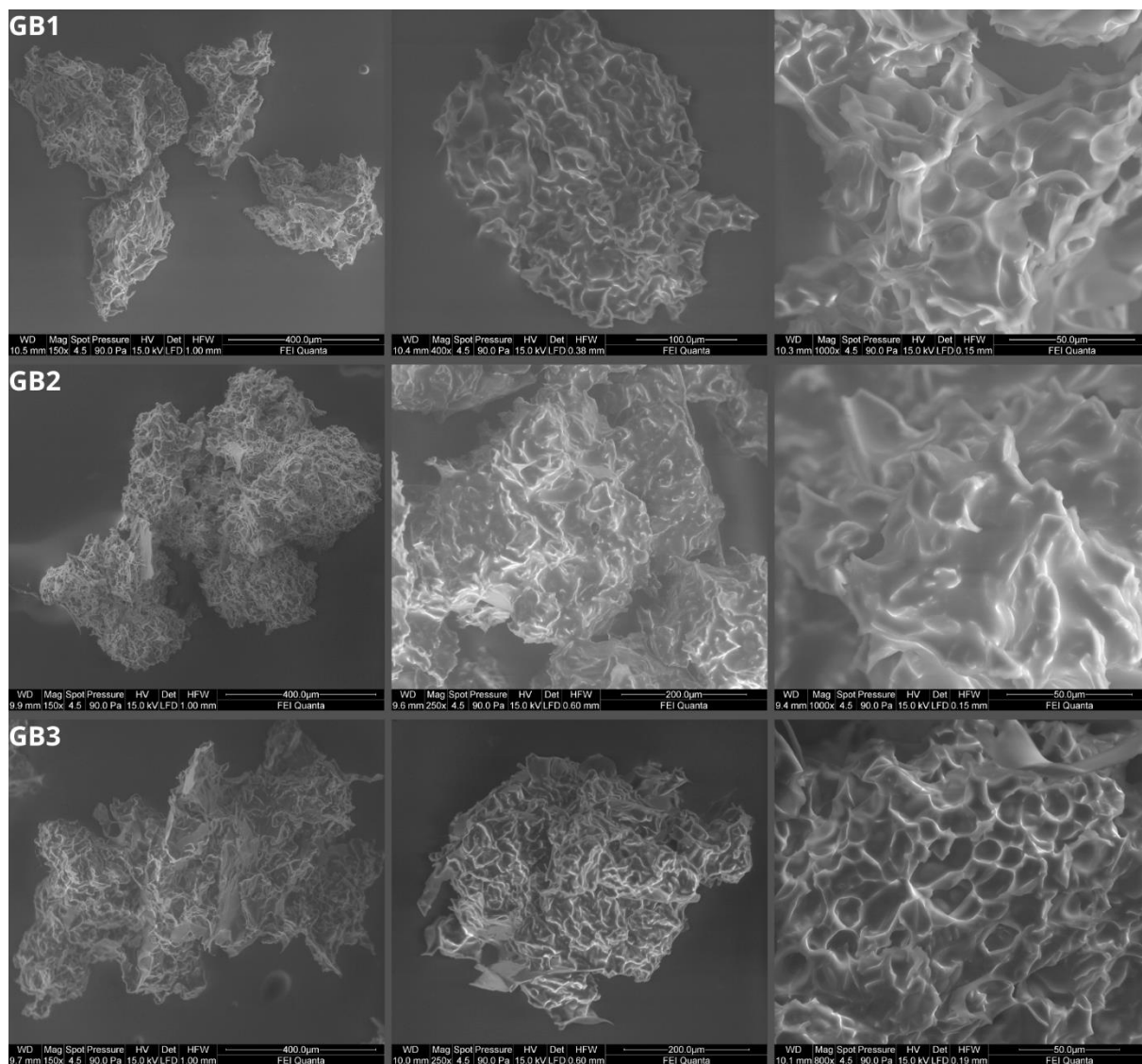
Wyniki w tej tabeli są wyrażone jako średnia \pm odchylenie standardowe. Średnie wartości oznaczone różnymi indeksami górnymi w obrębie wiersza różnią się istotnie przy $p \leq 0,05$.

S.E.M. – błąd standardowy średniej

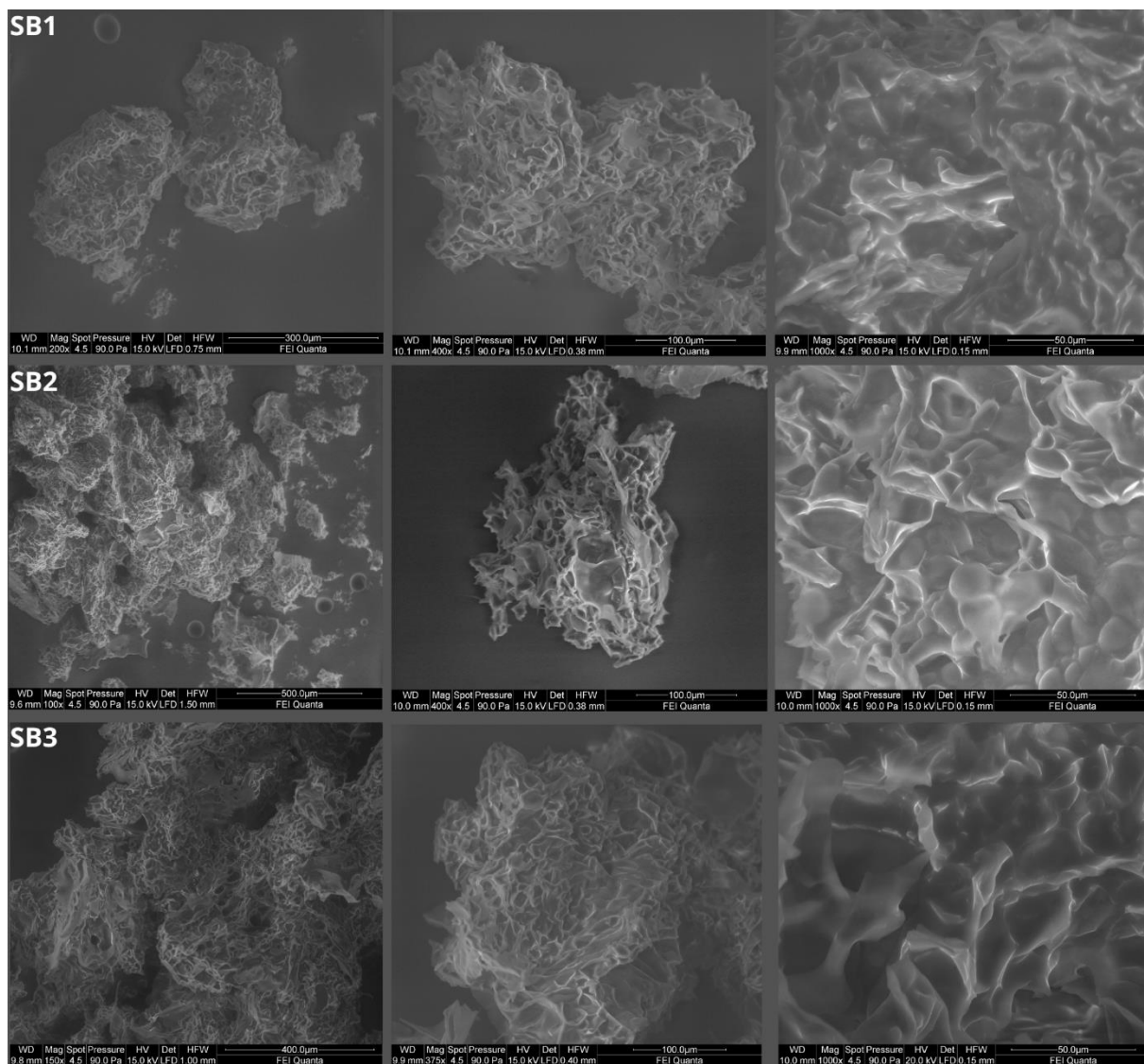
**= $p \leq 0,001$;

NS - brak istotnego wpływu = $p > 0,05$

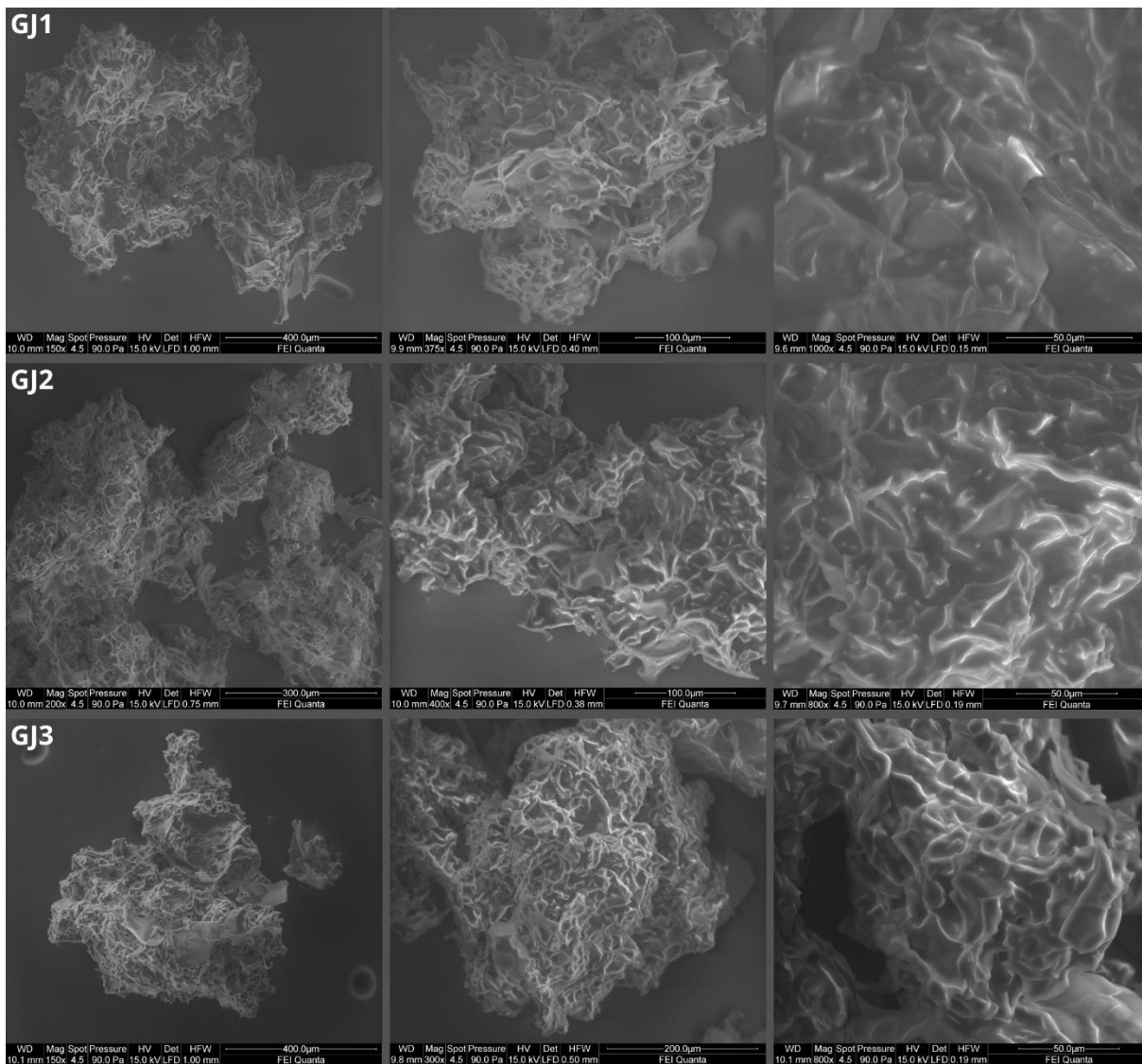
Niską wydajność enkapsulacji (42,7-64,09%) można wyjaśnić opisując morfologię otrzymanych mikrokapsulek – na rycinach 2-5 przedstawiono obrazy SEM. Otrzymany proszek charakteryzował się nieregularną, bardzo porowatą strukturą z dość rozwiniętą powierzchnią, co sugeruje, że materiał rdzeniowy nie został całkowicie pokryty. Zwiększona powierzchnia właściwa może prowadzić do większej interakcji z otoczeniem, co może sprzyjać wyciekom lub stratom materiału rdzeniowego (Marfil i wsp. 2018). Dodatkowo, wysoce porowata powierzchnia mikrokapsulek może ułatwiać parowanie olejku eterycznego zarówno jeszcze podczas liofilizacji, jak i podczas przechowywania.



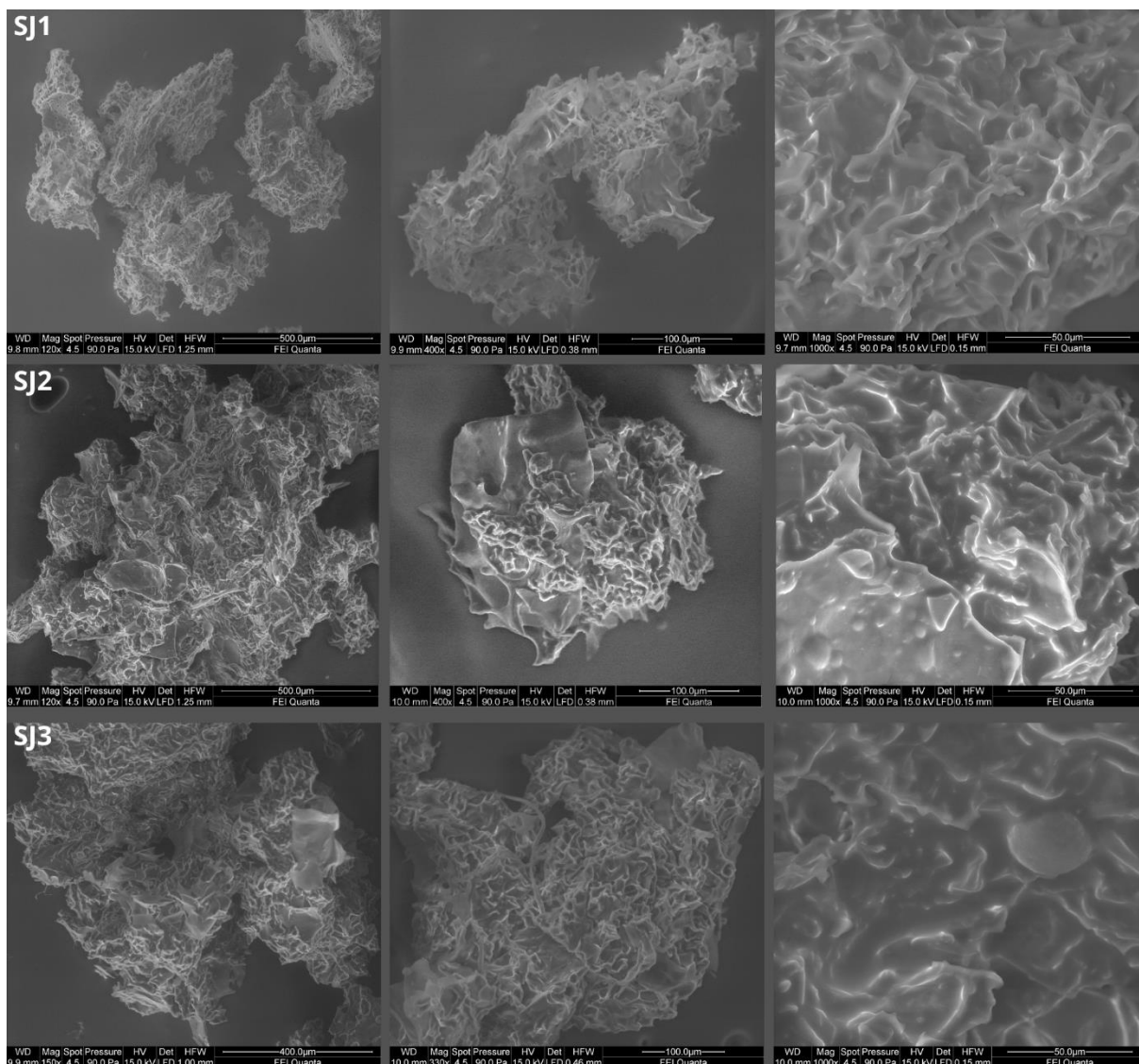
Ryc. 2: Obrazy SEM dla próbek **GB1** – próbka zawierająca żelatynę i gumę arabską w proporcji 1:1, olej z pestek winogron oraz olejek eteryczny z czarnego pieprzu, powiększenie odpowiednio: 150x, 400x i 1000x; **GB2** – próbka zawierająca żelatynę i gumę arabską w proporcji 1:2, olej z pestek winogron oraz olejek eteryczny z czarnego pieprzu, powiększenie odpowiednio: 150x, 250x i 1000x; **GB3** – próbka zawierająca żelatynę i gumę arabską w proporcji 2:1, olej z pestek winogron oraz olejek eteryczny z czarnego pieprzu, powiększenie odpowiednio: 150x, 250x i 800x



Ryc. 3: Obrazy SEM dla próbek **SB1** – próbka zawierająca żelatynę i gumę arabską w proporcji 1:1, olej sojowy oraz olejek eteryczny z czarnego pieprzu, powiększenie odpowiednio: 200x, 400x i 1000x; **SB2** – próbka zawierająca żelatynę i gumę arabską w proporcji 1:2, olej sojowy oraz olejek eteryczny z czarnego pieprzu, powiększenie odpowiednio: 100x, 400x i 1000x ; **SB3** – próbka zawierająca żelatynę i gumę arabską w proporcji 2:1, olej z pestek winogron oraz olejek eteryczny z czarnego pieprzu, powiększenie odpowiednio: 150x, 375x i 1000x



Ryc. 4: Obrazy SEM dla próbek **GJ1** – próbka zawierająca żelatynę i gumę arabską w proporcji 1:1, olej z pestek winogron oraz olejek eteryczny z jałowca, powiększenie odpowiednio: 150x, 375x i 1000x; **GJ2** – próbka zawierająca żelatynę i gumę arabską w proporcji 1:2, olej z pestek winogron oraz olejek eteryczny z jałowca, powiększenie odpowiednio: 200x, 400x i 800x ; **GJ3** – próbka zawierająca żelatynę i gumę arabską w proporcji 2:1, olej z pestek winogron oraz olejek eteryczny z jałowca, powiększenie odpowiednio: 150x, 300x i 800x



Ryc. 5: Obrazy SEM dla próbek **SJ1** – próbka zawierająca żelatynę i gumę arabską w proporcji 1:1, olej sojowy oraz olejek eteryczny z jałowca, powiększenie odpowiednio: 120x, 400x i 1000x; **SJ2** – próbka zawierająca żelatynę i gumę arabską w proporcji 1:2, olej sojowy oraz olejek eteryczny z jałowca, powiększenie odpowiednio: 120x, 400x i 1000x ; **SJ3** – próbka zawierająca żelatynę i gumę arabską w proporcji 2:1, olej sojowy oraz olejek eteryczny z jałowca, powiększenie odpowiednio: 150x, 330x i 1000x

Wykorzystanie koacerwacji złożonej pomiędzy białkami roślinnymi a gumą arabską do mikrokapsułkowania olejków eterycznych.

Wykorzystanie białka owsianego

Celem pracy była weryfikacja hipotezy 1: Białka roślinne mogą stanowić alternatywę dla żelatyny w procesie koacerwacji złożonej oraz hipotezy 2: Białka roślinne są równie skuteczne w mikrokapsułkowaniu olejków eterycznych, co żelatyna poprzez zastąpienie żelatyny białkiem grochowym. Dodatkowo ocenie poddano wpływ dodatku emulgatora na proces koacerwacji i właściwości otrzymanych mikrokapsulek.

Wpływ dodatku emulgatora na proces koacerwacji złożonej był niewątpliwie zauważalny (Tab. 2). Próbki zawierające Tween 80 charakteryzowały się wyższymi wartościami CY (najwyższe wartości: SBT2 = 92,40; SJT2 = 82,12; SJT1 = 95,34) w porównaniu do próbek bez emulgatora. Odwrotna sytuacja miała miejsce w przypadku parametrów SY i EE, gdzie wyższe wartości uzyskano dla próbek bez emulgatora. Najwyższe wartości tych parametrów osiągnęła próbka GJ1 (SY = 25,43; EE = 67%). Analiza statystyczna wykazała, że stosunek białka grochu do gumy arabskiej miał statystycznie mniej istotny wpływ na uzyskane wyniki ($p \leq 0,05$) niż dodatek emulgatora ($p \leq 0,001$). Dodatek emulgatora spowodował, co najmniej dwukrotne zmniejszenie uzyskanych wartości CY, SY i EE w porównaniu do próbek bez jego udziału. Wzajemny stosunek materiałów ściennych oraz interakcje między tymi czynnikami były statystycznie nieistotne.

Powyższe można wyjaśnić właściwościami emulgującymi Tween 80 – woda była dobrze włączana do struktury emulsji, a następnie łatwo uwalniana w procesie koacerwacji. To skutkowało wyższymi wartościami CY (ze względu na lepszą stabilność emulsji) i niższymi wartościami SY (z powodu odparowania niezwiązanej wody podczas procesu liofilizacji). Te obserwacje zostały potwierdzone wynikami dotyczącymi zawartości wody w próbkach (umieszczone w oryginalnym artykule). Niższe wartości EE dla próbek bez Tween 80 można wyjaśnić zbyt wysokim stosunkiem materiału rdzeniowego do emulgatora, co spowodowało zemulgowanie tylko części oleju zawartego w próbce (Xiao i wsp. 2016).

W porównaniu do wyników zawartych w pracy nr 2, nie zaobserwowano istotnych różnic w wartościach CY, SY ani EE, faworyzujących żelatynę lub białko grochu. Podobieństwo tych parametrów sugeruje, że oba materiały wykazują porównywalną wydajność w zakresie enkapsulacji i powiązanych cech, podkreślając ich potencjalną wymiennność.

Tab. 2: Wydajność koacerwacji (CY), wydajność mikrokapsułkowania (SY), efektywność kapsułkowania (EE) [%]

Próbka	CY	SY	EE
GJT1	76.10±3.02 ^{bB}	12.21±3.02 ^{bB}	0.21±0.11 ^{aA}
GJT2	65.53±2.09 ^{aB}	7.13±2.09 ^{aA}	0.20±0.16 ^{aA}
GJT3	37.16±0.25 ^{bA}	11.48±0.25 ^{aA}	0.34±0.17 ^{aA}
GJ1	34.31±1.13 ^{aA}	25.43±1.13 ^{bA}	0.67±0.07 ^{aA}
GJ2	24.21±2.37 ^{aA}	27.60±2.37 ^{aB}	0.41±0.43 ^{aA}

GJ3	38.74±0.76 ^{bA}	21.50±0.76 ^{aA}	0.33±0.01 ^{aA}
GBT1	42.75±0.91 ^{bA}	10.00±1.00 ^{bB}	0.18±0.02 ^{aA}
GBT2	69.85±0.95 ^{aA}	11.95±0.95 ^{abB}	0.23±0.20 ^{aA}
GBT3	55.55±0.97 ^{aA}	8.71±0.97 ^{bB}	0.28±0.01 ^{aA}
GB1	35.11±0.40 ^{aB}	24.79±0.40 ^{abA}	0.39±0.01 ^{aA}
GB2	29.94±0.73 ^{cB}	22.97±0.73 ^{bA}	0.38±0.12 ^{aA}
GB3	31.07±0.97 ^{bB}	20.68±0.97 ^{aA}	0.56±0.01 ^{aA}
SJT1	95.34±1.77 ^{bB}	6.61±1.77 ^{aB}	0.30±7.14 ^{aB}
SJT2	82.12±1.57 ^{aA}	6.14±1.57 ^{aB}	0.30±0.45 ^{aB}
SJT3	40.05±1.68 ^{aA}	9.45±1.68 ^{aB}	0.18±0.03 ^{aA}
SJ1	41.98±0.96 ^{cA}	20.86±0.96 ^{aA}	0.51±0.24 ^{aA}
SJ2	28.91±1.17 ^{bB}	21.17±1.17 ^{aA}	0.60±0.12 ^{aA}
SJ3	31.04±2.60 ^{aB}	24.59±2.6 ^{bA}	0.58±0.19 ^{aA}
SBT1	42.44±0.88 ^{bA}	9.04±0.88 ^{aB}	0.35±0.10 ^{aA}
SBT2	92.40±1.38 ^{aB}	6.45±1.38 ^{aB}	0.31±10.23 ^{aA}
SBT3	67.04±2.64 ^{cA}	6.40±2.64 ^{aB}	0.29±0.04 ^{aA}
SB1	36.04±3.45 ^{aB}	23.33±3.45 ^{bA}	0.64±0.09 ^{aA}
SB2	32.35±1.73 ^{cA}	23.23±1.73 ^{aA}	0.44±0.85 ^{aA}
SB3	44.93±0.28 ^{bB}	21.69±0.28 ^{aA}	0.48±0.18 ^{aA}
S.E.M.	166.8	6.41	0.02755
Efekt			
MR	*	NS	NS
T	**	**	**
MR*T	**	NS	NS

GJ1, GJ2, GJ3 – próbki zawierające żelatynę i gumę arabską w proporcji odpowiednio 1:1; 1:2; 2:1, olej z pestek winogron oraz olejek eteryczny z jałowca; **GB1, GB2, GB3** – próbki zawierające żelatynę i gumę arabską w proporcji odpowiednio 1:1; 1:2; 2:1, olej z pestek winogron oraz olejek eteryczny z czarnego pieprzu; **SJ1, SJ2, SJ3** – próbki zawierające żelatynę i gumę arabską w proporcji odpowiednio 1:1; 1:2; 2:1, olej sojowy oraz olejek eteryczny z jałowca; **SB1, SB2, SB3** – próbki zawierające żelatynę i gumę arabską w proporcji odpowiednio 1:1; 1:2; 2:1, olej sojowy oraz olejek eteryczny z czarnego pieprzu. **GJT1, GTJ2, GJT3** – próbki zawierające żelatynę i gumę arabską w proporcji odpowiednio 1:1; 1:2; 2:1, olej z pestek winogron, olejek eteryczny z jałowca oraz emulgator Tween 80; **GBT1, GBT2, GBT3** – próbki zawierające żelatynę i gumę arabską w proporcji odpowiednio 1:1; 1:2; 2:1, olej z pestek winogron, olejek eteryczny z czarnego pieprzu oraz emulgator Tween 80; **SJT1, SJT2, SJT3** – próbki zawierające żelatynę i gumę arabską w proporcji odpowiednio 1:1; 1:2; 2:1, olej sojowy, olejek eteryczny z jałowca oraz emulgator Tween 80; **SBT1, SBT2, SBT3** – próbki zawierające żelatynę

i gumę arabską w proporcji odpowiednio 1:1; 1:2; 2:1, olej sojowy, olejek eteryczny z czarnego pieprzu oraz emulgator Tween 80.

Wyniki w tej tabeli są wyrażone jako średnia \pm odchylenie standardowe. Średnie wartości oznaczone tymi samymi indeksami górnymi w obrębie wiersza nie różnią się istotnie przy $p \leq 0,05$.

S.E.M. – błąd standardowy średniej

*** = $p \leq 0,001$;

NS - brak istotnego wpływu = $p > 0,05$

Ciekawych wniosków dostarczyło badanie zachowania właściwości termicznych uzyskanych mikrokapsulek podczas ogrzewania w zakresie temperatur od 20°C do 230°C.

Tabela 3 przedstawia temperaturę początku, szczytu i końca reakcji endotermicznej, wraz z entalpią towarzyszącą tym zmianom. Próbkki bez emulgatora wykazały pojedynczą reakcję endotermiczną, przy czym temperatura początku reakcji wykazywała wyraźną zależność od MR. Co ciekawe, próbki zawierające większy udział białka grochu wykazywały zwiększoną stabilność termiczną. Wśród próbek bez emulgatora, SB1, SB2 i SB3 okazały się najbardziej odporne na podwyższone temperatury, z wartościami T_{on} w kolejności 137,21°C, 149,59°C i 162,35°C, wartościami T_{max} 138,33°C, 156,29°C i 163,53°C, oraz wartościami T_{end} 139,86°C, 178,18°C i 166,12°C, odpowiednio. Warto zauważyć, że SB2 wykazało najmniej dynamiczną reakcję. Wprowadzenie Tween 80 spowodowało dwie endotermiczne transformacje we wszystkich próbkach, a dodatek emulgatora znacznie obniżył T_{on} (dla pierwszej reakcji) w porównaniu do odpowiedników bez emulgatora.

Porównując te wyniki z naszymi wcześniejszymi badaniami zawartymi w pracy nr 2 wyłania się istotna tendencja – użycie białka grochu zamiast żelatyny prowadziło do poprawy stabilności termicznej mikrokapsulek.

Tab. 3: Wyniki analizy DSC, temperatura rozpoczęcia (T_{on}), temperatura szczytowa (T_{max}) i temperatura końcowa reakcji endotermicznej (T_{end}) wraz z towarzyszącą entalpią (ΔH)

Próbka	T_{on}	T_{max}	T_{end}	ΔH
GJT1	42.69 \pm 0.001	53.46 \pm 0.001	60.64 \pm 0.001	-25.14 \pm 0.001
	113.05 \pm 0.001	135.88 \pm 0.001	170.43 \pm 0.001	-559.32 \pm 0.001
GJT2	41.17 \pm 0.001	51.78 \pm 0.001	59.22 \pm 0.002	-28.75 \pm 0.001
	87.51 \pm 0.002	126.52 \pm 0.002	162.25 \pm 0.001	-581.48 \pm 0.001

GJT3	40.36±0.002	52.29±0.001	61.94±0.002	-37.59±0.001
	100.16±0.002	133.71±0.002	166.56±0.002	-382.50±0.001
GJ1	54.22±0.001	108.04±0.001	147.05±0.002	-698.4±0.002
GJ2	97.28±0.001	125.53±0.002	142.99±0.001	-624.34±0.002
GJ3	114.53±0.002	129.31±0.001	151.12±0.001	-533.84±0.001
GBT1	39.41±0.002	50.31±0.001	58.58±0.002	-30.46±0.001
	142.67±0.002	163.54±0.001	190.47±0.001	-348.33±0.001
GBT2	43.45±0.001	52.45±0.001	57.86±0.002	-12.44±0.002
	161.00±0.002	162.10±0.001	164.92±0.001	-407.63±0.002
GBT3	36.52±0.001	50.11±0.001	61.99±0.001	-27.95±0.001
	146.13±0.001	167.46±0.002	194.06±0.001	-538.82±0.001
GB1	71.98±0.001	118.72±0.002	164.97±0.002	-706.35±0.001
GB2	78.51±0.001	125.52±0.001	166.18±0.001	-759.67±0.001
GB3	97.63±0.002	98.61±0.001	99.98±0.001	-1.30±0.001
SJT1	41.89±0.002	52.45±0.001	59.38±0.002	-26.49±0.001
	121.98±0.002	137.02±0.001	159.89±0.002	-384.84±0.001
SJT2	31.21±0.001	42.11±0.002	50.20±0.002	-16.07±0.002
	101.12±0.001	129.97±0.002	157.38±0.001	-23.18±0.001
SJT3	32.86±0.001	43.80±0.001	53.09±0.001	-12.78±0.001
	81.85±0.001	128.41±0.001	149.81±0.001	-287.60±0.002
SJ1	69.44±0.001	117.71±0.001	157.23±0.001	-700.80±0.001
SJ2	117.21±0.001	135.84±0.001	159.13±0.002	-582.43±0.001
SJ3	146.79±0.001	155.17±0.001	176.31±0.001	-740.17±0.001
SBT1	41.55±0.002	51.93±0.002	59.08±0.002	-18.35±0.002
	143.75±0.001	149.58±0.001	150.44±0.001	-609.94±0.002
SBT2	37.13±0.001	50.44±0.001	57.91±0.001	-23.37±0.001
	117.83±0.001	157.97±0.001	190.42±0.002	-684.03±0.001
SBT3	38.87±0.002	50.94±0.001	59.35±0.001	-24.48±0.001
	134.53±0.001	167.33±0.002	200.93±0.001	-455.58±0.002
SB1	137.21±0.001	138.33±0.001	139.86±0.001	-15.43±0.001
SB2	149.59±0.002	156.29±0.002	178.18±0.001	-349.79±0.002
SB3	162.35±0.001	163.53±0.002	166.12±0.002	-549.57±0.002

GJ1, GJ2, GJ3 – próbki zawierające żelatynę i gumę arabską w proporcji odpowiednio 1:1; 1:2; 2:1, olej z pestek winogron oraz olejek eteryczny z jałowca; **GB1, GB2, GB3** – próbki zawierające żelatynę i gumę arabską

w proporcji odpowiednio 1:1; 1:2; 2:1, olej z pestek winogron oraz olejek eteryczny z czarnego pieprzu; **SJ1, SJ2, SJ3** – próbki zawierające żelatynę i gumę arabską w proporcji odpowiednio 1:1; 1:2; 2:1, olej sojowy oraz olejek eteryczny z jałowca; **SB1, SB2, SB3** – próbki zawierające żelatynę i gumę arabską w proporcji odpowiednio 1:1; 1:2; 2:1, olej sojowy oraz olejek eteryczny z czarnego pieprzu. **GJT1, GTJ2, GJT3** – próbki zawierające żelatynę i gumę arabską w proporcji odpowiednio 1:1; 1:2; 2:1, olej z pestek winogron, olejek eteryczny z jałowca oraz emulgator Tween 80; **GBT1, GBT2, GBT3** – próbki zawierające żelatynę i gumę arabską w proporcji odpowiednio 1:1; 1:2; 2:1, olej z pestek winogron, olejek eteryczny z czarnego pieprzu oraz emulgator Tween 80; **SJT1, SJT2, SJT3** – próbki zawierające żelatynę i gumę arabską w proporcji odpowiednio 1:1; 1:2; 2:1, olej sojowy, olejek eteryczny z jałowca oraz emulgator Tween 80; **SBT1, SBT2, SBT3** – próbki zawierające żelatynę i gumę arabską w proporcji odpowiednio 1:1; 1:2; 2:1, olej sojowy, olejek eteryczny z czarnego pieprzu oraz emulgator Tween 80.

Wykorzystanie białka grochowego

Celem pracy była weryfikacja hipotezy 1: Białka roślinne mogą stanowić alternatywę dla żelatyny w procesie koacerwacji złożonej oraz hipotezy 2: Białka roślinne są równie skuteczne w mikrokapsułkowaniu olejków eterycznych co żelatyna poprzez zastąpienie żelatyny białkiem owsianym (OP). Proces został zoptymalizowany przy użyciu metody analizy powierzchni odpowiedzi (RSM) zgodnie z wcześniejszym opisem.

Wydajność mikrokapsułkowania (SY) mieściła się w zakresie od 8,64% do 9,29% i była istotnie ($p \leq 0,05$) zależna od pH w sposób kwadratowy, co obniżało wartości SY. Skuteczność kapsułkowania mieściła się w zakresie od 23,39% do 26,46% i była znacząco uzależniona od zawartości OP w sposób kwadratowy, co obniżało skuteczność kapsułkowania. Najwyższą EE uzyskano dla próbki 4 (71:29, pH=5,4), a najniższą dla próbki 7 (20:80, pH=4) (Tab. 4, Ryc. 6).

Wartości SY i EE były niskie, co można przypisać ograniczonym interakcjom między OP i GA. Sieci koacerwatów tworzą się, gdy interakcje białko-polisacharyd są korzystne (Napiórkowska i Kurek, 2022; Nieto-Nieto i in., 2015; Nieto-Nieto i in., 2016). Kompleksowanie białka i polisacharydu zależy od pH i stosunku mieszania biopolimerów. pH odgrywa kluczową rolę w kontrolowaniu stopnia jonizacji grup funkcyjnych takich jak $-NH_2$ i $-COOH$, które są obecne w użytych materiałach ściennych. Reguluje również siłę oddziaływań elektrostatycznych w kompleksie. Z drugiej strony, proporcje mieszania biopolimerów wpływają na rozkład ładunków elektrycznych, wpływając na równowagę ładunków i oddziaływania elektrostatyczne (Naderi i in., 2020). Innym czynnikiem wpływającym na skuteczność kapsułkowania jest wybór materiału kapsułkującego oraz rodzaj materiału rdzeniowego, w tym konkretnego olejku

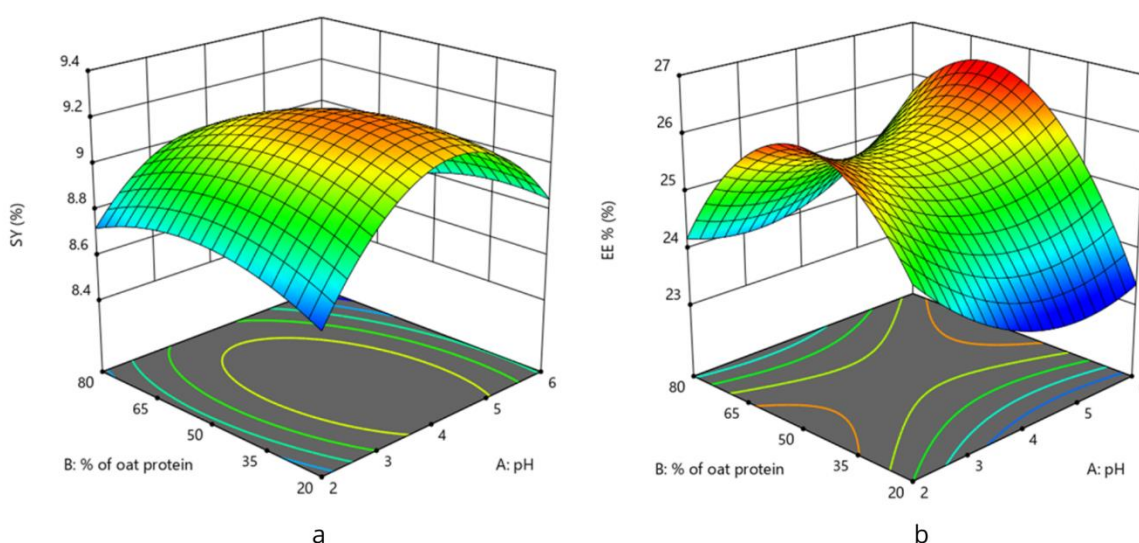
eterycznego. Połączenie różnych materiałów ściennych może skutkować zwiększeniem wartości EE dla tego samego materiału rdzenia w porównaniu do wartości EE otrzymywanych przy użyciu tych samych materiałów ściennych pojedynczo (Alvarez-Henao i wsp. 2018). Ponadto, zamiana materiału rdzeniowego (np. wybór innego olejku eterycznego) może spowodować wzrost lub spadek EE przy zastosowaniu tych samych materiałów ściennych i parametrów wytwarzania mikrokapsulek (Bringas-Lantigua i wsp. 2011; Bajac i in., 2022).

Tab. 4: Wydajność mikrokapsułkowania (SY) [%], efektywność kapsułkowania (EE) [%]

Podejście	Próbka	SY	EE
1	CS1	9.27 ^f ±0.002	25.65 ^a ±0.280
2	1S	8.89 ^c ±0.023	25.07 ^a ±5.650
3	2S	9.01 ^d ±0.002	26.30 ^a ±1.960
4	3S	8.64 ^a ±0.023	26.46 ^a ±5.520
5	4S	9.31 ^f ±0.002	23.46 ^a ±0.230
6	5S	9.04 ^d ±0.007	24.58 ^a ±0.800
7	6S	9.17 ^e ±0.023	23.39 ^a ±0.960
8	CS2	9.42 ^f ±0.003	25.69 ^a ±0.140
9	CS3	9.31 ^f ±0.072	25.71 ^a ±0.310
10	CS4	9.36 ^e ±0.008	26.05 ^a ±0.420
11	CS5	9.59 ^e ±0.001	25.13 ^a ±0.232
12	7S	8.91 ^c ±0.009	25.91 ^a ±4.160
13	8S	8.69 ^b ±0.012	25.43 ^a ±3.760
Współczynnik regresji			
	Model	9.23	25.62**
	A – pH	-0.0057	-0.001
	B – zawartość białka owsianego	-0.0514	0.2919
	AB	-0.05	0.3772
	A ²	-0.2046*	0.3977*
	B ²	-0.0662	-0.9436***
	R ²	0.995	0.997
	Brak dopasowania	0.787	0.206

CS1-5 – próbka centralna zawierająca 50% białka owsianego i 50% gumy arabskiej, olej z zarodków pszennych oraz olejek eteryczny z jałowca, otrzymana przy pH=4; **1S** – próbka zawierająca 29% białka owsianego i 71%

gumy arabskiej, olej z zarodków pszennych oraz olejek eteryczny z jałowca, otrzymana przy pH=2.6; **2S** – próbka zawierająca 50% białka owsianego i 50% gumy arabskiej, olej z zarodków pszennych oraz olejek eteryczny z jałowca, otrzymana przy pH=2.0; **3S** – próbka zawierająca 71% białka owsianego i 29% gumy arabskiej, olej z zarodków pszennych oraz olejek eteryczny z jałowca, otrzymana przy pH=5.4; **4S** – próbka zawierająca 80% białka owsianego i 20% gumy arabskiej, olej z zarodków pszennych oraz olejek eteryczny z jałowca, otrzymana przy pH=4.0; **5S** – próbka zawierająca 29% białka owsianego i 71% gumy arabskiej, olej z zarodków pszennych oraz olejek eteryczny z jałowca, otrzymana przy pH=5.4; **6S** – próbka zawierająca 20% białka owsianego i 80% gumy arabskiej, olej z zarodków pszennych oraz olejek eteryczny z jałowca, otrzymana przy pH=4.0; **7S** – próbka zawierająca 50% białka owsianego i 50% gumy arabskiej, olej z zarodków pszennych oraz olejek eteryczny z jałowca, otrzymana przy pH=6.0; **8S** – próbka zawierająca 71% białka owsianego i 29% gumy arabskiej, olej z zarodków pszennych oraz olejek eteryczny z jałowca, otrzymana przy pH=2.6.



Ryc. 6: Powierzchnia odpowiedzi dla (a) wydajności mikroksułowania (SY), (b) efektywności ksułowania (EE)

Analiza skaningowej kalorymetrii różnicowej (DSC) została przeprowadzona w celu oceny stabilności termicznej uzyskanych mikroksułowek.

Wszystkie badane próbki wykazały jedną reakcję endotermiczną (Tab. 5), wskazując na proces absorpcji ciepła podczas fazy grzania. Szczególnie wrażliwe na temperaturę były próbki CS1-5, 1S i 5S, z temperaturami T_{on} w zakresie 56,51-56,69°C, 47,64°C i 63,58°C. Interesujące jest to, że próbki 1S i 5S miały identyczny stosunek OP/GA (29:71), ale różne wartości pH (2,6 i 5,4). W przeciwieństwie do nich, pozostałe próbki wykazały odporność na temperatury przekraczające 115°C.

Próbka 2S (OP/GA = 50:50, pH = 2) charakteryzowała się szczególnie wyższą stabilnością termiczną. Zarejestrowane parametry to $T_{on}=179,20^{\circ}\text{C}$, $T_{max}=180,15^{\circ}\text{C}$, $T_{end}=182,37^{\circ}\text{C}$ i $\Delta H=-721,91$ mJ. Pomimo identycznego stosunku OP/GA z próbkami CS1-5, te ostatnie wykazały znacznie niższą stabilność termiczną, z $T_{on}=56,53^{\circ}\text{C}$. Ta rozbieżność podkreśla istotny wpływ pH, uwydatniając jego kluczową rolę w kształtowaniu właściwości końcowych produktu.

Tab. 5: Wyniki analizy DSC, temperatura rozpoczęcia (T_{on}), temperatura szczytowa (T_{max}) i temperatura końcowa reakcji endotermicznej (T_{end}) wraz z towarzyszącą entalpią (ΔH)

Podejście	Próbka	T_{on}	T_{max}	T_{end}	ΔH
1	CS1	56.53	114.23	155.16	-450.9
2	1S	47.64	92.58	131.67	-451.55
3	2S	179.20	180.15	182.37	-721.91
4	3S	126.98	148.91	162.19	-425.14
5	4S	176.54	177.98	183.23	-145.92
6	5S	63.58	117.22	163.71	-605.24
7	6S	119.98	136.21	165.78	-504.56
8	CS2	56.55	114.74	155.18	-451.94
9	CS3	56.69	115.00	154.86	-444.17
10	CS4	56.61	114.23	155.20	-450.30
11	CS5	56.51	114.23	155.60	-452.19
12	7S	163.87	164.84	168.20	-134.17
13	8S	147.10	148.08	148.92	-320.51

CS1-5 – próbka centralna zawierająca 50% białka owsianego i 50% gumy arabskiej, olej z zarodków pszennych oraz olejek eteryczny z jałowca, otrzymana przy pH=4; **1S** – próbka zawierająca 29% białka owsianego i 71% gumy arabskiej, olej z zarodków pszennych oraz olejek eteryczny z jałowca, otrzymana przy pH=2.6; **2S** – próbka zawierająca 50% białka owsianego i 50% gumy arabskiej, olej z zarodków pszennych oraz olejek eteryczny z jałowca, otrzymana przy pH=2.0; **3S** – próbka zawierająca 71% białka owsianego i 29% gumy arabskiej, olej z zarodków pszennych oraz olejek eteryczny z jałowca, otrzymana przy pH=5.4; **4S** – próbka zawierająca 80% białka owsianego i 20% gumy arabskiej, olej z zarodków pszennych oraz olejek eteryczny z jałowca, otrzymana przy pH=4.0; **5S** – próbka zawierająca 29% białka owsianego i 71% gumy arabskiej, olej z zarodków pszennych oraz olejek eteryczny z jałowca, otrzymana przy pH=5.4; **6S** – próbka zawierająca 20% białka owsianego i 80% gumy arabskiej, olej z zarodków pszennych oraz olejek eteryczny z jałowca, otrzymana przy pH=4.0; **7S** – próbka zawierająca 50% białka owsianego i 50% gumy arabskiej, olej z zarodków pszennych oraz olejek eteryczny z jałowca, otrzymana przy pH=6.0; **8S** – próbka zawierająca 71% białka owsianego i 29% gumy arabskiej, olej z zarodków pszennych oraz olejek eteryczny z jałowca, otrzymana przy pH=2.6

Podsumowując badania publikacji 2, wyraźnie wskazują na obecność interakcji między składnikami mikrokapsulek, co przyczyniło się do znacznego zwiększenia odporności termicznej w porównaniu do poszczególnych składników. Wyraźne różnice między próbkami, szczególnie pod względem pH, podkreślają kluczową rolę tego parametru w określaniu właściwości końcowych mikrokapsulek. Zwraca to uwagę na znaczenie uwzględnienia pH w projektowaniu i produkcji mikrokapsulek w celu osiągnięcia pożądanych właściwości.

Wykorzystanie koacerwacji złożonej pomiędzy białkiem bobowym a polisacharydami wyizolowanymi z nasion chia do mikrokapsułkowania olejków eterycznych

W pracy weryfikowano hipotezę nr 3: Zamiana gumy arabskiej na polisacharydy z nasion chia może zwiększyć efektywność kapsułkowania olejków eterycznych. W pracy zastosowano białko bobowe (FB) oraz polisacharydy wyizolowane z nasion chia (CHP).

Analiza statystyczna wykazała, że MR nie miał istotnego wpływu na efektywność produkcji mikrokapsulek (SY), której wartości wynosiły od 48,64% do 49,31% we wszystkich wariantach (Tab. 6). Próbkę RB1 charakteryzowała najniższą efektywność, podczas gdy próbka RB2 osiągnęła najwyższą.

Pod względem efektywności kapsułkowania, wartości mieściły się w zakresie od 65,64% do 87,85% (Tab. 6). Próbka RB2 wykazała najwyższą efektywność kapsułkowania, co było zgodne z jej lepszymi wynikami w produkcji mikrokapsulek. Próbki o stosunku FB/CHP równym 1:2 konsekwentnie wykazywały wyższą efektywność kapsułkowania w porównaniu do tych z innymi wartościami MR.

Tab. 6: Wydajność mikrokapsułkowania (SY), efektywność kapsułkowania (EE) [%]

Próbka	SY	EE
RJ1	49.27±0.00 ^a	83.23±6.99 ^{ab}
RJ2	48.89±0.02 ^c	84.61±6.68 ^{abc}
RJ3	49.01±0.00 ^b	74.39±6.60 ^{ab}
RB1	48.64±0.02 ^d	76.04±6.35 ^b
RB2	49.31±0.00 ^f	87.85±4.71 ^{ac}
RB3	49.04±0.01 ^g	77.08±3.21 ^{abc}
SJ1	49.17±0.02 ^c	79.49±7.25 ^{ab}

	SJ2	49.27±0.00 ^c	85.11±6.92 ^c
	SJ3	49.29±0.01 ^a	74.54±4.28 ^{ab}
	SB1	49.18±0.02 ^h	65.64±6.45 ^{ab}
	SB2	49.13±0.02 ^a	82.42±7.30 ^{ac}
	SB3	48.91±0.01 ^b	80.00±4.52 ^{ab}
	S.E.M	0.00	54.0
Efekt			
	Olej	**	NS
	MR	**	*
	EO	**	NS
	Olej*MR	**	NS
	Olej*EO	**	NS
	MR*EO	**	*
	Olej*MR*EO	**	NS

RJ1, RJ2, RJ3 – próbki zawierające białko bobowe i polisacharydy z nasion chia w proporcji odpowiednio 1:1; 1:2; 2:1, olej rzepakowy oraz olejek eteryczny z jałowca; **RB1, RB2, RB3** – próbki zawierające białko bobowe i polisacharydy z nasion chia w proporcji odpowiednio 1:1; 1:2; 2:1, olej rzepakowy oraz olejek eteryczny z czarnego pieprzu; **SJ1, SJ2, SJ3** – próbki zawierające białko bobowe i polisacharydy z nasion chia w proporcji odpowiednio 1:1; 1:2; 2:1, olej sojowy oraz olejek eteryczny z jałowca; **SB1, SB2, SB3** – próbki zawierające białko bobowe i polisacharydy z nasion chia w proporcji odpowiednio 1:1; 1:2; 2:1, olej sojowy oraz olejek eteryczny z czarnego pieprzu.

Wyniki w tej tabeli są wyrażone jako średnia ± odchylenie standardowe. Średnie wartości oznaczone różnymi indeksami górnymi w obrębie wiersza różnią się istotnie przy $p \leq 0,05$.

S.E.M. – błąd standardowy średniej

** = $p \leq 0,001$;

NS - brak istotnego wpływu = $p > 0,05$

Analiza DSC miała na celu zbadanie właściwości cieplnych uzyskanych mikrokapsulek podczas ogrzewania w zakresie temperatur od 20°C do 230°C. Uzyskane wyniki przedstawiono w Tab. 7, a ich analiza ujawnia wyraźny wpływ MR na odporność cieplną produkowanych mikrokapsulek. We wszystkich wariantach widoczne jest, że temperatura inicjacji reakcji była najniższa przy FP:CHP= 2:1 i najwyższa przy FP:CHP= 1:2. Spośród wszystkich próbek, RB2 wykazało najwyższą stabilność termiczną ($T_{on}=177,52^{\circ}\text{C}$, $T_{max}=177,55^{\circ}\text{C}$, $T_{end}=181,40^{\circ}\text{C}$,

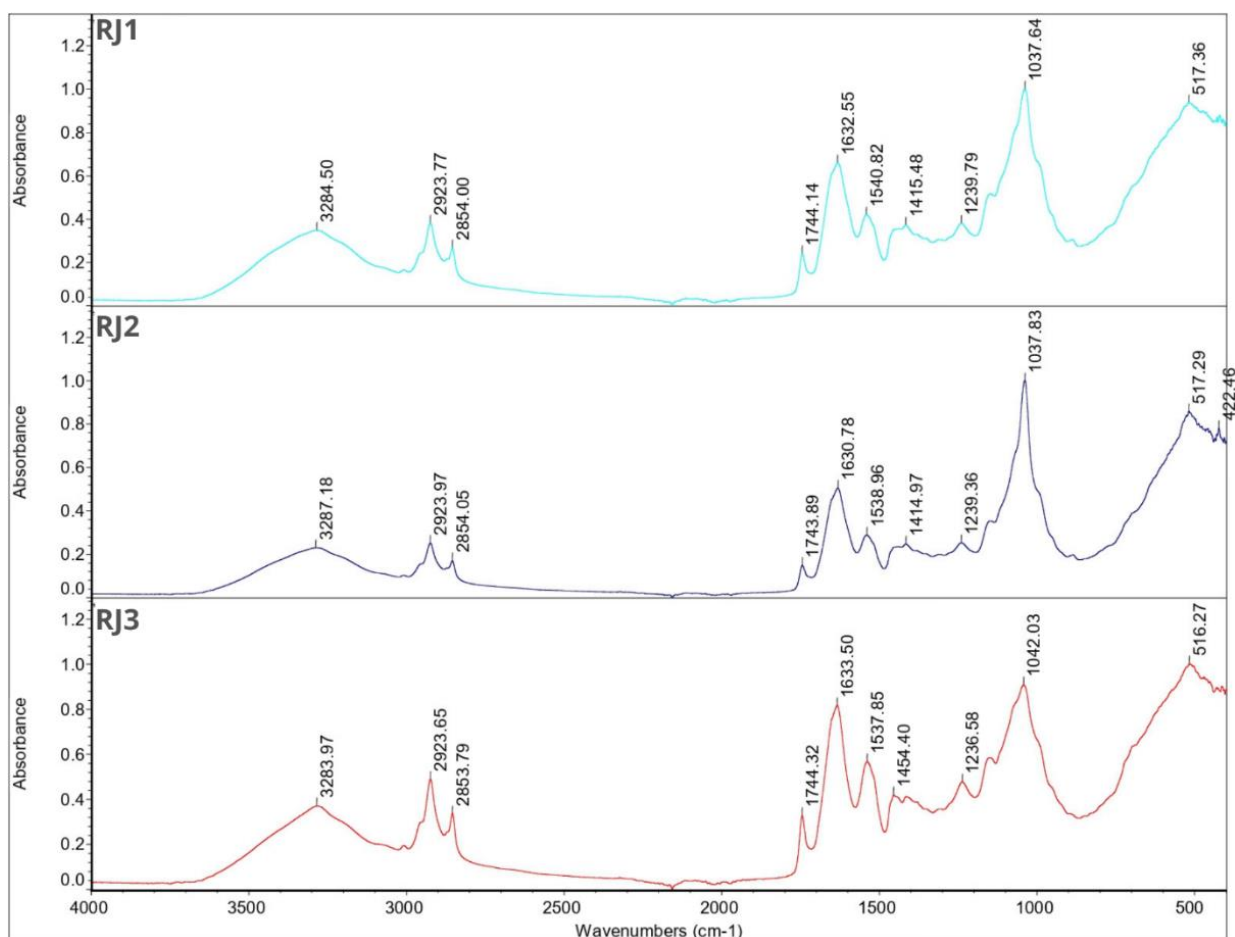
$\Delta H = -428,38$ mJ), podczas gdy SB3 wykazało najniższą stabilność termiczną ($T_{on} = 56,80^{\circ}\text{C}$, $T_{max} = 116,90^{\circ}\text{C}$, $T_{end} = 155,52^{\circ}\text{C}$, $\Delta H = -392,99$ mJ). Co ważne, temperatura inicjacji reakcji przekraczała T_{on} dla czystego białka bobu we wszystkich przypadkach, pozostając jednocześnie poniżej T_{on} dla CHP we wszystkich próbach. Podkreśla to interakcje między materiałami ścian mikrokapsulek, co zostało dodatkowo potwierdzone przez analizę FT-IR.

Tab. 7: Wyniki analizy DSC, temperatura rozpoczęcia (T_{on}), temperatura szczytowa (T_{max}) i temperatura końcowa reakcji endotermicznej (T_{end}) wraz z towarzyszącą entalpią (ΔH)

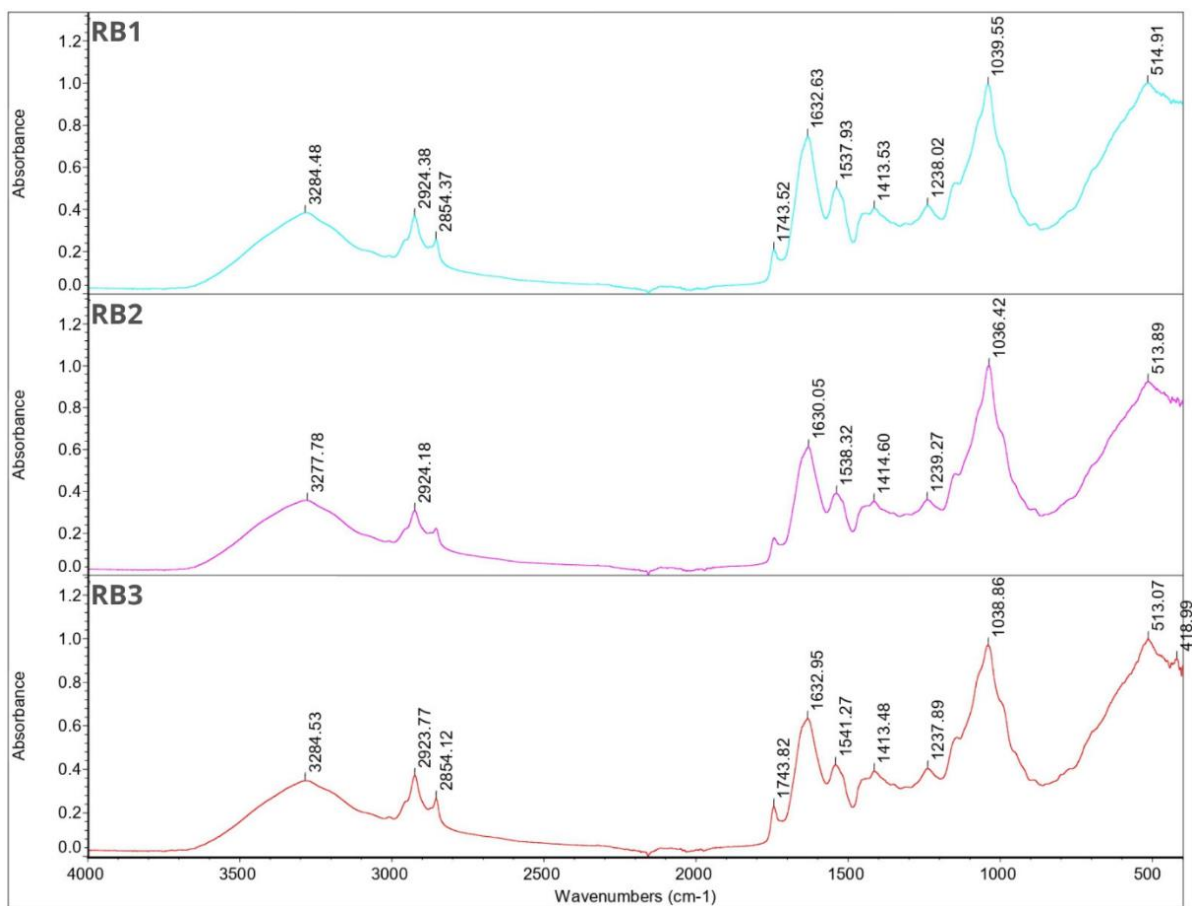
Próbka	T_{on}	T_{max}	T_{end}	ΔH
RJ1	122.81	133.79	156.11	-523.77
RJ2	154.70	173.79	195.12	-438.73
RJ3	87.01	132.08	157.47	-361.65
RB1	156.01	158.99	170.42	-120.11
RB2	177.52	177.55	181.40	-428.38
RB3	120.01	135.35	151.83	-376.06
SJ1	105.23	133.89	172.51	-398.25
SJ2	145.19	151.69	163.82	-413.72
SJ3	98.06	134.72	159.73	-369.17
SB1	128.33	128.58	174.08	-466.23
SB2	155.01	165.76	177.50	-490.12
SB3	56.80	116.90	155.52	-392.99
FB	48.97	63.60	76.94	-37.27
CHP	129.52	139.62	154.18	-9663.97
JEO	24.71	89.17	140.95	-80.00
BPO	26.81	97.10	148.11	-92.36
RSO	184.61	199.29	214.88	102.75
SBO	155.34	174.31	198.20	108.87
T80	116.40	138.82	154.42	58.61

RJ1, RJ2, RJ3 – próbki zawierające białko bobowe i polisacharydy z nasion chia w proporcji odpowiednio 1:1; 1:2; 2:1, olej rzepakowy oraz olejek eteryczny z jałowca; **RB1, RB2, RB3** – próbki zawierające białko bobowe i polisacharydy z nasion chia w proporcji odpowiednio 1:1; 1:2; 2:1, olej rzepakowy oraz olejek eteryczny z czarnego pieprzu; **SJ1, SJ2, SJ3** – próbki zawierające białko bobowe i polisacharydy z nasion chia w proporcji odpowiednio 1:1; 1:2; 2:1, olej sojowy oraz olejek eteryczny z jałowca; **SB1, SB2, SB3** – próbki zawierające białko bobowe i polisacharydy z nasion chia w proporcji odpowiednio 1:1; 1:2; 2:1, olej sojowy oraz olejek eteryczny z czarnego pieprzu.

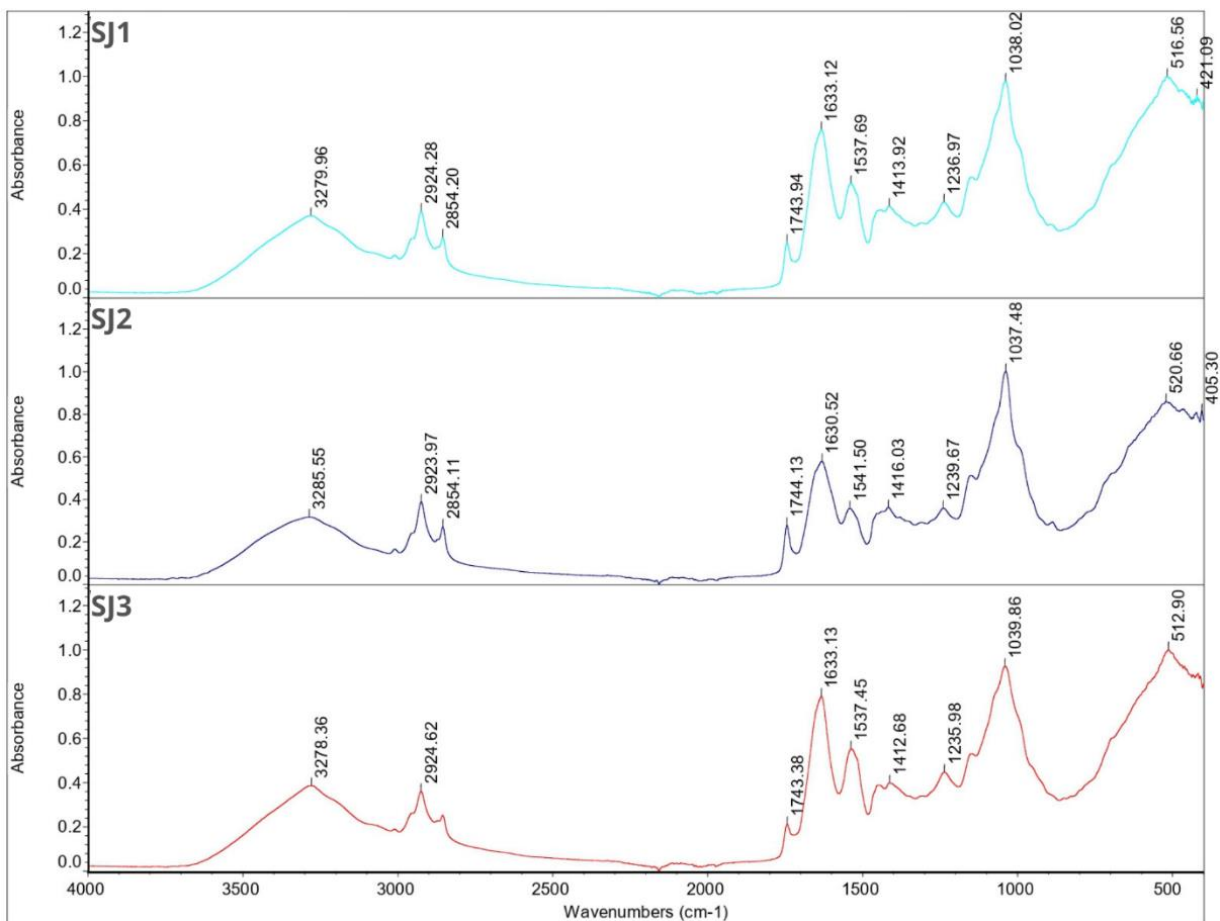
Opis widm FT-IR poszczególnych składników mikrokapsulek przedstawiony został w pracy nr 5. Ryciny 7-10 ilustrują widma FT-IR dla wszystkich uzyskanych mikrokapsulek. Brak charakterystycznych pików dla RSO, SBO, JEO i BPO w widmach sugeruje skuteczną mikroenkapsulację, co potwierdzają wyniki testu EE (Tab. 10). Widma te są bliskie widmom FB, zgodne z ich składem, przy czym koncentracja FB jest najwyższa we wszystkich przypadkach. Zaobserwowano zmienność w intensywności pików, zwłaszcza z wyższą intensywnością w określonych długościach fal dla niektórych stosunków mieszania. Zauważalny pik charakterystyczny dla RSO i SBO pojawił się we wszystkich próbkach z wyjątkiem RB2, która wykazała najwyższą efektywność enkapsulacji (87,85). Wskazuje to na korelację między składem mikrokapsulek, intensywnością pików a efektywnością enkapsulacji.



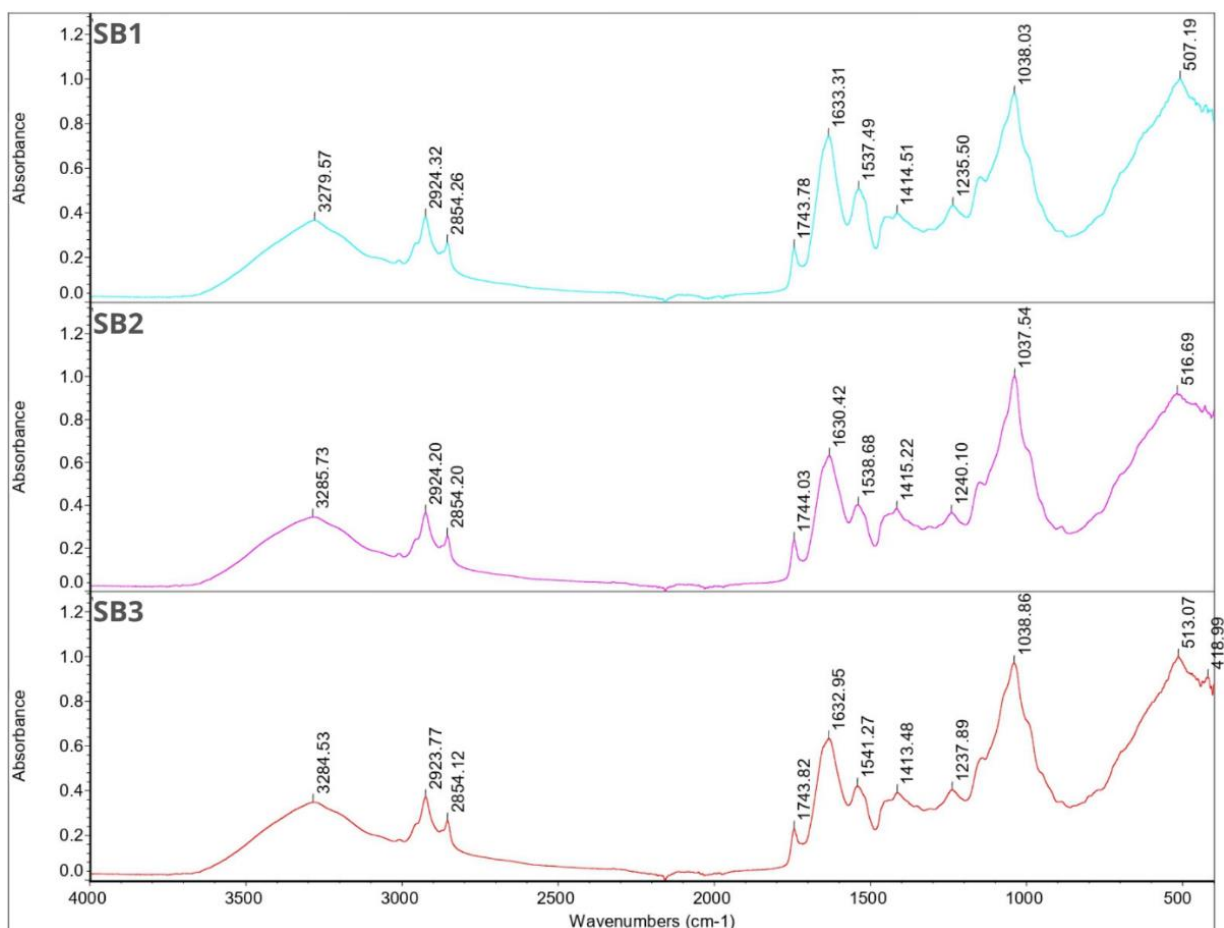
Ryc. 7: Widma FT-IR dla próbek RJ1, RJ2, RJ3 zawierających białko bobowe i polisacharydy z nasion chia w proporcji odpowiednio 1:1; 1:2; 2:1, olej rzepakowy oraz olejek eteryczny z jałowca



Ryc. 8: Widma FT-IR dla próbek RB1, RB2, RB3 zawierających białko bobowe i polisacharydy z nasion chia w proporcji odpowiednio 1:1; 1:2; 2:1, olej rzepakowy oraz olejek eteryczny z czarnego pieprzu



Ryc. 9: Widma FT-IR dla próbek SJ1, SJ2, SJ3 zawierających białko bobowe i polisacharydy z nasion chia w proporcji odpowiednio 1:1; 1:2; 2:1, olej sojowy oraz olejek eteryczny z jałowca



Ryc. 10: Widma FT-IR dla próbek SB1, SB2, SB3 zawierających białko bobowe i polisacharydy z nasion chia w proporcji odpowiednio 1:1; 1:2; 2:1, olej sojowy oraz olejek eteryczny z czarnego pieprzu.

Wnioski

Na podstawie otrzymanych wyników badań stwierdzono, że proces koacerwacji złożonej może być z powodzeniem stosowany do utrwalaania olejków eterycznych, pozwalając na otrzymanie mikrokapsulek o pożądaných właściwościach. Mikrokapsułki zawierające białka roślinne charakteryzują się niską zawartością wody i niską higroskopijnością co jest istotne z punktu widzenia ich przechowywania jak i trwałości materiału rdzenia. Ponadto, z pracy wynika, że białka roślinne mogą stanowić alternatywę dla żelatyny w tym procesie, a polisacharydy z nasion chia mogą zwiększać efektywność kapsułkowania. Najwyższe wartości EE otrzymano dla mikrokapsulek zawierających białko bobowe i polisacharydy z nasion chia. Istotny jest dobór zarówno białka i polisacharydu, jak i stosunku zmieszania ich ze sobą – ma to bezpośredni wpływ na właściwości otrzymywanych mikrokapsulek, jak i na efektywność enkapsulacji. Wyniki niniejszej pracy pozwalają na potwierdzenie postawionych hipotez:

1. Białka roślinne mogą stanowić alternatywę dla żelatyny w procesie koacerwacji złożonej.
2. Białka roślinne są równie skuteczne w mikrokapsułkowaniu olejków eterycznych, co żelatyna.
3. Zamiana gumy arabskiej na polisacharydy z nasion chia może zwiększyć efektywność kapsułkowania olejków eterycznych.

Bibliografia

1. Akseli, I., Hilden, J., Katz, J. M., Kelly, R. C., Kramer, T. T., Mao, C., Osei-Yeboah, F., & Strong, J. C. (2019). Reproducibility of the measurement of bulk/tapped density of pharmaceutical powders between pharmaceutical laboratories. *Journal of Pharmaceutical Sciences*, *108*, 1081-1084.
2. Almas, I., Innocent, E., Machumi, F., & Kisinza, W. (2021). Chemical composition of essential oils from *Eucalyptus globulus* and *Eucalyptus maculata* grown in Tanzania. *Scientific African*, *12*, e00758.
3. Alvarez-Henao, M. V., Saavedra, N., Medina, S., Jiménez Cartagena, C., Alzate, L. M., & Londoño-Londoño, J. (2018). Microencapsulation of lutein by spray-drying: Characterization and stability analyses to promote its use as a functional ingredient. *Food Chemistry*, *256*, 181-187.
4. Amalraj, A., Haponiuk, J. T., Thomas, S., & Gopi, S. (2020). Preparation, characterization and antimicrobial activity of polyvinyl alcohol/gum arabic/chitosan composite films incorporated with black pepper essential oil and ginger essential oil. *International Journal of Biological Macromolecules*, *151*, 366-375.
5. Amani, F., Azadi, A., Rezaei, A., Kharazmi, M. S., & Jafari, S. M. (2022). Preparation of soluble complex carriers from Aloe vera mucilage/gelatin for cinnamon essential oil: Characterization and antibacterial activity. *Journal of Food Engineering*, *334*, 111160.
6. Aminzare, M., Hashemi, M., Hassanzad, A. H., & Hejazi, J. (2016). The use of herbal extracts and essential oils as a potential antimicrobial in meat and meat products: A review. *Journal of Human and Environmental Health Promotion*, *1*, 63-74.
7. Arenas-Jal, M., Suñé-Negre, J. M., & García-Montoya, E. (2020). An overview of microencapsulation in the food industry: Opportunities, challenges, and innovations. *European Food Research and Technology*, *246*, 1371-1382.
8. Asioli, D., Aschemann-Witzel, J., Caputo, V., Vecchio, R., Annunziata, A., Næs, T., & Varela, P. (2017). Making sense of the “clean label” trends: A review of consumer food choice behavior and discussion of industry implications. *International Food Research Journal*, *99*, 58-71.
9. Atgié, M., Garrigues, J. C., Chennevière, A., Masbernat, O., & Roger, K. (2019). Gum Arabic in solution: Composition and multi-scale structures. *Food Hydrocolloids*, *91*, 319-330.
10. Bajac, J., Nikolovski, B., Lončarević, I., Petrović, J., Bajac, B., Đurović, S., & Petrović, L. (2022). Microencapsulation of juniper berry essential oil (*Juniperus communis* L.) by spray drying: Microcapsule characterization and release kinetics of the oil. *Food Hydrocolloids*.
11. Bakry, A. M., Abbas, S., Ali, B., Majeed, H., Abouelwafa, M. Y., Mousa, A. H., & Liang, L. (2016). Microencapsulation of oils: A comprehensive review of benefits, techniques, and applications. *Comprehensive Reviews in Food Science and Food Safety*, *15*, 143-182.
12. Bedoya-Serna, C. M., Dacanal, G. C., Fernandes, A. M., & Pinho, S. C. (2018). Antifungal activity of nanoemulsions encapsulating oregano (*Origanum vulgare*) essential oil: In vitro study and application in Minas padrão cheese. *Brazilian Journal of Microbiology*, *49*, 929-935.
13. Bento, R., Pagán, E., Berdejo, D., de Carvalho, R. J., García-Embida, S., Maggi, F., Magnani, M., Evandro de Souza, L., García-Gonzalo, D., & Pagán, R. (2020). Chitosan nanoemulsions of cold-pressed orange essential oil to preserve fruit juices. *International Journal of Food Microbiology*, *331*, 108786.
14. Boné Calvo, J., Clavero Adell, M., Guallar Abadía, I., Aznar, S. L., Sancho Rodríguez, M. L., Monzon, A. C., & Mazas, Y. A. (2021). As soon as possible in IgE-cow's milk allergy immunotherapy. *European Journal of Pediatrics*, *180*, 291-294.
15. Bringas-Lantigua, M., Expósito Molina, I., Reineccius, G. A., López-Hernández, O., & Pino, J. A. (2011). Influence of spray-dryer air temperatures on encapsulated mandarin oil. *Drying Technology*, *29*(5), 520-526.

16. Brüttsch, L. (2019). Chia seed mucilage—a vegan thickener: Isolation, tailoring viscoelasticity and rehydration. *Food & Function*, 8, 4854-4860.
17. Bustamante, M., Laurie-Martínez, L., Vergara, D., Campos-Vega, R., Rubilar, M., & Shene, C. (2020). Effect of three polysaccharides (Inulin, and Mucilage from Chia and Flax Seeds) on the survival of probiotic bacteria encapsulated by spray drying. *Applied Sciences*, 10, 4623.
18. Capitani, M. I., Ixtaina, V. Y., Nolasco, S. M., & Tomas, M. C. (2013). Microstructure, chemical composition and mucilage exudation of chia (*Salvia hispanica* L.) nutlets from Argentina. *Journal of the Science of Food and Agriculture*, 93, 3856-3862.
19. Carpentier, J., Conforto, E., Chaigneau, C., Vendeville, J. E., & Maugard, T. (2021). Complex coacervation of pea protein isolate and tragacanth gum: Comparative study with commercial polysaccharides. *Innovative Food Science & Emerging Technologies*, 69, 102641.
20. Carpentier, J., Conforto, E., Chaigneau, C., Vendeville, J. E., & Maugard, T. (2022). Microencapsulation and controlled release of α -tocopherol by complex coacervation between pea protein and tragacanth gum: A comparative study with arabic and tara gums. *Innovative Food Science & Emerging Technologies*, 77, 102951.
21. da Silva, S. F., de Campo, C., Paese, K., Guterres, S. S., Costa, T. M. H., & Flores, S. H. (2018). Nanoencapsulation of linseed oil with chia mucilage as structuring material: Characterization, stability and enrichment of orange juice. *Food Research International*, 120, 872-879.
22. De Melo Ramos, F., Silveira Júnior, V., & Prata, A. S. (2019). Assessing the vacuum spray drying effects on the properties of orange essential oil microparticles. *Food and Bioprocess Technology*, 12(11), 1917-1927.
23. Delshadi, R., Bahrami, A., Tafti, A. G., Barba, F. J., & Williams, L. L. (2020). Micro and nano-encapsulation of vegetable and essential oils to develop functional food products with improved nutritional profiles. *Trends in Food Science & Technology*, 104, 72-83.
24. Devi, N., Sarmah, M., Khatun, B., & Maji, T. (2017). Encapsulation of active ingredients in polysaccharide-protein complex coacervates. *Advances in Colloid and Interface Science*, 239, 136-145.
25. Dosoky, N. S., Satyal, P., Barata, L. M., da Silva, J. K. R., & Setzer, W. N. (2019). Volatiles of black pepper fruits (*Piper nigrum* L.). *Molecules*, 24(23), 4244.
26. Evans, M., Ratcliffe, I., & Williams, P. A. (2013). Emulsion stabilisation using polysaccharide-protein complexes. *Current Opinion in Colloid & Interface Science*, 18, 272-282.
27. Falleh, H., Benjemaa, M. B., Saada, M., & Ksouri, R. (2020). Essential oils: A promising eco-friendly food preservative. *Food Chemistry*, 330, 127268.
28. Falleh, H., Benjemaa, M., Djebblai, K., Abid, S., Saada, M., & Ksouri, R. (2019). Application of the mixture design for optimum antimicrobial activity: Combined treatment of *Syzygium aromaticum*, *Cinnamomum zeylanicum*, *Myrtus communis*, and *Lavandula stoechas* essential oils against *Escherichia coli*. *Journal of Food Processing and Preservation*, 43(1), e13983.
29. Gardeli, C., Evageliou, V., Poulos, C., Yanniotis, S., & Komaitis, M. (2010). Drying of fennel plants: Oven, freeze drying, effect of freeze-drying time, and use of biopolymers. *Drying Technology*, 28(4), 542-549.
30. Ghorbanzadeh, A., Ghasemnezhad, A., Sarmast, M. K., & Ebrahimi, S. N. (2021). An analysis of variations in morphological characteristics, essential oil content, and genetic sequencing among and within major Iranian Juniper (*Juniperus* spp.) populations. *Phytochemistry*, 186, 1-10.
31. Giacometti, J., Kovačević, D. B., Putnik, P., Gabrić, D., Bilušić, T., Krešić, G., Stulić, V., Barba, F. J., Chemat, F., & Barbosa-Cánovas, G. (2018). Extraction of bioactive compounds and essential oils from Mediterranean herbs by conventional and green innovative techniques: A review. *International Journal of Food Research*, 113, 245-262.
32. Goh, K. K. T., Matia-Merino, L., Chiang, J. H., Quek, R., Soh, S. J. B., & Lentle, R. G. (2016). The physicochemical properties of chia seed polysaccharide and its microgel dispersion rheology. *Carbohydrate Polymers*, 149, 297-307.
33. Górska-Horczyk, E., Wojtasik-Kalinowska, I., Guzek, D., Sun, D. W., & Wierzbicka, A. (2017). Differentiation of chill-stored and frozen pork necks using electronic nose with ultra-fast gas chromatography. *Journal of Food Process Engineering*, 40, e12305.
34. Grogan, K. A. (2015). The value of added sulfur dioxide in French organic wine. *Agriculture and Food Economics*, 3(1), 1-25.
35. Gyawali, R., & Ibrahim, S. A. (2014). Natural products as antimicrobial agents. *Food Control*, 46, 412-429.
36. Hashemi, S. M. B., Khaneghah, A. M., Tavakolpour, Y., Asnaashari, M., & Mehr, H. M. (2015). Effects of ultrasound treatment, UV irradiation and *Avishan-e-Denaei* essential oil on oxidative stability of sunflower oil. *Journal of Essential Oil Bearing Plants*, 18, 1083-1092.

37. Hernandez-Nava, R., Lopez-Malo, A., Palou, E., Ramirez-Corona, N., & Jimenez-Munguia, M. T. (2020). Encapsulation of oregano essential oil (*Origanum vulgare*) by complex coacervation between gelatin and chia mucilage and its properties after spray drying. *Food Hydrocolloids*, *109*, 106077.
38. Hernandez-Nava, R., Lopez-Malo, A., Palou, E., Ramirez-Corona, N., & Jimenez-Munguia, M. T. (2020). Encapsulation of oregano essential oil (*Origanum vulgare*) by complex coacervation between gelatin and chia mucilage and its properties after spray drying. *Food Hydrocolloids*, *109*, 106077.
39. Hojjati, F., Sereshti, H., & Hojjati, M. (2019). Leaf essential oils and their application in systematics of *Juniperus excelsa* complex in Iran. *Biochemical Systematics and Ecology*, *84*, 29-34.
40. Hussein, M. A., Gobba, N. A., & El Bishbishy, M. H. (2014). Composition, in vitro antioxidant and antitumor properties of essential oil from the seeds of *Moringa oleifera*. *International Journal of Pharmaceutical Sciences*, *4*, 532-540.
41. Hyldgaard, M., Mygind, T., & Meyer, R. L. (2012). Essential oils in food preservation: Mode of action, synergies, and interactions with food matrix components. *Frontiers in Microbiology*, *3*, 12.
42. Jannasari, N., Milad, F., Moshtaghian, S. J., & Abbaspourrad, A. (2019). Microencapsulation of vitamin D using gelatin and cress seed mucilage: Production, characterization and in vivo study. *International Journal of Biological Macromolecules*, *129*, 972-979.
43. Kassem, I. A. A., Ashaolu, T. J., Kamel, R., Elkasabgy, N. A., Afifi, S. M., & Farag, M. A. (2021). Mucilage as a functional food hydrocolloid: Ongoing and potential applications in prebiotics and nutraceuticals. *Food Function*, *12*, 4738-4748.
44. Kavooosi, G., Rahmatollahi, A., Dadfar, S. M. M., & Purfard, A. M. (2014). Effects of essential oil on the water binding capacity, physico-mechanical properties, antioxidant and antibacterial activity of gelatin films. *LWT - Food Science and Technology*, *57*, 556-561.
45. Klemmer, K. J., Waldner, L., Stone, A., Low, N. H., & Nickerson, M. T. (2012). Complex coacervation of pea protein isolate and alginate polysaccharides. *Food Chemistry*, *130*, 710-715.
46. Kocatepe, D., Turan, H., Altan, C. O., Keskin, I., Ceylan, A., Köstekli, B., & Candan, C. (2019). Influence of different essential oils on marinated anchovy (*Engraulis encrasicolus* L.) during refrigerated storage. *Food Science and Technology*, *39*, 255-260.
47. Kontogiorgos, V. (2019). Polysaccharides at fluid interfaces of food systems. *Advances in Colloid and Interface Science*, *270*, 28-37.
48. Kunicka-Styczyńska, A. (2016). Olejki eteryczne jako alternatywa dla syntetycznych konserwantów żywności – Praca przeglądowa. W T. Tarko, I. Drożdż, D. Najgebauer-Lejko, & A. Duda-Chodak (Eds.), *Innowacyjne rozwiązania w technologii żywności i żywieniu człowieka* (tom 122, s. 175-184). Kraków, Polska: Oddział Małopolski Polskiego Towarzystwa Technologów Żywności.
49. Kurek, M., Wyrwisz, J., Piwinska, M., & Wierzbicka, A. (2016). Application of the response surface methodology in optimizing oat fiber particle size and flour replacement in wheat bread rolls. *CyTA - Journal of Food*, *14*(1), 18-26.
50. Lages, L. Z., Radünz, M., Timm Gonçalves, B., Silva da Rosa, R., Fouchy, M. V., de Cássia dos Santos da Conceição, R., Gualarte, M. A., Barboza Mendonça, C. R., & Gandra, E. A. (2021). Microbiological and sensory evaluation of meat sausage using thyme (*Thymus vulgaris*, L.) essential oil and powdered beet juice (*Beta vulgaris* L., Early Wonder cultivar). *LWT*, *148*, 111794.
51. Lan, Y., Ohm, J. B., Chen, B., & Rao, J. (2020). Microencapsulation of hemp seed oil by pea protein isolate-sugar beet pectin complex coacervation: Influence of coacervation pH and wall/core ratio. *Food Hydrocolloids*, *113*, 106423.
52. Laranjo, M., Fernandez-Leon, A., Potes, M., & Santos, A. M. (2017). Use of essential oils in food preservation. In A. Mendez-Vilas (Ed.), *Antimicrobial research: Novel bioknowledge and educational programs* (vol. 6, pp. 177-188). Formatex Research Center: Badajoz, Spain.
53. Lashkari, H., Khosrowshahi, A. A., Madadlou, A., & Alizadeh, M. (2014). Chemical composition and rheology of low-fat Iranian white cheese incorporated with guar gum and gum arabic as fat replacers. *Journal of Food Science and Technology*, *51*, 2584-2591. <https://doi.org/10.1007/s13197-012-0768-y>
54. Li, Y., Zhang, X., Zhao, Y., Ding, J., & Lin, S. (2018). Investigation on complex coacervation between fish skin gelatin from cold-water fish and gum arabic: Phase behavior, thermodynamic, and structural properties. *International Food Research Journal*, *107*, 596-604.
55. Liang, Y., Matia-Merino, L., Gillies, G., Patel, H., Ye, A., & Golding, M. (2017). The heat stability of milk protein-stabilized oil-in-water emulsions: A review. *Current Opinion in Colloid and Interface Science*, *28*, 63-73.
56. Luo, X., Sedman, J., & Ismail, A. A. (2019). Microencapsulation of oregano (*Origanum vulgare* L.), rosemary (*Rosmarinus officinalis* L.), and sage (*Salvia officinalis* L.) essential oils in β -lactoglobulin. *Journal of Food Science & Technology*, *4*(9), 970-985.

57. Mahanta, B. P., Bora, P. K., Kemprai, P., Borah, G., Lal, M., & Haldar, S. (2021). Thermolabile essential oils, aromas and flavours: Degradation pathways, effect of thermal processing and alteration of sensory quality. *Food Research International*, *145*, 110404.
58. Manaf, M. A., Subuki, I., Jai, J., Raslan, R., & Mustapa, A. N. (2018). Encapsulation of volatile citronella essential oil by coacervation: Efficiency and release study. W *Proceedings of the 3rd International Conference on Global Sustainability and Chemical Engineering (ICGSCE)* (vol. 358). IOP Conference Series: Materials Science and Engineering, Putrajaya, Malaysia.
59. Maruyama, S., Streletskaya, N. A., & Lim, J. (2020). Clean label: Why this ingredient but not that one? *Food Quality and Preference*, *87*, 104062.
60. Mohammadalinejad, S., & Kurek, M. (2021). Microencapsulation of anthocyanins—Critical review of techniques and wall materials. *Applied Sciences*, *11*(9), 3936.
61. Moore-Neibel, K., Gerber, C., Patel, J., Friedman, M., Jaroni, D., & Ravishankar, S. (2013). Antimicrobial activity of oregano oil against antibiotic-resistant *Salmonella enterica* on organic leafy greens at varying exposure times and storage temperatures. *Food Microbiology*, *34*, 123–129.
62. Muhammad, D. R. A., Saputro, A. D., Rottiers, H., Van de Walle, D., & Dewettinck, K. (2018). Physicochemical properties and antioxidant activities of chocolates enriched with engineered cinnamon nanoparticles. *European Food Research and Technology*, *244*, 1185–1202.
63. Muhoza, B., Xia, S., & Zhang, X. (2019). Gelatin and high methyl pectin coacervates crosslinked with tannic acid: The characterization, rheological properties, and application for peppermint oil microencapsulation. *Food Hydrocolloids*, *97*, 105174.
64. Muhoza, B., Xia, S., Wang, X., Zhang, X., Li, Y., & Zhang, S. (2020). Microencapsulation of essential oils by complex coacervation method: preparation, thermal stability, release properties and applications. *Critical Reviews in Food Science and Nutrition*, *62*, 1363-1382.
65. Muhoza, B., Xia, S., Wang, X., Zhang, X., Li, Y., & Zhang, S. (2022). Microencapsulation of essential oils by complex coacervation method: Preparation, thermal stability, release properties and applications. *Critical Reviews in Food Science and Nutrition*, *62*(6), 1363–1382.
66. Naderi, B., Keramat, J., Nasirpour, A., & Aminifar, M. (2020). Complex coacervation between oak protein isolate and gum Arabic: Optimization & functional characterization. *International Journal of Food Properties*, *23*(1), 1854–1873.
67. Napiórkowska, A., & Kurek, M. (2022). Coacervation as a novel method of microencapsulation of essential oils—A review. *Molecules*, *27*(16), 5142.
68. Napiórkowska, A., Szpicer, A., Wojtasik-Kalinowska, I., Perez, M. D. T., González, H. D., & Kurek, M. A. (2023). Microencapsulation of juniper and black pepper essential oil using the coacervation method and its properties after freeze-drying. *Foods*, *12*(23), 4345.
69. Nedovic, V., Kalusevic, A., Manojlovic, V., Levic, S., & Bugarski, B. (2011). An overview of encapsulation technologies for food applications. *Procedia Food Science*, *1*, 1806–1815.
70. Nieto Nieto, T. V., Wang, Y., Ozimek, L., & Chen, L. (2016). Improved thermal gelation of oat protein with the formation of controlled phase-separated networks using dextrin and carrageenan polysaccharides. *Food Research International*, *82*, 95-103.
71. Nieto-Nieto, T. V., Wang, Y. X., Ozimek, L., & Chen, L. (2015). Inulin at low concentrations significantly improves the gelling properties of oat protein – A molecular mechanism study. *Food Hydrocolloids*, *50*, 116-127.
72. Nikolić, M., Stojković, D., Glamočlija, J., Ćirić, A., Marković, T., Smiljković, M., & Soković, M. (2015). Could essential oils of green and black pepper be used as food preservatives? *Journal of Food Science and Technology*, *52*, 1-9. <https://doi.org/10.1007/s13197-015-1792-5>
73. Nowak, D., & Jakubczyk, E. (2020). The freeze-drying of foods—the characteristic of the process course and the effect of its parameters on the physical properties of food materials. *Foods*, *9*(10), 1488.
74. Ogilvie-Battersby, J. D., Nagarajan, R., Mosurkal, R., & Orbey, N. (2022). Microencapsulation and controlled release of insect repellent geraniol in gelatin/gum arabic microcapsules. *Colloids and Surfaces A: Physicochemical and Engineering Aspects*, *640*, 128494.
75. Otálora, M. C., Castaño, J. A. G., & Wilches-Torres, A. (2019). Preparation, study and characterization of complex coacervates formed between gelatin and cactus mucilage extracted from cladodes of *Opuntia ficus-indica*. *LWT*, *112*, 108234.
76. Otálora, M. C., Wilches-Torres, A., & Gómez Castaño, J. A. (2023). Spray-drying microencapsulation of Andean blueberry (*Vaccinium meridionale* Sw.) anthocyanins using prickly pear (*Opuntia ficus-indica* L.) peel mucilage or gum arabic: A comparative study. *Foods*, *12*(9), 1811.
77. Paans, E. (2013). *Investigating consumers' avoidance of E-numbers*. Paans.
78. Pakzad, H., Alemzadeh, I., & Kazemi, A. (2013). Encapsulation of peppermint oil with arabic gum-gelatin by complex coacervation method. *International Journal of Engineering*, *26*, 807–814.

79. Pateiro, M., Barba, F. J., Domínguez, R., Sant'Ana, A. S., Khaneghah, A. M., Gavahian, M., Gómez, B., & Lorenzo, J. M. (2018). Essential oils as natural additives to prevent oxidation reactions in meat and meat products: A review. *International Food Research Journal*, *113*, 156–166.
80. Patrignani, F., Siroli, L., Braschi, G., & Lanciotti, R. (2020). Combined use of natural antimicrobial-based nanoemulsions and ultra-high-pressure homogenization to increase safety and shelf life of apple juice. *Food Control*, *111*, 107051.
81. Reis, D. R., Ambrosi, A., & Di Luccio, M. (2022). Encapsulated essential oils: A perspective in food preservation. *Future Foods*, *5*, 100126.
82. Rios-Mera, J. D., Saldaña, E., Ramírez, Y., Auquiñivín, E. A., Alvim, I. D., & Contreras-Castillo, C. J. (2019). Encapsulation optimization and pH- and temperature-stability of the complex coacervation between soy protein isolate and inulin entrapping fish oil. *LWT*, *116*, 108555.
83. Rogozińska, I., & Wichrowska, D. (2011). Najpopularniejsze dodatki utrwalające stosowane w nowoczesnej technologii żywności. *Inżynieria i Aparatura Chemiczna*, *50*, 19–21.
84. Rohman, A., Windarsih, A., Erwanto, Y., & Zakaria, Z. (2020). Review on analytical methods for analysis of porcine gelatine in food and pharmaceutical products for halal authentication. *Trends in Food Science & Technology*, *101*, 122–132.
85. Rojas-Moreno, S., Cárdenas-Bailón, F., Osorio-Revilla, G., Gallardo-Velázquez, T., & Proal-Nájera, J. (2017). Effects of complex coacervation-spray drying and conventional spray drying on the quality of microencapsulated orange essential oil. *Journal of Food Measurement and Characterization*, *12*, 650–660.
86. Rojas-Moreno, S., Osorio-Revilla, G., Gallardo-Velázquez, T., Cárdenas-Bailón, F., & Meza-Márquez, G. (2018). Effect of the cross-linking agent and drying method on encapsulation efficiency of orange essential oil by complex coacervation using whey protein isolate with different polysaccharides. *Journal of Microencapsulation*, *35*(2), 165–180.
87. Sanchez, C., Nigen, M., Mejia, T. V., Doco, T., Williams, P., Amine, C., & Renard, D. (2018). Acacia gum: History of the future. *Food Hydrocolloids*, *78*, 140–160.
88. Sarma, Y. R., Nirmal Babu, K., & Aziz, S. (2014). Spices and aromatics. In N. K. Van Alfen (Ed.), *Encyclopedia of Agriculture and Food Systems* (pp. 211–234). Academic Press.
89. Shaddel, R., Hesari, J., Azadmard-Damirchi, S., Hamishehkar, H., Fathi-Achachlouei, B., & Huang, Q. (2018). Use of gelatin and gum Arabic for encapsulation of black raspberry anthocyanins by complex coacervation. *International Journal of Biological Macromolecules*, *107*, 1800–1810.
90. Shah, B., Davidson, P. M., & Zhong, Q. (2013). Nanodispersed eugenol has improved antimicrobial activity against *Escherichia coli* O157: H7 and *Listeria monocytogenes* in bovine milk. *International Journal of Food Microbiology*, *161*, 53–59.
91. Shishir, M. R. I., Xie, L., Sun, C., Zheng, X., & Chen, W. (2018). Advances in micro and nano-encapsulation of bioactive compounds using biopolymer and lipid-based transporters. *Trends in Food Science & Technology*, *78*, 34–60.
92. Singletary, K. (2016). Rosemary, an overview of potential health benefits. *Nutrition Today*, *51*, 102–112.
93. Snoussi, A., Chouaibi, M., Ben Haj Koubaier, H., & Bouzouita, N. (2022). Encapsulation of Tunisian thyme essential oil in O/W nanoemulsions: Application for meat preservation. *Meat Science*, *188*, 108785.
94. Stojanović-Radić, Z., Pejčić, M., Joković, N., Jakanović, M., Ivić, M., Šojić, B., Škaljac, S., Stojanović, P., & Mihajilov-Krstev, T. (2022). Inhibition of *Salmonella Enteritidis* growth and storage stability in chicken meat treated with basil and rosemary essential oils alone or in combination. *Food Control*, *90*, 332–343.
95. Tamargo, A., Cueva, C., Laguna, L., Moreno-Arribas, M. V., & Muñoz, L. A. (2018). Understanding the impact of chia seed mucilage on human gut microbiota by using the dynamic gastrointestinal model simgi®. *Journal of Functional Foods*, *50*, 104–111.
96. Tang, C. H. (2017). Emulsifying properties of soy proteins: A critical review with emphasis on the role of conformational flexibility. *Critical Reviews in Food Science and Nutrition*, *57*, 2636–2679.
97. Tavares, L., & Noreña, C. P. Z. (2020). Encapsulation of ginger essential oil using complex coacervation method: Coacervate formation, rheological property, and physicochemical characterization. *Food and Bioprocess Technology*.
98. Timilsena, Y. P., Adhikari, R., Barrow, C. J., & Adhikari, B. (2017). Digestion behaviour of chia seed oil encapsulated in chia seed protein-gum complex coacervates. *Food Hydrocolloids*, *66*, 71–81.
99. Timilsena, Y. P., Taiwo, O. A., Nauman, K., Benu, A., & Colin, J. B. (2019). Complex coacervation: Principles, mechanisms and applications in microencapsulation. *International Journal of Biological Macromolecules*, *121*, 1276–1286.
100. Turek, C., & Stintzing, F. C. (2013). Stability of essential oils: A review. *Comprehensive Reviews in Food Science and Food Safety*, *12*, 40–53.

101. Valderrama, F., & Ruiz, F. (2018). An optimal control approach to steam distillation of essential oils from aromatic plants. *Computers & Chemical Engineering*, *117*, 25–31.
102. Valková, V., Dúranová, H., Galovičová, L., Vukovic, N. L., Vukic, M., & Kačániová, M. (2021). In vitro antimicrobial activity of lavender, mint, and rosemary essential oils and the effect of their vapours on growth of *Penicillium* spp. in a bread model system. *Molecules*, *26*, 3859.
103. Van Gunst, A., & Roodenburg, A. J. (2019). Consumer distrust about E-numbers: A qualitative study among food experts. *Foods*, *8*(5), 178.
104. Vargas, S. A., Delgado-Macuil, R. J., Ruiz-Espinosa, H., Rojas-Lopez, M., & Amador-Espejo, G. G. (2021). High-intensity ultrasound pretreatment influence on whey protein isolate and its use on complex coacervation with kappa carrageenan: Evaluation of selected functional properties. *Ultrasonics Sonochemistry*, *70*, 105340.
105. Veiga, R. D. S. D., Aparecida Da Silva-Buzanello, R., Corso, M. P., & Canan, C. (2019). Essential oils microencapsulated obtained by spray drying: A review. *Journal of Essential Oil Research*, *31*, 457–473.
106. Voltolini, S., Pellegrini, S., Contatore, M., Bignardi, D., & Minale, P. (2014). New risks from ancient food dyes: Cochineal red allergy. *European Annals of Allergy and Clinical Immunology*, *46*, 232–233.
107. Warnakulasuriya, S. N., & Nickerson, M. T. (2018). Review on plant protein-polysaccharide complex coacervation, and the functionality and applicability of formed complexes. *Journal of the Science of Food and Agriculture*, *98*, 5559–5571.
108. Wojtasik-Kalinowska, I., Guzek, D., Górska-Horczyzak, E., Brodowska, M., Sun, D. W., & Wierzbicka, A. (2018). Diet with linseed oil and organic selenium yields low n-6/n-3 ratio pork Semimembranosus meat with unchanged volatile compound profiles. *International Journal of Food Science*, *53*, 1838–1846.
109. Xiao, Z., Li, W., Zhu, G., Zhou, R., & Niu, Y. (2016). Study of production and the stability of styrallyl acetate nanocapsules using complex coacervation. *Flavour and Fragrance Journal*, *31*(4), 283–289.
110. Xin, X., Essien, S., Dell, K., Woo, M. W., & Baroutian, S. (2022). Effects of spray-drying and freeze-drying on bioactive and volatile compounds of smoke powder food flavouring. *Food Bioprocess Technology*, *15*, 785–794.
111. Xu, X., Liu, A., Hu, S., Ares, I., Martínez-Larrañaga, M. R., Wang, X., Martínez, M., Anadón, A., & Martínez, M.-A. (2021). Synthetic phenolic antioxidants: Metabolism, hazards and mechanism of action. *Food Chemistry*, *353*, 129488.
112. Yaman, D. M., Koçak Yanık, D., Elik Demir, A., Uzun Karka, H., Güçlü, G., Selli, S., Kelebek, H., Göğüş, F. (2023). Effect of encapsulation techniques on aroma retention of *Pistacia terebinthus* L. fruit oil: Spray drying, spray freeze drying, and freeze drying. *Foods*, *12*(17), 3244.
113. Yang, X., Gao, N., Hu, L., Li, J., & Sun, Y. (2015). Development and evaluation of novel microcapsules containing poppy-seed oil using complex coacervation. *Journal of Food Engineering*, *161*, 87–93.
114. Yuan, Y., Li, M. F., Chen, W. S., Zeng, Q. Z., Su, D. X., Tian, B., & He, S. (2018). Microencapsulation of shiitake (*Lentinula edodes*) essential oil by complex coacervation: Formation, rheological property, oxidative stability and odour attenuation effect. *International Journal of Food Science*, *53*, 1681–1688.
115. Zedan, H., Hosseini, S. M., & Mohammadi, A. (2021). The effect of tarragon (*Artemisia dracunculus*) essential oil and high molecular weight chitosan on sensory properties and shelf life of yogurt. *LWT*, *147*, 111613.
116. Zheljzkov, D. V., Kacaniova, M., Dincheva, I., Radoukova, T., Semerdjieva, I. B., Astatkie, T., & Schlegel, V. (2018). Essential oil composition, antioxidant and antimicrobial activity of the galbuli of six juniper species. *Industrial Crops and Products*, *124*, 449–458.

Pozostały dorobek naukowy

Artykuły w czasopismach recenzowanych

1. Hać-Szymańczuk, E., Cegiełka, A., Piwowarek, K., & **Napiórkowska, A.** (2020). Jakość mikrobiologiczna mrożonych surowców roślinnych i sposoby jej poprawy. *Chłodnictwo: organ Naczelnej Organizacji Technicznej*, 55(6), 2–4.
2. Hać-Szymańczuk, E., Cegiełka, A., Piwowarek, K., & **Napiórkowska, A.** (2020). Mycie i dezynfekcja – efektywność i skuteczność działania środków myjących wobec drobnoustrojów. *Gospodarka mięsna*, 7, 22–25.
3. Uncu, O., **Napiórkowska, A.**, Szajna, T. K., & Ozen, B. (2020). Evaluation of three spectroscopic techniques in determination of adulteration of cold pressed pomegranate seed oils. *Microchemical Journal*, 158, 105128. <https://doi.org/10.1016/j.microc.2020.105128>
4. Hać-Szymańczuk, E., Cegiełka, A., Piwowarek, K., & **Napiórkowska, A.** (2021). Przyprawy – naturalne składniki żywności. *Przemysł Spożywczy*, 75(2).
5. Hać-Szymańczuk, E., Cegiełka, A., Piwowarek, K., & **Napiórkowska, A.** (2021). Jakość mikrobiologiczna mrożonych owoców i warzyw i sposoby jej poprawy. *Przemysł Fermentacyjny i Owocowo-Warzywny*.
6. Kurek, M. A., Majek, M., Onopiuk, A., Szpicer, A., **Napiórkowska, A.**, & Samborska, K. (2023). Encapsulation of anthocyanins from chokeberry (*Aronia melanocarpa*) with plasmolyzed yeast cells of different species. *Food and Bioprocess Processing*, 137, 84–92. <https://doi.org/10.1016/j.fbp.2023.02.003>
7. **Napiórkowska, A.**, & Kurek, M. A. (2023). Plant proteins and polysaccharides in microencapsulation of essential oils for development of functional food sector. *Przemysł Spożywczy*, 77.
8. Aktaş, H., **Napiórkowska, A.**, Szpicer, A., Custodio-Mendoza, J. A., Paraskevopoulou, A., Pavlidou, E., & Kurek, M. A. (2024). Microencapsulation of green tea polyphenols: Utilizing oat oil and starch-based double emulsions for improved delivery. *International Journal of Biological Macromolecules*, 274, 133295.
9. **Napiórkowska, A.**, Khaneghah, A. M., & Kurek, M. A. (2024). Essential oil nanoemulsions—A new strategy to extend the shelf life of smoothies. *Foods*, 13(12), 1854.
10. Custodio-Mendoza, J. A., Pokorski, P., Aktaş, H., **Napiórkowska, A.**, & Kurek, M. A. (2024). Advances in chromatographic analysis of phenolic phytochemicals in foods: Bridging gaps and exploring new horizons. *Foods*, 13(14), 2268.

Monografie

1. **Napiórkowska, A.**, Maziński, K., & Hać-Szymańczuk, E. (2021). Aktywność przeciwdrobnoustrojowa wybranych miódów krajowych. W M. Janiszewska (Red.), *Mikrobiologia i toksykologia – przegląd wybranych zagadnień* (s. 118). Wydawnictwo Naukowe TYGIEL Sp. z o. o. ISBN 978-83-66489-78-3
2. Kurek, M., Aktas, H., Custodio Mendoza, J., & **Napiórkowska, A.** (2023). Zastosowanie nowoczesnych technik mikrokapsułkowania dla substancji bioaktywnych w wegańskich produktach spożywczych. W K. Gutkowska (Red.), *Partnerstwo instytucjonalne w kształtowaniu zachowań żywieniowych w trosce o zdrowie publiczne*

(s. 642). Szkoła Główna Gospodarstwa Wiejskiego w Warszawie (SGGW). ISBN 978-83-8237-205-2

3. Kurek, M. A., **Napiórkowska, A.**, & Aktaş, H. (2024). Plant sources for functional ingredients—proteins. W F. Boukid, C. M. Rosell, & N. Gasparre (Red.), *Handbook of Plant-Based Food and Drinks Design* (s. 3–18). Academic Press.

Podsumowanie dorobku naukowego

Łączna liczba punktów MNiSW: 1 285 (w tym 630 stanowiących pracę doktorską)

Łączna liczba IF: 45,6 (w tym 22.9 stanowiących pracę doktorską)

Stáže naukowe i zawodowe

Staż naukowy w Instytucie Technologicznym w Izmirze (Izmir Technology Institute),
1.06.2023 r. – 1.10.2023 r.

Staż zawodowy w zakładzie produkującym wino Kup Sarapçilik w Denizli, 19.01.2024 –
01.04.2024 r oraz 1.06.2024 – 1.10.2024 r.

**Publikacje stanowiące rozprawę doktorską wraz z oświadczeniami
współautorów**

Review

Coacervation as a Novel Method of Microencapsulation of Essential Oils—A Review

Alicja Napiórkowska  and Marcin Kurek * 

Department of Technique and Food Development, Institute of Human Nutrition Sciences, Warsaw University of Life Sciences (WULS-SGGW), Nowoursynowska 159 c, 02-776 Warszawa, Poland

* Correspondence: marcin_kurek@sggw.edu.pl

Abstract: These days, consumers are increasingly “nutritionally aware”. The trend of “clean label” is gaining momentum. Synthetic additives and preservatives, as well as natural ones, bearing the E symbol are more often perceived negatively. For this reason, substances of natural origin are sought for replacing them. Essential oils can be such substances. However, the wider use of essential oils in the food industry is severely limited. This is because these substances are highly sensitive to light, oxygen, and temperature. This creates problems with their processing and storage. In addition, they have a strong smell and taste, which makes them unacceptable when added to the product. The solution to this situation seems to be microencapsulation through complex coacervation. To reduce the loss of essential oils and the undesirable chemical changes that may occur during their spray drying—the most commonly used method—complex coacervation seems to be an interesting alternative. This article collects information on the limitations of the use of essential oils in food and proposes a solution through complex coacervation with plant proteins and chia mucilage.

Keywords: complex coacervation; essential oils; nutraceuticals; proteins; mucilage



Citation: Napiórkowska, A.; Kurek, M. Coacervation as a Novel Method of Microencapsulation of Essential Oils—A Review. *Molecules* **2022**, *27*, 5142. <https://doi.org/10.3390/molecules27165142>

Academic Editor: Natasa Poklar Ulrih

Received: 28 June 2022

Accepted: 10 August 2022

Published: 12 August 2022

Publisher’s Note: MDPI stays neutral with regard to jurisdictional claims in published maps and institutional affiliations.



Copyright: © 2022 by the authors. Licensee MDPI, Basel, Switzerland. This article is an open access article distributed under the terms and conditions of the Creative Commons Attribution (CC BY) license (<https://creativecommons.org/licenses/by/4.0/>).

1. Introduction

Consumer interest in foods with high nutritional value, longer shelf life, and health benefits (functional food—FF) is growing year by year. This leads to the restriction of the use of preservatives and synthetic food additives in favor of bioactive substances of natural origin, e.g., from fruits, vegetables, and other plant sources. However, many of them are characterized by high instability—they are prone to oxidation, which is intensified by light, temperature, moisture, and changes in pH. The fashion for “healthy eating” and concern for the natural environment make food producers try to reduce or eliminate the addition of synthetic food preservatives and make them interested in technologies that allow the stabilization of bioactive substances to maintain their functional properties during processing and storage and to modify their physical properties to facilitate dosing [1–3].

2. Types of Functional Food

Food products known as functional, bioactive, enriched, modified, FOSHU (Foods for Specified Health Use), nutraceuticals, or food designed for the specific needs of the organism have appeared on the global market. The richness of the terminology used results from the variety of products classified as such food [4].

In the US, the Food and Drug Administration (FDA) defines functional food as food and its components that provide health benefits beyond their basic function. Similarly, in Canada, functional food is understood as food that, in addition to having basic nutritional functions, has a proven beneficial effect on health and/or reduces the risk of chronic diseases. In turn, in the European Union, since 1999, there has been a definition according to which functional food exerts a beneficial effect on one or more bodily functions in addition to its nutritional effect. The effect is to improve health and well-being and/or reduce the

risk of diseases. It must resemble conventional food and it cannot be tablets, capsules, or dietary supplements. In addition, it is a requirement to prove the beneficial effect on the human body and the statement: nutritional and health. The concept of functional food is associated with the term enriched food, but these are not identical concepts. Fortified food means adding one or more nutrients to a food, whether or not they are naturally present in the food, e.g., yogurt with probiotics and margarine with phytosterol [4,5].

Nutraceuticals are an interesting concept. This term means ingredients isolated from food, dietary supplements, and herbal products that are used individually or combined to use their synergistic effects. They include biologically active substances with proven health-promoting properties, e.g., dietary fiber, proteins, lactic acid bacteria, antioxidant substances, etc. [4].

3. Trends among Consumers

Consumers nowadays are much more interested in information about the food products' production method and ingredients production. Some production methods are perceived as less "natural", and some food ingredients are perceived as "unhealthy" and "foreign" (i.e., artificial additives). This phenomenon, often referred to as the "clean label" trend, prompts the food industry to replace synthetic agents widely used in food with ingredients of natural origin, e.g., of plant origin [6].

Preservatives are used to prevent or inhibit unfavorable changes such as microbiological (growth of bacteria or fungi), chemical (oxidation, non-enzymatic browning), and biochemical (inactivation of certain enzymes, metabolites, and components necessary for the development of microorganisms), whereas food additives are substances that are added to food products to modify or improve their sensory qualities [2,7,8]. Unfortunately, more and more examples show that the consumption of artificial (chemical) additives and preservatives can lead to allergies, food poisoning, or the development of cancer. The most famous additives causing allergic reactions are sulfites (e.g., sulfur dioxide and sodium sulphite), which are traditionally used to preserve fruit and vegetable products. In addition, the addition of SO₂ is a longstanding and common practice utilized to preserve the quality of wine (prevention against oxidation and browning) [9]. The significant reduction in vitamin B₁ absorption caused by these compounds is responsible for the development of allergic reactions. Carmine and Cochineal Red are the other best-known food additives to cause allergies. These red pigments come from the bodies of female *Dactylopius coccus*, insects that grow on cochineal cacti (Central and South America, Southern Europe, and India). These dyes are widely used as colorants in processed foods and beverages. Most often it can be found in burgers, sausages, red alcohols, soft drinks, sweets, and fruit yogurts [10–13].

To meet the demands of consumers, food producers have taken great efforts to eliminate commonly used additives and preservatives from their products. In addition in recent years, more and more researchers have been developing methods that enable the use of natural substances for this purpose. For example, the use of antioxidants such as butylated hydroxytoluene (BHT), butylated hydroxyanisole (BHA), and tert-butyl hydroquinone (TBHQ) is not as popular in recent decades due to raised concerns about their adverse effects on human health. Even though it is believed that those substances are effective against oxidation reactions, substances of natural origin are sought for replacing them [14,15]. This, along with the traditional popularity of consuming natural products, has encouraged not only food producers but also scientists to explore the applicability and effectiveness of natural compounds such as essential oils as alternatives to harmful chemical antioxidants in food products [15]. Compounds derived from natural sources have great potential to extend the shelf life of food due to their antimicrobial properties against foodborne pathogens. However, this is not their only advantage. These types of substances can provide additional health benefits since they are very often bioactive compounds with antioxidant properties [9,10,12,13].

4. Essential Oils—Natural Preservatives and Functional Additives?

Essential oils (EO) are called essential in the sense that it contains the essence of the aroma of the plant it is derived from, whereas the term “oil” is used because it contains the oil-soluble chemicals in the plant, not only because it feels oily. EOs are also known as volatile oils, ethereal oils, or aetheroleum. Essential oils are secondary metabolites synthesized by oil-yielding plants. EOs are multi-component, hydrophobic mixtures containing up to several hundred volatile compounds (usually 100 to 200 chemicals per essential oil) in different concentrations. Essential oils can be characterized by two or three major components at relatively high concentrations (20–70%), which determines the biological properties of EOs (Figure 1). The main ingredients chemically are terpenes, aldehydes, ketones, phenols, alcohols, and others [16–18]. This complex chemistry gives them their therapeutic properties and explains why different essential oils may have overlapping effects [1,2,19,20]. Some examples of major components can be cited—carvacrol and thymol represent, respectively, 30% and 27% of the composition of EO from oregano (*Origanum compactum*). EOs from coriander (*Coriandrum sativum*) have in their constitution 65% linalool. Menthol (59%) and menthone (19%) are found in EOs from peppermint (*Mentha piperita*) [21,22].

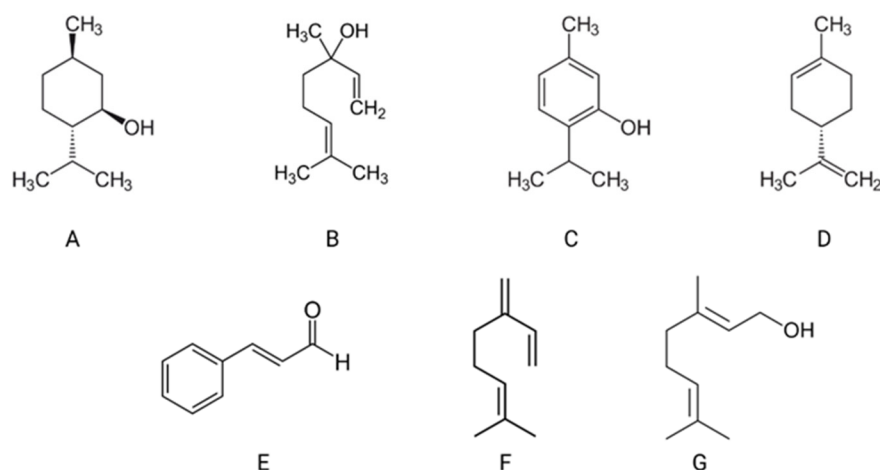


Figure 1. Examples of the main compounds of essential oils: menthol (A), linalool (B), thymol (C), limonene (D), geraniol (E), cinnamaldehyde (F), myrcene (G), own elaboration [21].

Essential oils are characterized by having many pharmacological properties, including anti-inflammatory, antispasmodic, sedative, analgesic, and digestive-supporting properties. Due to their very rich and diverse chemical composition, one essential oil can have several positive effects. For example, rosemary essential oil has the effect of improving digestion, enhancing appetite, and being anti-flatulence. In addition, they have well-documented antimicrobial activity against bacteria, yeasts, and molds [1–3]. Again, thanks to its complex composition, one essential oil can effectively inhibit the growth of both bacteria and fungi. The same rosemary EO inhibits the growth of Gram-positive (*Enterococcus* spp.) and Gram-negative (*Salmonella* spp.) bacteria, yeasts (*Candida* spp.), and molds (*Penicillium* spp.) [23–25]. For this reason, EOs can be an alternative to the commonly used food-preservation agents.

This is indicated by studies conducted, inter alia, by Coimbra et al. [26]. The team tested the applicability of thyme essential oil (*Thymus zygis*) to *Listeria monocytogenes* in four food matrices (chicken juice, lettuce leaf model, ultra-high-temperature (UHT)-treated skim, and whole milk). EO inhibited the growth of *L. monocytogenes* 13305 in a model medium with chicken juice and lettuce. A significant reduction in the number was observed for the two highest concentrations of EO tested from 4 to 14 days for chicken juice and from 2 to 14 days for the model medium with lettuce. Research on the possibility of using essential oils for preserving food products was also conducted by Shah et al. [27]. Thymol concentrations used in apple cider resulted in complete bacterial inhibition or were

bacteriostatic at 35 °C for *E. coli* and 32 °C for *L. monocytogenes*. Attempts have been made to use essential oils also for preserving such products as romaine lettuce, iceberg lettuce, mature bunched spinach, and baby spinach [28], snacks based on meat and seafood [29–31], juices [32], milk, yogurts, and other milk products [33–35] or chocolates [36], but also fruits or vegetables coated with edible coatings with the addition of EO [37,38].

Nanodispersion of eugenol (the basic ingredient of clove oil) in whey protein isolate and maltodextrin did not change its antimicrobial properties against *E. coli* O157: H7 and *Listeria monocytogenes*. However, nanodispersion allowed eugenol to be evenly distributed in the milk at concentrations above the solubility limit of the antimicrobial agent, which improved the antimicrobial efficacy in milk. Thus, nano-delivery systems hope to reduce the amount of antimicrobials without altering the turbidity of food products [33].

The stability of meat products during storage is a primary factor that is compromised by lipid oxidation and microbial growth. Hemmatkhak et al. [39] researched the use of active papers soaked in a nanoemulsion or Pickering emulsion containing cummin seed essential oil (CSEO). The effect of active papers on the quality and shelf-life of beef hamburgers stored at 4 °C for 7 days and at −18 °C for 60 days was investigated. Research results indicate good antioxidant and antimicrobial activity of cellulose papers impregnated in CSEO capsules. Packing beef burgers in contact with the produced active papers had a significant effect on extending the shelf life of hamburger samples by significantly reducing TBARS, the total number of mesophilic bacteria and psychrophilic. Furthermore, the sensory characteristics of the hamburgers did not changed.

It also seems important that many essential oils are on the Generally Recognized As Safe (GRAS) list published by the US Food and Drug Agency (FDA). Among the EOs that are approved for use in food are clove, rosemary, oregano, basil, mint, lavender, sage, cinnamon, and laurel [15,40,41]. Considering the above, essential oils can be not only a natural replacement for artificial preservatives but also a functional additive.

5. Microencapsulation as a Solution for EOs Application Limitations

However, there are limitations to the use of pure essential oils in food products. First of all, their characteristic strong aroma and taste can cause undesirable organoleptic changes. In addition, EOs are very sensitive to the influence of the external environment—light, oxygen, and temperature. Other limitations are their lipophilic nature and hence low water solubility, low bio-accessibility, and bio-availability [18,42]. These problems can be solved by microencapsulation—an effective method of preserving the quality of sensitive substances. Microencapsulation is defined as a method of coating or encapsulating a given material or mixture of materials within the shell of a specific material or system. The substance that is encapsulated is called “active”, “encapsulate”, “payload”, or “core” and constitutes 30–99% of the total weight of the capsule. The core material can be a single substance or a mixture of solid, liquid, and gaseous forms. The enclosing polymer is called “shell”, “wall”, “matrix”, or “coating” [42–44]. The wall material is usually insoluble and non-reactive with the core material. The wall can be made of gums, proteins, lipids, and synthetic polymers. The wall material is generally applied as a liquid (solution, suspension, or molten material) to permit enrobing of the core material. Because the task of the shell is to protect the encapsulated substance, it should have excellent film-forming and barrier properties against oxygen, water, pressure, heat, and/or light [44,45]. A single microcapsule may have a round or irregular shape, depending on the method of producing the microcapsule, the type of active, and wall materials (Figure 2). The average size of the microcapsules is 100–500 µm [46]. Therefore, this process can provide many benefits to the use of EOs in food recipes, including protecting them from harsh conditions (light, shear, oxygen, moisture, heat, and others), improving their solubility and bioavailability, increasing their controlled release, and preventing their interaction with other food ingredients. This also allows for the reduction of volatilization of volatile substances, slowing mass transfer or modifying the physical properties of the core material. It reduces the evaporative loss of liquids and the reactivity of the core material, and extends the duration

of its activity [43]. Encapsulation facilitates application by transforming the liquid into a solid phase, ensuring precise dosing, improving stability, and masking the encapsulated substance's taste and/or smell. In addition, microencapsulation of essential oils can be a viable and effective approach to liquid food matrices with high water content by increasing their dispersibility. Facilitating the distribution of EOs in food areas where microorganisms thrive (water phase) and minimizing their particle diameter may also contribute to improving their antimicrobial properties. The smaller size of the molecules favors the migration and attachment to the bacterial cell walls [18,47]. Commonly used microencapsulation techniques are emulsification, spray-drying, coaxial electro-spray system, freeze-drying, coacervation, in situ polymerization, extrusion, fluidized-bed-coating, and supercritical fluid technology [42,44].

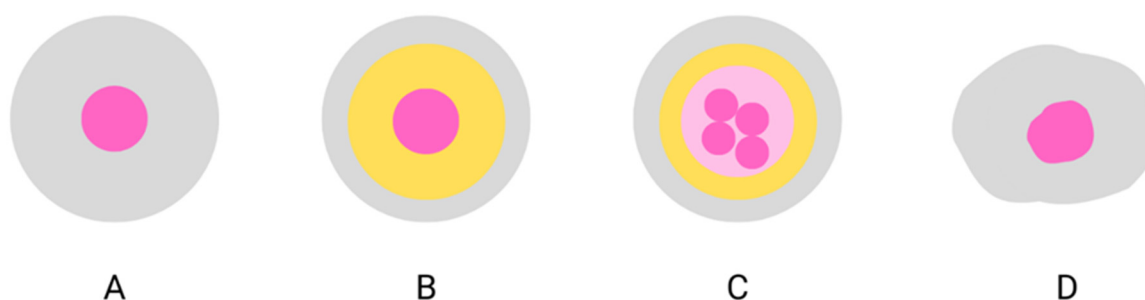


Figure 2. Schematic illustration of various morphologies formed by microencapsulation: monolayer and mononuclear microcapsule (A), multilayer and mononuclear microcapsule (B), multilayer and multinuclear microcapsule (C), and microparticle (D), own elaboration [46].

6. Spray Drying—The Most Commonly Used Method for Encapsulation of Essential Oils

Microencapsulation by spray drying is the oldest (has been used since the 1930s) and most common process used for microencapsulation in the food industry to preserve the physicochemical properties of volatile compounds such as essential oils. This method is most often used in the food industry due to its low production costs, large-scale production in a continuous mode, variety of encapsulating matrices, and adequate retention and stability of volatile compounds [22,42]. It consists of atomizing the emulsion in a drying medium at a relatively high temperature, which allows for quick evaporation of water and almost instantaneous encapsulation of the core material [42,44]. Microencapsulation with the use of spray drying is characterized by high retention of volatile substances during processing and their protection during storage. During this process, multinuclear capsules are formed in which the essential oil is distributed both inside and on the surface of the microcapsule, and thus volatile substances may be lost. This loss might occur during the process at three stages: during atomization, after the drop formation on the surface when a stable membrane has not been formed, and where the water inside the drop exceeds the boiling point and bubbles formed within the drop burst, cracking the surface and releasing volatiles [48]. Essential oils are substances highly sensitive to temperature. Ambient temperature crucially influences EOs stability; because of this, EOs may be degraded during this process. In general, chemical reactions are accelerated by increasing temperature (according to the Arrhenius equation). On this basis, van't Hoff's law states that a 10 °C increase in temperature approximately doubles the rate of chemical reactions. The degradation of essential oils by heat is a chemical phenomenon and can occur by various pathways, which can be broadly classified as oxidative degradation, cleavage of the C-C bond, elimination, hydrolysis, and thermal rearrangement. Under the influence of elevated temperature and due to their structural relationship within the same chemical groups, components of essential oils can easily transform into each other mutually, which may cause changes in their taste, smell, and antimicrobial activity [21,48,49]. For this reason, it seems legitimate to look for alternative methods for the spray-drying of essential oils. To

reduce the loss of essential oils and the undesirable chemical changes that may occur during their spray drying, the use of complex coacervation seems to be an interesting alternative.

7. Simple and Complex Coacervation—What Is the Difference?

Coacervation is one of the oldest and most widely used encapsulation techniques. It is a relatively simple method that can be compared to a modified emulsification technique. Coacervation name comes from the Latin word *acervus*, which means aggregation, and the prefix *co* indicates the fusion of colloid particles [43]. The mechanism of this process consists of the separation of the hydrocolloid from the primary solution followed by agglomeration into a separate, liquid phase which is called “coacervate”. The coacervates are called the “continuous phase”, whereas the second phase is called the “equilibrium solution” [43,50]. The coacervation process can be divided into four stages: suspending the core material particles in the liquid phase, production of a three-phase system, i.e., secretion of the second liquid phase (coacervate), deposition of liquid polymer around the core, gelling, and solidification of the microcapsule wall (Figure 3).

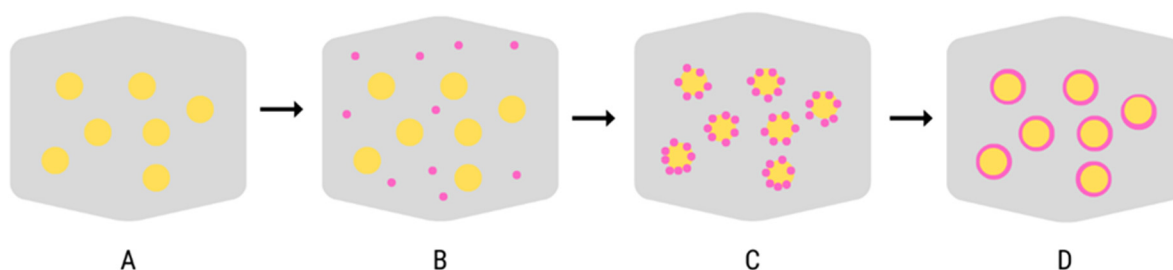


Figure 3. The mechanism of microcapsules formation in the coacervation method, liquid phase (A), suspending the core material in the liquid phase (B), deposition of liquid polymer around the core (C), gelling, and solidification of the microcapsule wall (D), own elaboration [43].

Coacervation has been classified into simple (SC) and complex coacervation (CC). Simple coacervation refers to the cases where only one polymer is involved and salted out by the action of electrolytes (sodium sulfate) or desolvated by the addition of a water-miscible nonsolvent (ethanol) or by increasing/decreasing the temperature [50,51]. Complex coacervation is a phase separation process caused by the interaction of two or more oppositely charged colloids (biopolymers), usually proteins and polysaccharides. The term complex coacervation was first introduced by Bungenberg de Jong and Kruyt in the 1940s to distinguish it from simple single polymer coacervation [43]. In this technique, the liquid phase separates from the polymer-rich (coacervate) phase.

The main driving force for complex coacervation is the reduction in free electrostatic energy of the reaction system resulting from the interaction between oppositely charged ions [52]. This process is also influenced by parameters such as pH (coacervates formation occurs over a narrow pH range below the isoelectric point), ionic strength, protein-polysaccharide ratio, total biopolymer concentration, type of core material, and the core:wall ratio [42,48,53,54]. The speed of agitation plays an important role in controlling the size of the coacervates formed. In addition, the difference between the polymer loads must be large enough to cause interaction, but not large enough to cause precipitation. Highly charged molecules are reported to have an extended molecular conformation resulting in unfavorable coacervation [52]. Microcapsules prepared in this way are insoluble in water and heat-resistant but the main advantages of complex coacervation compared to other microencapsulation methods are the overall higher encapsulation efficiency and the possibility of using controlled release. The process results in a circular microcapsule in which the core is surrounded by a wall material that protects the active compound [48,53,54].

8. Wall Materials Used in Complex Coacervation

8.1. Gelatin and Arabic Gum—Standard in Complex Coacervation

The most common system used in complex coacervation is gelatin (G)–Arabic gum (AG) [54–57] in Table 1. It is recommended due to its abundance, biocompatibility, and biodegradability [36,38]. Two types of gelatin can be distinguished—A and B. Gelatin A is formed by partial hydrolysis of collagen in an acidic environment, whereas gelatin B is in an alkaline environment. The isoelectric point (pI) of gelatin A produced ranges from pH 6–9, whereas gelatin B possesses a pI of 4.8–5 [58,59]. During the complex coacervation, the electrostatic attraction between gelatin and the anionic polysaccharide (i.e., Arabic gum) occurs at a pH below 9 for gelatin A and a pH below 5 for gelatin B [59]. In the case of G and AG, the mechanism of complex coacervation can be explained by the electrostatic attraction between the positive protein charges (NH_3^+) and negative charges derived from AG (COO^-) [59,60]. Gelatin and Arabic gum when exposed to electrostatic interactions form a coacervate layer that hardens in the process of gelatin cross-linking. In a chemically induced cross-linking process, the insoluble network is formed by the reaction of the aldehyde residues of the cross-linking agent and the amino groups of the protein. This newly formed network strengthens the wall of the capsule, thus facilitating the drying process and increasing the storage stability of the capsules [38]. However, this process is chemically induced by formaldehyde, glutaraldehyde, glyoxal, or epichlorohydrin, which are considered toxic to the human body, and are most often used to cause this process. This is one of the major limitations of the production of microcapsules for the food industry using the (G)–(AG) system [50,52,61]. This is not the only drawback of this combination. Preparation of a gelatin solution generally requires a relatively high temperature (50–60 °C) to completely dissolve the gelatin [52,56]. For that reason, the quality of sensitive compounds such as essential oil could deteriorate at this temperature. Another disadvantage of gelatin is its animal origin and, in the case of beef gelatin, its possible association with bovine spongiform encephalopathy (“mad cow disease”). Therefore, the most popular gelatin is that of porcine origin—not acceptable by a certain group of consumers based on their religious and dietary preferences [52]. Moreover, due to the increasing popularity of vegetarian and vegan diets, the current aim in the food industry is to minimize the use of ingredients of animal origin.

Arabic gum, also known as gum acacia, is a complex anionic polysaccharide with fractions of 90–99% arabinogalactan and 1% glycoprotein. This amazing composition gives it effective surface properties. Furthermore, it has a molecular structure with a galactan main chain carrying the highly branched galactose/arabinose side chains which contributes to a much higher negative charge density in comparison to a linear polysaccharide of the same composition. Moreover, Arabic gum has good cold solubility due to the presence of residual charged groups and peptide fragments [43,62]. It also has low solution viscosity and the ability to form a protective film around emulsion droplets. All of this above makes Arabic gum an effective emulsifier and good encapsulating agent [43,63].

As already mentioned, the combination of G and AG is the most commonly used combination of wall materials in complex coacervation. After pioneering systematic studies of the complex coacervation of gelatin and acacia in 1949, the first practical application of this system was the microencapsulation of dyes [43,64]. Since then, a huge amount of work on the microencapsulation of various active substances using the complex coacervation of this pair of polymers as one of the leading applications of protein-polysaccharide coacervation in encapsulation technology has been studied over the last few decades. Coacervation between G and AG is induced with an aqueous solution of both polymers at pH 6–7 and a temperature of 50–60 °C, above the gelatin gelling point. This system has already been used to encapsulate various types of flavors and colorants [65], oils [50,54,66,67], food ingredients [56], and medicines [68]. It has also been used for the complex coacervation of essential oils. A research team led by Lv et al. [62] confirmed that the pH of 4.80 and the mixing ratio 1:1 between G and AG were suitable for the preparation of spherical nanoparticles with trapped jasmine essential oil. Analysis of structural properties and volatile flavor

compounds showed that such nanocapsules have good heat resistance capability against humid heat (80 °C). The results suggested that the G-GA system may have potential use as a delivery vehicle for functional ingredients food. The results of another study examining the G-GA system [69,70] showed that the obtained coacervate microcapsules can be used for the sustainable release of EOs during food storage and as promising organic preservatives to inhibit foodborne pathogens.

8.2. Milk Proteins and Polysaccharides

Milk proteins (MP) have been extensively used in the food industry because of their amphiphilic nature, which allows them to adsorb and spread around the oil/water matrix. Those proteins are also popular as food additives for their nutritional, functional, and active properties. Milk proteins can be divided into whey proteins (WPI) (alpha with pI ranges from 4.3–4.7 and beta lactalbumin, pI = 5.2) and caseins, with pI ranges from 4.9–5.6 [59,71,72]. Many authors [71–74] have conducted complex coacervation with the use of milk proteins and various types of polysaccharides. From the research carried out so far, it is possible to conclude that increasing the concentration of MP and biopolymer ratio leads to an increase in the pH at which the CC process occurs including. This, in turn, leads to an increase in the average size of the microcapsules formed. This phenomenon can be explained by the decreasing force of electrostatic repulsion between proteins and polysaccharides [59]. The limitation in the use of milk proteins in the coacervation process is the fact that during the preparation of emulsions (ultrasound, temperature, high pressure), their partial denaturation and conformational changes may occur. This negatively affects the process of coacervate formation. As already mentioned, the food industry is trying to reduce the use of animal products. In addition, milk proteins are strong allergens [75].

Arabic gum is used as a polysaccharide for complex coacervation, along with milk proteins, e.g., chitosan, carrageenan, or alginates, which are also often used.

Chitosan (CH) is a cationic polysaccharide produced by the deacetylation of chitin in the hydrolysis of acetyl amino groups in a highly alkaline environment and at elevated temperatures. Its structure consists of D-glucosamine and N-acetyl-D-glucosamine, linked by β (1 \rightarrow 4) O-glycosidic bonds. Its low toxicity and allergenicity, as well as hydrophobicity, biodegradability, tissue biocompatibility, and antimicrobial activity, allow it to be used in edible film formulations or microencapsulation of bioactive compounds [76]. A study conducted by Tavares et al. [76] aimed to encapsulate garlic aqueous extract by complex coacervation between WPI and CH. FTIR analysis confirmed that garlic compounds were intact and encapsulated. Scanning electron microscopy images showed all microparticles with a spherical shape and no evidence of cracking or fissures on the surface. Therefore, it can be concluded that the combination of WPI and CH is a good alternative for use as wall systems to protect the bioactive compounds.

Carrageenan (CG) is the general name for a group of high molecular weight sulfated anionic polysaccharides extracted from red seaweeds formed by alternate units of D-galactose and 3, 6-anhydro-galactose (3, 6-AG) joined by α -1, 3, and β -1, 4-glycosidic linkage [72,77]. There are three main types of carrageenan, called kappa (κ), iota (ι), and lambda (λ). They are differentiated based on the number and position of sulfate groups on the galactose/anhydrogalactose chain. κ -carrageenan contains one sulfate group, whereas ι and λ have two and three per disaccharide repeating unit, respectively [72,78]. Since CG is a sulfated polysaccharide, it has a negative net charge in a wide pH range, which allows it to interact with positively charged compounds such as WPI under its isoelectric point where the protein has a positive net charge [72].

Alginates are natural polysaccharides isolated from the cell walls of various species of brown algae. They consist of linear chains (1–4)-connected b-D-mannuronic acid residues and A-L-guluronic acid in various proportions [79]. Bastos et al. [80] conducted extensive research on the microcapsule structure of black pepper essential oil (BPEO) obtained in the process of complex coacervation between lactoferrin (LF) and sodium alginate (SA). The authors indicate that the LF-SA system resulted in high encapsulation efficiency (>80%), and

the essential oil components were retained. The main identified component of BPEO was β -caryophyllene. After the encapsulation process, 97.5% of this compound was protected. In addition, the researchers presented the results of studies obtained with the use of an artificial gastrointestinal tract. The black pepper EO capsule demonstrated resistance under oral and gastric conditions and release in the intestine, contributing to absorption in the *in vitro* simulation.

An interesting study was also conducted by Rojas-Moreno et al. [81] to compare the microencapsulation of orange essential oil by complex coacervation with whey protein isolate (WPI) and different polysaccharides: carboxymethylcellulose (CMC), SA, and CH. The process was successfully performed with an encapsulation efficiency of 94% (WPI:CMC), 88% (WPI:SA), and 91% (WPI:CH). Another study conducted by Soliman et al. [82] showed that EO microcapsules (thyme, cinnamon, cloves) made with calcium alginate can retain 30–50% of the antifungal activity of EO after a storage period of 8 days, whereas all of these EOs have lost all their antifungal activity after two days of storage.

8.3. Plant Proteins and Polysaccharides

Due to the above-described trends among consumers and the limitations connected with the use of gelatin and milk proteins for the process of complex coacervation, plant-origin proteins were of growing interest. Another reason is they are environmentally friendly, low cost, available, and have interesting functional properties [45]. Among various plant proteins, soy protein (SP) is the most well-studied and most commonly employed in the microencapsulation technique. This is because SP has functional properties for encapsulation, such as emulsification, solubility, film-forming, and water binding capacity, in addition to presenting high nutritional value (contains at least 90% protein; it is thus virtually free from lipids and carbohydrates) [83]. Due to their amphipathic nature (hydrophilic and hydrophobic), these proteins exhibit a good ability to diffuse and/or adsorb, and stabilize the interface of, oil droplets during emulsification, thus acting as effective emulsifiers to form and stabilize oil-in-water emulsions [84]. These properties of SP make it widely used in the microencapsulation process. However, the hydrophilicity/hydrophobicity balance of a protein's surface is also thought to impact protein solubility, and this is crucial for the process of comprehensive coacervation. Soy protein is characterized by low solubility, but it can be increased by adding a polymer. Complexation-enhanced protein solubility is well observed in the literature [43,48,50,73,85]. It has been identified that the biopolymer mixing ratio is the factor most responsible for the solubility of proteins when they are in complexes. Significantly improved protein solubility for mixtures of soy protein isolate and xanthan gum at mixing ratios of 1:1 to 1:4 was observed [85]. Many research teams have confirmed that the use of soy protein together with polymer results in good stability of the core material during storage [70,86] or high process yield and the encapsulation efficiency [70,83].

Yuan et al. [70] conducted a study in which they proved that the use of soy protein and chitosan as wall materials for the complex coacervation of algae oil is effective in reducing its oxidation during storage. In similar studies [87] of the same SPI-CH system, DSC thermograms revealed increased denaturation temperature of SPI from 78 to 85 °C and elevated network thermal stability from about 38 to 43 °C.

However, proteins such as peas (PP), rice (RP), lentils (LP), or wheat (WP) are becoming popular in recent years. They possess different molecular weights and isoelectric points depending on the extraction method and plant source. As a result of using them instead of those of animal origin, the coacervation process can take place at room temperature. Yellow Pea (*Pisum sativum* L.) isolates are attractive for food and nutraceutical applications among plant proteins. This is due to their health properties, and the fact that PP is not allergenic and is gluten-free. In addition, PP is characterized by wide availability and low price [88].

The interactions between PP and different polysaccharides were applied (AG, tragacanth gum—TCG, tara gum—TG) to the microencapsulation of α -tocopherol by spray drying of complex coacervates. The effect of the protein/polysaccharide ratio was demonstrated—an increase

in the proportion of polysaccharides increased the size of the particles in the suspension. In the presence of proteolytic enzymes, the PP-TCG mixture retained a stronger gastro-protective effect compared to the PP-AG matrices. The results of this study demonstrated the ability of PP to bind to plant polysaccharides, especially gum tragacanth, to form an interesting microencapsulation coating that is resistant to gastric digestion [89].

The influence of pH on the course of the complex coacervation process and the wall:core ratio on the physicochemical properties of the produced microcapsules have already been investigated [90]. The results indicate that the pH of the coacervation formation had a great influence on the microstructure of the coacervates. As a result, the technical characteristics of microencapsulation such as powder yield (PY), encapsulation efficiency (EE), and oil distribution in the microcapsules, as well as the oxidative stability of the encapsulated oil, dictated different results. PP and sugar beet pectin (SBP) were used as wall materials, and hemp seed oil (HSO) was the core material. Microcapsules spray dried from PP-SBP coacervates at pH 3.5 showed lower EE than those at pH 2.5. However, holes and/or partially broken particles were observed in the spray-dried microcapsules prepared at pH 2.5 (SEM observation), which had the effect of deteriorating the protection against oxidation of the encapsulated oil. Thus, the choice of the wall:core ratio and the pH of the coacervation formation is extremely important and should be determined by taking into account the balance between technical performance and the oxidative stability of the core material [Tab. 1]. Further research into pea protein as wall material is advisable.

At present, there are no studies on the use of PP or any other plant protein for the complex coacervation of essential oils. Nevertheless, it is known that they are able to form microcapsules in the process of complex coacervation, increasing oxidative and thermal stability of core substances. They can be successfully used for the controlled release of the core material and as a delivery system for the active ingredient. Therefore, we believe that complex coacervation using plant proteins has a bright future ahead of it.

8.4. Mucilage Instead of Commonly Used Polysaccharides

It is not only animal proteins that can be a starting point for the discussion. Additionally, Arabic gum, widely used in CC, which, despite its natural origin, has recently been negatively perceived by consumers. This is because AG is assigned the symbol E. The consumer approach has led scientists to try to replace Arabic gum with polysaccharides derived from mucilage raw materials such as chia seeds (*Salvia hispanica*), cress seeds (*Cardamine*), flax seeds (*Linum usitatissimum*), marshmallow (*Althaea officinalis*), aloe vera, prickly pear (*Opuntia ficus-indica*), etc. [91–94]. The combination of gelatin and chia mucilage results in a high encapsulation efficiency (>90%) of the essential oil [93].

Chia (*Salvia hispanica* L.) was eaten centuries ago as a staple food by the Mayas and Aztecs of Central and North America. It fell into oblivion after the Spanish conquest and is now experiencing its renaissance. It can be found in many different products, mainly for breakfast-bread, rolls, muesli, yogurts, ready-to-eat porridge, or smoothies. Chia seeds have a unique nutritional profile, hence the increase in popularity. Chia is an excellent source of ω -3 and ω -6 fatty acids, proteins with high biological value, antioxidants, vitamins, and minerals. In addition, it has been reported that the consumption of seeds is able to prevent inflammation and the occurrence of civilization diseases [95–98]. What is most important, chia seeds are capable of absorbing large amounts of water through swelling. Upon hydration, a hydrogel network is formed—soluble fiber, known as chia seed mucilage (CM)—which is and can be used in emulsification and foaming processes. Chia seed polysaccharides consist of, inter alia, D-xylose, D-glucose, β -d-xylopyranosyl acid, α -d-glucopyranosyl, and 4-O-methyl- α -d-glucopyranosyluronic acid [96,99]. CM is a promising material for the food industry because like popular vegan thickeners such as alginate, polyvinyl alcohol, and carrageenan, CM is biodegradable and digestible [95,100]. Consumption of CM has a positive effect on health by facilitating the passage of the contents in the intestines, thanks to which the peristalsis is improved. Additionally, CM has prebiotic properties [100,101].

Table 1. Cont.

Wall Material	Wall Material Ratio	Core Material—Essential Oil	Wall:Core Ratio	pH	Method of Emulsification	Encapsulation Efficiency [%]	Reference
Gelatin	Chia mucilage	Oregano	1:1	3.6	Ultrasonication	91–79	[93]
Whey protein isolate	Quince mucilage	No core material		4.0	Magnetic stirrer	80–67	[74]

9. Complex Coacervation of Essential Oils

The process of microencapsulating essential oils by complex coacervation occurs in stages. The first one is hydration and preparation of wall materials solution. The essential oils and an emulsifier (e.g., Tween 20, 60, 80) are then added to these solutions, and the emulsification process is carried out. This step is essential because the quality of the emulsion and the interaction between its droplets directly affect the stability of the microcapsules produced later. The final step is curing by spray drying or freeze-drying [59,93].

Microencapsulation of essential oils using complex coacervation allows for their controlled release. It is the process of delivering EO delayed after administration or incorporation into the food matrix for an extended period [59,105]. This process is influenced by environmental conditions (type of food matrix), type of EO, the composition of microcapsules (proteins, polysaccharides), and microcapsule architecture. Essential oils can be released from their microcapsules through a variety of mechanisms (Figure 4). The swelling mechanism involves increasing the pore size as the matrix swells, which promotes the release of the encapsulated Eos. The mechanism of erosion is the dissolution of the outer part of the support (surface erosion) or all of the support (bulk erosion), often due to enzymatic or chemical hydrolysis. The mechanism of fragmentation is the rupture or breakage of the support matrix, which often occurs due to mechanical forces. The resulting increase in surface area and shorter diffusion paths mean that the bioactive agents are released from the fragments faster than the original carrier. The diffusion mechanism involves the diffusion of the bioactive component through the carrier matrix into the surrounding environment. EO microcapsules should be designed to be used in a specific product because food is exposed to a variable temperature, ionic strength, pH and mechanical conditions and stress during processing and storage [76,104,106,107]. The preparation of microcapsules of essential oils produced by complex coacervation can be an effective method to preserve their physicochemical properties. At the same time, it can contribute to increasing the applicability of essential oils in food as natural additives with a preservative effect and increasing the nutritional value of the final product. EO microcapsules can be an effective way to reduce the use of synthetic food additives while enabling the creation of interesting products placed in the functional food segment.

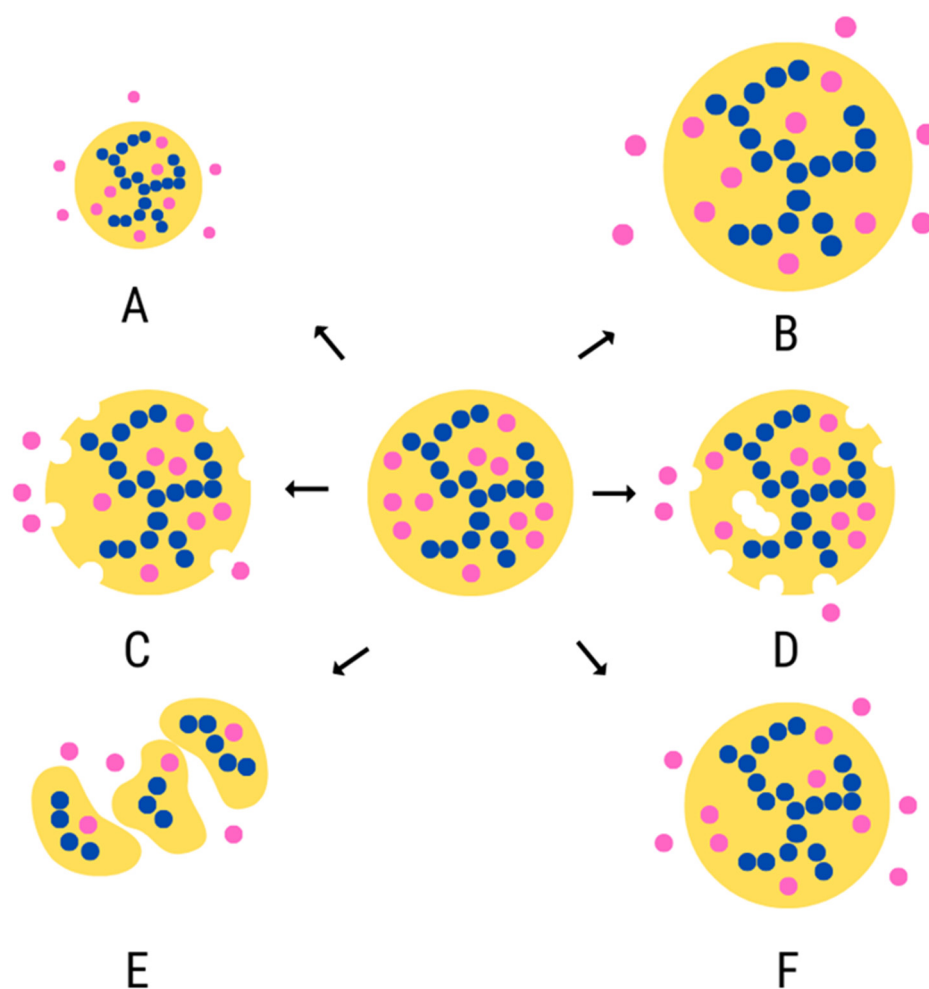


Figure 4. Various types of release mechanisms for EO-encapsulated component: shrinkage (A), swelling (B), surface erosion (C), bulk erosion (D), fragmentation (E), diffusion (F), own elaboration [106].

10. Conclusions and Future Perspectives

The food industry is trying to move away from the use of artificial additives and preservatives in food. Currently, substances of plant origin, including essential oils, are gaining more and more popularity. Despite the strongly documented pro-health and antimicrobial properties, the use of essential oils on a larger scale is currently not possible due to their very strong taste and aroma, which negatively affects the acceptability of the products in which they are found. In addition, they are characterized by high instability (sensitivity to light, oxygen, and temperature) and a hydrophobic nature, which prevents their solubility in the water phase of food where microorganisms develop. Therefore, scientists are looking for solutions that will preserve their properties during storage and at the same time mask their strong taste and smell and reduce their hydrophobicity.

All these limitations may be solved by microencapsulating EOs using complex coacervation. It is an alternative method to the most commonly used spray drying. It allows not only to eliminate the elevated temperature during the encapsulation process, but also to better enclose the core material and its protection from the external environment. Additionally, the fact that microcapsules of essential oils obtained through complex coacervation would constitute a kind of nutraceutical deserves attention. The use of non-allergenic proteins of plant origin (peas, rice) and polysaccharides from chia seeds with properties improving intestinal motility would significantly increase the nutritional value and health-promoting effect of the product to which microcapsules prepared in this way would be added.

Future research should focus on the possibility of producing microcapsules of essential oils as described. There is also no information on the in situ use of essential oils as antimicrobial agents.

Author Contributions: A.N. invented and prepared a manuscript, made figures and tables. M.K. critically reviewed and revised the manuscript. All authors have read and agreed to the published version of the manuscript.

Funding: This research received no external funding.

Institutional Review Board Statement: Not applicable.

Informed Consent Statement: Not applicable.

Data Availability Statement: Not applicable.

Conflicts of Interest: The authors declare no conflict of interest.

References

1. Kunicka-Styczyńska, A. Olejki eteryczne jako alternatywa dla syntetycznych konserwantów żywności—Praca przeglądowa. In *Innowacyjne Rozwiązania w Technologii Żywności i Żywieniu Człowieka*; Tarko, T., Drożdż, I., Najgebauer-Lejko, D., Duda-Chodak, A., Eds.; Oddział Małopolski Polskiego Towarzystwa Technologów Żywności: Kraków, Poland, 2016; Volume 122, pp. 175–184.
2. Falleh, H.; Benjemaa, M.; Djebblai, K.; Abid, S.; Saada, M.; Ksouri, R. Application of the mixture design for optimum antimicrobial activity: Combined treatment of *Syzygium aromaticum*, *Cinnamomum zeylanicum*, *Myrtus communis*, and *Lavandula stoechas* essential oils against *Escherichia coli*. *J. Food Process. Preserv.* **2019**, *43*, 1–11. [[CrossRef](#)]
3. Patrignani, F.; Siroli, L.; Braschi, G.; Lanciotti, R. Combined use of natural antimicrobial based nanoemulsions and ultra-high pressure homogenization to increase safety and shelflife of apple juice. *Food Control* **2020**, *111*, 107051. [[CrossRef](#)]
4. Korbutowicz, T. Żywność funkcjonalna na rynku światowym. *Gosp. Reg. Międz.* **2018**, *53*, 1–12. [[CrossRef](#)]
5. Topolska, K.; Florkiewicz, A.; Filipiak-Florkiewicz, A. Functional Food—Consumer Motivations and Expectations. *Int. J. Environ. Res. Public Health* **2021**, *18*, 5327. [[CrossRef](#)] [[PubMed](#)]
6. Asioli, D.; Aschemann-Witzel, J.; Caputo, V.; Vecchio, R.; Annunziata, A.; Næs, T.; Varela, P. Making sense of the “clean label” trends: A review of consumer food choice behavior and discussion of industry implications. *Int. Food Res. J.* **2017**, *99*, 58–71. [[CrossRef](#)]
7. Rogozińska, I.; Wichrowska, D. Najpopularniejsze dodatki utrwalające stosowane w nowoczesnej technologii żywności. *Inż. Apar. Chem.* **2011**, *50*, 19–21.
8. Maruyama, S.; Streletskaia, N.A.; Lim, J. Clean label: Why this ingredient but not that one? *Food Qual. Prefer.* **2020**, *87*, 104062. [[CrossRef](#)]
9. Grogan, K.A. The value of added sulfur dioxide in French organic wine. *Agric. Food Econ.* **2015**, *3*, 1–25. [[CrossRef](#)]
10. Gyawali, R.; Ibrahim, S.A. Natural products as antimicrobial agents. *Food Control* **2014**, *46*, 412–429. [[CrossRef](#)]
11. Voltolini, S.; Pellegrini, S.; Contatore, M.; Bignardi, D.; Minale, P. New risks from ancient food dyes: Cochineal red allergy. *Eur. Ann. Allergy Clin. Immunol.* **2014**, *46*, 232–233.
12. Aminzare, M.; Hashemi, M.; Hassanzad, A.H.; Hejazi, J. The Use of Herbal Extracts and Essential Oils as a Potential Antimicrobial in Meat and Meat Products; A review. *J. Hum. Environ. Health Promot.* **2016**, *1*, 63–74. [[CrossRef](#)]
13. Laranjo, M.; Fernandez-Leon, A.; Potes, M.; Santos, A.M. Use of essential oils in food preservation. In *Antimicrobial Research: Novel Bioknowledge and Educational Programs*; Mendez-Vilas, A., Ed.; Formatex Research Center: Badajoz, Spain, 2017; Volume 6, pp. 177–188.
14. Hashemi, S.M.B.; Khaneghah, A.M.; Tavakolpour, Y.; Asnaashari, M.; Mehr, H.M. Effects of ultrasound treatment, UV irradiation and Avishan-e-Denaee essential oil on oxidative stability of sunflower oil. *J. Essent. Oil Bear. Plants* **2015**, *18*, 1083–1092. [[CrossRef](#)]
15. Pateiro, M.; Barba, F.J.; Domínguez, R.; Sant’Ana, A.S.; Khaneghah, A.M.; Gavahian, M.; Gómez, B.; Lorenzo, J.M. Essential oils as natural additives to prevent oxidation reactions in meat and meat products: A review. *Int. Food Res. J.* **2018**, *113*, 156–166. [[CrossRef](#)]
16. Hyldgaard, M.; Mygind, T.; Meyer, R.L. Essential oils in food preservation: Mode of action, synergies, and interactions with food matrix components. *Front. Microbiol.* **2012**, *3*, 12. [[CrossRef](#)]
17. Giacometti, J.; Kovačević, D.B.; Putnik, P.; Gabrić, D.; Bilušić, T.; Krešić, G.; Stulić, V.; Barba, F.J.; Chemat, F.; Barbosa-Cánovas, G.; et al. Extraction of bioactive compounds and essential oils from Mediterranean herbs by conventional and green innovative techniques: A review. *Int. Food Res. J.* **2018**, *113*, 245–262. [[CrossRef](#)] [[PubMed](#)]
18. Delshadi, R.; Bahrami, A.; Tafti, A.G.; Barba, F.J.; Williams, L.L. Micro and nano-encapsulation of vegetable and essential oils to develop functional food products with improved nutritional profiles. *Trends Food Sci. Technol.* **2020**, *104*, 72–83. [[CrossRef](#)]
19. Valderrama, F.; Ruiz, F. An optimal control approach to steam distillation of 936 essential oils from aromatic plants. *Comput. Chem. Eng.* **2018**, *117*, 25–31. [[CrossRef](#)]

20. Falleh, H.; Benjemaa, M.B.; Saada, M.; Ksouri, R. Essential oils: A promising eco-friendly food preservative. *Food Chem.* **2020**, *330*, 127268. [[CrossRef](#)] [[PubMed](#)]
21. Turek, C.; Stintzing, F.C. Stability of Essential Oils: A Review. *Compr. Rev. Food Sci.* **2013**, *12*, 40–53. [[CrossRef](#)]
22. Veiga, R.D.S.D.; Aparecida Da Silva-Buzanello, R.; Corso, M.P.; Canan, C. Essential oils microencapsulated obtained by spray drying: A review. *J. Essent. Oil Res.* **2019**, *31*, 457–473. [[CrossRef](#)]
23. Singletary, K. Rosemary, An Overview of Potential Health Benefits. *Nutr. Today* **2016**, *51*, 102–112. [[CrossRef](#)]
24. Valková, V.; Ďuranová, H.; Galovičová, L.; Vukovic, N.L.; Vukic, M.; Kačaniová, M. In Vitro Antimicrobial Activity of Lavender, Mint, and Rosemary Essential Oils and the Effect of Their Vapours on Growth of *Penicillium* spp. in a Bread Model System. *Molecules* **2021**, *26*, 3859. [[CrossRef](#)] [[PubMed](#)]
25. Stojanović-Radić, Z.; Pejić, M.; Joković, N.; Jokanović, M.; Ivić, M.; Šojić, B.; Škaljac, S.; Stojanović, P.; Mihajilov-Krstev, T. Inhibition of *Salmonella* Enteritidis growth and storage stability in chicken meat treated with basil and rosemary essential oils alone or in combination. *Food Control* **2022**, *90*, 332–343. [[CrossRef](#)]
26. Coimbra, A.; Carvalho, F.; Duarte, A.P.; Ferreira, S. Antimicrobial activity of *Thymus zygis* essential oil against *Listeria monocytogenes* and its application as food preservative. *Innov. Food Sci. Emerg. Technol.* **2022**, *80*, 103077. [[CrossRef](#)]
27. Shah, B.; Davidson, P.M.; Zhong, Q. Nanocapsular Dispersion of Thymol for Enhanced Dispersibility and Increased Antimicrobial Effectiveness against *Escherichia coli* O157:H7 and *Listeria monocytogenes* in Model Food Systems. *Appl. Environ. Microbiol.* **2012**, *78*, 8448–8453. [[CrossRef](#)] [[PubMed](#)]
28. Moore-Neibel, K.; Gerber, C.; Patel, J.; Friedman, M.; Jaroni, D.; Ravishankar, S. Antimicrobial activity of oregano oil against antibiotic-resistant *Salmonella enterica* on organic leafy greens at varying exposure times and storage temperatures. *Food Microbiol.* **2013**, *34*, 123–129. [[CrossRef](#)]
29. Kocatepe, D.; Turan, H.; Altan, C.O.; Keskin, I.; Ceylan, A.; Köstekli, B.; Candan, C. Influence of different essential oils on marinated anchovy (*Engraulis encrasicolus* L.) during refrigerated storage. *Food Sci. Technol.* **2019**, *39*, 255–260. [[CrossRef](#)]
30. Lages, L.Z.; Radünz, M.; Timm Gonçalves, B.; Silva da Rosa, R.; Fouchy, M.V.; de Cássia dos Santos da Conceição, R.; Gularte, M.A.; Barboza Mendonça, C.R.; Gandra, E.A. Microbiological and sensory evaluation of meat sausage using thyme (*Thymus vulgaris*, L.) essential oil and powdered beet juice (*Beta vulgaris* L., Early Wonder cultivar). *LWT* **2021**, *148*, 111794. [[CrossRef](#)]
31. Snoussi, A.; Chouaibi, M.; Ben Haj Koubaier, H.; Bouzouita, N. Encapsulation of Tunisian thyme essential oil in O/W nanoemulsions: Application for meat preservation. *Meat Sci.* **2022**, *188*, 108785. [[CrossRef](#)] [[PubMed](#)]
32. Bento, R.; Pagán, E.; Berdejo, D.; de Carvalho, R.J.; García-Embid, S.; Maggi, F.; Magnani, M.; Evandro de Souza, L.; García-Gonzalo, D.; Pagán, R. Chitosan nanoemulsions of cold-pressed orange essential oil to preserve fruit juices. *Int. J. Food Microbiol.* **2020**, *331*, 108786. [[CrossRef](#)] [[PubMed](#)]
33. Shah, B.; Davidson, P.M.; Zhong, Q. Nanodispersed eugenol has improved antimicrobial activity against *Escherichia coli* O157:H7 and *Listeria monocytogenes* in bovine milk. *Int. J. Food Microbiol.* **2013**, *161*, 53–59. [[CrossRef](#)] [[PubMed](#)]
34. Bedoya-Serna, C.M.; Dacanal, G.C.; Fernandes, A.M.; Pinho, S.C. Antifungal activity of nanoemulsions encapsulating oregano (*Origanum vulgare*) essential oil: In vitro study and application in minas padrão cheese Braz. *J. Microbiol.* **2018**, *49*, 929–935. [[CrossRef](#)]
35. Zedan, H.; Hosseini, S.M.; Mohammadi, A. The effect of tarragon (*Artemisia dracunculus*) essential oil and high molecular weight Chitosan on sensory properties and shelf life of yogurt. *LWT* **2021**, *147*, 111613. [[CrossRef](#)]
36. Muhammad, D.R.A.; Saputro, A.D.; Rottiers, H.; Van de Walle, D.; Dewettinck, K. Physicochemical properties and antioxidant activities of chocolates enriched with engineered cinnamon nanoparticles. *Eur. Food Res. Technol.* **2018**, *244*, 1185–1202. [[CrossRef](#)]
37. Wang, H.; Guo, L.; Liu, L.; Han, B.; Niu, X. Composite chitosan films prepared using nisin and *Perilla frutescens* essential oil and their use to extend strawberry shelf life. *Food Biosci.* **2021**, *41*, 101037. [[CrossRef](#)]
38. Reis, D.R.; Ambrosi, A.; Di Luccio, M. Encapsulated essential oils: A perspective in food preservation. *Future Foods* **2022**, *5*, 100126. [[CrossRef](#)]
39. Hemmatkhah, F.; Zeynali, F.; Almasi, H. Encapsulated Cumin Seed Essential Oil-Loaded Active Papers: Characterization and Evaluation of the Effect on Quality Attributes of Beef Hamburger. *Food Bioproc. Tech.* **2020**, *13*, 533–547. [[CrossRef](#)]
40. Tajkarimi, M.M.; Ibrahim, S.A.; Cliver, D.O. Antimicrobial herb and spice compounds in food. *Food Control* **2010**, *21*, 1199–1218. [[CrossRef](#)]
41. Generally Recognized as Safe, §182.20 Essential Oils, Oleoresins (Solvent-Free), and Natural Extractives (Including Distillates). Available online: <https://www.accessdata.fda.gov/scripts/cdrh/cfdocs/cfcfr/cfrsearch.cfm?fr=182.20> (accessed on 10 June 2022).
42. Bakry, A.M.; Abbas, S.; Ali, B.; Majeed, H.; Abouelwafa, M.Y.; Mousa, A.H.; Liang, L. Microencapsulation of Oils: A Comprehensive Review of Benefits, Techniques, and Applications. *Compr. Rev. Food Sci.* **2016**, *15*, 143–182. [[CrossRef](#)]
43. Devi, N.; Sarmah, M.; Khatun, B.; Maji, T. Encapsulation of active ingredients in polysaccharide-protein complex coacervates. *Adv. Colloid Interface Sci.* **2017**, *239*, 136–145. [[CrossRef](#)]
44. Arenas-Jal, M.; Suñé-Negre, J.M.; García-Montoya, E. An overview of microencapsulation in the food industry: Opportunities, challenges, and innovations. *Eur. Food Res. Technol.* **2020**, *246*, 1371–1382. [[CrossRef](#)]
45. Shishir, M.R.I.; Xie, L.; Sun, C.; Zheng, X.; Chen, W. Advances in micro and nano-encapsulation of bioactive compounds using biopolymer and lipid-based transporters. *Trends Food Sci. Technol.* **2018**, *78*, 34–60. [[CrossRef](#)]

46. Mohammadalnejhad, S.; Kurek, M. Microencapsulation of Anthocyanins—Critical Review of Techniques and Wall Materials. *Appl. Sci.* **2021**, *11*, 3936. [[CrossRef](#)]
47. Almas, I.; Innocent, E.; Machumi, F.; Kisinza, W. Chemical composition of essential oils from *Eucalyptus globulus* and *Eucalyptus maculata* grown in Tanzania. *Sci. Afr.* **2021**, *12*, e00758. [[CrossRef](#)]
48. Rojas-Moreno, S.; Cárdenas-Bailón, F.; Osorio-Revilla, G.; Gallardo-Velázquez, T.; Proal-Nájera, J. Effects of complex coacervation-spray drying and conventional spray drying on the quality of microencapsulated orange essential oil. *J. Food Meas. Charact.* **2017**, *12*, 650–660. [[CrossRef](#)]
49. Mahanta, B.P.; Bora, P.K.; Kemprai, P.; Borah, G.; Lal, M.; Haldar, S. Thermolabile essential oils, aromas and flavours: Degradation pathways, effect of thermal processing and alteration of sensory quality. *Food Res. Int.* **2021**, *145*, 110404. [[CrossRef](#)]
50. Pakzad, H.; Alemzadeh, I.; Kazemi, A. Encapsulation of Peppermint Oil with Arabic Gum-gelatin by Complex Coacervation Method. *Int. J. Eng.* **2013**, *26*, 807–814. [[CrossRef](#)]
51. Gu, X.L.; Zhu, X.; Kong, X.Z.; Tan, Y. Comparisons of simple and complex coacervations for preparation of sprayable insect sex pheromone microcapsules and release control of the encapsulated pheromone molecule. *J. Microencapsul.* **2010**, *27*, 355–364. [[CrossRef](#)]
52. Timilsena, Y.P.; Taiwo, O.A.; Nauman, K.; Benu, A.; Colin, J.B. Complex coacervation: Principles, mechanisms and applications in microencapsulation. *Int. J. Biol. Macromol.* **2019**, *121*, 1276–1286. [[CrossRef](#)]
53. Evans, M.; Ratcliffe, I.; Williams, P.A. Emulsion stabilisation using polysaccharide–protein complexes. *Curr. Opin. Colloid. Interface Sci.* **2013**, *18*, 272–282. [[CrossRef](#)]
54. Yang, X.; Gao, N.; Hu, L.; Li, J.; Sun, Y. Development and evaluation of novel microcapsules containing poppy-seed oil using complex coacervation. *J. Food Eng.* **2015**, *161*, 87–93. [[CrossRef](#)]
55. Li, Y.; Zhang, X.; Zhao, Y.; Ding, J.; Lin, S. Investigation on complex coacervation between fish skin gelatin from cold-water fish and gum arabic: Phase behavior, thermodynamic, and structural properties. *Int. Food Res. J.* **2018**, *107*, 596–604. [[CrossRef](#)] [[PubMed](#)]
56. Shaddel, R.; Hesari, J.; Azadmard-Damirchi, S.; Hamishehkar, H.; Fathi-Achachlouei, B.; Huang, Q. Use of gelatin and gum Arabic for encapsulation of black raspberry anthocyanins by complex coacervation. *Int. J. Biol. Macromol.* **2018**, *107*, 1800–1810. [[CrossRef](#)]
57. Ogilvie-Battersby, J.D.; Nagarajan, R.; Mosurkal, R.; Orbey, N. Microencapsulation and controlled release of insect repellent geraniol in gelatin/gum arabic microcapsules. *Colloids Surf. A Physicochem. Eng. Asp.* **2022**, *640*, 128494. [[CrossRef](#)]
58. Elzoghby, A.O. Gelatin-based nanoparticles as drug and gene delivery systems: Reviewing three decades of research. *J. Control. Release* **2013**, *172*, 1075–1091. [[CrossRef](#)]
59. Muhoza, B.; Xia, S.; Wang, X.; Zhang, X.; Li, Y.; Zhang, S. Microencapsulation of essential oils by complex coacervation method: Preparation, thermal stability, release properties and applications. *Crit. Rev. Food Sci. Nutr.* **2022**, *62*, 1363–1382. [[CrossRef](#)]
60. Kontogiorgos, V. Polysaccharides at fluid interfaces of food systems. *Adv. Colloid Interface Sci.* **2019**, *270*, 28–37. [[CrossRef](#)] [[PubMed](#)]
61. Muhoza, B.; Xia, S.; Zhang, X. Gelatin and high methyl pectin coacervates crosslinked with tannic acid: The characterization, rheological properties, and application for peppermint oil microencapsulation. *Food Hydrocoll.* **2019**, *97*, 105174. [[CrossRef](#)]
62. Lv, Y.; Yang, F.; Li, X.; Zhang, X.; Abbas, S. Formation of heat-resistant nanocapsules of jasmine essential oil via gelatin/gum arabic based complex coacervation. *Food Hydrocoll.* **2014**, *35*, 305–314. [[CrossRef](#)]
63. Niu, F.; Kou, M.; Fan, J.; Pan, W.; Zhi-Juan, F.; Su, Y.; Yang, Y.; Zhou, W. Structural characteristics and rheological properties of ovalbumin-gum Arabic complex coacervates. *Food Chem.* **2018**, *260*, 1–6. [[CrossRef](#)]
64. Hernández-Nava, R.; López-Malo, A.; Palou, E.; Ramírez-Corona, N.; Jiménez-Munguía, M.T. Complex Coacervation Between Gelatin and Chia Mucilage as an Alternative of Encapsulating Agents. *J. Food Sci.* **2019**, *84*, 1281–1287. [[CrossRef](#)]
65. Zuanon, L.A.C.; Malacrida, C.R.; Nicoletti Telis, V.R. Production of Turmeric Oleoresin Microcapsules by Complex Coacervation with Gelatin–Gum Arabic. *J. Food Process Eng.* **2013**, *36*, 364–373. [[CrossRef](#)]
66. Habibi, A.; Keramat, J.; Hojjatoleslami, M.; Tamjidi, F. Preparation of fish oil microcapsules by complexcoacervation of gelatin–gum arabic and theirutilization for fortification of pomegranate juice. *J. Food Process Eng.* **2016**, *40*, e12385. [[CrossRef](#)]
67. Marfil, P.H.M.; Paulo, B.B.; Alvim, I.D.; Nicoletti, V.R. Production and characterization of palm oil microcapsules obtained by complex coacervation in gelatin/gum Arabic. *J. Food Process Eng.* **2018**, *41*, e12673. [[CrossRef](#)]
68. de Almeida Paula, D.; Furtado Martins, E.M.; de Almeida Costa, N.; de Oliveira, P.M.; de Oliveira, E.B.; Ramos, A.M. Use of gelatin and gum arabic for microencapsulation of probiotic cells from *Lactobacillus plantarum* by a dual process combining double emulsification followed by complex coacervation. *Int. J. Biol. Macromol.* **2019**, *133*, 722–731. [[CrossRef](#)]
69. Khatibi, S.A.; Ehsani, A.; Nemat, M.; Javadi, A. Microencapsulation of *Zataria multiflora* Boiss. essential oil by complex coacervation using gelatin and gum arabic: Characterization, release profile, antimicrobial and antioxidant activities. *J. Food Process. Preserv.* **2021**, *45*, e15823. [[CrossRef](#)]
70. Yuan, Y.; Kong, Z.Y.; Sun, Y.E.; Zeng, Q.Z.; Yang, X.Q. Complex coacervation of soy protein with chitosan: Constructing antioxidant microcapsule for algal oil delivery. *LWT* **2017**, *75*, 171–179. [[CrossRef](#)]
71. Liang, Y.; Matia-Merino, L.; Gillies, G.; Patel, H.; Ye, A.; Golding, M. The heat stability of milk protein-stabilized oil-in-water emulsions: A review. *Curr. Opin. Colloid Interface Sci.* **2017**, *28*, 63–73. [[CrossRef](#)]

72. Vargas, S.A.; Delgado-Macuil, R.J.; Ruiz-Espinosa, H.; Rojas-Lopez, M.; Amador-Espejo, G.G. High-intensity ultrasound pretreatment influence on whey protein isolate and its use on complex coacervation with kappa carrageenan: Evaluation of selected functional properties. *Ultrason. Sonochem.* **2021**, *70*, 105340. [[CrossRef](#)]
73. Raei, M.; Rafe, A.; Shahidi, F. Rheological and structural characteristics of whey protein-pectin complex coacervates. *J. Food Eng.* **2018**, *228*, 25–31. [[CrossRef](#)]
74. Reza, G.; Asghar, K.A.; Fardin, T. Int. J. Biol. Macromol. Optimization of whey protein isolate-quince seed mucilage complex coacervation. *Int. J. Biol. Macromol.* **2019**, *131*, 368–377. [[CrossRef](#)]
75. Boné Calvo, J.; Clavero Adell, M.; Guallar Abadía, I.; Aznar, S.L.; Sancho Rodriguez, M.L.; Monzon, A.C.; Mazas, Y.A. As soon as possible in IgE-cow's milk allergy immunotherapy. *Eur. J. Pediatr.* **2021**, *180*, 291–294. [[CrossRef](#)] [[PubMed](#)]
76. Tavares, L.; Noreña, Z.; Pelayo, C. Encapsulation of garlic extract using complex coacervation with whey protein isolate and chitosan as wall materials followed by spray drying. *Food Hydrocoll.* **2018**, *89*, 360–369. [[CrossRef](#)]
77. Zia, K.M.; Tabasum, S.; Nasif, M.; Sultan, N.; Aslam, N.; Noreen, A.; Zuber, M. A review on synthesis, properties and applications of natural polymer based carrageenan blends and composites. *Int. J. Biol. Macromol.* **2017**, *96*, 282–301. [[CrossRef](#)]
78. Palanisamy, M.; Töpfl, S.; Aganovic, K.; Berger, R.G. Influence of iota carrageenan addition on the properties of soya protein meat analogues. *LWT* **2018**, *87*, 546–552. [[CrossRef](#)]
79. Martins, E.; Poncelet, D.; Rodrigues, R.C.; Renard, D. Oil encapsulation techniques using alginate as encapsulating agent: Applications and drawbacks. *J. Microencapsul.* **2017**, *34*, 754–771. [[CrossRef](#)]
80. Bastos, L.P.H.; Corrêa dos Santos, C.E.; de Carvalho, M.G.; Garcia-Rojas, E.E. Encapsulation of the black pepper (*Piper nigrum* L.) essential oil by lactoferrin-sodium alginate complex coacervates: Structural characterization and simulated gastrointestinal conditions. *Food Chem.* **2020**, *316*, 126345. [[CrossRef](#)]
81. Rojas-Moreno, S.; Osorio-Revilla, G.; Gallardo-Velázquez, T.; Cárdenas-Bailón, F.; Meza-Márquez, G. Effect of the cross-linking agent and drying method on encapsulation efficiency of orange essential oil by complex coacervation using whey protein isolate with different polysaccharides. *J. Microencapsul.* **2018**, *35*, 165–180. [[CrossRef](#)]
82. Soliman, E.A.; El-Moghazy, A.Y.; Mohy Eldin, M.S.; Massoud, M.A. Microencapsulation of Essential Oils within Alginate: Formulation and in Vitro Evaluation of Antifungal Activity. *J. Encapsulation Adsorpt. Sci.* **2013**, *3*, 48–55. [[CrossRef](#)]
83. Rios-Mera, J.D.; Saldaña, E.; Ramírez, Y.; Auquiñivín, E.A.; Alvim, I.D.; Contreras-Castillo, C.J. Encapsulation optimization and pH- and temperature-stability of the complex coacervation between soy protein isolate and inulin entrapping fish oil. *LWT* **2019**, *116*, 108555. [[CrossRef](#)]
84. Tang, C.H. Emulsifying properties of soy proteins: A critical review with emphasis on the role of conformational flexibility. *Crit. Rev. Food Sci. Nutr.* **2017**, *57*, 2636–2679. [[CrossRef](#)]
85. Warnakulasuriya, S.N.; Nickerson, M.T. Review on plant protein-polysaccharide complex coacervation, and the functionality and applicability of formed complexes. *J. Sci. Food Agric.* **2018**, *98*, 5559–5571. [[CrossRef](#)]
86. Tang, C.H.; Xin-Rong, L. Microencapsulation properties of soy protein isolate and storage stability of the correspondingly spray-dried emulsions. *Int. Food Res. J.* **2013**, *52*, 419–428. [[CrossRef](#)]
87. Huang, G.Q.; Sun, Y.T.; Xiao, J.X.; Yang, J. Complex coacervation of soybean protein isolate and chitosan. *Food Chem.* **2012**, *135*, 534–539. [[CrossRef](#)] [[PubMed](#)]
88. Carpentier, J.; Conforto, E.; Chaigneau, C.; Vendeville, J.E.; Maugard, T. Complex coacervation of pea protein isolate and tragacanth gum: Comparative study with commercial polysaccharides. *Innov. Food Sci. Emerg. Technol.* **2021**, *69*, 102641. [[CrossRef](#)]
89. Carpentier, J.; Conforto, E.; Chaigneau, C.; Vendeville, J.E.; Maugard, T. Microencapsulation and controlled release of α -tocopherol by complex coacervation between pea protein and tragacanth gum: A comparative study with arabic and tara gums. *Innov. Food Sci. Emerg. Technol.* **2022**, *77*, 102951. [[CrossRef](#)]
90. Lan, Y.; Ohm, J.B.; Chen, B.; Rao, J. Microencapsulation of hemp seed oil by pea protein isolate–sugar beet pectin complex coacervation: Influence of coacervation pH and wall/core ratio. *Food Hydrocoll.* **2020**, *113*, 106423. [[CrossRef](#)]
91. Jannasari, N.; Milad, F.; Moshtaghian, S.J.; Abbaspourrad, A. Microencapsulation of vitamin D using gelatin and cress seed mucilage: Production, characterization and in vivo study. *Int. J. Biol. Macromol.* **2019**, *129*, 972–979. [[CrossRef](#)]
92. Otálora, M.C.; Castaño, J.A.G.; Wilches-Torres, A. Preparation, study and characterization of complex coacervates formed between gelatin and cactus mucilage extracted from cladodes of *Opuntia ficus-indica*. *LWT* **2019**, *112*, 108234. [[CrossRef](#)]
93. Hernández-Nava, R.; López-Malo, A.; Palou, E.; Ramírez-Corona, N.; Jiménez-Munguía, M.T. Encapsulation of oregano essential oil (*Origanum vulgare*) by complex coacervation between gelatin and chia mucilage and its properties after spray drying. *Food Hydrocoll.* **2020**, *109*, 106077. [[CrossRef](#)]
94. Amani, F.; Azadi, A.; Rezaei, A.; Kharazmi, M.S.; Jafari, S.M. Preparation of soluble complex carriers from Aloe vera mucilage/gelatin for cinnamon essential oil: Characterization and antibacterial activity. *J. Food Eng.* **2022**, *334*, 111160. [[CrossRef](#)]
95. Brüttsch, L. Chia seed mucilage—a vegan thickener: Isolation, tailoring viscoelasticity and rehydration. *Food Funct.* **2019**, *8*, 4854–4860. [[CrossRef](#)] [[PubMed](#)]
96. Bustamante, M.; Laurie-Martínez, L.; Vergara, D.; Campos-Vega, R.; Rubilar, M.; Shene, C. Effect of Three Polysaccharides (Inulin, and Mucilage from Chia and Flax Seeds) on the Survival of Probiotic Bacteria Encapsulated by Spray Drying. *Appl. Sci.* **2020**, *10*, 4623. [[CrossRef](#)]

97. Capitani, M.I.; Ixtaina, V.Y.; Nolasco, S.M.; Tomas, M.C. Microstructure, chemical composition and mucilage exudation of chia (*Salvia hispanica* L.) nutlets from Argentina. *J. Sci. Food Agric.* **2013**, *93*, 3856–3862. [[CrossRef](#)] [[PubMed](#)]
98. Tamargo, A.; Cueva, C.; Laguna, L.; Moreno-Arribas, M.V.; Muñoz, L.A. Understanding the impact of chia seed mucilage on human gut microbiota by using the dynamic gastrointestinal model simgi[®]. *J. Funct. Foods* **2018**, *50*, 104–111. [[CrossRef](#)]
99. Goh, K.K.T.; Matia-Merino, L.; Chiang, J.H.; Quek, R.; Bing Soh, S.J.; Lentle, R.G. The physic-chemical properties of chia seed polysaccharide and its microgel dispersion rheology. *Carbohydr. Polym.* **2016**, *149*, 297–307. [[CrossRef](#)]
100. Kassem, I.A.A.; Ashaolu, T.J.; Kamel, R.; Elkasabgy, N.A.; Afifi, S.M.; Farag, M.A. Mucilage as a functional food hydrocolloid: Ongoing and potential applications in prebiotics and nutraceuticals. *Food Funct.* **2021**, *12*, 4738–4748. [[CrossRef](#)] [[PubMed](#)]
101. Manaf, M.A.; Subuki, I.; Jai, J.; Raslan, R.; Mustapa, A.N. Encapsulation of Volatile Citronella Essential Oil by Coacervation: Efficiency and Release Study. In Proceedings of the 3rd International Conference on Global Sustainability and Chemical Engineering (ICGSCE), Putrajaya, Malaysia, 15–16 February 2017; IOP Conference Series: Materials Science and Engineering: Bristol, UK, 2018; Volume 358.
102. da Silva, S.F.; de Campo, C.; Paese, K.; Guterres, S.S.; Costa, T.M.H.; Flores, S.H. Nanoencapsulation of linseed oil with chia mucilage as structuring material: Characterization, stability and enrichment of orange juice. *Food Res. Int.* **2018**, *120*, 872–879. [[CrossRef](#)] [[PubMed](#)]
103. Timilsena, Y.P.; Adhikari, R.; Barrow, C.J.; Adhikari, B. Digestion behaviour of chia seed oil encapsulated in chia seed protein-gum complex coacervates. *Food Hydrocoll.* **2017**, *66*, 71–81. [[CrossRef](#)]
104. Tavares, L.; Noreña, C.P.Z. Encapsulation of Ginger Essential Oil Using Complex Coacervation Method: Coacervate Formation, Rheological Property, and Physicochemical Characterization. *Food Bioprocess Technol.* **2020**, *13*, 1405–1420. [[CrossRef](#)]
105. Basu, S.; Banerjee, D.; Chowdhury, R.; Bhattacharya, P. Controlled release of microencapsulated probiotics in food matrix. *J. Food Eng.* **2018**, *238*, 61–69. [[CrossRef](#)]
106. Weisany, W.; Yousefi, S.; Tahir, N.A.R.; Golestanezhadeh, N.; McClements, D.J.; Adhikari, B.; Ghasemlou, M. Targeted delivery and controlled released of essential oils using nanoencapsulation: A review. *Adv. Colloid Interface Sci.* **2022**, *303*, 102655. [[CrossRef](#)] [[PubMed](#)]
107. Matalanis, A.; Jones, O.G.; McClements, D.J. Structured biopolymer-based delivery systems for encapsulation, protection, and release of lipophilic compounds. *Food Hydrocoll.* **2011**, *25*, 1865–1880. [[CrossRef](#)]

Warszawa, 8/10/2024

Alicja Kizildag
alicjakizildag@gmail.com

**Rada Dyscypliny Technologia
Żywności i Żywienia
Szkoły Głównej Gospodarstwa
Wiejskiego w Warszawie**

Oświadczenie o współautorstwie

Niniejszym oświadczam, że w pracy: *Napiórkowska A, Kurek M. Coacervation as a Novel Method of Microencapsulation of Essential Oils—A Review. Molecules. 2022; 27(16):5142* mój indywidualny udział w jej powstaniu polegał na przeanalizowaniu dostępnej literatury, napisaniu manuskryptu oraz jego korekcie po procesie recenzji.

Podpis



Warszawa, 8/10/2024

Marcin Andrzej Kurek
marcin_kurek@sggw.edu.pl

**Rada Dyscypliny Technologia
Żywności i Żywienia
Szkoły Głównej Gospodarstwa
Wiejskiego w Warszawie**

Oświadczenie o współautorstwie

Niniejszym oświadczam, że w pracy: *Napiórkowska A, Kurek M. Coacervation as a Novel Method of Microencapsulation of Essential Oils—A Review. Molecules. 2022; 27(16):5142* mój indywidualny udział w jej powstaniu polegał na ostatecznej korekcie treści manuskryptu.

Podpis



Article

Microencapsulation of Juniper and Black Pepper Essential Oil Using the Coacervation Method and Its Properties after Freeze-Drying

Alicja Napiórkowska ¹, Arkadiusz Szpicer ¹, Iwona Wojtasik-Kalinowska ¹, Maria Dolores Torres Perez ², Herminia Dominguez González ² and Marcin Andrzej Kurek ^{1,*}

¹ Department of Technique and Food Development, Warsaw University of Life Sciences, 02-787 Warsaw, Poland; alicja_napiorkowska@sggw.edu.pl (A.N.); arkadiusz_szpicer@sggw.edu.pl (A.S.); iwona_wojtasik_kalinowska@sggw.edu.pl (I.W.-K.)

² CINBIO, Departamento de Ingeniería Química, Campus Ourense, Universidade de Vigo, 32004 Ourense, Spain; matorres@uvigo.es (M.D.T.P.); herminia@uvigo.es (H.D.G.)

* Correspondence: marcin_kurek@sggw.edu.pl

Abstract: Essential oils are mixtures of chemical compounds that are very susceptible to the effects of the external environment. Hence, more attention has been drawn to their preservation methods. The aim of the study was to test the possibility of using the classical model of complex coacervation for the microencapsulation of essential oils. Black pepper (*Piper nigrum*) and juniper (*Juniperus communis*) essential oils were dissolved in grape seed (GSO) and soybean (SBO) oil to minimize their loss during the process, and formed the core material. Various mixing ratios of polymers (gelatin (G), gum Arabic (GA)) were tested: 1:1; 1:2, and 2:1. The oil content was 10%, and the essential oil content was 1%. The prepared coacervates were lyophilized and then screened to obtain a powder. The following analyses were determined: encapsulation efficiency (EE), Carr index (CI), Hausner ratio (HR), solubility, hygroscopicity, moisture content, and particle size. The highest encapsulation efficiency achieved was within the range of 64.09–59.89%. The mixing ratio G/GA = 2:1 allowed us to obtain powders that were characterized by the lowest solubility (6.55–11.20%). The smallest particle sizes, which did not exceed 6 µm, characterized the powders obtained by mixing G/GA = 1:1. All powder samples were characterized by high cohesiveness and thus poor or very poor flow (CI = 30.58–50.27, HR = 1.45–2.01).

Keywords: essential oils; complex coacervation; gum Arabic; gelatin



Citation: Napiórkowska, A.; Szpicer, A.; Wojtasik-Kalinowska, I.; Perez, M.D.T.; González, H.D.; Kurek, M.A. Microencapsulation of Juniper and Black Pepper Essential Oil Using the Coacervation Method and Its Properties after Freeze-Drying. *Foods* **2023**, *12*, 4345. <https://doi.org/10.3390/foods12234345>

Academic Editor: Shaojin Wang

Received: 16 October 2023

Revised: 16 November 2023

Accepted: 27 November 2023

Published: 1 December 2023



Copyright: © 2023 by the authors. Licensee MDPI, Basel, Switzerland. This article is an open access article distributed under the terms and conditions of the Creative Commons Attribution (CC BY) license (<https://creativecommons.org/licenses/by/4.0/>).

1. Introduction

In response to consumer expectations, food producers have begun to focus on the production of high-quality and less processed products. These products also come with the longest shelf life. Moreover, a commitment to environmental stewardship has prompted manufacturers to prioritize the reduction or elimination of synthetic preservatives and stabilizers [1]. This has led to a growing emphasis on plant-based alternatives, such as essential oils, to meet these evolving expectations. This is because essential oils have a strong antimicrobial effect, and their use minimizes the risk of foodborne pathogens acquiring resistance to antibiotics. In addition, essential oils have several health-promoting properties [1–3].

The main components of juniper essential oil (*Juniperus communis* L.) are α -pinene, limonene, and myrcene [4,5], while the main ingredients of black pepper essential oil (*Piper nigrum* L.) are α -pinene, sabinene, β -pinene, δ -3-carene, limonene, and β -caryophyllene [6–8]. Both plants are known worldwide as spices but also as pharmaceutical raw materials [9,10]. They have strong antioxidant and antimicrobial properties [7,11], but also have anti-inflammatory and antispasmodic properties [5].

The growing interest in essential oils and the escalating demand for natural additives in the food industry have prompted research into their powdered forms as potential food ingredients [12]. Encapsulating essential oils has become imperative as these substances are sensitive to external environmental factors such as light, temperature, pH, and oxygen. However, their challenges extend beyond environmental sensitivity. Their lipophilic nature, resulting in low water solubility, poor bio-accessibility, and limited bioavailability, hinders their widespread application in food products [13–15]. The application of microencapsulation techniques has been proven to be essential in safeguarding the active ingredients of essential oils, enabling their incorporation into various products, such as fruit and vegetable drinks, yogurts, and other dairy products.

Crucially, the choice of the wall material composition for each system is paramount, as the encapsulating material influences the numerous physicochemical properties of the powdered product and dictates its storage behavior [2]. An intriguing method that facilitates microencapsulation is complex coacervation. This process holds a distinctive advantage as it can occur at room temperature, a particularly noteworthy feature when dealing with essential oils [16].

Complex coacervation is one of the most important microencapsulation methods used to protect sensitive substances such as aromas, omega-3 fatty acids, vegetable oils, antioxidants, and essential oils [9,10,15,17,18]. This phenomenon takes place in an aqueous solution when two polymers with opposite charges are drawn together by electrostatic forces. Subsequently, this interaction leads to phase separation, creating two distinct phases: a concentrated coacervated phase referred to as the “continuous phase,” and a less concentrated liquid phase known as the “equilibrium solution” [11,19,20]. The coacervated phase consists of wall material deposited in a thin layer of the core material. The mixtures of proteins and polysaccharides are commonly used, and the most widely studied coacervation system is gelatin (G): gum Arabic (GA) [11,21,22]. This technique allows for high encapsulation efficiency (up to 99%) [14] and enables the encapsulation of more core material per unit mass of wall material compared with other microencapsulation techniques [12,16,17,19,20]. This process has been used to microencapsulate essential oils [9,10,14,16,19]. However, so far, it has been used to do so without first dissolving EO in the oil. Complex coacervation allows for one to obtain a high efficiency of oil encapsulation [23]. However, essential oils, as highly volatile compounds, may suffer significant losses during the spray drying or freeze drying processes [9,10,12,24].

The main aim of this research was to determine whether the classical model of complex coacervation (G:GA) could be used for the microencapsulation of essential oils. The aim of this study was to examine how varying mixing ratios of wall materials (specifically, gelatin and gum Arabic) impact encapsulation efficiency. Additionally, the research sought to explore the physicochemical properties of the resulting powders. In order to minimize the loss of essential oil (due to the increased temperature of the process), the essential oils were dissolved in the oil before being microencapsulated. The literature review shows that, so far, such a solution has not been used. The amount of research into the application of the classical model of complex coacervation to microencapsulation of essential oils is also limited.

The obtained results indicate that the use of the classical model of complex coacervation for microencapsulation of essential oils is possible. This allows a large part of EO to be retained in the microcapsule structures and gives hope for their possible use in food.

2. Materials and Methods

2.1. Materials

Gelatin (Agnex, Białystok, Poland), and gum Arabic (Warchem, Warsaw, Poland) were used as wall materials. Juniper berry (*Juniperus communis*) essential oil and black pepper peppercorn (*Piper nigrum*) essential oil (Ancient Wisdom, Sheffield, Great Britain) were firstly dissolved in soybean oil (Dary Natury, Koryciny, Poland) or grape seed oil (Basso Fedele e figli s.r.l., Avellino, Italy) and used as the core material. Essential oils were

dissolved in oil at a concentration of 1% *v/v* to reduce the risk of their evaporation during the freeze drying process.

2.2. Preparation of Coacervates

As a wall material, 5% gelatin solution with 5% gum Arabic solution was used. Gelatin (G) (Agnex, Białystok, Poland) and gum Arabic (GA) (Warchem, Warsaw, Poland) were dissolved at the temperature of 50 °C. The solutions were mixed in different mixing ratios: 1:1; 1:2, and 2:1. The mass of each system was 300 g. After the solutions were mixed together, they were subjected to high shear homogenization using Ultra turrax (IKA T18 basic, Staufen, Germany) for 5 min at 15,000 rpm/min at room temperature. In the homogenization process, every variant received an addition of 10% (30 g) of either soybean oil (SBO) or grape seed oil (GSO), within which 1% of the system mass (3 g) had juniper essential oil (JEO) or black pepper essential oil (BPEO) dissolved in SBO or GSO previously. After emulsification, the pH was adjusted to 4.0 (under the isoelectric point) using 1M HCl solution (Firma Chempur, Piekary Śląskie, Poland). Each emulsion underwent a storage process at 4 °C for 24 h, followed by transfer to −20 °C for an additional 24 h. Subsequently, the samples were further transferred to −60 °C for an additional 24 h. The frozen samples were then subjected to lyophilization for a duration of 72 h at −80 °C. After this period, the lyophilized products were sieved using a laboratory sieve with a mesh size of 710 μm. The screened material was vacuum packed and stored at 4 °C for subsequent analyses.

The samples were coded for easier identification (Table 1). The mixing ratio was marked as 1—1:1, 2—1:2, 3—2:1, juniper essential oil—J, black pepper oil—B, soybean oil—S, grape seed oil—G. For example, the sample in which G/GA = 1:1 and which contains juniper essential oil dissolved in soybean oil was coded as SJ1.

Table 1. Coding of samples.

Oil	Essential Oil	Mixing Ratio G/GA	Code
Grape seed	Juniper	1:1	GJ1
		1:2	GJ2
		2:1	GJ3
	Black pepper	1:1	GB1
		1:2	GB2
		2:1	GB3
Soybean	Juniper	1:1	SJ1
		1:2	SJ2
		2:1	SJ3
	Black pepper	1:1	SB1
		1:2	SB2
		2:1	SB3

2.3. Complex Coacervation Yield, Solid Yield, and Encapsulation Efficiency

To determine the efficiency of the complex, coacervation yield (CY) was calculated according to the equation [25]:

$$CY = \frac{CM}{SM} * 100\% \quad (1)$$

CM—coacervate mass collected after the process,

SM—total mass of the freeze-dried powder.

To determine the losses during the freeze drying process, the solid yield (SY %) was calculated according to the equation [25]:

$$SY = \frac{PM}{LCM} * 100\% \quad (2)$$

where:

PM—powder mass collected after freeze drying,

LCM—liquid coacervate mass, before the freeze drying process.

Encapsulation efficiency (EE) was measured according to the method described by Hernandez-Nava [26] with slight modifications. Briefly, it was calculated by measuring the surface oil (SO) and total oil (TO) of the freeze-dried powders. All measurements were completed in triplicate.

SO was determined by weighing 1 g of sample and dispersion in 30 mL of n-hexane with constant stirring (60 rpm) for 15 min. The oil phase with n-hexane was filtered into the pre-weighted round-bottom flask and evaporated on a rotary evaporator (R-100 Büchi, Switzerland). Then, the sample was stored in the oven at 105 °C for 30 min to ensure all n-hexane had evaporated. After this, the sample was left in the desiccator until it had cooled (1 h). The round-bottom flask was weighed, and the SO was calculated as:

$$S_O = OM_1 - OM_2 \quad (3)$$

where:

OM₁—oil mass after extraction and evaporation of the solvent,

OM₂—the theoretical weight of oil from the sample.

T_O was determined by weighing 1.5 g of the sample and spreading it in 4 mL of KCl. In the next step, 4 mL of acetone and 8 mL of chloroform were added to the sample. The sample prepared was constantly stirred (60 rpm) for 15 min and then centrifuged (5000 rpm, 5 min). The sample was separated during centrifugation. The top layer was poured, and the bottom layer containing chloroform and the oil phase was passed through a filter paper with anhydrous sodium sulfate into a weighed round-bottom flask, so the test sample remained in the falcon test tube. After that, 4 mL of double-distilled water, 4 mL of acetone, and 8 mL of chloroform were added to the residue. The sample was centrifuged again, the top layer was poured, and the bottom layer was soaked through filter paper. Then the solvent was evaporated on a rotary evaporator (R-100 Büchi, Switzerland). After that, the sample was stored in the oven at 105 °C for 30 min to evaporate the excess chloroform. After this, the sample was left in the desiccator until it was cooled down (1 h). The round-bottom flask was weighed, and the T_O was calculated as:

$$T_O = OM_1 - OM_2 \quad (4)$$

where:

OM₁—oil mass after extraction and evaporation of the solvent,

OM₂—the theoretical weight of oil from the sample.

Having the results for S_O and T_O, EE (%) was calculated according to the formula:

$$EE = \frac{T_O - S_O}{T_O} * 100\% \quad (5)$$

2.4. Bulk and Tapped Density, Carr Index (CI), and Hausner Ratio (HR)

The bulk density (ρ_{bulk}) was determined by measuring the volume occupied by a known quantity of powder in a 10 mL measuring cylinder, measuring its weight before and after adding the powder [26]. Similarly, the tapped density (ρ_{tap}) was determined in a 10 mL measuring cylinder by repeatedly tapping manually by lifting and dropping the cylinder under its own weight at a vertical distance of 14 ± 2 mm high for one minute (one tap per second) [27]. Determinations were made in triplicate. Bulk and tapped densities were expressed in g/cm³.

The compressibility index (CI) and Hausner ratio (HR) are measures of the tendency of a powder to be compressed. Determinations were made in triplicate. To calculate the CI and HR, ρ_{bulk} and ρ_{tap} were used in these equations [28]:

$$CI = \frac{\rho_{\text{tap}} - \rho_{\text{bulk}}}{\rho_{\text{tap}}} * 100\% \quad (6)$$

$$HR = \frac{\rho_{\text{tap}}}{\rho_{\text{bulk}}} \quad (7)$$

2.5. Color Measurement

The color of the microcapsules was examined using a Minolta CR-400 colorimeter (Konica Minolta Inc., Tokyo, Japan) (D65 illuminate, measuring surface—8 mm, standard 2° observers). The measurement results are expressed following the system of the International Commission on Lighting (Commission Internationale de L'Eclairage) in the CIELab color space. The following parameters were determined and tested: L* (L = 0 (black), L = 100 (white)), a* (−a = green, +a = red), and b* (−b = blue, +b = yellow) [29]. Determinations were made in triplicate immediately after production.

2.6. Solubility, Hygroscopicity, and Moisture Content

The solubility of samples was measured according to the method described by Shaddel et al. [30]. Briefly, 0.5 g of freeze-dried sample was weighed into a falcon test tube containing 50 mL of double-distilled H₂O. The sample prepared in this way was homogenized for 30 min and then centrifuged (5000 rpm, 5 min). After centrifugation, 25 mL aliquot of the supernatant was transferred into a dried and pre-weighed Petri dish and immediately oven dried at 105 °C for 6 h. Then, the solubility (%) was calculated by weight difference. Determinations were made in triplicate.

The hygroscopicity of samples was measured according to the method described by Shaddel et al. [30]. Briefly, 0.2 g of each freeze-dried sample was placed in a Petri dish and stored in a container containing the saturated solution of Na₂SO₄ for one week. Hygroscopicity was expressed as g of water absorbed per 100 g sample (%). Determinations were made in triplicate.

The moisture content of microcapsules was determined gravimetrically by drying in a Binder FP 115 drying oven (Binder, Tuttlingen, Germany) at 70 °C for at least 24 h, then cooling to room temperature in desiccators until a constant weight was reached. Determinations were made in triplicate.

2.7. Particle Size Distribution

The measurement was carried out with the Morphologi[®] G3SE apparatus (Malvern Instruments Ltd., Malvern, UK) equipped with a dispersion unit for dry samples. The particle size distribution was calculated as the relative volume of molecules in the band, shown as size distribution curves (Malvern Microsoft ware v.5.40, Malvern Instruments Ltd.). The examined parameters of the size distribution contained the largest particle size (D (v, 0.9)), mean particle volume (D (v, 0.5)), and the smallest particle size (D (v, 0.1)) [31]. The particle size distribution (Span index (SI)) was estimated using the following formula [32]:

$$SI = \frac{D_{90} - D_{10}}{D_{50}} \quad (8)$$

2.8. Fourier Transform Infrared Spectroscopy (FT-IR)

FT-IR spectra were recorded on a Nicolet™ iS™ 5 FTIR Spectrometer (Thermo Scientific, Waltham, MA, USA), with horizontal device for attenuated reflectance and diamond crystal, on a spectral window ranging from 4000 to 400 cm^{−1}, at a spectral resolution of 2 cm^{−1}. Spectra were recorded without any sample preparation and were processed with the OMNIC program (Thermo Scientific, Waltham, MA, USA).

2.9. Differential Scanning Calorimetry (DSC)

The thermal properties of the samples were evaluated using differential scanning calorimetry (DSC 1) from Mettler Toledo (Schwerzenbach) under an argon atmosphere at

a flow rate of 100 cm³/min, as per the method described by Zhao et al. [33] with some modifications. The instrument was calibrated with pure indium and zinc. Each sample (5.0 ± 0.1 mg) was placed in a standard 40 µL aluminum crucible (ME-51119870) and covered with a lid (ME-51119871) using the Mettler Toledo Crucible Sealing Press. DSC scans were recorded from 10 °C to 230 °C at a rate of 10 °C/min (β). The thermograms were analyzed using STARe Software (Version 9.30) to determine the start (T_{on}), maximum (T_{max}), and end (T_{end}) temperatures, as well as the areas under the peaks (ΔH).

2.10. Electronic Nose Analysis

Volatile compounds within the microcapsules were extracted using the Heracles II electronic nose (Alpha M.O.S., Toulouse, France) following the methodology outlined in the works of Wojtasik-Kalinowska et al. [34] and Górska-Horzyczak et al. [35]. This electronic nose employs ultra-fast gas chromatography with headspace and features a detection system comprising two metal columns of varying polarities (nonpolar MXT-5 and slightly polar MXT1701, diameter = 180 µm, length = 10 m) and two flame ionization detectors (FID). Kovats indexes were established using alkane standards (n-butane to n-hexadecane) (Restek) measured under the same conditions as the samples. Identification of volatile compounds was accomplished using the AroChemBase (Alpha MOS Co., Toulouse, France), containing 44,000 compounds and a base of sensory descriptors for each compound.

For analysis, 10% solutions of each sample were placed in 20 mL headspace vials sealed with a Teflon-faced silicon rubber cap. These vials were then incubated at 35 °C for 900 s under an agitation speed of 8.33 Hz. Hydrogen was used as the carrying gas at a constant flow rate of 1 mL/min. The injector temperature was set at 200 °C, with an injected volume of 3500 µL and an injection speed of 125 mL s⁻¹. The analytes were collected in the trap at 15 °C and subsequently divided and simultaneously transferred into the two columns. The carrying gas was maintained at a constant pressure of 80 kPa, with a split flow rate of 10 mL min⁻¹ at the column heads. The temperature program in the oven was as follows: 60 °C for 2 s, a ramp of 3 °C s⁻¹ to 270 °C, held for 20 s, and FID1/FID2 at 280 °C. Flavor data profiles were presented through principal component analysis (PCA) using AlphaSoft Version 8.0 software. All samples were analyzed in triplicate.

2.11. Scanning Electron Microscopy Analysis (SEM)

A scanning electron microscope (Jeol JSM6010LA, Tokyo, Japan) was employed to analyze the samples' surface morphologies after the different treatments. Each sample was fixed on an adhesive carbon tape and coated (approximately 15 nm) with gold. Secondary electron images were taken at several magnifications and an accelerating voltage of 10 kV.

2.12. Statistical Analysis

For statistical analysis, the STATISTICA computer program was used. To check significant differences between the results, one-way and multivariate analyses of variance ANOVA and the Fisher LSD test (*p*-value < 0.05, α = 95%) were used.

3. Results

3.1. Evaluation of Coacervation Efficacy

The critical factor influencing the complex coacervation process is the protein-polysaccharide mass ratio. Different ratios impact the intensity of interaction and complexation due to the charge balance between protein and polysaccharide [26,36,37]. The statistical analysis demonstrated that the obtained results had been affected by the mixing ratio, essential oil, the type of oil used, and their interactions. However, the mixing ratio had the most significant impact on the resulting coacervation yield (CY) and solid yield (SY), closely followed by the essential oil (EO) (Table 2). The mixing ratio exhibited a strong positive effect on CY but had a negative impact on SY. Similarly, the type of oil had a small effect, with a slight decrease in CY and a slight increase in SY values. Notably, the content of essential oil caused an opposite effect—it led to a slight decrease in CY and a slight increase

in SY values. In this study, both CY and SY values were relatively low, not exceeding 50%. Samples GJ3, GB3, SJ3, and SB3 exhibited the highest CY values, with significant differences ($p < 0.05$) among them. Despite having the highest CY values, these samples did not reflect the highest SY. The highest SY values were observed for samples SB2, GB2, GJ2, and SB1, characterized by the lowest CY values. The specific molar mixing ratio for the achievement of maximum coacervate yield occurs when protein and polysaccharide have the exact opposite charge density, leading to charge neutralization [14,38,39]. This likely occurred at a mixing ratio of 2:1, where the ratio of gelatin to gum Arabic was the highest, resulting in the highest CY. Gelatin, rich in positively charged NH_3^+ ions, and gum Arabic, with primarily negatively charged COO^- ions, undergo electrostatic attraction in the coacervation process [40]. Despite gelatin's high water-binding capacity, these polymers form weak hydrogen bonds with water, which disintegrate and release water during the freeze drying process [41].

Table 2. Complex coacervation yield (CY), solid yield (SY), and encapsulation efficiency (EE) values [%].

Sample	CY%	SY%	EE%
GJ1	30.93 ± 0.44 ^b	29.79 ± 1.21 ^c	49.3 ± 0.07 ^{abe}
GJ2	28.01 ± 0.16 ^a	37.11 ± 0.49 ^e	59.89 ± 0.01 ^{cdf}
GJ3	39.22 ± 0.16 ^g	21.32 ± 0.25 ^a	49.65 ± 0.02 ^{abe}
GB1	30.49 ± 0.56 ^b	29.25 ± 1.29 ^c	42.7 ± 0.11 ^e
GB2	29.45 ± 0.08 ^d	36.23 ± 0.08 ^{de}	55.25 ± 0.01 ^{abcd}
GB3	41.64 ± 0.15 ⁱ	23.01 ± 0.36 ^b	47.21 ± 0.04 ^{ae}
SJ1	33.78 ± 0.46 ^f	26.58 ± 0.36 ^g	64.09 ± 0.09 ^f
SJ2	31.91 ± 0.12 ^e	33.8 ± 0.02 ^h	53.4 ± 0.04 ^{abcd}
SJ3	46.58 ± 0.19 ^j	22.02 ± 0.18 ^{ab}	56.8 ± 0.01 ^{bcd}
SB1	23.95 ± 0.16 ^c	35.44 ± 0.47 ^d	54.14 ± 0.05 ^{abcd}
SB2	28.34 ± 0.12 ^a	38.45 ± 0.34 ⁱ	52.33 ± 0.01 ^{abc}
SB3	41.04 ± 0.51 ^h	20.21 ± 0.61 ^f	61.92 ± 0.04 ^{df}
S.E.M	0.369	0.096	26.524
Oil	**	NS	**
Essential oil	**	**	NS
Mixing ratio	**	**	NS
Oil × essential oil	**	**	NS
Essential oil × mixing ratio	**	**	**
Oil × mixing ratio	**	**	NS
Oil × essential oil × mixing ratio	**	**	NS

Results in this table are expressed as mean ± standard deviation. Mean values with the same superscript letters within a row are not significantly different at $p \leq 0.05$. S.E.M.—standard error of the mean. ** = $p < 0.001$; NS—non-significant effect = $p > 0.05$.

Encapsulation efficiency (EE) represents the percentage of the core material enclosed within the powder particles, a critical parameter for essential oils given their volatility and susceptibility to loss during the drying process. Statistical analysis revealed that the results had been significantly influenced by the interaction between the mixing ratio of polymers and oil (Table 2). The type of oil exhibited a notable positive impact on EE, leading to an increase in its values. The highest EE was observed for sample SJ1 (64.09% ± 0.09). Additionally, notable encapsulation efficiency was achieved for samples SB3 and GJ2 (61.92 ± 0.04 and 59.89 ± 0.01, respectively), with significant differences ($p < 0.05$) in EE. Samples GB2, SB1, and SJ2 did not show significant differences ($p < 0.05$) in EE, with values falling within the middle of the obtained range (53.4–55.25%). Notably, similarities were identified in samples SB1 and GB2, which shared the same oil and essential oil, as well as in samples GB2 and SJ2, featuring the same mixing ratio (1:2). The influence of the interaction between mixing ratio and oil on the EE value is evident in these cases. Samples GJ1 and GJ3 were also within the same statistical group (49.30 ± 0.07 and 49.65 ± 0.02, respectively), containing the same essential oil. The lowest EE value was recorded for sample GB1 (Table 2).

3.2. Bulk Density, Tapped Density, Carr Index (CI), and Hausner Ratio (HR)

Bulk density (ρ_{bulk}) is defined as the ratio of the mass to the volume (including the inter-particle void volume) of an untapped (loose) powder sample. If the bulk density is high, the volume of the powder is lower; when the bulk density is low, the same powder mass takes up a larger volume. The tapped density (ρ_{tap}) is defined as an increased bulk density attained after mechanically tapping a cylinder containing the powder sample. This property influences the appropriate selection of the size of the containers for packing the powder (e.g., barrels, bags). Analysis of bulk and tapped density of powder gives a possibility to calculate the compressibility index (Carr index) and Hausner ratio of the powder [28].

The Carr index (CI) serves as an indicator of powder bridge strength and stability, while the Hausner ratio (HR) reflects interparticulate friction [42]. These metrics are instrumental in assessing the flow characteristics of powders. Powder bridging takes place when particles interlock or bond, forming an arch above the container outlet. The cohesive strength and internal friction of individual particles together play a crucial role in determining the stability and strength of this arch. In instances where a powder experiences bridging, the arch effectively holds the remaining contents within the container, impeding the discharge of the remaining powder. A powder's lower CI or lower HR indicates better flow properties than higher ones. A CI of <10 or HR of <1.11 is considered 'excellent' flow, whereas CI > 38 or HR > 1.60 is considered 'very very poor' flow [43]. In CI and HR, the obtained values were influenced by the mixing ratio and its interaction with the oil. The increase in the mixing ratio resulted in a decrease in the cohesiveness of the obtained powders, and thus a decrease in the CI and HR values. The samples differed statistically significantly ($p < 0.05$). The GB2, GB3, SJ2, and SB2 samples were in the same statistical group (Table 3), presenting the CI in the range of 31.81–34.74 and the HR in the range of 1.47–1.53, thus demonstrating high cohesiveness and very poor flow [44]. These were also the lowest CI and HR values obtained in this study. The highest values were recorded for the GJ1 and GB1 samples, which were also together in the same statistical group ($p < 0.05$). CI values were 50.27 ± 2.53 and 48.84 ± 7.73 , respectively, and HR values were 2.01 ± 0.11 and 2.98 ± 0.28 , respectively. These powders had the highest cohesiveness and virtually no flow [45].

Table 3. Bulk density, tapped density, Carr index, Hausner ratio [g/cm^3], and solubility, hygroscopicity and moisture content ($\text{g}/100 \text{ g}$).

Sample	Bulk Density g/cm^3	Tapped Density g/cm^3	Carr Index g/cm^3	Hausner Ratio g/cm^3	Solubility $\text{g}/100 \text{ g}$	Hygroscopicity $\text{g}/100 \text{ g}$	Moisture Content $\text{g}/100 \text{ g}$	
GJ1	0.12 ± 0.01^c	0.24 ± 0.00^{abc}	50.27 ± 2.53^d	2.01 ± 0.11^d	19.4 ± 2.92^{be}	2.53 ± 0.32^a	0.27 ± 0.04^a	
GJ2	0.16 ± 0.01^a	0.23 ± 0.01^{ab}	30.58 ± 4.93^a	1.45 ± 0.10^a	12.54 ± 3.76^{acd}	7.29 ± 8.02^a	0.18 ± 0.12^a	
GJ3	0.16 ± 0.01^{ab}	0.24 ± 0.01^{abc}	31.81 ± 4.45^a	1.47 ± 0.09^{ab}	7.85 ± 3.54^a	2.87 ± 2.15^a	0.56 ± 0.62^a	
GB1	0.11 ± 0.01^c	0.22 ± 0.02^{ab}	48.84 ± 7.73^d	1.98 ± 0.28^d	18.22 ± 3.35^{bd}	3.77 ± 2.51^a	0.29 ± 0.42^a	
GB2	0.17 ± 0.01^b	0.26 ± 0.00^{de}	33.56 ± 3.46^{ab}	1.51 ± 0.08^{ab}	20.7 ± 4.15^{be}	6.98 ± 3.85^a	0.05 ± 0.05^a	
GB3	0.16 ± 0.01^a	0.24 ± 0.01^{abc}	34.64 ± 2.13^{ab}	1.53 ± 0.05^{ab}	6.58 ± 2.69^a	6.00 ± 4.84^a	0.36 ± 0.29^a	
SJ1	0.12 ± 0.00^c	0.22 ± 0.03^a	44.35 ± 6.21^{cd}	1.81 ± 0.21^{cd}	16.39 ± 4.46^{bcd}	4.92 ± 4.18^a	0.30 ± 0.21^a	
SJ2	0.16 ± 0.00^{ab}	0.25 ± 0.00^{cd}	34.74 ± 0.64^{ab}	1.53 ± 0.02^{ab}	18.72 ± 5.65^{bd}	4.32 ± 3.06^a	0.44 ± 0.66^a	
SJ3	0.17 ± 0.01^{ab}	0.28 ± 0.00^e	40.28 ± 4.6^{bc}	1.68 ± 0.13^{bc}	11.14 ± 3.01^{ac}	2.71 ± 1.97^a	0.36 ± 0.30^a	
SB1	0.14 ± 0.02^d	0.23 ± 0.01^{ab}	38.05 ± 8.82^{abc}	1.64 ± 0.22^{abc}	10.74 ± 2.41^{ac}	2.63 ± 0.17^a	0.24 ± 0.25^a	
SB2	0.16 ± 0.00^{ab}	0.25 ± 0.01^{bcd}	34.33 ± 2.05^{ab}	1.52 ± 0.05^{ab}	25.86 ± 6.81^e	2.86 ± 0.82^a	0.28 ± 0.24^a	
SB3	0.15 ± 0.01^{ad}	0.24 ± 0.01^{abcd}	37.75 ± 2.98^{abc}	1.61 ± 0.08^{abc}	7.47 ± 1.34^a	1.48 ± 0.48^a	0.49 ± 0.08^a	
Effect	S.E.M	0.000	0.000	23.152	0.020	15.466	12.105	0.113
	Oil	NS	NS	NS	NS	NS	NS	NS
	Essential oil	NS	NS	NS	NS	NS	NS	NS
	Mixing ratio	*	**	**	**	**	**	**
	Oil \times Essential oil	NS	*	NS	NS	NS	NS	NS
	Essential oil \times mixing ratio	*	*	*	*	*	NS	NS
	Oil \times mixing ratio	NS	*	NS	NS	*	NS	NS
	Oil \times essential oil \times mixing ratio	*	*	NS	NS	NS	NS	NS

Results in this table are expressed as mean \pm standard deviation. Mean values with the same superscript letters within a row are not significantly different at $p \leq 0.05$. S.E.M.—standard error of the mean. * = $p \leq 0.05$; ** = $p \leq 0.001$; NS—non-significant effect = $p > 0.05$.

The powders obtained in this study were characterized by a very low bulk density in the range of 0.11–0.17 and a tapped density from 0.22 to 0.28 (Table 3). The tapped density exceeded the bulk density because smaller particles filled the voids between larger particles, achieving a more compact packing condition due to the tapping process [46]. The greatest influence on the obtained bulk density was the mixing ratio and the interaction between the mixing ratio, oil, and essential oil. All factors caused an increase in bulk density. The samples showed statistically significant differences among themselves ($p < 0.05$). Similarly, in the case of tapped density, the mixing ratio and interactions between it and the oil and essential oil had the greatest impact on the obtained results. The influence of the mixing ratio was so positive that it caused the tapped density value to increase as it increased. Oil also had a slight positive effect while EO had a slight negative effect. The samples differed statistically significantly ($p < 0.05$).

3.3. Solubility, Hygroscopicity, and Moisture Content

In the food industry, the solubility of powders in water is a crucial factor to expand their range of applications. However, complex coacervation aims to produce water-insoluble microcapsules, allowing for controlled release of the core material. In this study, all samples exhibited low solubility in water (>26%) (Table 3). The solubility of the powders was primarily influenced by the mixing ratio of polymers, as well as the interaction between the mixing ratio and the oil, and the interaction between the mixing ratio and essential oil ($p < 0.05$). These interactions led to a decrease in the solubility of the powders. The least soluble samples were GJ3, GB3, and SB3, forming a homogeneous statistical group with solubility below 8%. The impact of the mixing ratio and the oil used to dissolve the essential oil is evident here, with sample SB2 showing the highest solubility ($25.86\% \pm 6.81$).

Hygroscopicity is a critical factor affecting the stability of food products, storage conditions, and packaging materials. Powders with hygroscopic values exceeding 15.1% are considered highly hygroscopic [47]. However, the hygroscopicity of the powders in this study ranged from 1.49% to 7.29% (Table 3), indicating low hygroscopicity. The examined factors did not have a statistically significant influence on the hygroscopicity of the obtained powders ($p < 0.05$), with no statistical differences found between samples.

Moisture content is another important property related to storage stability and shelf life. The moisture content in the obtained powders was low, ranging from 0.05% to 0.56% (Table 3). Similar to hygroscopicity, the examined factors did not have a statistically significant influence on the moisture content of the powders ($p < 0.05$), and no statistical differences were observed between samples.

3.4. Color Measurement

The color of the resulting powders was primarily influenced by the oil used to dissolve the essential oil, with grape seed oil imparting a slight greenish tint and soybean oil exhibiting a vivid yellow hue. However, the powder color was also affected by the mixing ratio, essential oil, and the interactions among these factors.

Statistical analysis revealed significant differences ($p < 0.05$) in each of the color components among the samples (Table 4). Regarding the brightness of the samples (L^*), the variations were not substantial, with L^* parameter values ranging from 78.72 ± 0.34 to 88.52 ± 0.25 for samples containing soybean oil and grape seed oil. Statistical homogeneity was determined for GJ3, GB3, and SJ1 samples, as well as for SJ2 and SB2. The a^* parameter, indicative of the green color, exhibited negative values for all samples. For samples containing grape seed oil, the a^* values ranged from -1.19 ± 0.02 to -3.83 ± 0.15 . The mixing ratio played a significant role in influencing the a^* value, with an increase corresponding to a higher proportion of green color. Samples containing soybean oil showed a^* values ranging from -7.06 ± 0.27 to -7.66 ± 0.05 , and a homogeneous group was identified for samples SB1 and SB2. In terms of the b^* parameter, representing the yellow color, positive values were observed for all samples. For samples containing grape seed oil, b^* ranged

from 5.61 ± 0.04 to 12.3 ± 0.47 , while for those with soybean oil, the range was 41.87 ± 1.05 to 51.71 ± 0.47 .

Table 4. Color parameters of obtained powders.

Sample	L*	a*	b*
GJ1	86.99 ± 0.32 ^{cd}	-1.74 ± 0.14 ^h	6.3 ± 0.19 ^{bc}
GJ2	88.52 ± 0.25 ^g	-2.09 ± 0.02 ^g	6.56 ± 0.13 ^c
GJ3	84.46 ± 0.97 ^a	-3.05 ± 0.08 ^e	9.47 ± 0.37 ^d
GB1	87.08 ± 0.23 ^c	-1.19 ± 0.02 ⁱ	5.61 ± 0.04 ^b
GB2	87.00 ± 0.11 ^c	-2.91 ± 0.01 ^e	9.24 ± 0.02 ^d
GB3	84.10 ± 0.87 ^a	-3.83 ± 0.15 ^f	12.30 ± 0.47 ^f
SJ1	84.52 ± 0.05 ^a	-7.66 ± 0.05 ^c	46.52 ± 0.13 ^{ae}
SJ2	85.64 ± 0.33 ^b	-7.38 ± 0.14 ^{ab}	45.82 ± 0.31 ^e
SJ3	78.72 ± 0.34 ^d	-7.06 ± 0.27 ^d	51.71 ± 0.47 ^h
SB1	86.07 ± 1.03 ^{bc}	-7.37 ± 0.21 ^{ab}	41.87 ± 1.05 ^g
SB2	85.70 ± 0.30 ^b	-7.49 ± 0.11 ^{ac}	46.86 ± 0.38 ^a
SB3	82.29 ± 0.56 ^f	-7.2 ± 0.07 ^{bd}	47.06 ± 0.64 ^a
S.E.M	0.302	0.017	0.201
Effect			
Oil	**	**	**
Essential oil	*	**	**
Mixing ratio	**	**	**
Oil × essential oil	**	**	**
Essential oil × mixing ratio	**	**	NS
Oil × mixing ratio	**	**	**
Oil × essential oil × mixing ratio	*	**	**

Results in this table are expressed as mean \pm standard deviation. Mean values with the same superscript letters within a row are not significantly different at $p \leq 0.05$. S.E.M.—standard error of the mean. * = $p \leq 0.05$; ** = $p \leq 0.001$; NS—non-significant effect = $p > 0.05$.

3.5. Particle Size Distribution

The size of microcapsules should be in the range of $0.1 \mu\text{m}$ to $100 \mu\text{m}$ [12]. The particle sizes in all tested trials met these assumptions. The obtained results depend on all examined factors individually and their interactions. However, the mixing ratio of polymers had the greatest influence ($p < 0.05$). The highest values of the SI characterized the GJ3, GB3, SB3, and SJ3 samples. This means they had the highest diversity in terms of particle size (Table 5) [48]. In sample GJ3, the SI was the closest to 1.0 (SI = 0.96), so this powder contained particles with the most uniform size distribution in the tested ranges [48]. The smallest range of particle sizes and the smallest SI value were found for samples SB2 and GB2 ($D_{10} = 59.04 \pm 1.18 \mu\text{m}$, $D_{90} = 96.72 \pm 0.5 \mu\text{m}$, SI = 0.43 ± 0.01 and $D_{10} = 60.13 \pm 0.74 \mu\text{m}$, $D_{90} = 96.86 \pm 0.41 \mu\text{m}$, SI = 0.44 ± 0.01 , respectively). The smallest powder particles were obtained for a mixing ratio of 1:1 (GB1, SJ1, SB1). However, no clear relationship was observed between the increase in the content of one polymer and the size of the obtained powder particles.

Table 5. Particle size and particle size distribution index—span (SI) [μm].

Sample	Particle Size μm	D ₁₀ μm	D ₅₀ μm	D ₉₀ μm	SI μm
GJ1	20.48 \pm 0.16 ^h	56.79 \pm 0.62 ^b	83.42 \pm 0.36 ^b	96.84 \pm 0.35 ^a	0.48 \pm 0.01 ^b
GJ2	9.18 \pm 0.14 ^f	53.66 \pm 0.54 ^h	81.98 \pm 0.64 ^a	95.55 \pm 0.41 ^b	0.47 \pm 0.01 ^b
GJ3	4.51 \pm 0.18 ^d	51.9 \pm 0.4 ^g	81.7 \pm 0.98 ^a	95.37 \pm 0.36 ^b	0.96 \pm 0.01 ^g
GB1	5.55 \pm 0.29 ^a	45.86 \pm 0.33 ^f	82.79 \pm 0.75 ^{ab}	95.7 \pm 0.34 ^b	0.6 \pm 0.00 ^e
GB2	10.5 \pm 0.25 ^c	60.13 \pm 0.74 ^c	85.82 \pm 1.46 ^d	96.86 \pm 0.41 ^a	0.44 \pm 0.01 ^a
GB3	12.74 \pm 0.34 ^g	43.14 \pm 1.01 ^e	77.77 \pm 0.18 ⁱ	95.38 \pm 0.26 ^b	1.17 \pm 0.01 ^h
SJ1	5.57 \pm 0.35 ^a	22.2 \pm 0.25 ^d	72.98 \pm 0.79 ^h	92 \pm 0.18 ^d	0.53 \pm 0.01 ^d
SJ2	6.67 \pm 0.29 ^b	57.59 \pm 0.88 ^b	84.11 \pm 0.29 ^{bc}	96.78 \pm 0.55 ^a	0.51 \pm 0.01 ^c
SJ3	6.48 \pm 0.46 ^b	17.42 \pm 0.5 ^a	51.6 \pm 1.16 ^e	90.01 \pm 0.14 ^b	1.41 \pm 0.02 ^j
SB1	5.71 \pm 0.38 ^a	17.37 \pm 0.46 ^a	68.25 \pm 0.58 ^g	97.24 \pm 0.1 ^a	0.67 \pm 0.01 ^f
SB2	10.61 \pm 0.35 ^c	59.04 \pm 1.18 ^c	84.82 \pm 0.22 ^{cd}	96.72 \pm 0.5 ^a	0.43 \pm 0.01 ^a
SB3	7.59 \pm 0.34 ^e	16.69 \pm 0.25 ^a	60.77 \pm 0.94 ^f	92.67 \pm 0.14 ^e	1.25 \pm 0.02 ⁱ
S.E.M	0.094	0.437	0.630	0.118	0.000
Oil	**	**	**	**	**
Essential oil	NS	**	*	**	**
Mixing ratio	**	**	**	**	**
Oil \times essential oil	**	**	**	**	**
Essential oil \times mixing ratio	**	**	**	**	**
Oil \times mixing ratio	**	**	**	**	**
Oil \times essential oil \times mixing ratio	**	**	**	**	**

Results in this table are expressed as mean \pm standard deviation. Mean values with the same superscript letters within a row are not significantly different at $p \leq 0.05$. S.E.M.—standard error of the mean. * = $p \leq 0.05$; ** = $p \leq 0.001$; NS—non-significant effect = $p > 0.05$.

3.6. FT-IR

The obtained FT-IR spectra for JEO showed characteristic peaks at 2917.56 cm^{-1} , 2878.29 cm^{-1} , 1446.07 cm^{-1} , 887.14 cm^{-1} , 786.52 cm^{-1} , and 418.96 cm^{-1} . For BPO, characteristic peaks occurred at 2954.86 cm^{-1} , 2922.95 cm^{-1} , 2867.06 cm^{-1} , 1446.24 cm^{-1} , 885.83 cm^{-1} , 875.20 cm^{-1} , 786.32 cm^{-1} , 543.65 cm^{-1} , 421.49 cm^{-1} , and 442.11 cm^{-1} . Based on the obtained results, the compositional similarity of both essential oils can be seen, which was confirmed by the analysis of volatile compounds using the e-nose (3.8).

In the FT-IR spectra for wall materials, characteristic peaks were observed at wavenumber 3300.05 cm^{-1} , 2893.28 cm^{-1} , 1596.88 cm^{-1} , 1413.05 cm^{-1} , 1017.17 cm^{-1} , 448.52 cm^{-1} , 437.30 cm^{-1} and 416.39 cm^{-1} for gum Arabic and at 1627.16 cm^{-1} , 1526.30 cm^{-1} , 1444.40 cm^{-1} , 1332.90 cm^{-1} , 1235.97 cm^{-1} , 1078.27 cm^{-1} , 597.00 cm^{-1} , 507.22 cm^{-1} , 490.10 cm^{-1} , 469.20 cm^{-1} , 448.82 cm^{-1} , 416.66 cm^{-1} , 409.46 cm^{-1} and 402.23 cm^{-1} for gelatin. Regular soy oil contains approximately 54% linoleic acid (18:2), 23% oleic acid (18:1), 11% palmitic acid (16:0), 8% linolenic acid (18:3), and 4% steric acid (18:0) [49]. Grape seed oil contains the same fatty acids in similar amounts, hence the similarity of the obtained FT-IR spectra [50]. Characteristic peaks were observed at wavenumber 3008.09 cm^{-1} , 2922.44 cm^{-1} , 2852.97 cm^{-1} , 1742.88 cm^{-1} , 1457.23 cm^{-1} , 1377.09 cm^{-1} , 1159.43 cm^{-1} , 1097.51 cm^{-1} and 721.59 cm^{-1} for grapeseed oil. For soybean oil characteristic peaks were found at 3008.58 cm^{-1} , 2922.40 cm^{-1} , 2852.84 cm^{-1} , 1742.92 cm^{-1} , 1456.95 cm^{-1} , 1377.02 cm^{-1} , 1159.01 cm^{-1} , 1097.76 cm^{-1} , and 720.99 cm^{-1} .

For gum Arabic a broad absorption band was observed at wavenumber 3300.05 cm^{-1} which corresponds to hydrogen bond. Because this was followed by the presence of spectra at the 1600–1300 cm^{-1} (1596.88 cm^{-1} , 413.05 cm^{-1}) frequencies, we can confirm the existence of a hydroxyl (-OH) group. The next narrow band was found at 2893.28 cm^{-1} followed by peaks between 1470–720 cm^{-1} , which can correspond with absorption band for long-chain linear aliphatic compounds. A characteristic peak at 1017.17 cm^{-1} corresponds to the fingerprint of carbohydrates, which, along with peaks at 448.52 cm^{-1} and 437.30 cm^{-1} , is characteristic for CCO, COC, symmetrical, and asymmetrical ring breathing vibration. For gelatin, characteristic peaks were found at 1627.16 cm^{-1} , which corresponds to COO asymmetric stretching, and at 1526.30 cm^{-1} and 1444.40 cm^{-1} which can be associated with COO symmetric stretching. Peaks at 1332.90 cm^{-1} , 1235.97 cm^{-1} ,

and 1078.27 cm^{-1} can be attributed to C=O stretching. The remaining characteristic peaks at 597.00 cm^{-1} , 507.22 cm^{-1} , 490.10 cm^{-1} , 469.20 cm^{-1} , 448.82 cm^{-1} , 416.66 cm^{-1} , 409.46 cm^{-1} and 402.23 cm^{-1} are CCO, COC, symmetrical and asymmetrical ring breathing vibrations [51].

Figures 1 and 2 show the FT-IR spectra for individual microcapsules. The spectra of the microcapsules were similar to those of the wall materials. Most of the peaks corresponding to the essential oils disappeared in these spectra. This phenomenon can be related to the overlapping of the peaks of the matrix, oils, and essential oils, which is due to the low concentration of essential oils in the total weight of the microcapsules [24]. Nevertheless, the obtained results confirm that both oils were successfully encapsulated. This is evident from the characteristic peaks at 1455.95 cm^{-1} , 1454.10 cm^{-1} , 1454.84 cm^{-1} and 1453.80 cm^{-1} seen in samples GJ3, GB3, SJ1 and SB3, respectively. It is also worth noting that samples SJ1 and SB3 have the highest encapsulation efficiency among the remaining samples.

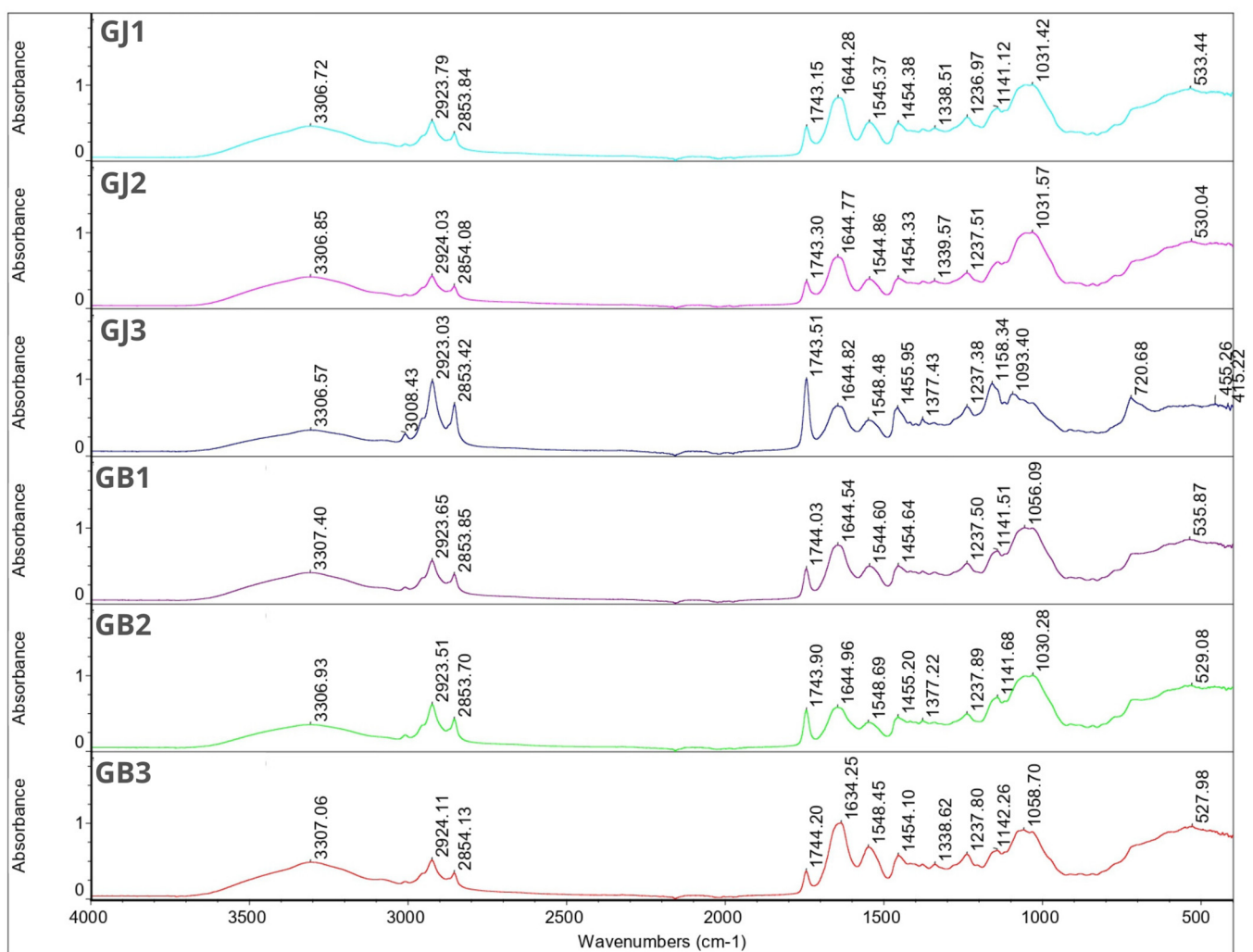


Figure 1. FT-IR spectra for samples GJ1, GJ2, GJ3, GB1, GB2 and GB3.

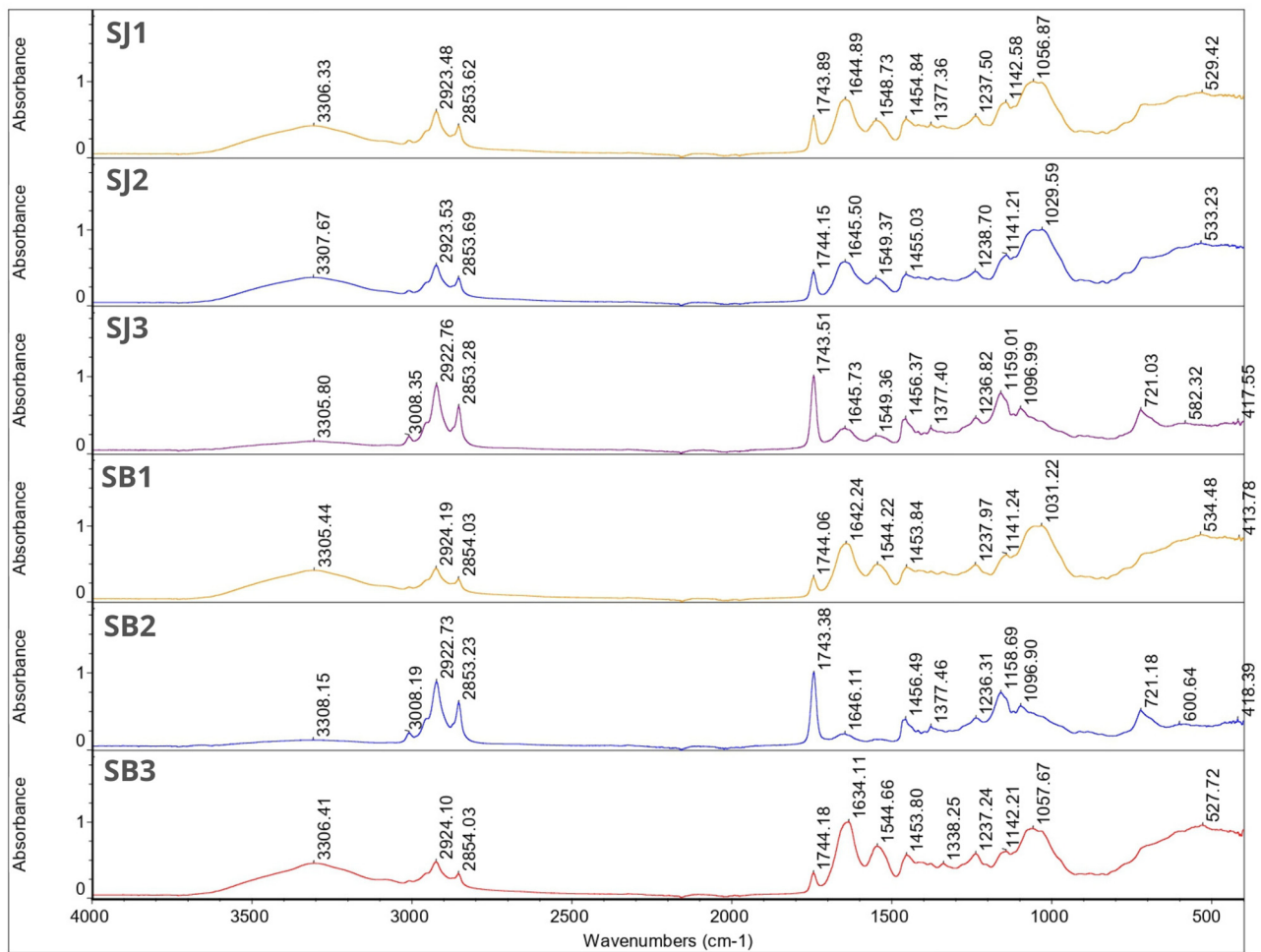


Figure 2. FT-IR spectra for samples SJ1, SJ2, SJ3, SB1, SB2 and SB3.

In all samples, a characteristic broad absorption band between $3305.44\text{--}3308.15\text{ cm}^{-1}$ can be seen. This is characteristic for gum Arabic and hydroxyl groups [52]. For samples SB2, SJ3 and GJ3 this peak is followed by characteristic narrow peaks between wavenumber $3008.19\text{--}3008.43\text{ cm}^{-1}$ which can be linked with unsaturated compounds or aromatic rings characteristic for essential oils. Those peaks are not visible in other sample spectra. For all samples, peaks between $2922.73\text{--}2924.19\text{ cm}^{-1}$ and $2853.23\text{--}2854.13\text{ cm}^{-1}$ were found. Since it was found in the single bond area those peaks can contribute to long-chain aliphatic compounds [53]. There were no characteristic peaks in the triple-bond region ($2000\text{--}2500\text{ cm}^{-1}$). In the double-bond region ($1500\text{--}2000\text{ cm}^{-1}$) for all samples, peaks were found between $1743.15\text{--}1744.20\text{ cm}^{-1}$. Those peaks can describe carbonyl compounds such as aldehydes, ketones or esters characteristic for essential oils, at the same time being a proof for successful EOs encapsulation. These peaks for samples SB2, SJ3 and GJ3 were much more intense compared with the rest of the graphs, which may indicate a higher content of essential oils in these samples (according to the EE% results). In the same region we found peaks at $1634.11\text{--}1646.11\text{ cm}^{-1}$, which might be because of the presence of unsaturated bonds, probably $\text{C}=\text{C}$. The rest of the peaks are characteristic for the fingerprint region ($600\text{--}1500\text{ cm}^{-1}$)—those peaks can contribute to the methylene C-H bond ($1485\text{--}1445\text{ cm}^{-1}$), methyne C-H bond ($1350\text{--}1330\text{ cm}^{-1}$), C-O stretch ($\sim 1200\text{ cm}^{-1}$, $\sim 1150\text{ cm}^{-1}$), and CN stretch ($1210\text{--}1150\text{ cm}^{-1}$). Again, only for samples SB2, SJ3 I GJ3 were characteristic peaks at $720.68\text{--}721.18\text{ cm}^{-1}$ found and these can be linked with the aromatic ring coming from essential oils [53].

3.7. DSC

DSC analysis was performed to verify the thermal behavior after encapsulation of the essential oils. In the curves showing the thermal behavior of the wall materials (gelatin, gum Arabic), an endothermic peak can be seen in each case— 60.58 ± 0.002 °C (-1430.91 ± 0.001 mJ) for gelatin and 137.93 ± 0.001 °C (-696.52 ± 0.001 mJ) for gum Arabic. Those peaks probably refer to a glass transition. DSC curves for juniper and black pepper essential oils show an endothermic event at $24\text{--}25 \pm 0.001$ °C (-80.00 ± 0.001 mJ and -87.04 ± 0.002 mJ, respectively) related to the residual water and at $150 \pm 0.001\text{--}158 \pm 0.001$ °C (-350.87 ± 0.001 mJ and -367.14 ± 0.001 mJ, respectively) related to the decomposition of JEO and BPO [24]. Table 6 shows DSC onset, peaks and endset temperatures with corresponding enthalpies for all designed microcapsules. Onset and endset temperatures for GJ1, GJ2, and GJ3 were found to be $63.67 \pm 0.002\text{--}87.18 \pm 0.002$ °C, $56.93 \pm 0.002\text{--}161.87 \pm 0.002$ °C and $68.75 \pm 0.001\text{--}87.94 \pm 0.002$ °C, respectively, with different enthalpy values (-36.31 ± 0.001 mJ, -14.00 ± 0.001 mJ and -20.52 ± 0.002 mJ, respectively). Onset and endset temperatures for GB1, GB2 and GB3 were found to be $46.21 \pm 0.001\text{--}113.29 \pm 0.001$ °C, $83.46 \pm 0.001\text{--}99.21 \pm 0.001$ °C and $94.72 \pm 0.001\text{--}151.31 \pm 0.002$ °C, respectively, with the following respective enthalpy values: -222.81 ± 0.001 mJ, -14.00 ± 0.001 mJ and -327.77 ± 0.001 mJ. For samples SJ1, SJ2 and SJ3 onset and endset temperatures were $55.23 \pm 0.001\text{--}175.95 \pm 0.001$ °C, $82.32 \pm 0.001\text{--}108.89 \pm 0.001$ °C and $68.86 \pm 0.001\text{--}89.36 \pm 0.001$ °C, respectively. Each sample exhibited unique enthalpy values, indicative of the heat absorbed during thermal transitions. The respective enthalpy values were: -186.11 ± 0.001 mJ, -51.25 ± 0.001 mJ and -0.45 ± 0.002 mJ. Similarly, for samples SB1, SB2 and SB3, onset and endset temperatures were $59.94 \pm 0.001\text{--}178.75 \pm 0.001$ °C, $70.13 \pm 0.001\text{--}84.80 \pm 0.001$ °C and $71.79 \pm 0.001\text{--}161.17 \pm 0.001$ °C, respectively, with enthalpy values of -285.82 ± 0.002 mJ, -14.50 ± 0.001 mJ and -210.46 ± 0.001 mJ, respectively. Due to the lack of peaks characteristic of JEO and BPO, it can be assumed that these essential oils have been successfully encapsulated in the wall material [24]. In terms of thermal stability, samples containing soybean oil were found to be the most stable. Additionally, the samples with the G/GA ratio of 1:1 were characterized by the highest onset temperature. From this it can be concluded that those samples would be the best variant of EO microcapsules, allowing their use in processes requiring the use of elevated temperature (not higher than 68 °C).

Table 6. Temperatures of the onsets, peaks and endsets of endothermic reactions with enthalpy.

Sample	Onset (°C)	Peak (°C)	Endset (°C)	Enthalpy (mJ)
GJ1	63.67 ± 0.002	76.61 ± 0.001	87.18 ± 0.002	-36.31 ± 0.001
GJ2	56.93 ± 0.002	98.08 ± 0.001	161.87 ± 0.002	-353.88 ± 0.001
GJ3	68.75 ± 0.001	79.31 ± 0.002	87.94 ± 0.002	-20.52 ± 0.002
GB1	46.21 ± 0.001	98.60 ± 0.001	113.29 ± 0.001	-222.81 ± 0.001
GB2	83.46 ± 0.001	92.76 ± 0.002	99.21 ± 0.001	-14.00 ± 0.001
GB3	94.72 ± 0.001	121.90 ± 0.001	151.31 ± 0.002	-327.77 ± 0.001
SJ1	55.23 ± 0.001	107.75 ± 0.001	175.95 ± 0.001	-186.11 ± 0.001
SJ2	82.32 ± 0.001	89.61 ± 0.001	108.89 ± 0.001	-51.25 ± 0.001
SJ3	68.86 ± 0.001	80.62 ± 0.001	89.36 ± 0.001	-0.45 ± 0.002
SB1	59.94 ± 0.001	109.09 ± 0.002	178.75 ± 0.001	-285.82 ± 0.002
SB2	70.13 ± 0.001	78.48 ± 0.002	84.80 ± 0.001	-14.50 ± 0.001
SB3	71.79 ± 0.001	121.62 ± 0.002	161.17 ± 0.001	-210.46 ± 0.001

3.8. Electronic Nose Analysis

Figure 3 presents the classification of scent profiles in relation to their experimental groups. Samples are represented in a two-dimensional plane with reference to selected components: principal component 1 and principal component 2. When considering essential oils separately, it can be concluded that, in the case of grape seed with juniper as an essential

oil, the total contribution variances of PC1 and PC2 for direct electronic nose measurements were 60.6% and 14.27%, respectively. The combination of grape seed and black pepper as essential oil resulted in values explaining 65.23% of the data variance, where 10.81% was intercepted by the horizontal axis, explaining differences among samples along that axis. For soybean with juniper, the total contribution variances of PC1 and PC2 for direct electronic nose measurements were 63.21% and 14.10%, respectively. Soybean with black pepper caused a 67.56% data variance, with 10.51% intercepted by the horizontal axis. Additionally, there was no overlap between the mixing ratios of the single samples for all essential oils.

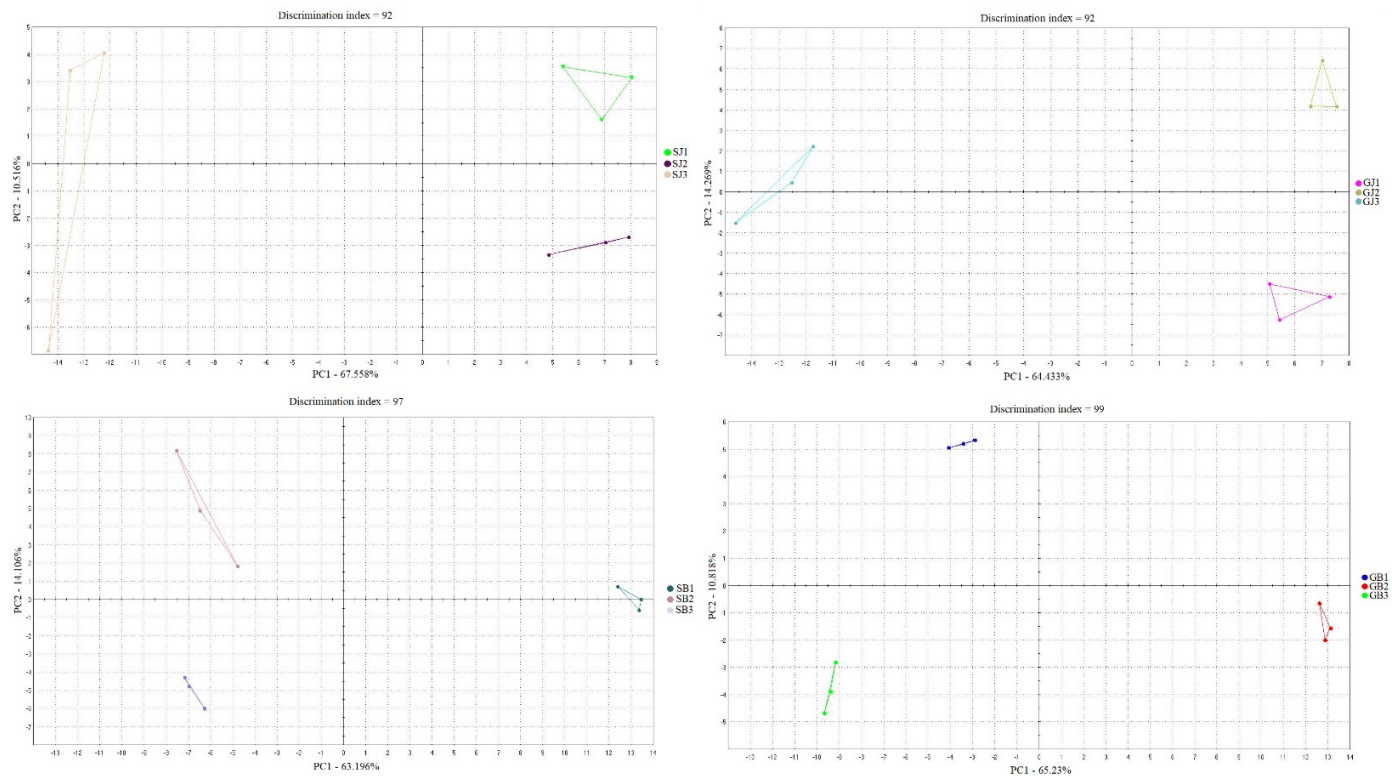


Figure 3. Classification of scent profiles of microcapsules containing juniper and black pepper essential oils.

Table 7 lists the Kovats indexes along with the volatiles identified in each sample and their corresponding sensory descriptors. According to literature data, juniper (*Juniperus communis*) essential oil contains mainly α -pinene (25.3%), β -pinene (2.98%), sabinene (5.99%), β -myrcene (12.6%), α -terpinene (0.21%), γ -terpinene (0.80%), and limonene (2.99%) [7]. All of the abovementioned compounds except for sabinene and α -terpinene were identified in all of the samples containing juniper essential oil. These two compounds are highly volatile, and their absence in the samples can be explained by their probable evaporation during the freeze drying process [54]. Samples containing EO from juniper dissolved in soybean oil were also characterized by the content of 3-methyl-octane, 2-butylfuran and dimethyl disulfide. In turn, those with grape seed oil were the only ones that contained 3-methyl-2-butene-1-thiol, geranial and thymol. All JEO capsules contained nonane and propyl nonanoate. From this it can be seen that the oil in which the EO is dissolved has an effect on the composition of the EO volatiles after freeze drying. Similarly, in the samples containing black pepper essential oil, the compounds characteristic of this oil were identified as α -pinene, β -pinene, myrcene, and limonene. Sabinene and β -caryophyllene were not identified [55]. In addition, 5-pentanolide and isoamylacetate were identified in samples containing BPO.

In each of the samples, ethanol and 2-propanol were identified, which are probably residues from the extraction process [56].

Table 7. Kovats indexes, identified volatile compounds and sensory descriptors assigned to them.

Kovats Index	Identified Volatile Compound	Sensory Descriptors	GJ1	GJ2	GJ3	SJ1	SJ2	SJ3	GB1	GB2	GB3	SB1	SB2	SB3
437	ethanol	alcoholic	+	+	+	+	+	+	+	+	+	+	+	+
508	2-propanol	alcoholic	+	+	+	+	+	+	+	+	+	+	+	+
519	ethanethiol	earthy, fruity, garlic												
541	2-methylpropanal	aldehydic	+	+	+	+	+	+	+	+	+	+	+	+
567	butanal	chocolate, green, malty	+	+	+	+	+	+	+	+	+	+	+	+
594	butan-2-one	acetone, butter	+	+	+	+	+	+	+	+	+	+	+	+
608	2-methylfuran	acetone, burnt						+						
610	methyl propanoate	apple, ethereal, fresh									+			
617	acetic acid	acetic, acidic				+							+	
618	1-propanethiol	alliaceous, cabbage, onion, sweet				+								
638	1-butanamine	ammoniacal, fish										+	+	+
643	1-propanethiol	alliaceous, cabbage, onion, sweet									+			
437	ethanol	alcoholic	+	+	+	+	+	+	+	+	+	+	+	+
508	2-propanol	alcoholic	+	+	+	+	+	+	+	+	+	+	+	+
519	ethanethiol	earthy, fruity, garlic												
541	2-methylpropanal	aldehydic	+	+	+	+	+	+	+	+	+	+	+	+
567	butanal	chocolate, green, malty	+	+	+	+	+	+	+	+	+	+	+	+
594	butan-2-one	acetone, butter	+	+	+	+	+	+	+	+	+	+	+	+
608	2-methylfuran	acetone, burnt						+						
610	methyl propanoate	apple, ethereal, fresh									+			
617	acetic acid	acetic, acidic				+							+	
618	1-propanethiol	alliaceous, cabbage, onion, sweet				+								
638	1-butanamine	ammoniacal, fish										+	+	+
643	1-propanethiol	alliaceous, cabbage, onion, sweet									+			
437	ethanol	alcoholic	+	+	+	+	+	+	+	+	+	+	+	+
508	2-propanol	alcoholic	+	+	+	+	+	+	+	+	+	+	+	+
519	ethanethiol	earthy, fruity, garlic												
541	2-methylpropanal	aldehydic	+	+	+	+	+	+	+	+	+	+	+	+
567	butanal	chocolate, green, malty	+	+	+	+	+	+	+	+	+	+	+	+
594	butan-2-one	acetone, butter	+	+	+	+	+	+	+	+	+	+	+	+
608	2-methylfuran	acetone, burnt						+						
610	methyl propanoate	apple, ethereal, fresh									+			
617	acetic acid	acetic, acidic				+							+	
618	1-propanethiol	alliaceous, cabbage, onion, sweet				+								
638	1-butanamine	ammoniacal, fish										+	+	+
643	1-propanethiol	alliaceous, cabbage, onion, sweet									+			
658	n-butanol	alcoholic, cheese, fermented										+	+	+
667	trichloroethane	chloroform, ethereal	+	+	+	+		+	+	+	+	+	+	+
673	1-methoxy-2-propanol	mild					+	+	+					
684	pentan-2-one	acetone, banana, ethereal					+	+	+			+	+	+
700	pentan-2-ol	alcoholic, ethereal, fermented	+	+	+							+	+	+
700	heptane	alkane, fruity									+			
735	dimethyl disulfide	cabbage, cheese, garlic					+	+	+					
735	butanethiol	coffee, garlic	+	+	+									
742	(e)-2-pentanal	apple, fruity, green									+			
745	propanoic acid	cheese, fruity	+	+	+	+	+	+	+			+	+	+
759	pentanol	alcoholic, anise, balsamic												
767	3-methylbut-2-en-1-ol	herbaceous, lavender					+	+						+
780	toluene	caramelized, ethereal, fruity	+	+	+				+	+	+	+	+	+
767	2-methylpentane	-				+	+	+						
792	hexanal	acorn, aldehydic, fatty					+	+	+	+	+	+	+	+
801	ethyl butyrate	acetone, banana	+	+	+	+	+	+						
812	octane	alkane, fruity, fusel				+	+	+				+	+	
810	(e)-2-octene	-								+	+			
847	4-ethylheptane	-					+	+	+					
847	3-methyl-2-butene-1-thiol	amine, leek, onion	+	+	+									
852	methyl pentanoate	apple, ethereal, fruity, green									+			
866	ethyl isovalerate	anise, apple, blackcurrant	+	+	+			+						
873	3-methyl-octane	-						+						
884	nonane	alkane, fusel	+	+	+	+	+	+						
896	2-butylfuran	fruity, mild				+	+	+						
898	isoamyl acetate	apple, banana, ester, fresh	+	+					+	+	+	+	+	+
907	nonane	alkane, fusel									+			
922	1s(-)-a-pinene	fresh, herbaceous	+	+	+	+	+	+	+	+	+	+	+	+
940	5-pentanolide	-										+	+	+
962	alpha-pinene	camphore, citrus	+	+	+	+	+	+	+	+	+	+	+	+
974	beta-pinene	dry, green, hay	+	+	+	+	+	+	+	+	+	+	+	+
966	myrcene	balsamic, ethereal, fruity	+	+	+	+	+	+	+	+	+	+	+	+
1033	beta-phellandrene	fruity, herbaceous	+	+	+	+	+	+	+	+	+	+	+	+
1049	limonene	citrus, fruity	+	+	+	+	+	+	+	+	+	+	+	+
1076	gamma-terpinene	citrus, ethereal, fruity	+	+	+	+	+	+	+	+	+	+	+	+
1106	methylacetophenone	-				+	+	+						
1107	ethyl heptanoate	fruity	+	+	+				+	+	+	+	+	+
1135	n-nonanal	aldehydic, chlorine, citrus	+	+	+	+	+	+	+	+	+	+	+	+
1150	ethyl cyclohexanecarboxylate	-										+		
1153	2,3-diethyl-5-methylpyrazin	fragrant, hazelnut					+	+	+					
1153	e-2-nonen-1-ol	green, melon	+	+	+								+	+
1164	benzyl acetate	burnt, floral, fresh, fruity	+	+	+	+	+	+	+	+	+	+	+	+
1187	p-methylacetophenone	almond, bitter almond, cherry	+	+	+	+	+		+	+	+	+	+	+
1205	decanal	aldehydic, burnt, citrus	+	+	+				+	+	+	+	+	+
1207	6-decenal	-												
1217	dodecane	alkane, fusel					+	+	+				+	+
1248	ethyl phenylacetate	anise, cinnamon, cocoa, flaral, rose							+	+	+			
1265	2-butenic acid, hexyl ester	fruity, green, oily, walnut												
1277	tridecane	alkane, citrus, fruity												
1300	ethyl nonanoate	fruity, rose, rum					+							
1313	nonyl acetate	fruity, leafy, sweet											+	
1272	tridecane	-									+			
1278	geranial	-	+	+										
1293	thymol	aromatic, earthy, herbaceous	+	+										
1301	tricdecane	alkane, citrus, fruity										+		
1313	butyl heptanoate	fresh, fruity, grassy, green							+					
1316	anethole	anise, herbaceous,	+	+										
1330	nonyl acetate	fruity, leafy, sweet												+
1365	3-ethyl dodecane	-												
1367	eugenol	balsamic, camphore, floral					+	+						
1371	tetradecane	alkane, fusel, herbaceous	+	+	+				+	+		+	+	+
1386	n-hexyl-hexanoate	apple, fresh, fruity					+	+						
1369	butyl octanoate	butter, floral, fruity, green, oily		+	+							+	+	+
1421	propyl nonanoate	fermented, melon	+	+	+	+	+	+				+	+	+
1468	n-octylbenzene	-					+	+	+					

3.9. SEM

Figure 4 shows SEM images of lyophilized microcapsules. As described earlier, the encapsulation efficiency was not very high (42.7–64.09%). This fact can be explained by the morphology of the microcapsules. The obtained powder was characterized by an irregular, very porous structure with a large surface area, suggesting that the core material was not completely covered. For this reason, oxygen availability can be high, causing oxidation of both the oil and the essential oil [51]. In addition, the highly porous surface of the microcapsules may make it easier for the essential oil to evaporate during storage. An increase in the concentration of polymers can make the wall of the microcapsule thicker, which can have a direct effect on the size of the resulting capsules [54]—in figures 12–15 it is clear that the microcapsules containing G:GA = 1:1 were smaller than those where the concentration of G:GA was 1:2 or 2:1.

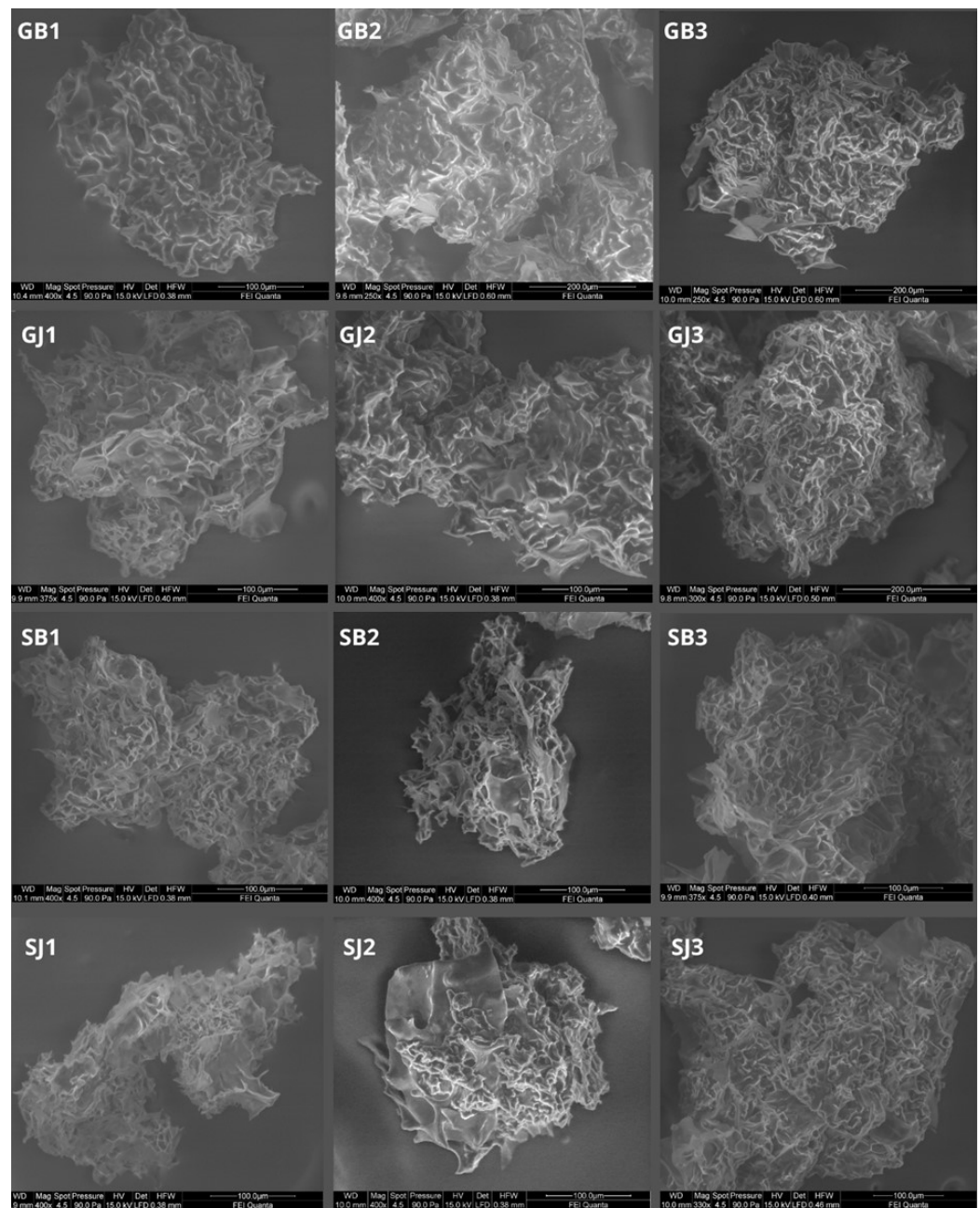


Figure 4. SEM photos.

4. Discussion

4.1. Evaluation of Coacervation Efficacy

Karagozlu [57], using a complex coacervation between gelatin and acacia, obtained a SY of about 26.66%. Hernandez-Nava [26] used G and GA as wall material (mixing ratio 2:1) and obtained an SY in the 72–88% range. These differences may be caused primarily by the difference in pH during the coacervation process and the difference in the selection of the drying method.

The most common method of encapsulating essential oils is spray drying with the use of various types of carriers—whey protein (WP), maltodextrin (MD), inulin (IN), gelatin, gum Arabic, various types of modified starches (MS), etc. The use of this method allows for encapsulation efficiencies at levels of 47.13% for WPI, 61.64% for WPI:MD, 48.14% for WPI:IN [12], 87.5–94.5% for G:GA (depending on the air temperature used at the inlet) [26] or even 98.87% for MD:MS [42]. The encapsulation efficiency for spray drying depends largely on the wall materials used, as is the case with complex coacervation. Here, however, the mixing ratio of the polymers is also important. It is well known that encapsulation efficiency increases with increasing polymer concentration, however, this is not the only factor affecting EE. The interactions between the polymers used and the amount of core material also play an important role, as shown by the results of our research. Manaf et al. [44] used simple and complex coacervation to encapsulate citronella EO. For simple coacervation they used GA (12,5% *w/v*), for complex coacervation they used G:GA (mixing ratio 1:1, 12,5% *v/w*), and in both cases they used 1% of core material. The encapsulation efficiencies of the system prepared in this way were 93.91% and 94.42%, respectively. The team did not use any method of drying the obtained coacervates, liquid forms were used for the research. Various concentrations of wall and core material were tested by Samakradhamrongthai et al. [45]. A complex coacervation with spray drying was performed between G and GA at pH = 4.0 with a mixing ratio of 1:1; 1:2, and 2:1. The results show that the lowest EE was obtained with a mixing ratio of 1:1 and a core material content of 10% (38.56%). The highest was obtained with a mixing ratio of 2:1 and a content of core material of 5% (95.15%). Much less research is available where lyophilization has been used to dry the coacervates. This method gives good results. Freeze drying of complex coacervates made between WPI and carbomethylcellulose (CMC), WPI and sodium alginate (SA) as well as WPI and chitosan (CH), has resulted in EE at the levels of 83.94%, 79.28% and 82.88%, respectively [19]. A complex coacervation with freeze drying has also been performed between G and GA [57]. The encapsulation efficiency reported was 64.31%. In our research, the encapsulation efficiency was similar to that obtained by Karagozlu et al. [57] and slightly lower compared with results obtained by Rojas-Moreno et al. [19] (max. 64.09%, min. 42.7%). To increase the efficiency of encapsulation, in our case, the amount of core material should probably be reduced (less than 10%) or the concentration of wall materials should be increased (more than 5%).

4.2. Bulk density, Tapped Density, Carr Index (CI), and Hausner Ratio (HR)

Bulk and tapped density depend not only on composition of the wall material, but also on the drying method. The use of WPI:IN (3:1, 1:1, 1:3) as a wall material for rosemary EO encapsulation by spray drying (170 °C) resulted in powders with bulk densities of 0.20 g/cm³, 0.24 g/cm³, and 0.26 g/cm³, respectively. Tapped densities were slightly higher—0.30 g/cm³, 0.34 g/cm³, and 0.41 g/cm³, respectively [12]. On the other hand, Yekdane et al. [58], using spray drying (170 °C), microencapsulated pomegranate seed oil and reported that the bulk density, depending on the content of pomegranate juice in the wall material, ranged from 0.4 to 0.5 g/cm³. Hernandez-Nava et al. [26], used the complex coacervation with spray drying between G:GA and gelatin and chia mucilage (CM) to microencapsulate oregano EO. Depending on the spray drying parameters (160 °C or 180 °C), the bulk density in their study was in the range of G:GA 0.157–0.202 g/cm³ and 0.234–0.282 g/cm³ for G:CM. In contrast, the tapped density for G:GA was 0.314–0.404 g/cm³, and for G:CM 0.335–0.403 g/cm³. However, a low bulk

density may indicate a high air content in the microcapsules, which in turn may favor the negative effect of lipid oxidation. The authors of [57], investigating the bulk density of freeze-dried coacervates (G:GA) containing oregano essential oil, indicated that the bulk density of the powders thus obtained was 0.527 g/cm^3 . In our case, the bulk density was lower, probably due to different solid content.

The use of MD:WPI as wall materials for spray drying and thus encapsulation of olive oil allowed us to obtain a CI in the range of 25.61–54.70 [59]. Such a large dispersion of values was caused by different mixing ratios of polymers. Hernandez-Nava et al. [26], have reported that the powders obtained by spray drying G:GA coacervates were characterized by a Carr index of approximately 50, while the HR was approximately 2. Similarly, for the G:CM system, CI was approximately 30 and HR approximately 1.43. Another team used complex coacervation between soy protein and GA to microencapsulate chia seed oil. The obtained coacervates were spray dried ($130 \text{ }^\circ\text{C}$) and were characterized by $\text{CI} = 35$ and $\text{HR} = 1.25$ [23]. In turn, freeze drying of MD-based emulsions (10, 15 and 20% *v/w*) allowed for the obtaining of powders characterized by a CI in the range of 11.62 to 17.64 and HR in the range of 1.13–1.21 [60]. These values were much lower than in our case, where we freeze dried coacervates (CI min. 30.58, max. 50.27, HR min. 1.45, max. 2.01). Therefore, it can be concluded that the powders obtained as a result of complex coacervation are characterized by very high cohesiveness and virtually no flow.

4.3. Solubility, Hygroscopicity, and Moisture Content

Fernandez et al. [12] investigated the solubility of spray-dried powders containing ginger EO. Depending on the wall material used (WPI, WPI:MD, WPI:IN), the solubility of the powders was in the range of 76.94–81.58%. Another team [19], using MD:MS as a wall material for microencapsulation of orange EO (by spray drying), obtained powders with a solubility of 57.10%. Caparino et al. [27] investigated the water solubility of mango powders obtained from the emulsion with MD by spray and freeze drying. Powders obtained by spray drying had a solubility of 95.31%, while those obtained by freeze drying had a lower solubility—89.70%. Thus, the influence of the choice of method on the solubility of the obtained powder is visible—lyophilization makes the powders less soluble. In our case, the solubility was low and did not exceed 26%. These results correlate with those obtained by Shaddel et al. [30]. The powders obtained by freeze drying coacervates (5% *v/v* G/GA) were characterized by low water solubility, not exceeding 30%. Similarly, in the case of freeze-dried coacervates obtained by mixing G:GA in the ratio 1:1 with the addition of shrimp lipid extract [61]—the solubility of the obtained powder was low—approximately 9.6%. The above indicates that not only the method of drying, but also the type of dried material (emulsion, coacervates), has a significant impact on the solubility of powders. Powders obtained by the freeze drying of complex coacervates show much lower solubility in water than those obtained from the classical emulsion.

Zotarelli et al. [47] found that mango powders obtained by the spray drying of mango pulp with maltodextrin (MD) displayed high hygroscopicity in the range of 23.9–26.9%. In a study by Caparino et al. [27], the hygroscopicity of mango powders obtained by spray and freeze drying of mango puree with MD was reported to be around 16.5% for spray-dried samples and approximately 18% for freeze-dried samples. Similarly, in the case of the spray drying (at $170 \text{ }^\circ\text{C}$) of an emulsion containing WPI:IN and rosemary essential oil, the hygroscopicity of the resulting powders varied from 15.7% to 17.1%, depending on the mixing ratio of the wall materials [32].

In contrast, powders obtained by the freeze drying of coacervates showed significantly lower hygroscopicity. Tavares et al. [62] have reported that coacervates with ginger essential oil exhibited lower hygroscopicity than coacervates without, ranging from 6.64% to 9.65%, which is below the threshold of 15.1%. This aligns more closely with the values obtained in our study. Gomez-Estaca [59] demonstrated that coacervates (G:GA, freeze dried) containing shrimp lipid extract had hygroscopicity at the level of $2.33 \pm 0.12 \text{ g/100 g}$. Consequently, it can be inferred that both the addition of essential oil and the utilization of

complex coacervation as a microencapsulation method have a positive effect on reducing the hygroscopicity of the obtained powders. Based on the results obtained and their comparison with literature data, it can be concluded that the obtained microcapsules could be stored for a longer time without compromising their properties.

The moisture content of powders obtained through various encapsulation methods and wall materials can vary significantly. Fernandes et al. [12] demonstrated that ginger essential oil (EO) powders obtained by spray drying had moisture content ranging from 1.05% to 1.98%, depending on the wall material used (WPI, WPI:MD, WPI:IN). Similar results were reported by Zotarelli et al. [47], where the moisture content of spray-dried mango powders with maltodextrin (MD) was 1.5%. Slightly higher hygroscopicity was observed in spray-dried coacervates, with moisture content ranging from 3.86% to 4.55% (G:GA) and 3.49% to 4.58% (G:CM) [26]. Rojas-Moreno et al. [19] found that the moisture content of spray-dried microcapsules containing orange essential oil varied from 1% to 4.5%, while freeze-dried samples exhibited slightly higher moisture content (2% to 5.5%). This difference in moisture content between spray-dried and freeze-dried samples could be attributed to the presence of oil droplets, which act as a vapor transport barrier, reducing the evaporation of water and increasing the hydrophobicity of the microcapsules. The freeze drying of coacervates containing ginger essential oil, with different wall materials (GA:CH, WPI:GA), resulted in powders with moisture contents of approximately 3.04% and 3.10%, respectively. The addition of essential oil significantly reduced these values, as coacervates without essential oil had moisture contents of approximately 6.01% and 8.02%, respectively [63]. The freeze drying of coacervates (G:GA) containing oregano essential oil produced powders with a water content of 3.39% [57].

The selection and concentration of wall materials play a crucial role in determining the moisture content of the obtained powders. The results obtained in our study (moisture content = 0.05% to 0.56%) are consistent with those obtained by Samakradhamrongthai et al. [45], who, by mixing gelatin and gum Arabic in a 1:1 ratio, obtained powders with moisture content ranging from 0.32% to 0.72% for different concentrations of core material. Based on the above, it can be concluded that the use of gelatin with gum Arabic in the coacervation process allows one to obtain powders with low moisture content, and that are thus suitable for long-term storage.

4.4. Color Measurement

Syed et al. [63] conducted color measurements of, inter alia, unrefined soybean oil. The results obtained in the study correlate with those obtained in this study in terms of the b^* parameter—the researchers indicate the value of b^* as 40.0 ± 0.60 . There is some discrepancy in the case of the a^* parameter. The team indicated positive values (4.0 ± 0.65), while the results we obtained clearly indicate negative a^* values. Such a change in the a^* parameter should be attributed to the wall materials used for encapsulation and to the presence of EO. Bruhl and Unbehend [64] carried out measurements of the color of grape seed oil. The L^* parameter obtained by the researchers was similar to the results obtained in this study $L^* = 99.44$. In turn, parameters a^* and b^* had higher values, although with the same sign: $a^* = -4.68$, $b^* = 12.49$. Again, the discrepancy in the results was largely caused by wall materials and essential oil.

4.5. Particle Size Distribution

Several studies have investigated particle size and similar parameters for powders produced by various methods, such as spray drying and complex coacervation. Rojas-Moreno et al. [19] examined powders obtained by spray drying coacervates (WPI:CMC, WPI:SA, WPI:CH), reporting particle sizes of 6.31 μm , 10.59 μm , and 9.44 μm , respectively, along with surface index (SI) values of 0.95 μm , 1.03 μm , and 10.6 μm , respectively.

Hernandez-Nava et al. [26] conducted similar studies involving complex coacervation between gelatin (G) and gum Arabic (GA). Depending on the parameters, they observed particle sizes (D10, D50, and D90) ranging from 6.08 μm to 30.31 μm . It is worth noting

that spray drying generally allows for smaller particle sizes [25]. For instance, the particle size of spray-dried smoke powder food flavoring has been reported to be 6.3–6.9 μm , significantly smaller than freeze-dried preparations (134.7–580.4 μm) [65]. Freeze-dried G:GA coacervates had a particle size of 41.26 μm . Tavares et al. [63] conducted complex coacervation between WPI:CH and GA:CH, followed by freeze drying. Their results include D10 of approximately 25.06 μm , D50 of approximately 103.39 μm , D90 of approximately 293.51 μm , and an SI of approximately 2.60 for WPI:CH. For GA:CH, the results were D10 \approx 19.18 μm , D50 \approx 74.23 μm , D90 \approx 189.21 μm , and SI \approx 2.29. In our study, the screening of the obtained lyophilizates on a laboratory sieve played a crucial role in achieving size uniformity and obtaining relatively small particles, consistent with the standard for lyophilizates. This method allowed for the control and standardization of particle sizes.

Particle size stands as a crucial quality parameter in the determination of microcapsules' application areas. It significantly influences delivery properties and the flowability of the powder, playing a pivotal role in the selection process. Complex coacervation between CH and GA [66] in the ratio 1:1, 1:2 and 2:1 has shown that the ratio of the wall material has a significant effect on the particle size of the microcapsules. The particle size for the samples was 16.39 μm , 28.98 μm , and 49.53 μm , respectively. Particle size is significantly affected by the proportion of polymer used in the wall material, and as the particle size decreases, particle–particle interactions become easier due to the increase in surface area [66].

4.6. SEM

Marfil et al. [67], using the same mixing ratios G:GA (1:1, 1:2, 2:1), obtained microcapsules with a completely different surface—smooth, without pores—and individual microcapsules were connected with each other via solid bridges, characteristic of freeze-dried products. This type of surface suggests that the entire core material was covered with wall material and the encapsulation efficiency should be high. Meanwhile, in the case of capsules that had the same concentration of wall materials and core material as in the present study, the encapsulation efficiency was quite similar, ranging from 50.08 to 83.5%. Differences in the obtained structure may be due to the difference in lyophilization temperature, which in the case of studies conducted by Marfil et al. [68] was higher ($-40\text{ }^{\circ}\text{C}$) than in this study ($-80\text{ }^{\circ}\text{C}$). As described by Krokida et al. [69]—where the porosity of the obtained product depends on the lyophilization conditions, including the temperature—the lower the temperature, the higher the porosity. The same was later confirmed by Barresi et al. [70]. Perhaps increasing the lyophilization temperature would allow for higher encapsulation efficiency in the case of this study.

5. Conclusions

Complex coacervation between gelatin and gum Arabic can be used to microencapsulate essential oils. However, not all of the combinations of mixing ratios were equally effective. The highest encapsulation efficiency characterized the SJ1 sample.

A relatively low EE was obtained, influenced by the interaction between the mixing ratio and the oil. A low efficiency was probably caused by a too-high concentration of core material in relation to the wall material. The highest EE value was obtained for sample SJ1 ($64.09\% \pm 0.09$). Similarly, high encapsulation efficiency was obtained for samples SB3 and GJ2 (61.92 ± 0.04 and 59.89 ± 0.01 , respectively). Thus, no clear influence of the mixing ratio between gelatin and gum Arabic was demonstrated on the obtained efficiency of the encapsulation process. The powders obtained because of lyophilization of the coacervates with a 1:1 mixing ratio were characterized by the smallest particle sizes. However, this did not reflect an increase in bulk and tapped density, and did not reflect an increase in their hygroscopicity. However, the powders containing G/GA = 1:1 were the most soluble among the powders tested. The least dissolving microcapsules were obtained with a mixing ratio of G/GA = 2:1.

The aim of this research was to determine whether the classical model of complex coacervation (G: GA) could be used for microencapsulation of essential oils. These findings

suggest that such a combination of wall materials can be used for this purpose. Further research should be carried out to find the optimal mixing ratio between gelatin and gum Arabic that would allow for higher encapsulation efficiency. Future investigations may also focus on optimizing all process parameters for the microencapsulation of essential oils to obtain powders with better properties.

Author Contributions: A.N.—conceptualization, methodology, formal analysis, writing—original draft, investigation, A.S.—investigation, I.W.-K.—investigation, M.D.T.P.—investigation, H.D.G.—investigation, M.A.K.—supervision, writing—review and editing. All authors have read and agreed to the published version of the manuscript.

Funding: This research received no external funding.

Data Availability Statement: Data is contained within the article.

Conflicts of Interest: The authors declare no conflict of interest.

References

1. Kunicka-Styczyńska, A. Olejki eteryczne jako alternatywa dla syntetycznych konserwantów żywności—Praca przeglądowa. In *Innowacyjne Rozwiązania w Technologii Żywności i Żywieniu Człowieka*; Tarko, T., Drożdż, I., Najgebauer-Lejko, D., Duda-Chodak, A., Eds.; Oddział Małopolski Polskiego Towarzystwa Technologów Żywności: Kraków, Poland, 2016; pp. 175–184.
2. Tajkarimi, M.M.; Ibrahim, S.A.; Cliver, D.O. Antimicrobial herb and spice compounds in food. *Food Control* **2010**, *21*, 1199–1218. [[CrossRef](#)]
3. Maruyama, S.; Streletskaia, N.A.; Lim, J. Clean label: Why this ingredient but not that one? *Food Qual. Prefer.* **2020**, *87*, 1–9. [[CrossRef](#)]
4. Hojjati, F.; Sereshti, H.; Hojjati, M. Leaf essential oils and their application in systematics of *Juniperus excelsa* complex in Iran. *Biochem. Syst. Ecol.* **2019**, *84*, 29–34. [[CrossRef](#)]
5. Ghorbanzadeh, A.; Ghasemnezhad, A.; Sarmast, M.K.; Ebrahimi, S.N. An analysis of variations in morphological characteristics, essential oil content, and genetic sequencing among and within major Iranian Juniper (*Juniperus* spp.) populations. *Phytochem* **2021**, *186*, 1–10. [[CrossRef](#)] [[PubMed](#)]
6. Nikolić, M.; Stojković, D.; Glamočlija, J.; Ćirić, A.; Marković, T.; Smiljković, M.; Soković, M. Could essential oils of green and black pepper be used as food preservatives? *J. Food Sci. Technol.* **2015**, *52*, 1–9. [[CrossRef](#)]
7. Zheljzkov, D.V.; Kacaniova, M.; Dincheva, I.; Radoukova, T.; Semerdjieva, I.B.; Astatkie, T.; Schlegel, V. Essential oil composition, antioxidant and antimicrobial activity of the galbula of six juniper species. *Ind. Crops Prod.* **2018**, *124*, 449–458. [[CrossRef](#)]
8. Dosoky, N.S.; Satyal, P.; Barata, L.M.; da Silva, J.K.R.; Setzer, W.N. Volatiles of Black Pepper Fruits (*Piper nigrum* L.). *Molecules* **2019**, *24*, 4244. [[CrossRef](#)]
9. Bastos, L.P.H.; de Sá Costa, B.; Siqueira, R.P.; Garcia-Rojas, E.E. Complex coacervates of β -lactoglobulin/sodium alginate for the microencapsulation of black pepper (*Piper nigrum* L.) essential oil: Simulated gastrointestinal conditions and modeling release kinetics. *Int. J. Biol. Macromol.* **2020**, *160*, 861–870. [[CrossRef](#)]
10. Bastos, L.P.H.; Corrêa dos Santos, C.H.; de Carvalho, M.G.; Garcia-Rojas, E.E. Encapsulation of the black pepper (*Piper nigrum* L.) essential oil by lactoferrin-sodium alginate complex coacervates: Structural characterization and simulated gastrointestinal conditions. *Food Chem.* **2020**, *316*, 861–870. [[CrossRef](#)]
11. Amalraj, A.; Haponiuk, J.T.; Thomas, S.; Gopi, S. Preparation, characterization and antimicrobial activity of polyvinyl alcohol/gum arabic/chitosan composite films incorporated with black pepper essential oil and ginger essential oil. *Int. J. Biol. Macromol.* **2020**, *151*, 366–375. [[CrossRef](#)]
12. Fernandes, R.V.d.B.; Silva, E.K.; Borges, S.V.; de Oliveira, C.R.; Yoshida, M.I.; da Silva, Y.F.; do Carmo, E.L.; Azevedo, V.M.; Botrel, D.A. Proposing Novel Encapsulating Matrices for Spray-Dried Ginger Essential Oil from the Whey Protein Isolate-Inulin/Maltodextrin Blends. *Food Bioproc. Technol.* **2017**, *10*, 115–130. [[CrossRef](#)]
13. Napiórkowska, A.; Kurek, M. Coacervation as a Novel Method of Microencapsulation of Essential Oils—A Review. *Molecules* **2022**, *27*, 5142. [[CrossRef](#)] [[PubMed](#)]
14. Bakry, A.M.; Shabbar, A.; Barkat, A.; Majeed, H.; Abouelwafa, M.Y.; Mousa, A.; Li, L. Microencapsulation of Oils: A Comprehensive Review of Benefits, Techniques, and Applications. *CRFSFS* **2016**, *15*, 143–182. [[CrossRef](#)] [[PubMed](#)]
15. Delshadi, R.; Bahrami, A.; Tafti, A.G.; Barba, F.J.; Williams, L.L. Micro and nano-encapsulation of vegetable and essential oils to develop functional food products with improved nutritional profiles. *Trends Food. Sci. Technol.* **2020**, *104*, 72–83. [[CrossRef](#)]
16. Timilsena, Y.P.; Taiwo, O.A.; Nauman, K.; Benu, A.; Colin, J.B. Complex coacervation: Principles, mechanisms and applications in microencapsulation. *Int. J. Biol. Macromol.* **2019**, *121*, 1276–1286. [[CrossRef](#)]
17. Kralovec, J.; Zhang, S.; Zhang, W.; Barrow, C. A review of the progress in enzymatic concentration and microencapsulation of omega-3 rich oil from fish and microbial sources. *Food Chem.* **2020**, *131*, 639–644. [[CrossRef](#)]
18. Ogilvie-Battersby, J.D.; Nagarajan, R.; Mosurkal, R.; Orbey, N. Microencapsulation and controlled release of insect repellent geraniol in gelatin/gum arabic microcapsules. *Colloids Surf. A Physicochem. Eng.* **2022**, *640*, 1–11. [[CrossRef](#)]

19. Rojas-Moreno, S.; Osorio-Revilla, G.; Gallardo-Velázquez, T.; Cárdenas-Bailón, F.; Meza-Márquez, G. Effect of the cross-linking agent and drying method on encapsulation efficiency of orange essential oil by complex coacervation using whey protein isolate with different polysaccharides. *J. Microencapsul.* **2018**, *35*, 165–180. [[CrossRef](#)]
20. Pakzad, H.; Alemzadeh, I.; Kazemi, A. Encapsulation of Peppermint Oil with Arabic Gum-gelatin by Complex Coacervation Method. *Int. J. Eng.* **2013**, *26*, 807–814. [[CrossRef](#)]
21. Devi, N.; Sarmah, M.; Khatun, B.; Tarun, K.M. Encapsulation of active ingredients in polysaccharide-protein complex coacervates. *Adv. Colloid Interface Sci.* **2017**, *239*, 136–145. [[CrossRef](#)]
22. Warnakulasuriya, S.N.; Nickerson, M.T. Review on plant protein-polysaccharide complex coacervation, and the functionality and applicability of formed complexes. *J. Sci. Food Agric.* **2018**, *98*, 5559–5571. [[CrossRef](#)] [[PubMed](#)]
23. Bordón, M.G.; Paredes, A.J.; Camacho, N.M.; Penci, M.C.; González, A.; Palma, S.D.; Ribotta, P.D.; Martínez, M.L. Formulation, spray-drying and physicochemical characterization of functional powders loaded with chia seed oil and prepared by complex coacervation. *J. Powder Technol.* **2021**, *391*, 479–493. [[CrossRef](#)]
24. Mehran, M.; Masoum, S.; Memarzadeh, M. Microencapsulation of *Mentha spicata* essential oil by spray drying: Optimization, characterization, release kinetics of essential oil from microcapsules in food models. *Ind. Crops Prod.* **2020**, *154*, 1–8. [[CrossRef](#)]
25. Xin, X.; Essien, S.; Dell, K.; Woo, M.W.; Baroutian, S. Effects of Spray-Drying and Freeze-Drying on Bioactive and Volatile Compounds of Smoke Powder Food Flavouring. *Food Bioproc. Technol.* **2022**, *15*, 785–794. [[CrossRef](#)]
26. Hernandez-Nava, R.; Lopez-Malo, A.; Palou, E.; Ramírez-Corona, N.; Jimenez-Munguía, M.T. Encapsulation of oregano essential oil (*Origanum vulgare*) by complex coacervation between gelatin and chia mucilage and its properties after spray drying. *Food Hydrocoll.* **2020**, *109*, 1–36. [[CrossRef](#)]
27. Caparino, O.A.; Tang, J.; Nindo, C.I.; Sablani, S.S.; Powers, J.R.; Fellman, J.K. Effect of drying methods on the physical properties and microstructures of mango (*Philippine 'Carabao' var.*) powder. *J. Food Eng.* **2012**, *111*, 135–148. [[CrossRef](#)]
28. Akseli, I.; Hilden, J.; Katz, J.M.; Kelly, R.C.; Kramer, T.T.; Mao, C.; Osei-Yeboah, F.; Strong, J.C. Reproducibility of the Measurement of Bulk/Tapped Density of Pharmaceutical Powders Between Pharmaceutical Laboratories. *J. Pharm. Sci.* **2019**, *108*, 1081–1084. [[CrossRef](#)]
29. Kurek, M.A.; Moczowska-Wyrwicz, M.; Wyrwicz, J.; Karp, S. Development of Gluten-Free Muffins with β -Glucan and Pomegranate Powder Using Response Surface Methodology. *Foods* **2021**, *10*, 2551. [[CrossRef](#)]
30. Shaddel, R.; Hesari, J.; Azadmard-Damirchi, S.; Hamishehkar, H.; Fathi-Achachlouei, B.; Huang, Q. Use of gelatin and gum Arabic for encapsulation of black raspberry anthocyanins by complex coacervation. *Int. J. Biol. Macromol.* **2018**, *107*, 1800–1810. [[CrossRef](#)]
31. Pieczykolan, E.; Kurek, M.A. Use of guar gum, gum arabic, pectin, beta-glucan and inulin for microencapsulation of anthocyanins from chokeberry. *Int. J. Biol. Macromol.* **2019**, *129*, 665–671. [[CrossRef](#)]
32. Fernandes, R.V.d.B.; Borges, S.V.; Botrel, D.A.; Oliveira, C. Physical and chemical properties of encapsulated rosemary essential oil by spray drying using whey protein–inulin blends as carriers. *Int. J. Food Sci.* **2014**, *49*, 1–8. [[CrossRef](#)]
33. Zhao, Y.; Khalid, N.; Shu, G.; Neves, M.A.; Kobayashi, I.; Nakajima, M. Complex Coacervates from Gelatin and Octenyl Succinic Anhydride Modified Kudzu Starch: Insights of Formulation and Characterization. *Food Hydrocoll.* **2019**, *86*, 70–77. [[CrossRef](#)]
34. Wojtasik-Kalinowska, I.; Guzek, D.; Górska-Horczyk, E.; Brodowska, M.; Sun, D.W.; Wierzbicka, A. Diet with linseed oil and organic selenium yields low n-6/n-3 ratio pork Semimembranosus meat with unchanged volatile compound profiles. *Int. J. Food Sci.* **2018**, *53*, 1838–1846. [[CrossRef](#)]
35. Górska-Horczyk, E.; Wojtasik-Kalinowska, I.; Guzek, D.; Sun, D.W.; Wierzbicka, A. Differentiation of chill-stored and frozen pork necks using electronic nose with ultra-fast gas chromatography. *J. Food Process Eng.* **2017**, *40*, 1–9. [[CrossRef](#)]
36. Yuan, Y.; Li, M.F.; Chen, W.S.; Zeng, Q.Z.; Su, D.X.; Tian, B.; He, S. Microencapsulation of shiitake (*Lentinula edodes*) essential oil by complex coacervation: Formation, rheological property, oxidative stability and odour attenuation effect. *Int. J. Food Sci.* **2018**, *53*, 1681–1688. [[CrossRef](#)]
37. Klemmer, K.J.; Waldner, L.; Stone, A.; Low, N.H.; Nickerson, M.T. Complex coacervation of pea protein isolate and alginate polysaccharides. *Food Chem.* **2012**, *130*, 710–715. [[CrossRef](#)]
38. Rohman, A.; Windarsih, A.; Erwanto, Y.; Zakaria, Z. Review on analytical methods for analysis of porcine gelatine in food and pharmaceutical products for halal authentication. *Trends Food Sci. Technol.* **2020**, *101*, 122–132. [[CrossRef](#)]
39. Atgié, M.; Garrigues, J.C.; Chennevière, A.; Masbernat, O.; Roger, K. Gum Arabic in solution: Composition and multi-scale structures. *Food Hydrocoll.* **2019**, *91*, 319–330. [[CrossRef](#)]
40. Muhoza, B.; Xia, S.; Wang, X.; Zhang, X.; Li, Y.; Zhang, S. Microencapsulation of essential oils by complex coacervation method: Preparation, thermal stability, release properties and applications. *Crit. Rev. Food Sci. Nutr.* **2020**, *62*, 1363–1382. [[CrossRef](#)]
41. Kavooosi, G.; Rahmatollahi, A.; Dadfar, S.M.M.; Purfard, A.M. Effects of essential oil on the water binding capacity, physico-mechanical properties, antioxidant and antibacterial activity of gelatin films. *LWT* **2014**, *57*, 556–561. [[CrossRef](#)]
42. de Melo Ramos, F.; Silveira Júnior, V.; Prata, A.S. Assessing the Vacuum Spray Drying Effects on the Properties of Orange Essential Oil Microparticles. *Food Bioproc. Technol.* **2019**, *12*, 1917–1927. [[CrossRef](#)]
43. Shah, R.B.; Tawakkul, M.A.; Khan, M.A. Comparative Evaluation of Flow for Pharmaceutical Powders and Granules. *AAPS Pharmscitech* **2008**, *9*, 250–258. [[CrossRef](#)] [[PubMed](#)]
44. Manaf, M.A.; Subuki, I.; Jai, J.; Raslan, R.; Mustapa, A.N. Encapsulation of Volatile Citronella Essential Oil by Coacervation: Efficiency and Release Study. In *IOP Conference Series: Materials Science and Engineering*, 358, *Proceedings of the 3rd International Conference on Global Sustainability and Chemical Engineering (ICGSCE) Putrajaya, Malaysia, 15–16 February 2017*; IOP Publishing: Bristol, UK, 2018.

45. Samakradhamrongthai, R.S.; Angeli, P.T.; Kopermsub, P.; Utama-ang, N. Optimization of gelatin and gum arabic capsule infused with pandan flavor for multi-core flavor powder encapsulation. *Carbohydr. Polym.* **2019**, *226*, 2584–2591. [[CrossRef](#)] [[PubMed](#)]
46. Mitra, H.; Pushpadass, H.A.; Franklin, M.E.E.; Ambrose, R.K.; Ghoroi, C.; Battula, S. Influence of moisture content on the flow properties of basundi mix. *J. Powder Technol.* **2017**, *312*, 133–143. [[CrossRef](#)]
47. Zotarelli, M.F.; da Silva, V.M.; Durigon, A.; Hubinger, M.D.; Laurindo, J.B. Production of mango powder by spray drying and cast-tape drying. *Powder Technol.* **2017**, *305*, 447–454. [[CrossRef](#)]
48. Drozińska, E.; Kanclerz, A.; Kurek, M.A. Microencapsulation of sea buckthorn oil with β -glucan from barley as coating material. *Int. J. Biol. Macromol.* **2019**, *131*, 1014–1020. [[CrossRef](#)] [[PubMed](#)]
49. Walsh, M.K. Immobilized enzyme technology for food applications. In *Novel Enzyme Technology for Food Applications*; Rastall, R., Ed.; Woodhead Publishing: Sawston, UK, 2007; pp. 60–84. [[CrossRef](#)]
50. Kapcsándi, V.; Lakatos, E.H.; Sik, B.; Linka, L.A.; Székelyhidi, R. Characterization of fatty acid, antioxidant, and polyphenol content of grape seed oil from different *Vitis vinifera* L. varieties. *OCL* **2021**, *28*, 1–6. [[CrossRef](#)]
51. Cui, S.W.; Phillips, G.O.; Blackwell, B.; Nikiforuk, J. Characterisation and properties of *Acacia senegal* (L.) Willd. var. senegal with enhanced properties (Acacia (sen) SUPERGUM™): Part 4. Spectroscopic characterisation of Acacia senegal var. senegal and Acacia (sen) SUPERGUM™ Arabic. *Food Hydrocoll.* **2007**, *21*, 347–352. [[CrossRef](#)]
52. Nandiyanto, A.B.D.; Oktiani, R.; Ragadhita, R. How to read and interpret FTIR spectroscopy of organic material. *Indones. J. Sci. Technol.* **2019**, *4*, 97–118. [[CrossRef](#)]
53. Musa, H.H.; Ahmed, A.A.; Musa, T.H. Chemistry, Biological, and Pharmacological Properties of Gum Arabic. In *Bioactive Molecules in Food. Reference Series in Phytochemistry*; Mérillon, J.M., Ramawat, K.G., Eds.; Springer: Cham, Switzerland, 2019; pp. 797–814. [[CrossRef](#)]
54. Marković, M.S.; Radosavljević, D.B.; Pavićević, V.P.; Ristić, M.S.; Milojević, S.Z.; Bošković-Vragolović, N.M.; Veljković, V.B. Influence of common juniper berries pretreatment on the essential oil yield, chemical composition and extraction kinetics of classical and microwave-assisted hydrodistillation. *Ind. Crops Prod.* **2018**, *122*, 402–413. [[CrossRef](#)]
55. Bastos, L.P.H.; Vicente, J.; Corrêa dos Santos, C.H.; Geraldo de Carvalho, M.; Garcia-Rojas, E.E. Encapsulation of black pepper (*Piper nigrum* L.) essential oil with gelatin and sodium alginate by complex coacervation. *Food Hydrocoll.* **2019**, *102*, 1–8. [[CrossRef](#)]
56. Roohinejad, S.; Koubaa, M.; Barba, F.J.; Leong, S.Y.; Khalefa, A.; Greiner, R.; Chemat, F. Extraction methods of essential oils from herbs and spices. In *Essential Oils in Food Processing: Chemistry, Safety and Applications*; Hashemi, S.M.B., Khaneghah, A.M., de Souza Sant'Ana, A., Eds.; John Wiley & Sons Ltd.: Hoboken, NJ, USA, 2017; pp. 21–55. [[CrossRef](#)]
57. Karagozlu, M.; Ocak, B.; Özdestand-Ocak, Ö. Effect of Tannic Acid Concentration on the Physicochemical, Thermal, and Antioxidant Properties of Gelatin/Gum Arabic-Walled Microcapsules Containing *Origanum onites* L. Essential Oil. *Food Bioproc. Technol.* **2021**, *14*, 1231–1243. [[CrossRef](#)]
58. Yekdane, N.; Goli, S.A.H. Effect of Pomegranate Juice on Characteristics and Oxidative Stability of Microencapsulated Pomegranate Seed Oil Using Spray Drying. *Food Bioproc. Technol.* **2019**, *12*, 1614–1625. [[CrossRef](#)]
59. Koç, M.; Güngör, Ö.; Zungur, A.; Yalçın, B.; Selek, I.; Ertekin, F.K.; Ötles, S. Microencapsulation of Extra Virgin Olive Oil by Spray Drying: Effect of Wall Materials Composition, Process Conditions, and Emulsification Method. *Food Bioproc. Technol.* **2015**, *8*, 301–318. [[CrossRef](#)]
60. Rafiq, S.; Sofi, S.A.; Kumar, H.; Kaul, R.K.; Mehra, R.; Awuchi, C.G.; Okpala, C.O.R.; Korzeniowska, M. Physicochemical, antioxidant, and polyphenolic attributes of microencapsulated freeze-dried kinnnow peel extract powder using maltodextrin as wall material. *J. Food Process. Preserv.* **2022**, *46*, 1–10. [[CrossRef](#)]
61. Gomez-Estaca, J.; Comunian, T.A.; Montero, P.; Favaro-Trindade, C.S. Physico-Chemical Properties, Stability, and Potential Food Applications of Shrimp Lipid Extract Encapsulated by Complex Coacervation. *Food Bioproc. Technol.* **2018**, *11*, 1596–1604. [[CrossRef](#)]
62. Tavares, L.; Noreña, C.P.Z. Encapsulation of Ginger Essential Oil Using Complex Coacervation Method: Coacervate Formation, Rheological Property, and Physicochemical Characterization. *Food Bioproc. Technol.* **2020**, *13*, 1405–1420. [[CrossRef](#)]
63. Syed, N.; Mahesar, S.A.; Sherazi, S.T.H.; Soylak, M. Quality assessment and safety measurement of different industrial processing stages of soybean oil. *TURJFAS* **2020**, *1*, 28–33. [[CrossRef](#)]
64. Bruhl, L.; Unbehemd, G. Precise Color Communication by Determination of the Color of Vegetable Oils and Fats in the CIELAB 1976 (L*a*b*) Color Space. *Eur. J. Lipid Sci. Technol.* **2021**, *123*, 1–9. [[CrossRef](#)]
65. Sanchez, C.; Nige, M.; Meji, T.; Doco, T.; Williams, P.; Amine, C.; Renard, D. Acacia gum: History of the future. *Food Hydrocoll.* **2018**, *78*, 140–160. [[CrossRef](#)]
66. Ocak, B. Gum arabic and collagen hydrolysate extracted from hide fleshing wastes as novel wall materials for microencapsulation of *Origanum onites* L. essential oil through complex coacervation. *Environ. Sci. Pollut. Res.* **2020**, *27*, 42727–42737. [[CrossRef](#)] [[PubMed](#)]
67. Marfil, P.H.M.; Paulo, B.B.; Alvim, I.D.; Nicoletti, R. Production and characterization of palm oil microcapsules obtained by complex coacervation in gelatin/gum Arabic. *J. Food Process Eng.* **2018**, *41*, 1–11. [[CrossRef](#)]
68. Tavares, L.; Barros, H.L.; Barbosa, J.C.P.; Vagheti, C.P.Z. Noreña, Microencapsulation of Garlic Extract by Complex Coacervation Using Whey Protein Isolate/Chitosan and Gum Arabic/Chitosan as Wall Materials: Influence of Anionic Biopolymers on the Physicochemical and Structural Properties of Microparticles. *Food Bioproc. Technol.* **2019**, *12*, 2093–2106. [[CrossRef](#)]

69. Krokida, M.K.; Karathanos, V.T.; Maroulis, Z.B. Effect of freeze-drying conditions on shrinkage and porosity of dehydrated agricultural products. *J. Food Eng.* **1998**, *35*, 369–380. [[CrossRef](#)]
70. Barresi, A.A.; Ghio, S.; Fissore, D.; Pisano, R. Freeze Drying of Pharmaceutical Excipients Close to Collapse Temperature: Influence of the Process Conditions on Process Time and Product Quality. *Dry Technol.* **2009**, *27*, 805–816. [[CrossRef](#)]

Disclaimer/Publisher’s Note: The statements, opinions and data contained in all publications are solely those of the individual author(s) and contributor(s) and not of MDPI and/or the editor(s). MDPI and/or the editor(s) disclaim responsibility for any injury to people or property resulting from any ideas, methods, instructions or products referred to in the content.

Warszawa, 8/10/2024

Alicja Kizildag
alicjakizildag@gmail.com

**Rada Dyscypliny Technologia
Żywności i Żywienia
Szkoły Głównej Gospodarstwa
Wiejskiego w Warszawie**

Oświadczenie o współautorstwie

Niniejszym oświadczam, że w pracy: *Napiórkowska A, Szpicer A, Wojtasik-Kalinowska I, Perez MDT, González HD, Kurek MA. Microencapsulation of Juniper and Black Pepper Essential Oil Using the Coacervation Method and Its Properties after Freeze-Drying. Foods. 2023; 12(23):4345* mój indywidualny udział w jej powstaniu polegał na wykonaniu części badawczej, napisaniu manuskryptu oraz jego korekcie po procesie recenzji.

Podpis



Warszawa, 8/10/2024

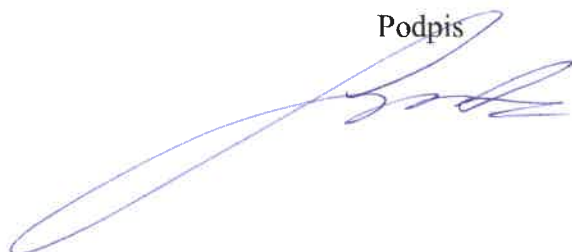
Arkadiusz Szpicer
arkadiusz_szpicer@sggw.edu.pl

**Rada Dyscypliny Technologia
Żywności i Żywnienia
Szkoły Głównej Gospodarstwa
Wiejskiego w Warszawie**

Oświadczenie o współautorstwie

Niniejszym oświadczam, że w pracy: *Napiórkowska A, Szpicer A, Wojtasik-Kalinowska I, Perez MDT, González HD, Kurek MA. Microencapsulation of Juniper and Black Pepper Essential Oil Using the Coacervation Method and Its Properties after Freeze-Drying. Foods. 2023; 12(23):4345* mój indywidualny udział w jej powstaniu polegał na nadzorowaniu analizy Skaningowej Kalorymetrii Różnicowej oraz ostatecznej korekcie treści manuskryptu w tym zakresie.

Podpis



Warszawa, 8/10/2024

Iwona Wojtasik-Kalinowska
iwona_wojtasik-kalinowska@sggw.edu.pl

**Rada Dyscypliny Technologia
Żywności i Żywienia
Szkoły Głównej Gospodarstwa
Wiejskiego w Warszawie**

Oświadczenie o współautorstwie

Niniejszym oświadczam, że w pracy: *Napiórkowska A, Szpicer A, Wojtasik-Kalinowska I, Perez MDT, González HD, Kurek MA. Microencapsulation of Juniper and Black Pepper Essential Oil Using the Coacervation Method and Its Properties after Freeze-Drying. Foods. 2023; 12(23):4345* mój indywidualny udział w jej powstaniu polegał na przeprowadzeniu analizy ultra-szybkiej chromatografii gazowej „e-nos” oraz opracowaniu otrzymanych wyników.



Podpis

Warsaw, 05.09.2024 r.

dr Maria Dolores Torres Perez
matorres@uvigo.gal

CINBIO
Department of Chemical Engineering
University of Vigo, Spain

CO-AUTHORSHIP STATEMENT

I hereby declare that in the paper: *Napiórkowska A, Szpicer A, Wojtasik-Kalinowska I, Perez MDT, González HD, Kurek MA. Microencapsulation of Juniper and Black Pepper Essential Oil Using the Coacervation Method and Its Properties after Freeze-Drying. Foods. 2023; 12(23):4345* my contribution consisted of performing Scanning Electron Microscopy (SEM) analysis .

TORRES PEREZ,
MARIA DOLORES
(AUTENTICACIÓN)



Firmado digitalmente
por TORRES PEREZ,
MARIA DOLORES
(AUTENTICACIÓN)
Fecha: 2024.09.11
18:12:22 +02'00'

Signature

.....

Warsaw, 05.09.2024 r.

dr Herminia Dominguez González
herminia@uvigo.gal

CINBIO
Department of Chemical Engineering
University of Vigo, Spain

CO-AUTHORSHIP STATEMENT

I hereby declare that in the paper: *Napiórkowska A, Szpiczer A, Wojtasik-Kalinowska I, Perez MDT, González HD, Kurek MA. Microencapsulation of Juniper and Black Pepper Essential Oil Using the Coacervation Method and Its Properties after Freeze-Drying. Foods. 2023; 12(23):4345* my contribution consisted of performing Scanning Electron Microscopy (SEM) analysis .

Firmado por DOMINGUEZ
GONZALEZ HERMINIA - DNI
***5727** el día 11/09/2024
con un certificado emitido
por AC Sector Público

Signature

.....

Warszawa, 8/10/2024

Marcin Andrzej Kurek
marcin_kurek@sggw.edu.pl

**Rada Dyscypliny Technologia
Żywności i Żywienia
Szkoły Głównej Gospodarstwa
Wiejskiego w Warszawie**

Oświadczenie o współautorstwie

Niniejszym oświadczam, że w pracy: *Napiórkowska A, Szpicer A, Wojtasik-Kalinowska I, Perez MDT, González HD, Kurek MA. Microencapsulation of Juniper and Black Pepper Essential Oil Using the Coacervation Method and Its Properties after Freeze-Drying. Foods. 2023; 12(23):4345* mój indywidualny udział w jej powstaniu polegał na nadzorowaniu badań, ocenie poprawności metodologii, konsultacjach merytorycznych oraz pomocy w analizie wyników i opracowaniu części tekstu artykułu.

Podpis



ORIGINAL ARTICLE

Food Engineering, Materials Science, and Nanotechnology

Understanding emulsifier influence on complex coacervation: Essential oils encapsulation perspective

Alicja Napiórkowska  | Arkadiusz Szpicer | Elżbieta Górka-Horzyczak | Marcin Kurek

Department of Technique and Product Development, Warsaw University of Life Sciences, Warszawa, Poland

Correspondence

Alicja Napiórkowska and Marcin Kurek, Department of Technique and Product Development, Warsaw University of Life Sciences, ul. Nowoursynowska 159C, bud. 32, pok. 109B, 02-776 Warsaw, Poland.
Email: alicja_napiorkowska@sggw.edu.pl and marcin_kurek@sggw.edu.pl

Abstract

The objective of this research was to explore the viability of pea protein as a substitute for gelatin in the complex coacervation process, with a specific focus on understanding the impact of incorporating an emulsifier into this process. The study involved the preparation of samples with varying polymer mixing ratios (1:1, 1:2, and 2:1) and emulsifier content. As core substances, black pepper and juniper essential oils were utilized, dissolved beforehand in grape seed oil or soybean oil, to minimize the loss of volatile compounds. In total, 24 distinct samples were created, subjected to freeze-drying to produce powder, and then assessed for their physicochemical properties.

Results revealed the significant impact of emulsifier addition on microcapsule parameters. Powders lacking emulsifiers exhibited higher water solubility (57.10%–81.41%) compared to those with emulsifiers (24.64%–40.13%). Moreover, the emulsifier significantly decreased thermal stability (e.g., without emulsifier, $T_{on} = 137.21^{\circ}\text{C}$; with emulsifier, $T_{on} = 41.55^{\circ}\text{C}$) and adversely impacted encapsulation efficiency (highest efficiency achieved: 67%; with emulsifier: 21%).

KEYWORDS

complex coacervation, emulsifier, essential oil, gum arabic, pea protein

1 | INTRODUCTION

Complex coacervation is the process of phase separation caused by the change in the environment of the colloidal solution. Such a change can occur by changing the pH, temperature, ionic strength, or solubility of the system. Complex coacervation usually occurs between systems containing oppositely charged proteins and polysaccharides, and the main driving mechanism is electrostatic interactions between them. The ratio of polymers in the system also has an impact on the coacervates formed (Duhoranimana et al., 2017; Timilsena et al., 2019). This process is used to microencapsulate various types of compounds, such as food flavorings and dyes, omega-3 acids,

essential oils, probiotic microorganisms, anthocyanins, and other bioactive compounds (Napiórkowska & Kurek, 2022).

The process of complex coacervation is most often carried out in the classical model between gelatin and gum Arabic (GA) (Napiórkowska & Kurek, 2022). Following a strong trend among consumers, proteins of plant origin are sought that could constitute a wall material in this process while allowing for similar process efficiency and encapsulation efficiency. One such vegetable protein may be pea protein (PP). PP (*Pisum sativum*, Fabaceae family) is considered a high-quality protein as well as a functional ingredient. This is due to the fact that it is well soluble in water, has good emulsifying properties, does not

contain gluten, and is less allergenic. Due to its properties, PP can be an interesting alternative to gelatin in the process of complex coacervation (Shanthakumar et al., 2022). Previously, PP has been used in complex coacervation between different types of pectins (beet and apple) (Lan et al., 2020; Salminen et al., 2022), alginates (Klemmer et al., 2012), and gums (tragacanth and Arabic) (Carpentier et al., 2021; Comunian et al., 2022). To the authors' knowledge, this protein has not yet been used for coacervation of essential oils.

Essential oils (EO) are compounds produced by essential plants (containing more than 0.1% EO). They are a mixture of such compounds as ketones, aldehydes, esters, alcohols, and so on. Most often, these plants are used as spices or medicinal preparations (e.g., mint, lemon balm, lavender, juniper, and sage). In addition, essential oils are known for their antimicrobial properties—antibacterial, antifungal, and antiviral (Bakkali et al., 2008; Baptista-Silva et al., 2020). Due to these properties, EO has gained popularity in recent years. Methods are sought to enable their use in food, which is a challenge due to their strong sensory properties. One of the methods that may contribute to the diffusion of essential oils in the food industry may be complex coacervation. We selected juniper and black pepper essential oils for microencapsulation based on their appealing sensory attributes and well-documented health benefits. Both oils boast potent anti-inflammatory and antioxidant properties (Ashokkumar et al., 2021; Han & Parker, 2017), contributing to overall wellness. Juniper oil offers additional benefits such as antispasmodic, carminative, and digestive properties (Albrecht & Madisch, 2022), while black pepper oil is known for its liver-protective effects (Zhang et al., 2021).

The study aims to assess PP's viability as a gelatin alternative in complex coacervation of essential oils, building upon our previous research (Napiórkowska et al., 2023). An additional aim was to investigate the impact of emulsifier addition on coacervation and encapsulation efficiency and analyze the resulting powder properties.

2 | MATERIALS AND METHODS

2.1 | Materials

PP (Hortimex) and Arabic gum (Warchem) were used as wall materials. Juniper berry essential oil (*Juniperus communis*) and black peppercorn essential oil (*Piper nigrum*) (Ancient Wisdom) were first dissolved in soybean oil (Dary Natury) or grape seed oil (Basso Fedele e figli s.r.l.) and used as core materials. The essential oils were dissolved in the oil at a concentration of 50% v/v

to reduce the risk of their evaporation during the freeze-drying process. The samples were divided into two parts: 12 were prepared with the addition of the emulsifier Tween 80 (Sigma Aldrich), and 12 were prepared without this emulsifier.

2.2 | Preparation of coacervates

As a wall material, 3% (w/w) PP solution with 3% (w/w) GA solution was used (in double-distilled water). PP was dissolved in water at room temperature, and GA was dissolved at 50°C. After cooling down the GA solution, both were mixed in different mixing ratios: 1:1, 1:2, and 2:1. The mass of each system was 200 g. We employed the same wall material ratio as in our previous studies incorporating gelatin to ensure direct comparison of results (Napiórkowska et al., 2023). Material concentrations were selected based on a literature review. After mixing, they were subjected to high shear homogenization using Ultra turrax (IKA T18 basic) for 10 min at 15,000 rpm min⁻¹ at room temperature. During homogenization, each variant was supplemented with mixture of soybean oil (SBO) or grape seed oil (GSO) with juniper (JEO) or black pepper (BPO) essential oil (6% core material). The total concentration of essential oil in the system was 3%. Note that 12 samples were prepared with 0.5% Tween 80 emulsifier and 12 samples without. After emulsification, the pH was adjusted to 4.0 (under the isoelectric point) using 1 M HCl. All emulsions were stored at 4°C for 24 h, then transferred at -20°C for 24 h, and then again transferred at -60°C for the next 24 h. The frozen samples were lyophilized for 72 h. After this time, the lyophilizates were grinded and screened on a laboratory sieve with a mesh size of 710 µm, then vacuum packed and stored at 4°C for further determinations.

The samples were coded as presented in Table 1. The mixing ratio was marked as (a) 1:1, (b) 1:2, and (c) 2:1 (juniper essential oil—J, black pepper oil—B, soybean oil—S, and grape seed oil—G).

2.3 | Complex coacervation yield, solid yield, and encapsulation efficiency

The efficiency of the coacervation process (CY) was estimated based on the ratio of liquid coacervates to sample mass. Freeze-drying losses (SY) were also assessed, expressed as the ratio of the mass of the obtained powder to the mass of liquid coacervates before drying (Rojas-Moreno et al., 2018). All measurements were done in triplicates.

TABLE 1 Coding of samples.

Oil	Essential oil	Mixing ratio PP/GA	Tween 80 (emulsifier)	Code	
Grape seed	Juniper	1:1	Yes	GJT1	
		1:2		GJT2	
		2:1		GJT3	
		1:1		No	GJ1
		1:2			GJ2
		2:1			GJ3
	Black pepper	1:1	Yes	GBT1	
		1:2		GBT2	
		2:1		GBT3	
		1:1		No	GB1
		1:2			GB2
		2:1			GB3
Soybean	Juniper	1:1	Yes	SJT1	
		1:2		SJT2	
		2:1		SJT3	
		1:1		No	SJ1
		1:2			SJ2
		2:1			SJ3
	Black pepper	1:1	Yes	SBT1	
		1:2		SBT2	
		2:1		SBT3	
		1:1		No	SB1
		1:2			SB2
		2:1			SB3

Abbreviations: GA, gum Arabic; PP, pea protein.

Encapsulation efficiency (EE) was expressed as the ratio of internal oil to oil on the surface of the samples. For this purpose, total oil (TO) and surface oil (SO) were determined (Bastos et al., 2019; Hernandez-Nava et al., 2020). All measurements were done in triplicates.

$$EE = \frac{T_O - S_O}{T_O} \times 100\%$$

To determine SO, 1 g of the sample was dissolved in 30 mL of n-hexane with constant stirring (60 rpm) for 15 min. The extracted oil together with the solvent were filtered into a previously weighed 25-mL round-bottom flask and evaporated (R-100; Büchi). To ensure that all n-hexane was removed from the sample, the flasks were kept at 105°C for 30 min (Binder FP 115 drying oven) and then transferred to a desiccator to cool completely. The round bottom flasks were weighed again, and the SO (g) was calculated as:

$$S_O = OM_1 - OM_2$$

where OM_1 is the oil mass after extraction and evaporation of the solvent (g) and OM_2 is the theoretical weight of oil from the sample (g).

To determine the total oil content in the samples (TO), 4 mL of KCl, 4 mL of acetone, and 8 mL of chloroform were added to 1.5 g of powder and mixed (60 rpm) for 15 min. The samples prepared in this way were centrifuged (10,000 rpm, 10 min) to separate the layers. The chloroform layer containing the extracted oil was filtered into previously weighed 25-mL round-bottom flasks. The tested sample remained in the falcon. The procedure was repeated a second time, but instead of KCl, 4 mL of double-distilled water was added. Then the solvent was evaporated first on a rotary evaporator (R-100; Büchi), then at 105°C for 30 min (Binder FP 115 drying oven). The last stage was cooling the flasks in a desiccator.

The round bottom flasks were weighed, and the TO (g) was calculated as:

$$T_O = OM_1 - OM_2$$

2.4 | Bulk and tapped density, Carr index (CI), and Hausner ratio

Bulk density (BD) (ρ_{bulk}) was determined by loosely pouring 1 g of the sample into a 10 mL graduated cylinder and reading the volume it occupied. Then the tapped density (TD) (ρ_{tap}) was determined by repeatedly tapping manually by lifting and dropping the cylinder under its own weight at a vertical distance of 14 ± 2 mm high for 1 min. Determinations were made in triplicate and the densities were expressed in g cm^{-3} . Based on the obtained results, the average compressibility index (CI [%]) and Hausner ratio (HR) were calculated, which are a measure of the powder's flowability and tendency to compress (Xin et al., 2022).

$$\text{CI} = \frac{\rho_{\text{tap}} - \rho_{\text{bulk}}}{\rho_{\text{tap}}} \times 100\%$$

$$\text{HR} = \frac{\rho_{\text{tap}}}{\rho_{\text{bulk}}}$$

2.5 | Color measurement

The color of the microcapsules was assessed using a Minolta CR-400 colorimeter manufactured by Konica Minolta Inc. The measurements were conducted under D65 illuminant conditions with an 8 mm measuring surface and following the standard 2° observers protocol. The recorded data were expressed in accordance with the International Commission on Lighting's (Commission Internationale de L'Eclairage) system within the CIELab color space. These determinations were performed in triplicate immediately after the production process to ensure accuracy and consistency.

2.6 | Solubility, hygroscopicity, and moisture content

To evaluate the solubility of the obtained powders, a method involving the dispersion of 0.5 g of the sample in 50 mL of double-distilled water was employed. Subsequently, the sample was agitated for 30 min at 60 rpm and then subjected to centrifugation at 10,000 rpm for 5 min. Following centrifugation, 25 mL of the supernatant was carefully transferred onto a pre-weighed petri dish and dried at 105°C for a period of 6 h (Binder FP 115 drying oven). The solubility (%) was calculated as the percentage of dried supernatant in relation to the initially

added amount of powder (de Melo Ramos et al., 2019). Determinations were made in triplicate.

The hygroscopicity of the obtained powders was determined by placing 0.2 g of the sample in a pre-weighed petri dish. The dish was then stored in a desiccator containing a saturated Na_2SO_4 solution for a duration of 1 week. Hygroscopicity (HIG) was expressed as g of water absorbed per 100 g sample (%) (Tavares & Norena, 2020). Determinations were made in triplicate.

The moisture content of the obtained powders was determined by placing 0.2 g of the sample in a pre-weighed petri dish. The dish with the sample was then dried at 70°C for 24 h (Binder FP 115 drying oven). Subsequently, the dried samples were transferred to a desiccator to cool completely before being reweighed. The moisture content was calculated based on the observed difference in weight before and after the drying process (Tavares & Norena, 2020). Determinations were made in triplicate.

2.7 | Particle size distribution

The measurement was conducted using the Morphologi G3SE apparatus from Malvern Instruments Ltd. The apparatus was equipped with a dispersion unit specifically designed for dry samples. The particle size distribution was determined by calculating the relative volume of particles within the specified size range, as depicted in the size distribution curves. The data analysis was performed using Malvern Microsoftware v.5.40, a software provided by Malvern Instruments Ltd. The particle size distribution (span index [SI]) was estimated using the following formula (Fernandes et al., 2014):

$$\text{SI} = \frac{D_{90} - D_{10}}{D_{50}}$$

where D_{90} , D_{50} , and D_{10} are the equivalent volume diameters at 90%, 50%, and 10% cumulative volume, respectively.

2.8 | Differential scanning calorimetry

The thermal properties of the samples were evaluated using differential scanning calorimetry (DSC 1) from Mettler Toledo 820 under a nitrogen atmosphere at a flow rate of $100 \text{ cm}^3 \text{ min}^{-1}$, as per the method described (Kurek et al., 2023) with some modifications. The instrument was calibrated with pure indium and zinc. Each sample (5.0 ± 0.1 mg) was placed in an aluminum crucible

(ME-51,119,870) and covered with a lid (ME-51,119,871) using the Mettler Toledo Crucible Sealing Press. DSC scans were recorded from 10°C to 230°C at a rate of 10°C min⁻¹. The thermograms were analyzed using STARe Software (Version 9.30) to determine the start (T_{on}), maximum (T_{max}), and end (T_{end}) temperatures, as well as the areas under the peaks (ΔH).

2.9 | E-nose

The volatile compounds within the microcapsules were extracted using the Heracles II electronic nose (Alpha M.O.S.), which utilizes ultra-fast gas chromatography with headspace. The system features a detection system comprising two metal columns of varying polarities (nonpolar MXT-5 and slightly polar MXT1701, diameter = 180 μ m, length = 10 m) and two flame ionization detectors (FID).

For the analysis, 10% solutions (0.25 g in 5 g) of each sample were placed in standard headspace vials sealed with a Teflon-faced silicon rubber cap. Incubation was performed at 35°C for 900 s under an agitation speed of 8.33 Hz. The carrying gas was hydrogen (flow rate: 1 mL min⁻¹). The injector temperature was set at 200°C, with an injected volume of 3500 μ L and a speed of 125 mL s⁻¹. The analytes were collected in the trap at 15°C and subsequently divided and simultaneously transferred into the two columns. The carrying gas was maintained at a constant pressure of 80 kPa with a split flow rate of 10 mL min⁻¹ at the column heads. The temperature program in the oven was as follows: 60°C for 2 s, a ramp of 3°C s⁻¹ to 270°C, held for 20 s, and FID1/FID2 at 280°C.

The volatile compounds identified in the samples were presented in the form of a table with Kovats indexes. All samples were analyzed in triplicate. Kovats indexes were established using alkane standards (n-butane to n-hexadecane) (Restek) measured under the same conditions as the samples (Górska-Horczyzak et al., 2017; Wojtasik-Kalinowska et al., 2018).

2.10 | Statistical analysis

For statistical analysis, the STATISTICA (13.3 version) computer program was used. To assess whether the mixing ratio and the addition of the emulsifier had a statistically significant impact on the complex coacervation process and the final parameters of the obtained powders, a one-way analysis of variance and a Fisher least significant difference test (p -value < 0.05, α = 95%) were conducted.

3 | RESULTS AND DISCUSSION

3.1 | Complex coacervation yield, solid yield, and encapsulation efficiency

The influence of adding an emulsifier to the complex coacervation process is evident (Table 2). Samples containing Tween 80 exhibited higher CY values (with the highest values observed in SBT2 = 92.40, SJT2 = 82.12, and SJT1 = 95.34) compared to those without the emulsifier. Conversely, for SY and EE parameters, higher values were observed in samples without the emulsifier, with the GJ1 sample achieving the highest values (SY = 25.43 and EE = 67.36%). Statistical analysis showed that the mixing ratio of PP and GA had a statistically less significant impact on the obtained results ($p \leq 0.05$) than the addition of the emulsifier ($p \leq 0.001$). The addition of the emulsifier resulted in at least a twofold reduction in the obtained SY and EE values compared to samples without it. The mixing ratio and the interaction between these factors were statistically insignificant.

The above fact can be explained by the emulsification properties of Tween 80—water was well incorporated into the emulsion structure and then unbound in the coacervation process. This resulted in higher CY values (because of better emulsion stability) and lower SY values (due to the evaporation of unbound water during the freeze-drying process). This observation is supported by the results regarding sample moisture content (refer to Subsection 3.3). Lower EE values for samples without Tween 80 can be explained by a too-high ratio of core material to emulsifier. Xiao et al. (2016) conducted similar research examining the effect of the addition of the Tween 20 emulsifier in various concentrations on the complex coacervation process and observed that if the ratio of core material to emulsifier is greater than 1:1, this emulsifier does not have the ability to emulsify all the oil contained in the system. Based on this, it can be concluded that an imbalance in the core material to emulsifier ratio may lead to inadequate emulsification of the oil phase, resulting in reduced encapsulation efficiency. Therefore, conducting experiments to optimize this ratio may help explain the observed discrepancies in EE values between samples with and without Tween 80.

In comparison to our prior investigations (Napiórkowska et al., 2023), no significant differences were observed in terms of CY, SY, or EE values, favoring either gelatin or PP. The similarity in these parameters suggests that both materials exhibit comparable performance in terms of encapsulation and related characteristics, highlighting their potential interchangeability. Further

TABLE 2 Complex coacervation yield (CY), solid yield (SY), encapsulation efficiency (EE, %), bulk density (BD), tapped density (TD), tapped density (TD) (g cm^{-3}), Carr index (CI), Hausner ratio (HR), and hygroscopicity (HIG), solubility (SOL), and moisture content (MC) (%)

Sample	CY	SY	EE	BD	TD	CI	HR	HIG	SOL	MC	
1	GJT1	76.10 ± 3.02 ^{bb}	12.21 ± 3.02 ^{bb}	21.13 ± 0.11 ^{aa}	0.21 ± 0.01 ^{bb}	0.38 ± 0.10 ^{ab}	42.88 ± 15.84 ^{aa}	1.86 ± 0.60 ^{aa}	13.86 ± 0.00 ^{ab}	33.59 ± 0.01 ^{aa}	0.37 ± 0.00 ^{aa}
2	GJT2	65.53 ± 2.09 ^{ab}	7.13 ± 2.09 ^{aa}	20.34 ± 0.16 ^{aa}	0.23 ± 0.00 ^{cb}	0.39 ± 0.01 ^{ab}	40.12 ± 2.29 ^{aa}	1.71 ± 0.05 ^{aa}	17.54 ± 0.00 ^{ba}	25.81 ± 0.06 ^{ba}	0.17 ± 0.00 ^{ba}
3	GJT3	37.16 ± 0.25 ^{ba}	11.48 ± 0.25 ^{aa}	34.53 ± 0.17 ^{aa}	0.18 ± 0.01 ^{aa}	0.34 ± 0.07 ^{aa}	45.87 ± 10.68 ^{aa}	1.85 ± 0.33 ^{aa}	10.92 ± 0.01 ^{ca}	34.89 ± 0.01 ^{aa}	0.47 ± 0.00 ^{aa}
4	GJI	34.31 ± 1.13 ^{aa}	25.43 ± 1.13 ^{ba}	67.36 ± 0.07 ^{aa}	0.07 ± 0.03 ^{ba}	0.14 ± 0.07 ^{aa}	47.98 ± 8.19 ^{aa}	1.92 ± 0.32 ^{aa}	13.85 ± 0.00 ^{ab}	61.60 ± 0.01 ^{ab}	0.68 ± 0.00 ^{aa}
5	GJ2	24.21 ± 2.37 ^{ab}	27.60 ± 2.37 ^{ab}	41.29 ± 0.43 ^{aa}	0.07 ± 0.01 ^{ca}	0.15 ± 0.00 ^{aa}	48.57 ± 2.99 ^{aa}	1.95 ± 0.10 ^{aa}	11.07 ± 0.00 ^{ba}	57.10 ± 0.01 ^{bb}	0.51 ± 0.00 ^{ba}
6	GJ3	38.74 ± 0.76 ^{ba}	21.50 ± 0.76 ^{aa}	33.81 ± 0.01 ^{aa}	0.11 ± 0.00 ^{aa}	0.17 ± 0.00 ^{aa}	35.25 ± 0.77 ^{aa}	1.54 ± 0.02 ^{aa}	19.33 ± 0.01 ^{aa}	78.17 ± 0.00 ^{aa}	0.86 ± 0.00 ^{aa}
7	GBT1	42.75 ± 0.91 ^{ba}	10.00 ± 1.00 ^{bb}	18.22 ± 0.02 ^{aa}	0.22 ± 0.01 ^{ba}	0.33 ± 0.01 ^{ba}	33.06 ± 0.66 ^{bb}	1.49 ± 0.01 ^{bb}	10.29 ± 0.00 ^{ab}	40.13 ± 0.01 ^{ab}	0.54 ± 0.00 ^{aa}
8	GBT2	69.85 ± 0.95 ^{aa}	11.95 ± 0.95 ^{abb}	23.17 ± 0.20 ^{aa}	0.18 ± 0.01 ^{aa}	0.34 ± 0.01 ^{aa}	46.78 ± 0.29 ^{aa}	1.91 ± 0.00 ^{aa}	14.47 ± 0.00 ^{aa}	34.41 ± 0.01 ^{ab}	0.24 ± 0.00 ^{aa}
9	GBT3	55.55 ± 0.97 ^{aa}	8.71 ± 0.97 ^{bb}	28.53 ± 0.01 ^{aa}	0.21 ± 0.00 ^{aa}	0.33 ± 0.06 ^{aa}	36.61 ± 8.88 ^{ab}	1.58 ± 0.31 ^{ab}	12.59 ± 0.00 ^{aa}	25.10 ± 0.01 ^{bb}	0.41 ± 0.00 ^{aa}
10	GB1	35.11 ± 0.40 ^{ab}	24.79 ± 0.40 ^{ab}	39.34 ± 0.01 ^{aa}	0.07 ± 0.00 ^{ab}	0.15 ± 0.01 ^{ab}	55.81 ± 3.07 ^{aa}	2.27 ± 0.08 ^{aa}	15.43 ± 0.00 ^{aa}	70.20 ± 0.01 ^{ba}	0.60 ± 0.00 ^{ca}
11	GB2	29.94 ± 0.73 ^{cb}	22.97 ± 0.73 ^{ba}	38.45 ± 0.12 ^{aa}	0.09 ± 0.00 ^{bb}	0.18 ± 0.01 ^{ab}	49.69 ± 0.68 ^{ba}	1.99 ± 0.02 ^{ba}	14.21 ± 0.00 ^{aa}	67.07 ± 0.04 ^{aba}	0.47 ± 0.00 ^{aa}
12	GB3	31.07 ± 0.97 ^{bb}	20.68 ± 0.97 ^{aa}	56.49 ± 0.01 ^{aa}	0.10 ± 0.01 ^{ab}	0.18 ± 0.02 ^{ab}	45.81 ± 2.02 ^{aa}	1.85 ± 0.05 ^{aba}	13.12 ± 0.00 ^{aa}	59.12 ± 0.04 ^{aa}	0.58 ± 0.00 ^{ba}
13	SJT1	95.34 ± 1.77 ^{bb}	6.61 ± 1.77 ^{ab}	30.12 ± 7.14 ^{ab}	0.24 ± 0.00 ^{aa}	0.32 ± 0.00 ^{aa}	23.48 ± 2.31 ^{ab}	1.31 ± 0.08 ^{ab}	6.09 ± 0.00 ^{ab}	31.84 ± 0.00 ^{ab}	0.64 ± 0.01 ^{ba}
14	SJT2	82.12 ± 1.57 ^{aa}	6.14 ± 1.57 ^{ab}	30.81 ± 0.45 ^{ab}	0.20 ± 0.00 ^{aa}	0.37 ± 0.01 ^{ab}	43.59 ± 1.87 ^{aa}	1.80 ± 0.10 ^{aa}	4.07 ± 0.00 ^{ab}	24.64 ± 0.01 ^{bb}	0.42 ± 0.00 ^{aa}
15	SJT3	40.05 ± 1.68 ^{aa}	9.45 ± 1.68 ^{ab}	18.73 ± 0.03 ^{aa}	0.19 ± 0.00 ^{ba}	0.30 ± 0.00 ^{aa}	35.86 ± 1.39 ^{ab}	1.56 ± 0.05 ^{ab}	5.37 ± 0.00 ^{ab}	37.54 ± 0.01 ^{ab}	0.93 ± 0.00 ^{aa}
16	SJ1	41.98 ± 0.96 ^{ca}	20.86 ± 0.96 ^{aa}	51.36 ± 0.24 ^{aa}	0.11 ± 0.01 ^{cb}	0.26 ± 0.01 ^{ba}	53.24 ± 3.34 ^{ba}	2.31 ± 0.13 ^{aa}	14.68 ± 0.00 ^{aa}	71.65 ± 0.00 ^{aa}	0.47 ± 0.00 ^{ba}
17	SJ2	28.91 ± 1.17 ^{bb}	21.17 ± 1.17 ^{aa}	60.33 ± 0.12 ^{aa}	0.11 ± 0.00 ^{bb}	0.20 ± 0.00 ^{aa}	44.02 ± 0.80 ^{aa}	1.80 ± 0.02 ^{ba}	18.77 ± 0.00 ^{aa}	59.42 ± 0.01 ^{ba}	0.32 ± 0.00 ^{aa}
18	SJ3	31.04 ± 2.60 ^{ab}	24.59 ± 2.6 ^{ba}	58.88 ± 0.19 ^{aa}	0.06 ± 0.00 ^{ab}	0.14 ± 0.01 ^{ab}	55.71 ± 2.70 ^{aa}	2.26 ± 0.09 ^{aa}	14.64 ± 0.01 ^{aa}	81.41 ± 0.00 ^{aa}	0.49 ± 0.00 ^{ca}
19	SBT1	42.44 ± 0.88 ^{ba}	9.04 ± 0.88 ^{ab}	35.02 ± 0.10 ^{aa}	0.25 ± 0.00 ^{aa}	0.32 ± 0.01 ^{ba}	21.09 ± 14.18 ^{bb}	1.27 ± 0.85 ^{ab}	6.22 ± 0.00 ^{ab}	31.96 ± 0.01 ^{cb}	0.60 ± 0.00 ^{aa}
20	SBT2	92.40 ± 1.38 ^{ab}	6.45 ± 1.38 ^{bb}	31.11 ± 0.23 ^{aa}	0.19 ± 0.00 ^{ca}	0.30 ± 0.00 ^{ca}	37.76 ± 2.79 ^{ab}	1.61 ± 0.31 ^{ab}	3.65 ± 0.00 ^{ab}	35.14 ± 0.00 ^{bb}	0.32 ± 0.00 ^{aba}
21	SBT3	67.04 ± 2.64 ^{ca}	6.40 ± 2.64 ^{ab}	29.28 ± 0.04 ^{aa}	0.20 ± 0.01 ^{ba}	0.32 ± 0.01 ^{ba}	39.00 ± 5.20 ^{ab}	1.64 ± 0.16 ^{ab}	4.51 ± 0.00 ^{ab}	37.55 ± 0.00 ^{ab}	0.76 ± 0.00 ^{ca}
22	SBI	36.04 ± 3.45 ^{ab}	23.33 ± 3.45 ^{ba}	64.32 ± 0.09 ^{aa}	0.06 ± 0.00 ^{bb}	0.13 ± 0.00 ^{ab}	52.93 ± 2.16 ^{ba}	2.13 ± 0.10 ^{ba}	14.31 ± 0.00 ^{ba}	80.56 ± 0.00 ^{aa}	0.78 ± 0.01 ^{ba}
23	SB2	32.35 ± 1.73 ^{ca}	23.23 ± 1.73 ^{aa}	44.47 ± 0.85 ^{aa}	0.08 ± 0.00 ^{ab}	0.18 ± 0.00 ^{ab}	53.54 ± 1.24 ^{aa}	2.16 ± 0.06 ^{aa}	13.13 ± 0.00 ^{aa}	67.31 ± 0.01 ^{aa}	0.90 ± 0.05 ^{aa}
24	SB3	44.93 ± 0.28 ^{bb}	21.69 ± 0.28 ^{aa}	48.09 ± 0.18 ^{aa}	0.07 ± 0.00 ^{ab}	0.16 ± 0.00 ^{ab}	56.01 ± 1.55 ^{aa}	2.28 ± 0.08 ^{aa}	10.09 ± 0.00 ^{aba}	60.72 ± 0.01 ^{aa}	0.75 ± 0.05 ^{aa}
S.E.M.	166.8	6.41	0.02755	0.000379	0.001848	59.9	0.0845	19.026	51.7	2.81080	
Effect											
MR	*	NS	NS	*	NS	NS	NS	NS	*	*	*
T	**	**	**	**	**	**	**	**	**	**	*
MR × T	**	NS	NS	**	NS	**	*	NS	NS	NS	*

Note: Results in this table are expressed as mean ± standard deviation. Mean values with the same superscript letters within a row are not significantly different at $p \leq 0.05$.

Abbreviations: MR, mixing ratio; S.E.M., standard error of the mean; T, Tween 80.

* $p \leq 0.05$ and ** $p \leq 0.001$. NS, nonsignificant effect at $p > 0.05$.

analysis and interpretation of these findings may provide valuable insights into the formulation and optimization of the encapsulation process with the incorporation of complex coacervation.

3.2 | Bulk and tapped density, Carr index, and Hausner ratio

The obtained powders were characterized by quite low BD ranging from 0.06–0.11 g cm⁻³ for samples without an emulsifier and 0.18–0.25 g cm⁻³ for samples with an emulsifier (Table 2). The TD was higher than the BD and ranged from 0.13 to 0.26 g cm⁻³ for samples without an emulsifier and 0.30–0.39 for samples with Tween 80. In the case of BD, both factors (M and T) and the interaction between them had a significant effect ($p \leq 0.001$) on the received values. For TD, only the addition of the emulsifier had a statistically significant effect and resulted in an increase in values compared to samples without it. The highest values of CI and HR parameters were observed in samples SB3 (CI = 56.01 and HR = 2.28), GB1 (CI = 55.81 and HR = 2.27), and SJ3 (CI = 55.71 and HR = 2.26). Most powders except GJ3, GBT1, GBT3, SJT1, SJT3, and SBT1 were characterized by CI values above 38 and HR above 1.6, which indicates very high cohesiveness and therefore virtually no flow (Sonawane et al., 2021).

The TD is usually about twice the BD. This is confirmed by many different studies (Hernandez-Nava et al., 2020; Karagozlu et al., 2021; Mitra et al., 2017; Yekdane & Goli, 2019) and is due to the fact that when the powder is freely poured, spaces are created between its larger particles, which are filled by smaller particles during tapping (Mitra et al., 2017). In research conducted by Luna-Guevara et al. (2017), the team checked the BD and TD of powders obtained by spray-drying emulsions containing different types of nut oils (walnut, peanut, and pecan). The BD was in the range of 0.19–0.25 g cm⁻³ and the TD was 0.33–0.46 g cm⁻³. The analysis of BD and TD is crucial for calculating the CI (Carr's index) and HR parameters, which are important indicators characterizing the flow of powders. These parameters are extremely important for both the storage and dosing of powders because they affect their ability to move freely and distribute evenly (de Melo Ramos et al., 2019).

Powders obtained by spray or freeze drying are usually characterized by high CI and HR values and, therefore, low flow and high cohesiveness. These parameters also depend on what type of emulsion is dried. Pink pepper essential oil powder microencapsulated in a single emulsion layer was characterized by higher CI (31.9) and HR (1.47) values compared to powders obtained by drying the double emulsion. This resulted in a decrease in these parameters

TABLE 3 Interpretation of Carr index (CI) and Hausner ratio (HR) values (based on Akshay et al. [2021], own elaboration).

CI	HR	Flowability
0–10	1.00–1.11	Excellent
10–15	1.12–1.18	Good
16–20	1.19–1.25	Fair
21–25	1.26–1.34	Possible
26–31	1.35–1.45	Poor
32–37	1.46–1.59	Very poor
>38	>1.60	Virtually no flow

(CI = 24.5 and HR = 1.33) and had a direct impact on flowability (Table 3) (Pereira et al., 2019). Powders obtained by drying coacervates are usually characterized by high cohesiveness and virtually no flow (Bordon et al., 2021), as is the case in our study.

Once again, in comparison to our earlier studies where gelatin served as the protein in the complex coacervation process (Napiórkowska et al., 2023), there were no significant differences noted in the density or flowability of the resulting powders. This consistency in the observed characteristics suggests that the choice of protein source, whether gelatin or an alternative like PP, does not markedly influence the physical properties of the obtained powders.

3.3 | Solubility, hygroscopicity, and moisture content

The effect of the emulsifier addition on the solubility of powders was statistically significant ($p \leq 0.001$). Powders without an emulsifier were highly soluble in water (57.10%–81.41%), while those containing Tween 80 were much less soluble (24.64%–40.13%). The addition of Tween 80 also had a statistically significant effect on the HIG of powders, lowering its values. Even though all of them could be classified as nonhygroscopic, the differences between the samples were significant. The HIG value for samples containing Tween 80 was in the range of 1.27%–1.91%, and for samples without an emulsifier, it was in the range of 1.54%–2.28%. The moisture content was in the ranges of 0.32–0.90 for samples without an emulsifier and 0.17–0.93 for samples with an emulsifier.

The microcapsules without an emulsifier were highly soluble in water despite the hydrophobic nature of the core material. In turn, those containing an emulsifier dissolved much worse, and this could be due to the presence of hydrophobic, slightly water-soluble Tween 80 on their surface, which prevented better dissolution of the microcapsules in water. It is also worth noting that these samples

TABLE 4 Color parameters: L^* , a^* , and b^* , SI, D_{10} , D_{50} , and D_{90} .

Sample	L^*	a^*	b^*	SI	D_{10}	D_{50}	D_{90}
GJT1	78.81 ± 0.67 ^{aA}	3.79 ± 0.05 ^{bA}	13.99 ± 0.44 ^{bB}	0.88 ± 0.01 ^{bA}	31.63 ± 1.00 ^{bB}	67.76 ± 1.00 ^{aA}	91.30 ± 1.00 ^{aA}
GJT2	87.60 ± 0.70 ^{cB}	5.37 ± 0.09 ^{cB}	11.27 ± 0.10 ^{aB}	1.10 ± 0.01 ^{cB}	28.90 ± 1.00 ^{aA}	55.56 ± 1.00 ^{bA}	89.97 ± 1.00 ^{aA}
GJT3	75.93 ± 0.46 ^{bA}	2.64 ± 0.05 ^{aA}	26.22 ± 0.37 ^{cA}	0.84 ± 0.02 ^{aA}	36.99 ± 1.00 ^{cA}	68.06 ± 1.00 ^{aA}	93.97 ± 1.00 ^{bA}
GJ1	86.08 ± 0.98 ^{bB}	4.12 ± 0.05 ^{bB}	10.31 ± 0.66 ^{bA}	0.96 ± 0.01 ^{bB}	29.08 ± 1.00 ^{bA}	68.37 ± 1.00 ^{aA}	94.53 ± 1.00 ^{aB}
GJ2	85.50 ± 0.32 ^{cA}	4.74 ± 0.17 ^{cA}	7.04 ± 0.69 ^{aA}	0.98 ± 0.01 ^{cA}	29.15 ± 1.00 ^{aA}	65.33 ± 1.00 ^{bB}	93.44 ± 1.00 ^{aB}
GJ3	84.75 ± 0.44 ^{aA}	2.84 ± 0.20 ^{aA}	14.54 ± 0.25 ^{cA}	0.88 ± 0.02 ^{aA}	34.77 ± 1.00 ^{cA}	67.45 ± 1.00 ^{aA}	93.92 ± 1.00 ^{bA}
GBT1	88.94 ± 0.30 ^{bA}	3.98 ± 0.06 ^{aA}	9.74 ± 0.21 ^{cB}	0.78 ± 0.02 ^{aA}	37.84 ± 1.00 ^{cA}	73.91 ± 1.00 ^{cA}	95.44 ± 0.58 ^{aA}
GBT2	85.89 ± 1.43 ^{aA}	3.78 ± 0.55 ^{bA}	16.00 ± 2.11 ^{bA}	0.84 ± 0.01 ^{bA}	36.72 ± 1.00 ^{bA}	65.98 ± 1.00 ^{bB}	91.91 ± 1.00 ^{aA}
GBT3	86.13 ± 0.40 ^{aA}	4.20 ± 0.06 ^{cA}	13.43 ± 0.18 ^{aA}	0.95 ± 0.01 ^{cB}	33.20 ± 1.00 ^{aA}	62.24 ± 1.00 ^{aB}	92.04 ± 1.00 ^{aA}
GB1	83.30 ± 0.48 ^{bB}	2.91 ± 0.15 ^{abB}	15.30 ± 0.47 ^{aA}	0.78 ± 0.01 ^{aA}	39.18 ± 1.00 ^{aA}	71.89 ± 1.00 ^{cA}	94.96 ± 1.00 ^{bA}
GB2	84.59 ± 2.37 ^{aA}	3.77 ± 0.21 ^{aA}	14.08 ± 0.07 ^{cB}	0.84 ± 0.01 ^{bA}	35.49 ± 1.00 ^{aA}	69.22 ± 1.00 ^{bA}	93.83 ± 1.00 ^{aA}
GB3	84.52 ± 0.85 ^{aB}	4.23 ± 0.41 ^{bA}	10.69 ± 0.47 ^{bB}	1.00 ± 0.01 ^{cA}	28.09 ± 1.00 ^{bB}	65.98 ± 1.00 ^{aA}	94.27 ± 1.00 ^{aA}
SJT1	84.32 ± 0.35 ^{aA}	5.78 ± 0.05 ^{aB}	9.61 ± 0.18 ^{bA}	0.84 ± 0.01 ^{aB}	36.95 ± 1.00 ^{aA}	65.67 ± 1.00 ^{aA}	92.03 ± 1.00 ^{aB}
SJT2	85.78 ± 0.51 ^{aA}	6.46 ± 0.04 ^{cA}	8.92 ± 0.19 ^{aA}	0.88 ± 0.01 ^{aA}	36.43 ± 1.00 ^{aA}	63.95 ± 1.00 ^{aB}	92.93 ± 1.00 ^{aA}
SJT3	85.09 ± 1.14 ^{aA}	5.31 ± 0.04 ^{bA}	6.36 ± 0.32 ^{aA}	0.63 ± 0.02 ^{bB}	47.77 ± 1.00 ^{bA}	75.55 ± 1.00 ^{aA}	95.08 ± 1.00 ^{aA}
SJ1	84.87 ± 0.46 ^{aA}	4.09 ± 0.06 ^{bA}	4.18 ± 0.35 ^{cB}	0.91 ± 0.04 ^{bA}	35.51 ± 1.00 ^{aB}	66.77 ± 1.00 ^{aA}	94.09 ± 1.00 ^{aA}
SJ2	85.01 ± 1.06 ^{aA}	5.43 ± 0.04 ^{cB}	5.44 ± 0.39 ^{bB}	0.89 ± 0.01 ^{cA}	33.26 ± 1.00 ^{aB}	68.49 ± 1.00 ^{aA}	94.35 ± 1.00 ^{aA}
SJ3	85.43 ± 0.41 ^{aA}	4.70 ± 0.01 ^{aB}	5.50 ± 0.28 ^{aB}	0.85 ± 0.02 ^{aA}	36.01 ± 1.00 ^{cB}	68.33 ± 1.00 ^{bB}	94.09 ± 1.00 ^{bA}
SBT1	85.00 ± 1.26 ^{aA}	4.19 ± 0.13 ^{bA}	14.07 ± 0.27 ^{bA}	0.72 ± 0.01 ^{bB}	42.16 ± 1.00 ^{aA}	71.36 ± 1.00 ^{aA}	93.83 ± 1.00 ^{bA}
SBT2	87.32 ± 0.61 ^{bA}	5.60 ± 0.08 ^{aA}	7.59 ± 0.13 ^{cA}	0.88 ± 0.01 ^{aA}	36.09 ± 1.00 ^{aA}	64.00 ± 1.00 ^{aB}	91.61 ± 1.00 ^{abA}
SBT3	86.42 ± 0.63 ^{aA}	4.60 ± 0.08 ^{aB}	5.86 ± 0.22 ^{aA}	0.93 ± 0.01 ^{cA}	33.53 ± 1.00 ^{bA}	63.19 ± 1.00 ^{bA}	92.26 ± 1.00 ^{aA}
SB1	85.23 ± 0.48 ^{aA}	4.66 ± 0.04 ^{aA}	5.38 ± 0.07 ^{bB}	0.88 ± 0.02 ^{aA}	34.90 ± 1.00 ^{cB}	67.19 ± 1.00 ^{bB}	93.76 ± 1.00 ^{bA}
SB2	82.91 ± 0.83 ^{bB}	5.15 ± 0.05 ^{bB}	6.36 ± 0.12 ^{aB}	0.84 ± 0.01 ^{bA}	35.99 ± 1.00 ^{bA}	68.72 ± 1.00 ^{aA}	93.43 ± 1.00 ^{aA}
SB3	86.12 ± 0.57 ^{abA}	5.28 ± 0.08 ^{aA}	4.84 ± 0.16 ^{aB}	0.93 ± 0.01 ^{cA}	31.13 ± 1.00 ^{abB}	65.06 ± 1.00 ^{aA}	91.73 ± 1.00 ^{abA}
S.E.M	6.9	0.773	23.729	0.00778	17.00	12.0	1.9
Effect							
MR	NS	**	NS	NS	NS	**	*
T	NS	NS	*	NS	**	NS	**
MR × T	*	NS	NS	NS	NS	**	NS

Note: Results in this table are expressed as mean ± standard deviation. Mean values with the same superscript letters within a row are not significantly different at $p \leq 0.05$.

Abbreviations: MR, mixing ratio; S.E.M., standard error of the mean; T, tween.

* $p < 0.05$ and ** $p < 0.001$. NS, nonsignificant effect at $p > 0.05$.

had low EE, which may lead to the accumulation of superficial oil, forming a hydrophobic film, and reducing their solubility in water. The HIG of the obtained microcapsules was significantly lower than previously published results of other studies. Bajac et al. (2022) performed microencapsulation of JEO in various types of wall materials, obtaining significantly higher HIG values for each: GA HIG = 13.47 ± 0.11 , GA/maltodextrin HIG = 10.18 ± 0.20 , sodium alginate HIG = 25.66 ± 0.21 , and whey protein concentrate HIG = 8.0 ± 1.26 . Powders containing pink pepper essential oil were characterized by similar HIG (9.3 ± 0.4 , 8.5 ± 0.3) (Pereira et al., 2019). In comparison to the counterparts with gelatin instead of PP from our previous study (Napiórkowska et al., 2023), the microcapsules with PP

in the current variants exhibited significantly higher solubility in water, surpassing 26%. Additionally, there was a slight reduction in HIG. This undoubtedly has to do with the wall material used. Paying attention to the requirements of the food industry regarding the moisture content of powders for long-term storage (4%–6%) as well as HIG (15.1%) (Zotarelli et al., 2017), the obtained microcapsules meet the requirements (Bajac et al., 2022).

3.4 | Color measurement

The color of the powders depended mainly on the oil used to dissolve the essential oils. Naturally, samples containing

soybean oil (yellow in color) (Syed et al., 2020) were characterized by higher values of parameter a^* and lower values of parameter b^* compared to samples with GSO (Bruhl & Unbehemd, 2021). However, the oil had no effect on the brightness of the samples, which ranged from 75.93 to 88.94 (Table 4).

3.5 | Particle size distribution

Statistical analysis showed that the addition of the emulsifier had a statistically significant effect on the D_{10} diameter value ($p \leq 0.001$), while MR and the interaction between T and MR had no statistical significance. The D_{10} value for samples without an emulsifier was in the range of 29.08–39.18, for those with an emulsifier, it was in the range of 28.90–47.77. In the case of D_{50} diameter values, MR and the interaction between MR and T had a statistically significant effect ($p \leq 0.001$). D_{50} values for samples without an emulsifier were 65.06–71.89, for samples with an emulsifier, they were 62.24–75.55. In turn, for diameter D_{90} , the effect of the emulsifier on the obtained values was more statistically significant ($p \leq 0.001$) than the influence of the polymer mixing ratio ($p \leq 0.05$) and had a negative impact on the obtained values. D_{90} values were in the range of 91.73–94.96 for samples without an emulsifier and 89.97–95.44 for samples with Tween 80. Neither the mixing ratio, the addition of emulsifier, nor the interaction between these factors had a statistically significant impact on the obtained SI values (Table 4). Therefore, it can be concluded that the addition of Tween 80 in the amount of 0.1% does not affect the size of microcapsules obtained in the complex coacervation method. From the existing research, it is evident that the inclusion of an emulsifier has an impact on the particle size obtained during complex coacervation. The average size of microcapsules tends to decrease with an increase in emulsifier concentration, leading to the creation of smaller particles with a broad distribution (Hu et al., 2011; Xiao et al., 2016). This difference in the results obtained may be due to the use of 0.1% Tween 80, which may not have been sufficient to cause a significant effect on the size of microcapsules obtained in the complex coacervation process in this study.

3.6 | Differential scanning calorimetry

The DSC analysis aimed to investigate the thermal behavior of the obtained microcapsules in the temperature range from 20°C to 230°C. In our previous study (Napiórkowska et al., 2023), DSC results for GA, JEO, and BPO were presented. In summary, the thermal transition for GA began at 137.93°C and concluded

at $157.54 \pm 0.001^\circ\text{C}$ ($T_{\text{max}} = 139.98 \pm 0.001^\circ\text{C}$ and $\Delta H = -696.52 \pm 0.001$ mJ), indicating a glass transition. On the other hand, JEO and BPO exhibited an endothermic event at $24.15 \pm 0.001^\circ\text{C}$ and $24.92 \pm 0.001^\circ\text{C}$ (-80.00 ± 0.001 mJ and -87.04 ± 0.002 mJ, respectively), associated with residual water, and at 150.42 ± 0.001 and $158.04 \pm 0.001^\circ\text{C}$ ($\Delta H = -350.87 \pm 0.001$ mJ and -367.14 ± 0.001 mJ, respectively), related to the decomposition of essential oils (EOs) (data not presented).

For oils, the first peak is related to the formation of primary auto-oxidation products, and the next one is related to the oxidation and decomposition of oxidation products (Kozłowska & Gruczyńska, 2018). For both oils (SBO and GSO), only one peak was observed, indicating an exothermic reaction, which was related to the formation of peroxides (Kozłowska & Gruczyńska, 2018). For SBO, $T_{\text{on}} = 155.34 \pm 0.001^\circ\text{C}$, $T_{\text{max}} = 174.31 \pm 0.001^\circ\text{C}$, and $T_{\text{end}} = 198.20 \pm 0.001^\circ\text{C}$ with $\Delta H = 108.87$ mJ. For GSO $T_{\text{on}} = 149.68 \pm 0.001^\circ\text{C}$, $T_{\text{max}} = 154.94 \pm 0.001^\circ\text{C}$, and $T_{\text{end}} = 170.10 \pm 0.001^\circ\text{C}$ with $\Delta H = 73.80$ mJ (data not presented).

DSC analysis was also conducted for Tween 80, revealing an exothermic transformation associated with a flash point starting at 116.40°C and ending at 154.42°C (with a peak at $138.82 \pm 0.001^\circ\text{C}$ and an enthalpy of 58.61 mJ) (data not presented). These findings align with previously published studies (Kishore et al., 2011; Pramod et al., 2015).

Table 5 provides onset, peak, and endset temperatures, along with the enthalpy accompanying these changes. Samples without an emulsifier exhibited a single endothermic reaction, with the reaction start temperature showing a clear dependence on the mixing ratio. Interestingly, samples containing a higher proportion of PP demonstrated increased thermal stability. Among emulsifier-free samples, SB1, SB2, and SB3 proved to be the most resistant to elevated temperatures, with T_{on} values in the order of $137.21 \pm 0.001^\circ\text{C}$, $149.59 \pm 0.002^\circ\text{C}$, and $162.35 \pm 0.001^\circ\text{C}$, T_{max} values of $138.3 \pm 0.001^\circ\text{C}$, $156.29 \pm 0.002^\circ\text{C}$, and $163.53 \pm 0.002^\circ\text{C}$, and T_{end} values of $139.86 \pm 0.001^\circ\text{C}$, $178.18 \pm 0.001^\circ\text{C}$, and $166.12 \pm 0.002^\circ\text{C}$, respectively. Notably, SB2 exhibited the least dynamic reaction. The introduction of Tween 80 led to two endothermic transformations in all samples, and the addition of the emulsifier significantly reduced T_{on} (for the first reaction) compared to counterparts without an emulsifier. In a study conducted by Li et al. (2018), it was observed that chitosan-based microcapsules containing citrus essential oils without the addition of an emulsifier exhibited greater temperature resistance compared to samples containing an emulsifier. Comparative investigations focusing on the influence of various types of emulsifiers on the reaction start temperature revealed that emulsifiers with higher Hydrophilic-Lipophilic balance (HLB) numbers tend to

TABLE 5 Results of DSC (differential scanning calorimetry) analysis, T_{on} , T_{max} , T_{end} , and enthalpy (ΔH).

Sample	T_{on} (°C)	T_{max} (°C)	T_{end} (°C)	ΔH (mJ)
GJT1	42.69 ± 0.001	53.46 ± 0.001	60.64 ± 0.001	-25.14 ± 0.001
	113.05 ± 0.001	135.88 ± 0.001	170.43 ± 0.001	-559.32 ± 0.001
GJT2	41.17 ± 0.001	51.78 ± 0.001	59.22 ± 0.002	-28.75 ± 0.001
	87.51 ± 0.002	126.52 ± 0.002	162.25 ± 0.001	-581.48 ± 0.001
GJT3	40.36 ± 0.002	52.29 ± 0.001	61.94 ± 0.002	-37.59 ± 0.001
	100.16 ± 0.002	133.71 ± 0.002	166.56 ± 0.002	-382.50 ± 0.001
GJ1	54.22 ± 0.001	108.04 ± 0.001	147.05 ± 0.002	-698.4 ± 0.002
GJ2	97.28 ± 0.001	125.53 ± 0.002	142.99 ± 0.001	-624.34 ± 0.002
GJ3	114.53 ± 0.002	129.31 ± 0.001	151.12 ± 0.001	-533.84 ± 0.001
GBT1	39.41 ± 0.002	50.31 ± 0.001	58.58 ± 0.002	-30.46 ± 0.001
	142.67 ± 0.002	163.54 ± 0.001	190.47 ± 0.001	-348.33 ± 0.001
GBT2	43.45 ± 0.001	52.45 ± 0.001	57.86 ± 0.002	-12.44 ± 0.002
	161.00 ± 0.002	162.10 ± 0.001	164.92 ± 0.001	-407.63 ± 0.002
GBT3	36.52 ± 0.001	50.11 ± 0.001	61.99 ± 0.001	-27.95 ± 0.001
	146.13 ± 0.001	167.46 ± 0.002	194.06 ± 0.001	-538.82 ± 0.001
GB1	71.98 ± 0.001	118.72 ± 0.002	164.97 ± 0.002	-706.35 ± 0.001
GB2	78.51 ± 0.001	125.52 ± 0.001	166.18 ± 0.001	-759.67 ± 0.001
GB3	97.63 ± 0.002	98.61 ± 0.001	99.98 ± 0.001	-1.30 ± 0.001
SJT1	41.89 ± 0.002	52.45 ± 0.001	59.38 ± 0.002	-26.49 ± 0.001
	121.98 ± 0.002	137.02 ± 0.001	159.89 ± 0.002	-384.84 ± 0.001
SJT2	31.21 ± 0.001	42.11 ± 0.002	50.20 ± 0.002	-16.07 ± 0.002
	101.12 ± 0.001	129.97 ± 0.002	157.38 ± 0.001	-23.18 ± 0.001
SJT3	32.86 ± 0.001	43.80 ± 0.001	53.09 ± 0.001	-12.78 ± 0.001
	81.85 ± 0.001	128.41 ± 0.001	149.81 ± 0.001	-287.60 ± 0.002
SJ1	69.44 ± 0.001	117.71 ± 0.001	157.23 ± 0.001	-700.80 ± 0.001
SJ2	117.21 ± 0.001	135.84 ± 0.001	159.13 ± 0.002	-582.43 ± 0.001
SJ3	146.79 ± 0.001	155.17 ± 0.001	176.31 ± 0.001	-740.17 ± 0.001
SBT1	41.55 ± 0.002	51.93 ± 0.002	59.08 ± 0.002	-18.35 ± 0.002
	143.75 ± 0.001	149.58 ± 0.001	150.44 ± 0.001	-609.94 ± 0.002
SBT2	37.13 ± 0.001	50.44 ± 0.001	57.91 ± 0.001	-23.37 ± 0.001
	117.83 ± 0.001	157.97 ± 0.001	190.42 ± 0.002	-684.03 ± 0.001
SBT3	38.87 ± 0.002	50.94 ± 0.001	59.35 ± 0.001	-24.48 ± 0.001
	134.53 ± 0.001	167.33 ± 0.002	200.93 ± 0.001	-455.58 ± 0.002
SB1	137.21 ± 0.001	138.33 ± 0.001	139.86 ± 0.001	-15.43 ± 0.001
SB2	149.59 ± 0.002	156.29 ± 0.002	178.18 ± 0.001	-349.79 ± 0.002
SB3	162.35 ± 0.001	163.53 ± 0.002	166.12 ± 0.002	-549.57 ± 0.002

lower the temperature at which the reaction begins. While emulsifiers with higher HLB numbers may exhibit a stronger propensity to form stable structures under high-temperature conditions, potentially delaying the onset of thermal reactions, the opposite effect might be attributed to the interaction of Tween 80 with EO.

Comparing these outcomes to our previous studies (Napiórkowska et al., 2023), a noteworthy trend emerges—the use of PP instead of gelatin resulted in an enhancement of the thermal stability of the microcapsules.

3.7 | FT-IR

Four characteristic peaks were identified for GA, confirming its organic nature. In the single bond area (2500–4000 cm^{-1}), a broad absorption band at 3300.05 cm^{-1} suggests a hydrogen bond, specifically the presence of a hydroxyl group (—OH). A narrow absorption band at 2893.28 cm^{-1} indicates C—H stretching from long-chain linear aliphatic compounds, followed by a peak at 1413.05 cm^{-1} connected to —OH and —CH vibrations

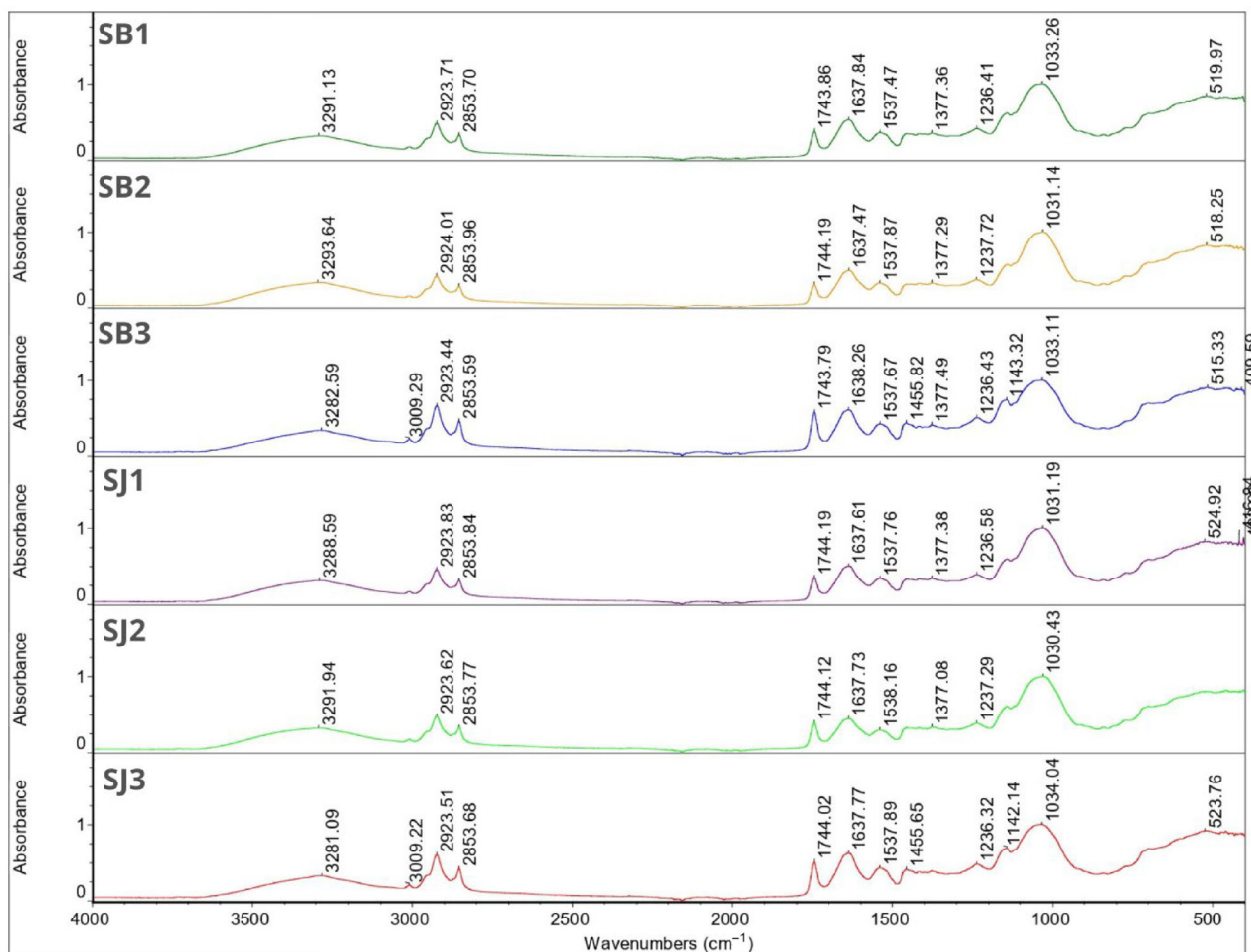


FIGURE 1 FT-IR spectra for samples SB1, SB2, SB3, SJ1, SJ2, and SJ3.

(Tavares & Norena, 2020). No peaks were identified in the triple bond region ($2000\text{--}2500\text{ cm}^{-1}$). In the double bond region ($1500\text{--}2000\text{ cm}^{-1}$), a peak at 1596.88 cm^{-1} may be attributed to carbonyl compounds ($\text{C}=\text{O}$). The peaks at 1413.05 and 1596.88 cm^{-1} also confirm the presence of the hydroxyl group identified in the single bond area (data not presented) (Cui et al., 2007; Nandiyanto et al., 2019; Napiórkowska et al., 2023).

Six characteristic peaks were identified for PP, confirming its complex nature. In the single bond area, a broad absorption band at 3280.24 cm^{-1} suggests the presence of hydrogen bonds, confirming the existence of a hydroxyl group ($-\text{OH}$), as well as ammonium and amino groups. A narrow absorption band at 2931.82 cm^{-1} may correspond to long-chain linear aliphatic compounds, especially since peaks in the range of $1470\text{--}720\text{ cm}^{-1}$ were also identified. No peaks were observed in the triple bond region. In the double bond area, a characteristic peak was observed at a wavelength of 1635.82 cm^{-1} , which may correspond to double and triple bonds between carbons. Together with the peak at 1537.45 cm^{-1} , it may also correspond to aromatic

rings and N-H bend derived from aromatic amino acids such as proline. In the fingerprint region ($600\text{--}1500\text{ cm}^{-1}$), characteristic peaks were identified at wavelengths 1395.17 , 1236.84 , and 1045.99 cm^{-1} , corresponding to N-H and $-\text{NH}_2$ bend, and 427.23 and 417.43 cm^{-1} corresponding to S-S stretch derived from sulfur amino acids that form disulfide bridges (data not presented) (Babault et al., 2015; Nandiyanto et al., 2019; Shanthakumar et al., 2022; Sokolowska et al., 2012).

FT-IR spectra for essential oils were reported in our previous work (Napiórkowska et al., 2023). Briefly, JEO showed characteristic peaks at 2917.56 and 2878.29 cm^{-1} , which refers to long-chain linear aliphatic compounds. The next peak at 1446.07 cm^{-1} corresponds to C-OH bend. Peaks at 887.14 , 786.52 , and 418.96 cm^{-1} may be associated with aromatic rings (Bastos et al., 2019; Nandiyanto et al., 2019). For BPO, characteristic peaks occurred at 2954.86 and 2922.95 cm^{-1} , which again refers to C-H stretching in long-chain linear aliphatic compounds; at 2867.06 cm^{-1} , what may be related to aliphatic chains (C-H); and at 1446.24 cm^{-1} , associated with C-OH bend. The rest of the

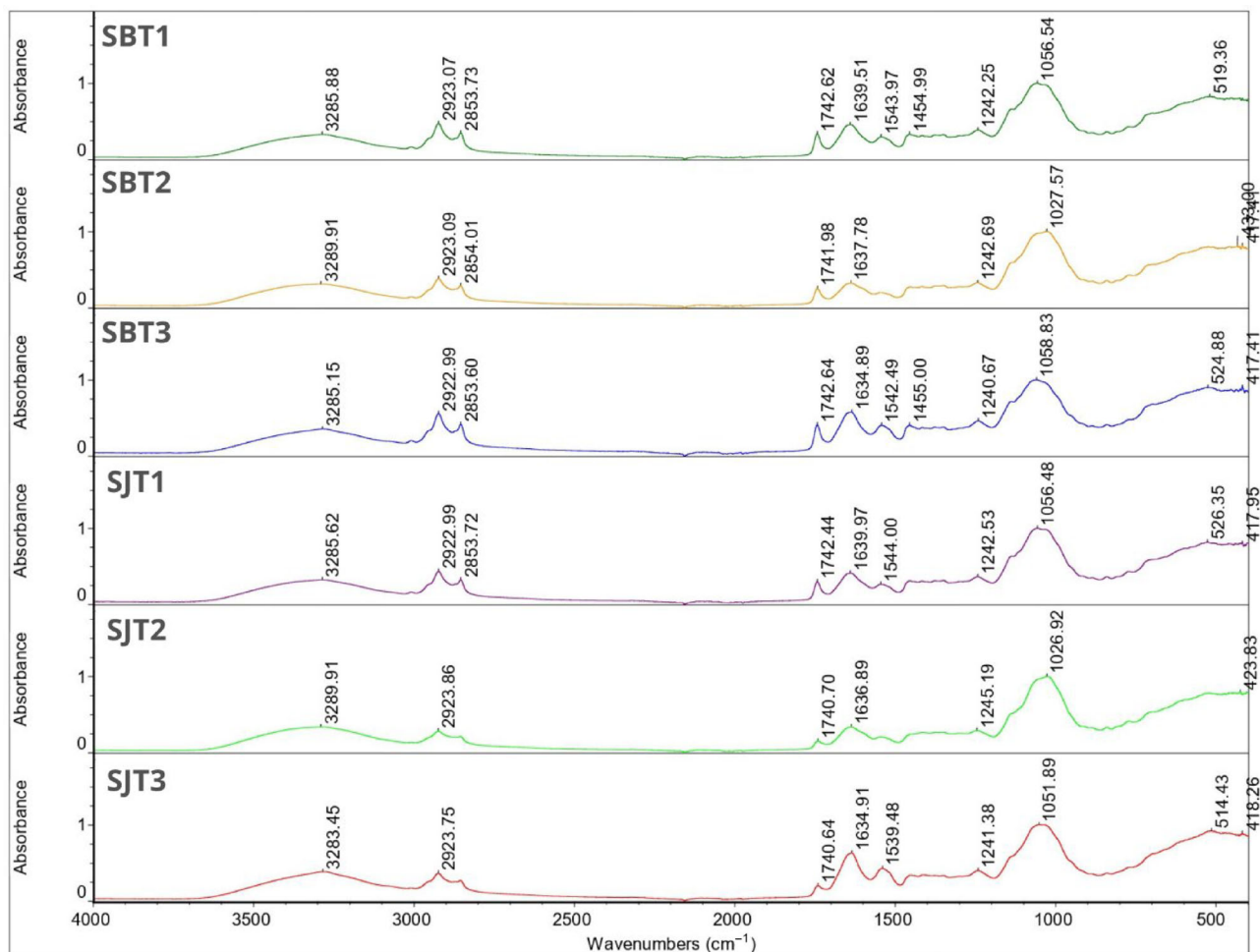


FIGURE 2 FT-IR spectra for samples SBT1, SBT2, SBT3, SJT1, SJT2, and SJT3.

identified peaks are 885.83, 875.20, 786.32, 543.65, 421.49, and 442.11 cm^{-1} , corresponding to aromatic rings (data not presented) (Bastos et al., 2019; Nandiyanto et al., 2019).

FT-IR spectra for soybean and grapeseed oil were also reported in our previous work (Napiórkowska et al., 2023). Briefly, for GSO, characteristic peaks were observed at wavenumber 3008.09, 2922.44, 2852.97, 1742.88, 1457.23, 1377.09, 1159.43, 1097.51, and 721.59 cm^{-1} , and for SBO, characteristic peaks were found at 3008.58, 2922.40, 2852.84, 1742.92, 1456.95, 1377.02, 1159.01, 1097.76, and 720.99 cm^{-1} (data not presented).

The analysis of Tween 80 emulsifier revealed 10 distinct peaks. The initial peak at a wavelength of 2855.75 cm^{-1} may signify the C—H bend. Its narrowness, coupled with the identification of peaks in the 1470–720 cm^{-1} range, suggests alignment with long-chain linear aliphatic compounds and —OH bend, consistent with the established chemical structure of Tween 80. The subsequent peak at 1734.71 cm^{-1} may correspond to aromatic bands. No indications of triple bonds were observed. The majority of peaks

were identified in the fingerprint region (1456.94, 1348.54, 1296.36, 1247.46, 1096.21, 946.67, 846.64, and 510.58 cm^{-1}), confirming the presence of aromatic rings and double bonds (data not presented) (Nair et al., 2003; Nandiyanto et al., 2019; Pramod et al., 2015).

Figures 1–4 depict the fourier-transform infrared spectroscopy (FT-IR) spectra for all microcapsules obtained. More than five characteristic peaks were identified in all the obtained spectra, confirming the complex nature of the samples. Samples containing Tween 80 were characterized by a reduced number of peaks compared to their counterparts without the emulsifier, which proves proper emulsification of the oils in the emulsion before the complex coacervation process. In all microcapsules, a broad absorption peak in the range of 3281.04–3293.64 cm^{-1} was identified, indicating the presence of pea protein and GA. For samples with an PP/GA ratio of 1:2, these peaks had lower intensity, while for samples with an PP/GA ratio of 2:1, the peaks had a shape more similar to the spectrum for PP. This proves the interaction between wall materials and reflects the mixing ratio well. The next two peaks were

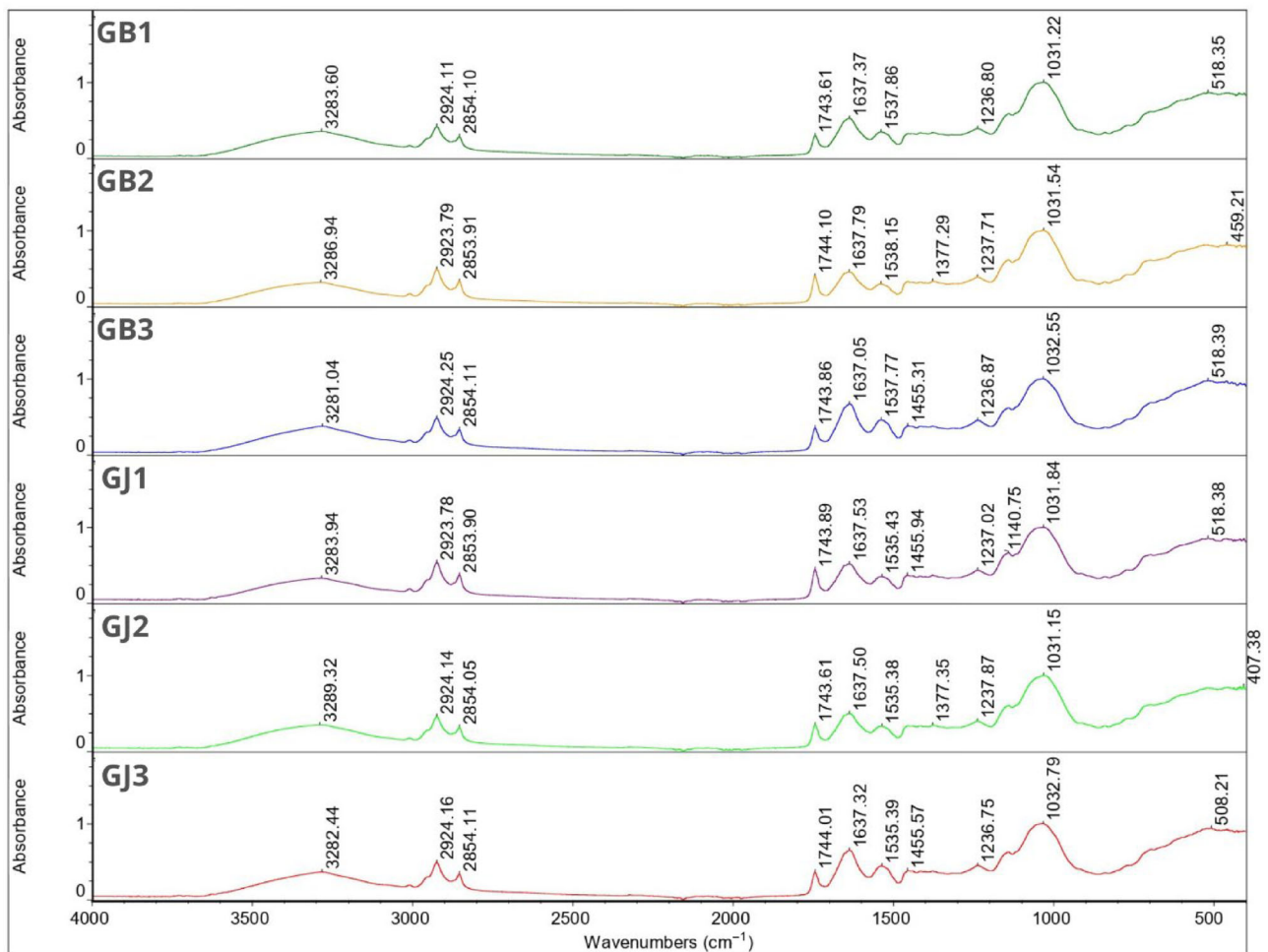


FIGURE 3 FT-IR spectra for samples GB1, GB2, GB3, GJ1, GJ2, and GJ3.

identified in the ranges $2922.99\text{--}2924.25\text{ cm}^{-1}$ and $2853.60\text{--}2854.39\text{ cm}^{-1}$, indicating the presence of GSO and SBO. This is particularly evident in the spectra of SB3 and SJ3, where a peak around $3009.22\text{--}3009.29\text{ cm}^{-1}$ is also visible. The spectra for samples GBT1, GJT3, SJT2, and SJT3 show the influence of the emulsifier (interaction between Tween 80 and oils), where only one peak is visible at a wavelength of $2922.99\text{--}2924.25\text{ cm}^{-1}$. The next peak identified in all samples (except GBT1) ($1740.64\text{--}1744.19\text{ cm}^{-1}$) also indicates the presence of GSO and SBO, and its significantly reduced intensity compared to the spectra of pure oils indicates their successful microencapsulation. The next two peaks, $1634.32\text{--}1640.59\text{ cm}^{-1}$ and $1535.38\text{--}1544.00\text{ cm}^{-1}$ (absent in samples with emulsifiers GBT2, SBT2, and SJT2), correspond to the presence of OP, as well as double and triple bonds between carbons, the --NH group, and aromatic rings. The next peaks were identified in the fingerprint region. The first one around the wavelength of $1454.30\text{--}1455.94\text{ cm}^{-1}$ was identifiable for samples SB3, SJ3, GBT3, SBT1, SBT3, GB3, GJ1, and GJ3, which may indicate the presence of GSO, SBO, as well as JEO and BPO. How-

ever, the shape and intensity of the peaks indicate more GSO and SBO oils, especially since the following peak is at a wavelength of $1377.08\text{--}1377.49\text{ cm}^{-1}$. In turn, for the GJT3 sample, the peak was identified only at 1410.92 cm^{-1} , which more indicates the peak resulting from the presence of GA in the sample. Another peak was identified in all samples ($1236.32\text{--}1245.19\text{ cm}^{-1}$), indicating the presence of PP, corresponding to N--H and --NH_2 bend. For samples SB3, SJ3, and GJ1, peaks were identified at wavelengths: 1143.32 , 1142.14 , and 1140.75 cm^{-1} , which may correspond to large aromatic rings and indicate the presence of JEO and BPO (Dosoky et al., 2019; Höferl et al., 2014; Nandiyanto et al., 2019). The peak at wavelength $1030.43\text{--}1033.26\text{ cm}^{-1}$ for samples without an emulsifier is characteristic of PP. A similar peak ($1026.92\text{--}1058.99\text{ cm}^{-1}$) was observed for samples from Tween 80; it is the result of overlapping peaks coming from the emulsifier and protein—the wavelength increased with the increase in protein concentration in the sample. Subsequent peaks in the fingerprint region correspond to the presence of essential oils and their successful microencapsulation.

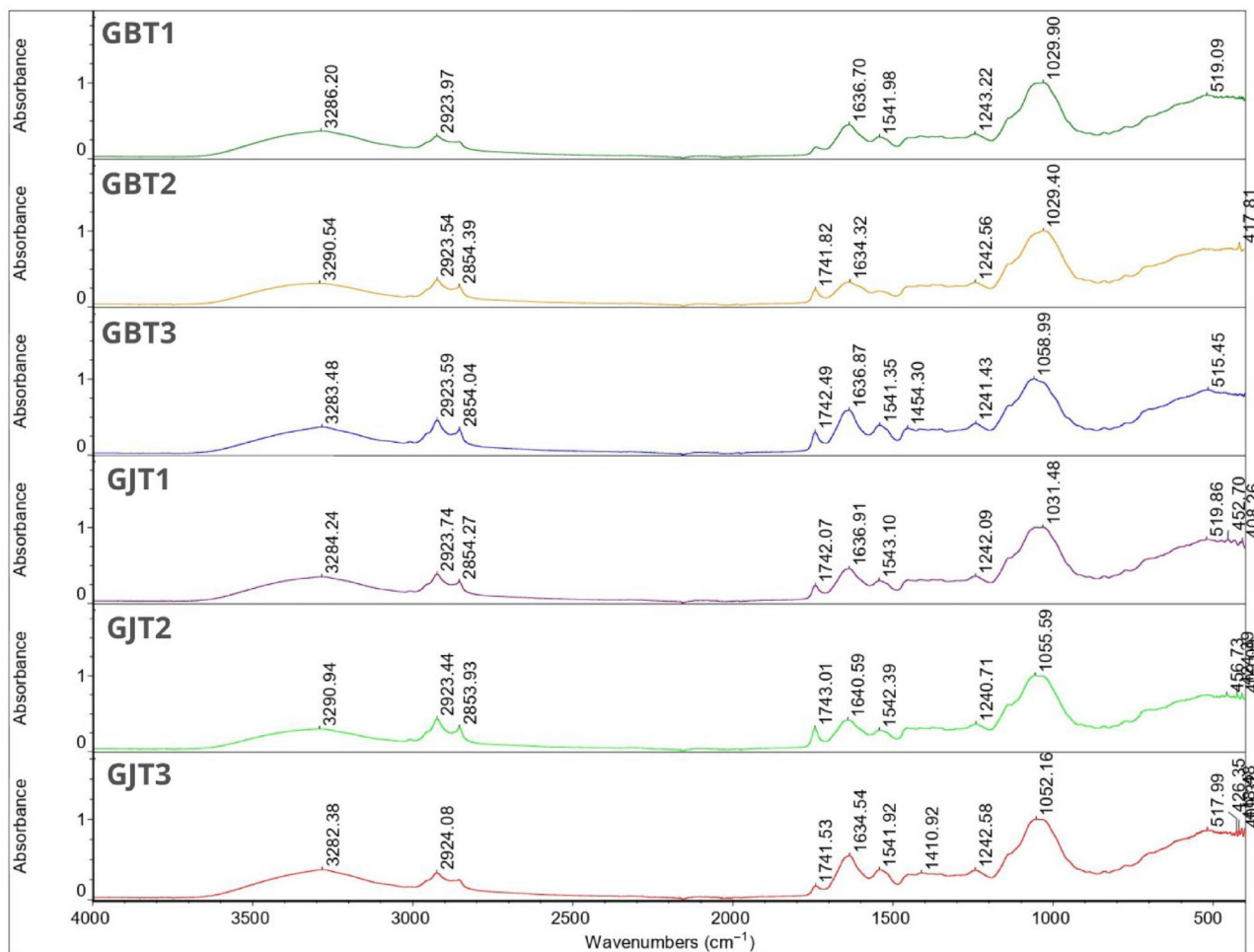


FIGURE 4 FT-IR spectra for samples GBT1, GBT2, GBT3, GJT1, GJT2, and GJT3.

3.8 | E-nose analysis

Table 6 presents the volatile compounds identified in the prepared microcapsules. Compounds characteristic of the essential oils used were identified in all samples. JEO contains the largest amounts of, among others, α -pinene and myrcene, which were identified in all samples containing JEO. The third most abundant compound, sabinene, has not been identified, but limonene and β -pinene, occurring in similar amounts to sabinene, have been identified. The samples also contained trace amounts of β -phellandrene and γ -terpinene (Höferl et al., 2014). BPO contains the most α -pinene, limonene, and β -pinene, which were identified in all samples. The next most common compounds in BPO (in similar amounts) are δ -3-carene and β -caryophyllene. The first of them was not identified in any of the samples, but β -caryophyllene was present in all of them (Dosoky et al., 2019). It appears that some of the highly volatile low boiling point compounds were either completely lost or present in trace amounts and were not detected during analysis (Ravi et al., 2013). Loss of compounds could occur

both during sample homogenization and lyophilization. Nevertheless, the identification of these compounds across all samples indicates the successful microencapsulation of essential oils.

Figures 5 and 6 illustrate the classification of scent profiles relative to their respective experimental groups. The samples are depicted in a two-dimensional plane based on principal component 1 (PC1) and principal component 2 (PC2). Based on the odor analysis, a clear difference can be seen between the samples without the addition of Tween 80 and those with the emulsifier. For samples without Tween 80 (Figure 5), the total variance contributions of PC1 and PC2 from direct electronic nose measurements were 98.592% and 1.072%, respectively. The differentiation index (DI) reached 99.92%, indicating clear discrimination among the samples. Samples were distinctly separated from each other, suggesting significant differences between them, with one exception where sample SJ3 overlapped with samples GJ1–GJ3. Generally, samples containing black pepper essential oil tend to be positioned on the right side of the chart. Those additionally containing

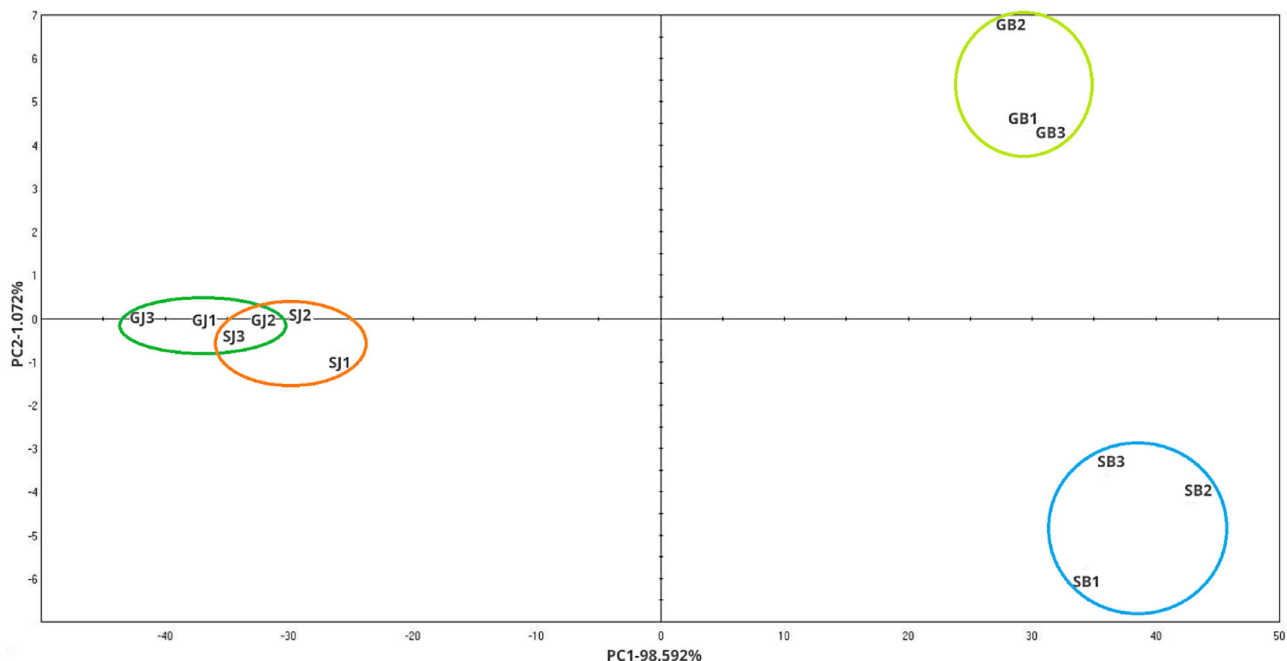


FIGURE 5 Smell pattern chart for samples without Tween 80. PC1, principal component 1; PC2, principal component 2.

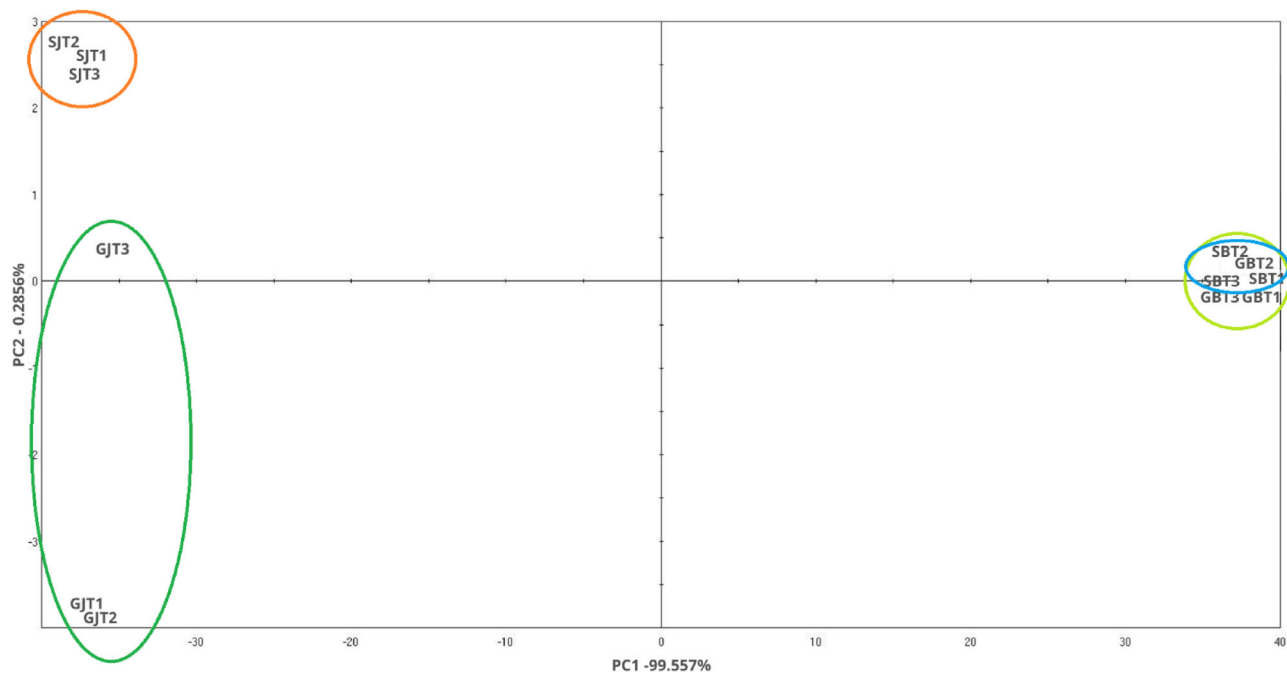


FIGURE 6 Smell pattern chart for samples containing Tween 80. PC1, principal component 1; PC2, principal component 2.

GSO were located in the upper part, while those with SBO were situated in the lower part. Moreover, samples with juniper essential oil were primarily positioned on the left side and approximately in the middle of the chart, without predominating on any side. For samples containing emulsifier (Figure 6), the DI was 98.82%, indicating clear

discrimination among the samples. Once more, samples containing juniper essential oil were positioned on the left side of the chart. This time, samples containing additional SBO were located in the upper part, while those containing GSO were in the lower part, except for the GJT3 sample. Samples containing black pepper essential oil were

positioned on the right side of the graph, and despite differences in SBO or GSO content, the distinctions between them were not significant as the samples overlapped.

Comparing the results to our previous studies (Napiórkowska et al., 2023), it can be seen that the compounds occurring in the largest amounts were identified in both cases; however, the use of PP allowed the retention of compounds occurring in trace amounts (β -caryophyllene, β -phellandrene, and γ -terpinene) in the samples. Interestingly, according to the findings from the odor profile analysis of samples encapsulated with broad bean protein and chia seed polysaccharides as the wall material (Napiórkowska et al., 2024), it is evident that the composition of the capsules directly influences the odor profile and the positioning of the samples on the chart. In the aforementioned research, samples containing juniper essential oil were positioned on the right side of the chart, while those containing black pepper oil were on the left (opposite to the current study).

4 | CONCLUSIONS

Based on the outcomes of the conducted research, it is evident that PP presents itself as a promising alternative to gelatin in the complex coacervation process. Microcapsules formulated with PP demonstrated several advantages that could significantly influence their applicability in the food industry.

Firstly, the microcapsules containing PP exhibited higher solubility, a characteristic that holds particular importance for the rapid release of active substances. Their lower HIG is a notable advantage, especially in terms of storage conditions. The diminished tendency to absorb moisture could contribute to maintaining the physicochemical stability of the microcapsules. Additionally, a crucial observation was the significantly higher temperature resistance of microcapsules with PP compared to gelatin capsules. This feature becomes particularly valuable in applications where microcapsules may be subjected to varying temperature conditions, such as during processing processes. It is worth noting that despite differences in some properties, no statistically significant distinctions were observed in encapsulation efficiency, density, or flowability between microcapsules with PP and those with gelatin. This suggests that, despite variations, both substances may prove equally effective in these parameters. Furthermore, it was noted that the addition of Tween 80 at a concentration of 0.5% had a negative impact on the efficiency of encapsulating the essential oil and the thermal stability of obtained powders.

Further research and optimization of process conditions are recommended to maximize the efficiency and quality

of the microcapsules obtained, emphasizing the need for continued investigation and refinement of the formulation and processing parameters.

AUTHOR CONTRIBUTIONS

Alicja Napiórkowska: Investigation; writing—original draft. **Arkadiusz Szpicer:** Investigation. **Elżbieta Górska-Horczyzak:** Investigation. **Marcin Kurek:** Writing—review and editing; supervision.

CONFLICT OF INTEREST STATEMENT

The authors declare no conflicts of interest.

ORCID

Alicja Napiórkowska  <https://orcid.org/0000-0001-9210-0823>

REFERENCES

- Albrecht, U. W., & Madisch, A. (2022). Therapeutic potentials associated with biological properties of Juniper berry oil (*Juniperus communis* L.) and its therapeutic use in several diseases—A Review. *Bioactive Compounds in Health and Disease*, 5(9), 174–185. <https://doi.org/10.31989/bchd.v5i9.999>
- Ashokkumar, K., Murugan, M., Dhanya, M. K., Pandian, A., & Warkentin, T. D. (2021). Phytochemistry and therapeutic potential of black pepper [*Piper nigrum* (L.)] essential oil and piperine: A review. *Clinical Phytoscience*, 7(1), Article 52. <https://doi.org/10.1186/s40816-021-00292-2>
- Babault, N., Païzis, C., Deley, G., Guérin-Deremaux, L., Saniez, M. H., Lefranc-Millot, C., & Allaert, F. A. (2015). Pea proteins oral supplementation promotes muscle thickness gains during resistance training: A double-blind, randomized, Placebo-controlled clinical trial vs. Whey protein. *Journal of the International Society of Sports Nutrition*, 12(1), Article 3. <https://doi.org/10.1186/s12970-014-0064-5>
- Bajac, J., Nikolovski, B., Lončarević, I., Petrović, J., Bajac, B., Đurović, S., & Petrović, L. (2022). Microencapsulation of juniper berry essential oil (*Juniperus communis* L.) by spray drying: Microcapsule characterization and release kinetics of the oil. *Food Hydrocolloids*, 125, 107430.
- Bakkali, F., Averbeck, S., Averbeck, D., & Idaomar, M. (2008). Biological effects of essential oils—A review. *Food and Chemical Toxicology*, 46(2), 446–475.
- Baptista-Silva, S., Borges, S., Ramos, O. L., Pintado, M., & Sarmiento, B. (2020). The progress of essential oils as potential therapeutic agents: A review. *Journal of Essential Oil Research*, 32(4), 279–295. <https://doi.org/10.1080/10412905.2020.1746698>
- Bastos, L. P. H., Vicente, J., Corrêa dos Santos, C. H., Geraldo de Carvalho, M., & Garcia-Rojas, E. E. (2019). Encapsulation of black pepper (*Piper nigrum* L.) essential oil with gelatin and sodium alginate by complex coacervation. *Food Hydrocolloids*, 102, 105605. <https://doi.org/10.1016/j.foodhyd.2019.105605>
- Bordón, M. G., Paredes, A. J., Camacho, N. M., Penci, M. C., González, A., Palma, S. D., Ribotta, P. D., & Martínez, M. L. (2021). Formulation, spray-drying and physicochemical characterization of functional powders loaded with chia seed oil and prepared by

- complex coacervation. *Journal of Powder Technology*, 391, 479–493. <https://doi.org/10.1016/j.powtec.2021.06.035>
- Bruhl, L., & Unbehemd, G. (2021). Precise color communication by determination of the color of vegetable oils and fats in the CIELAB 1976 (Lab*) color space. *European Journal of Lipid Science and Technology*, 123, 2000204. <https://doi.org/10.1002/ejlt.202000204>
- Carpentier, J., Conforto, E., Chaigneau, C., Vendeville, J.-E., & Maugard, T. (2021). Complex coacervation of pea protein isolate and tragacanth gum: Comparative study with commercial polysaccharides. *Innovative Food Science & Emerging Technologies*, 69, 102641. <https://doi.org/10.1016/j.ifset.2021.102641>
- Comunian, T. A., Archut, A., Gomez-Mascaraque, L. G., Brodkorb, A., & Drusch, S. (2022). The type of gum arabic affects interactions with soluble pea protein in complex coacervation. *Carbohydrate Polymers*, 295, 119851. <https://doi.org/10.1016/j.carbpol.2022.119851>
- Cui, S. W., Phillips, G. O., Blackwell, B., & Nikiforuk, J. (2007). Characterisation and properties of *Acacia senegal* (L.) Willd. var. *senegal* with enhanced properties (*Acacia* (sen) SUPERGUM™): Part 4. Spectroscopic characterisation of *Acacia senegal* var. *senegal* and *Acacia* (sen) SUPERGUM™ arabic. *Food Hydrocolloids*, 21(3), 347–352. <https://doi.org/10.1016/j.foodhyd.2006.05.009>
- de Melo Ramos, F., Silveira Júnior, V., & Prata, A. S. (2019). Assessing the vacuum spray drying effects on the properties of orange essential oil microparticles. *Food and Bioprocess Technology*, 12(11), 1917–1927. <https://doi.org/10.1007/s11947-019-02355-2>
- Dosoky, N. S., Satyal, P., Barata, L. M., da Silva, J. K. R., & Setzer, W. N. (2019). Volatiles of black pepper fruits (*Piper nigrum* L.). *Molecules*, 24(23), 4244. <https://doi.org/10.3390/molecules24234244>
- Duhoanimana, E., Karangwa, E., Lai, L., Xu, X., Yu, J., Xia, S., Zhang, X., Muhoza, B., & Habinshuti, I. (2017). Effect of sodium carboxymethyl cellulose on complex coacervates formation with gelatin: Coacervates characterization, stabilization and formation mechanism. *Food Hydrocolloids*, 69, 111–120. <https://doi.org/10.1016/j.foodhyd.2017.01.035>
- Fernandes, R. V. D. B., Borges, S. V., Botrel, D. A., & Oliveira, C. (2014). Physical and chemical properties of encapsulated rosemary essential oil by spray drying using whey protein–inulin blends as carriers. *International Journal of Food Science*, 49, 1522–1529. <https://doi.org/10.1080/09637486.2013.820556>
- Górska-Horczyk, E., Wojtasik-Kalinowska, I., Guzek, D., Sun, D. W., & Wierzbicka, A. (2017). Differentiation of chill-stored and frozen pork necks using electronic nose with ultra-fast gas chromatography. *Journal of Food Process Engineering*, 40, e12305. <https://doi.org/10.1111/jfpe.12305>
- Han, X., & Parker, T. L. (2017). Anti-inflammatory activity of Juniper (*Juniperus communis*) berry essential oil in human dermal fibroblasts. *Cogent Medicine*, 4(1), Article 1306200. <https://doi.org/10.1080/2331205X.2017.1306200>
- Hernandez-Nava, R., Lopez-Malo, A., Palou, E., Ramirez-Corona, N., & Jimenez-Munguia, M. T. (2020). Encapsulation of oregano essential oil (*Origanum vulgare*) by complex coacervation between gelatin and chia mucilage and its properties after spray drying. *Food Hydrocolloids*, 109, 106077. <https://doi.org/10.1016/j.foodhyd.2020.106077>
- Höferl, M., Stoilova, I., Schmidt, E., Wanner, J., Jirovetz, L., Trifonova, D., Krastev, L., & Krastanov, A. (2014). Chemical composition and antioxidant properties of juniper berry (*Juniperus communis* L.) essential oil. Action of the essential oil on the antioxidant protection of *saccharomyces cerevisiae* model organism. *Antioxidants*, 3(1), 81–98. <https://doi.org/10.3390/antiox3010081>
- Hu, J., Xiao, Z., Zhou, R., Li, Z., Wang, M., & Ma, S. (2011). Synthesis and characterization of polybutylcyanoacrylate-encapsulated rose fragrance nanocapsule. *Flavour and Fragrance Journal*, 26(3), 162–173.
- Karagozlu, M., Ocak, B., & Özdestan-Ocak, Ö. (2021). Effect of tannic acid concentration on the physicochemical, thermal, and antioxidant properties of gelatin/gum arabic-walled microcapsules containing *Origanum onites* L. essential oil. *Food Bioprocess Technology*, 14, 1231–1243. <https://doi.org/10.1007/s11947-021-02633-y>
- Kishore, R. S., Pappenberger, A., Dauphin, I. B., Ross, A., Buerger, B., Staempfli, A., & Mahler, H. C. (2011). Degradation of polysorbates 20 and 80: Studies on thermal autoxidation and hydrolysis. *Journal of Pharmaceutical Sciences*, 100, 721–731. <https://doi.org/10.1002/jps.22343>
- Klemmer, K. J., Waldner, L., Stone, A., Low, N. H., & Nickerson, M. T. (2012). Complex coacervation of pea protein isolate and alginate polysaccharides. *Food Chemistry*, 130(3), 710–715. <https://doi.org/10.1016/j.foodchem.2011.07.114>
- Kozłowska, M., & Gruczyńska, E. (2018). Comparison of the oxidative stability of soybean and sunflower oils enriched with herbal plant extracts. *Chemical Papers*, 72(10), 2607–2615. <https://doi.org/10.1007/s11696-018-05165>
- Kurek, M. A., Majek, M., Onopiuk, A., Szpicier, A., Napiórkowska, A., & Samborska, K. (2023). Encapsulation of anthocyanins from chokeberry (*Aronia melanocarpa*) with plasmolyzed yeast cells of different species. *Food and Bioprocess Technology*, 137, 84–92. <https://doi.org/10.1016/j.fbp.2022.11.001>
- Lan, Y., Ohm, J.-B., Chen, B., & Rao, J. (2020). Phase behavior and complex coacervation of concentrated pea protein isolate-beet pectin solution. *Food Chemistry*, 307, 125536. <https://doi.org/10.1016/j.foodchem.2019.125536>
- Li, Y., Wu, C., Wu, T., Wang, L., Chen, S., Ding, T., & Hu, Y. (2018). Preparation and characterization of citrus essential oils loaded in chitosan microcapsules by using different emulsifiers. *Journal of Food Engineering*, 217, 108–114. <https://doi.org/10.1016/j.jfoodeng.2017.08.026>
- Luna-Guevara, J. J., Ochoa-Velasco, C. E., Hernández-Carranza, P., & Guerrero-Beltrán, J. A. (2017). Microencapsulation of walnut, peanut and pecan oils by spray drying. *Food Structure*, 12, 26–32. <https://doi.org/10.1016/j.foostr.2017.04.001>
- Mitra, H., Pushpadass, H. A., Franklin, M. E. E., Ambrose, R. K., Ghoroi, C., & Battula, S. (2017). Influence of moisture content on the flow properties of basundi mix. *Journal of Powder Technology*, 312, 133–143. <https://doi.org/10.1016/j.powtec.2017.02.039>
- Nair, L. M., Stephens, N. V., Vincent, S., Raghavan, N., & Sand, P. J. (2003). Determination of polysorbate 80 in parental formulations by high-performance liquid chromatography and evaporative light scattering detection. *Journal of Chromatography A*, 1012(1), 81–86. [https://doi.org/10.1016/s0021-9673\(03\)01105-1](https://doi.org/10.1016/s0021-9673(03)01105-1)
- Nandiyanto, A. B. D., Oktiani, R., & Ragadhita, R. (2019). How to read and interpret FTIR spectroscopy of organic material. *Indonesian Journal of Science and Technology*, 4(1), 97–118. <https://doi.org/10.17509/ijost.v4i1.12351>
- Napiórkowska, A., & Kurek, M. (2022). Coacervation as a novel method of microencapsulation of essential oils: A review. *Molecules*, 27(16), 5142. <https://doi.org/10.3390/molecules27165142>

- Napiórkowska, A., Szpicer, A., Górską-Horczyzak, E., & Kurek, M. A. (2024). Microencapsulation of essential oils using faba bean protein and chia seed polysaccharides via complex coacervation method. *Molecules*, 29(9), 2019. <https://doi.org/10.3390/molecules29092019>
- Napiórkowska, A., Szpicer, A., Wojtasik-Kalinowska, I., Perez, M. D. T., González, H. D., & Kurek, M. A. (2023). Microencapsulation of juniper and black pepper essential oil using the coacervation method and its properties after freeze-drying. *Foods*, 12(23), 4345. <https://doi.org/10.3390/foods12234345>
- Pereira, A. R. L., Gonçalves Cattelan, M., & Nicoletti, V. R. (2019). Microencapsulation of pink pepper essential oil: Properties of spray-dried pectin/SPI double-layer versus SPI single-layer stabilized emulsions. *Colloids and Surfaces A: Physicochemical and Engineering Aspects*, 581, 123806. <https://doi.org/10.1016/j.colsurfa.2019.123806>
- Pramod, K., Suneesh, C. V., Shanavas, S., Ansari, S. H., & Ali, J. (2015). Unveiling the compatibility of eugenol with formulation excipients by systematic drug-excipient compatibility studies. *Journal of Analytical Science and Technology*, 6(1), Article 34.
- Ravi, R., Prakash, M., & Bhat, K. K. (2013). Characterization of aroma active compounds of cumin (*Cuminum cyminum* L.) by GC-MS, E-nose, and sensory techniques. *International Journal of Food Properties*, 16(5), 1048–1058. <https://doi.org/10.1080/10942912.2011.576356>
- Rojas-Moreno, S., Osorio-Revilla, G., Gallardo-Velázquez, T., Cárdenas-Bailón, F., & Meza-Márquez, G. (2018). Effect of the cross-linking agent and drying method on encapsulation efficiency of orange essential oil by complex coacervation using whey protein isolate with different polysaccharides. *Journal of Microencapsulation*, 35(2), 165–180. <https://doi.org/10.1080/02652048.2018.1449910>
- Salminen, H., Sachs, M., Schmitt, C., & Weiss, J. (2022). Complex coacervation and precipitation between soluble pea proteins and apple pectin. *Food Biophysics*, 17, 460–471. <https://doi.org/10.1007/s11483-022-09726-x>
- Shanthakumar, P., Klepacka, J., Bains, A., Chawla, P., Dhull, S. B., & Najda, A. (2022). The current situation of pea protein and its application in the food industry. *Molecules*, 27(16), 5354. <https://doi.org/10.3390/molecules27165354>
- Sokolowska, I., Ngounou Wetie, A. G., Woods, A. G., & Darie, C. C. (2012). Automatic determination of disulfide bridges in proteins. *Journal of Laboratory Automation*, 17(6), 408–416. <https://doi.org/10.1177/2211068212454737>
- Sonawane, A., Pathak, S. S., & Pradhan, R. C. (2021). Effect of drying on physical and flow properties of banana powder. *Carpathian Journal of Food Science and Technology*, 13(3), 173–184. <https://doi.org/10.34302/crpfjst/2021.13.3.14>
- Syed, N., Mahesar, S. A., Sherazi, S. T. H., & Soyak, M. (2020). Quality assessment and safety measurement of different industrial processing stages of soybean oil. *Turkish Journal of Agriculture—Food Science and Technology*, 1, 28–33. <https://doi.org/10.24925/turjaf.v1i1.28-33.26>
- Tavares, L., & Noreña, C. P. Z. (2020). Encapsulation of ginger essential oil using complex coacervation method: Coacervate formation, rheological property, and physicochemical characterization. *Food and Bioprocess Technology*, 13, 1405–1420. <https://doi.org/10.1007/s11947-020-02480-3>
- Timilsena, Y. P., Akanbi, T. O., Khalid, N., Adhikari, B., & Barrow, C. J. (2019). Complex coacervation: Principles, mechanisms and applications in microencapsulation. *International Journal of Biological Macromolecules*, 121, 1276–1286. <https://doi.org/10.1016/j.ijbiomac.2018.10.144>
- Wojtasik-Kalinowska, I., Guzek, D., Górską-Horczyzak, E., Brodowska, M., Sun, D. W., & Wierzbicka, A. (2018). Diet with linseed oil and organic selenium yields low n-6/n-3 ratio pork Semimembranosus meat with unchanged volatile compound profiles. *International Journal of Food Science*, 53, 1838–1846. <https://doi.org/10.1080/09637486.2018.1483144>
- Xiao, Z., Li, W., Zhu, G., Zhou, R., & Niu, Y. (2016). Study of production and the stability of styrallyl acetate nanocapsules using complex coacervation. *Flavour and Fragrance Journal*, 31(4), 283–289. <https://doi.org/10.1002/ffj.3306>
- Xin, X., Essien, S., Dell, K., Woo, M. W., & Baroutian, S. (2022). Effects of spray-drying and freeze-drying on bioactive and volatile compounds of smoke powder food flavouring. *Food Bioprocess Technology*, 15, 785–794.
- Yekdane, N., & Goli, S. A. H. (2019). Effect of pomegranate juice on characteristics and oxidative stability of microencapsulated pomegranate seed oil using spray drying. *Food Bioprocess Technology*, 12, 1614–1625. <https://doi.org/10.1007/s11947-019-02325-8>
- Zhang, C., Zhao, J., Famous, E., Pan, S., Peng, X., & Tian, J. (2021). Antioxidant, hepatoprotective and antifungal activities of black pepper (*Piper nigrum* L.) essential oil. *Food Chemistry*, 346, 128845. <https://doi.org/10.1016/j.foodchem.2020.128845>
- Zotarelli, M. F., da Silva, V. M., Durigon, A., Hubinger, M. D., & Laurindo, J. B. (2017). Production of mango powder by spray drying and cast-tape drying. *Powder Technology*, 305, 447–454. <https://doi.org/10.1016/j.powtec.2016.10.053>

How to cite this article: Napiórkowska, A., Szpicer, A., Górską-Horczyzak, E., & Kurek, M. (2024). Understanding emulsifier influence on complex coacervation: Essential oils encapsulation perspective. *Journal of Food Science*, 1–19. <https://doi.org/10.1111/1750-3841.17220>

Warszawa, 8/10/2024

Alicja Kizildag
alicjakizildag@gmail.com

**Rada Dyscypliny Technologia
Żywności i Żywnienia
Szkoly Głównej Gospodarstwa
Wiejskiego w Warszawie**

Oświadczenie o współautorstwie

Niniejszym oświadczam, że w pracy: *Napiórkowska, A., Szpicer, A., Górską-Horczyzak, E., & Kurek, M. Understanding emulsifier influence on complex coacervation: Essential oils encapsulation perspective. Journal of Food Science. 2024, 89(8)* mój indywidualny udział w jej powstaniu polegał na analizie dostępnej literatury, przygotowaniu metodologii badań, wykonaniu części badawczej, przygotowaniu manuskryptu oraz jego korekcie po procesie recenzji.

Podpis



Warszawa, 8/10/2024

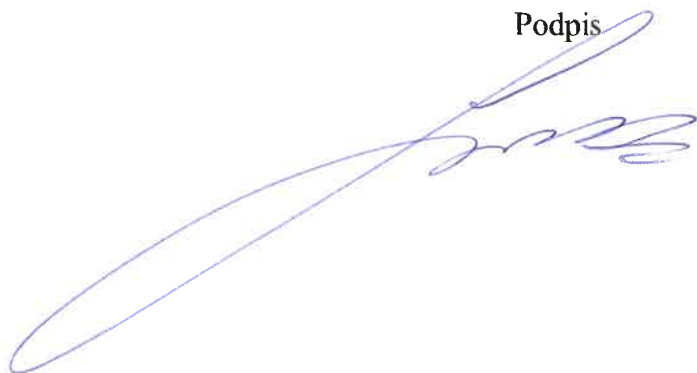
Arkadiusz Szpicer
arkadiusz_szpicer@sggw.edu.pl

**Rada Dyscypliny Technologia
Żywności i Żywienia
Szkoły Głównej Gospodarstwa
Wiejskiego w Warszawie**

Oświadczenie o współautorstwie

Niniejszym oświadczam, że w pracy: *Napiórkowska, A., Szpicer, A., Górską-Horczyzak, E., & Kurek, M. Understanding emulsifier influence on complex coacervation: Essential oils encapsulation perspective. Journal of Food Science. 2024, 89(8)* mój indywidualny udział w jej powstaniu polegał na wykonaniu analizy Skaningowej Kalorymetrii Różnicowej oraz pomocy w przygotowaniu treści manuskryptu w tym zakresie.

Podpis

A handwritten signature in blue ink, consisting of a large, sweeping loop followed by several smaller, connected strokes.

Warszawa, 8/10/2024

Elżbieta Górską-Horzyczak
elzbieta_gorska-horzyczak@sggw.edu.pl

**Rada Dyscypliny Technologia
Żywności i Żywnienia
Szkoly Głównej Gospodarstwa
Wiejskiego w Warszawie**

Oświadczenie o współautorstwie

Niniejszym oświadczam, że w pracy: *Napiórkowska, A., Szpicer, A., Górską-Horzyczak, E., & Kurek, M. Understanding emulsifier influence on complex coacervation: Essential oils encapsulation perspective. Journal of Food Science. 2024, 89(8)* mój indywidualny udział w jej powstaniu polegał na przeprowadzeniu analizy ultra-szybkiej chromatografii gazowej „e-nos” i pomocy w interpretacji otrzymanych wyników.

Podpis



Warszawa, 8/10/2024

Marcin Andrzej Kurek
marcin_kurek@sggw.edu.pl

**Rada Dyscypliny Technologia
Żywności i Żywnienia
Szkoły Głównej Gospodarstwa
Wiejskiego w Warszawie**

Oświadczenie o współautorstwie

Niniejszym oświadczam, że w pracy: *Napiórkowska, A., Szpicer, A., Górską-Horczyzak, E., & Kurek, M. Understanding emulsifier influence on complex coacervation: Essential oils encapsulation perspective. Journal of Food Science. 2024, 89(8)* mój indywidualny udział w jej powstaniu polegał na nadzorowaniu badań, ocenie poprawności metodologii, konsultacjach merytorycznych oraz pomocy w analizie wyników.

Podpis





Optimization of oat protein and gum Arabic microcapsules containing juniper essential oil using Response Surface Methodology

Alicja Napiórkowska, Havva Aktaş, Arkadiusz Szpicer, Elżbieta Górską-Horczyk, Marcin A. Kurek*

Department of Technique and Food Development, Institute of Human Nutrition Sciences, Warsaw University of Life Sciences, Poland

ARTICLE INFO

Keywords:

Juniper essential oil
Wheat germ oil
Complex coacervation
Microencapsulation
Oat protein

ABSTRACT

In this study, we explored the feasibility of using oat soluble protein and gum Arabic as wall materials for microencapsulation via complex coacervation of juniper dissolved in wheat germ oil EO. The process was optimized using Response Surface Methodology (RSM), varying mixing ratios (20–80%) and pH levels (2–6), followed by freeze-drying of the coacervates. Physicochemical properties of the resulting powders, including solubility, hygroscopicity, moisture content, color, particle size distribution, and bulk and tapped density, were assessed. Encapsulation efficiency (EE) was determined through surface and total oil content calculations, supported by FT-IR spectroscopy. Characterization involved e-nose sensor analysis and differential scanning calorimetry (DSC). The study findings revealed encapsulation efficiencies (EE) ranging from 23.38 % to 26.58%, accompanied by low bulk and tapped densities (0.11–0.17 g/cm³ and 0.20–0.28 g/cm³, respectively), as well as elevated Carr Index values (36.92–46.34) and Hausner ratios (1.59–1.86). Moisture content varied between 0.07 % and 0.93 % across the samples. Additionally, the research demonstrated that employing oat protein and gum Arabic as wall materials enables the production of microcapsules with thermal stability exceeding 100 °C, facilitating their potential application in the food industry.

1. Introduction

Oats (*Avena sativa* L., *Poaceae*, *Aveneae*) are characterized by a relatively high protein content (up to 20%) and better quality in terms of amino acid composition compared to other cereal grains (Table 1). Unlike other cereals, oats are unique in having the predominant storage protein soluble in salt solution, known as globulin. Oat globulins constitute a mixture of various proteins identified and separated into 12 S (the major component), 7 S, and 3 S fractions (Chang et al., 2011). They contain essential amino acids such as phenylalanine, lysine, histidine, and valine. The composition of essential amino acids in globulins aligns with the FAO recommended values for adults for all amino acids except methionine (Jing et al., 2016). While oats contain more lysine (the first limiting amino acid in other cereals), its content is still lower than the FAO requirement for infants. The levels of sulfur-containing amino acids and tryptophan exceed the FAO standard, making oats a valuable source of supplementary protein limited by methionine (Jing et al., 2016; Boukid, 2021). Due to its high nutritional value, oat protein is gaining popularity among consumers, and food producers are

increasingly incorporating it into their products. In contrast, while rice and wheat proteins are commonly used in microencapsulation processes, they exhibit lower protein content and less favorable amino acid profiles compared to oat protein (Table 1). Additionally, despite intensive literature search, no prior studies on utilizing oat protein for essential oil microencapsulation were found. This highlights the novelty and potential of oat protein in this application, underscoring its suitability for creating microcapsules with enhanced nutritional and functional properties.

Oat protein is industrially obtained using the isoelectric precipitation method, wherein alkaline extraction is employed because the protein dissolves well at pH ~ 7–8. Subsequently, the protein is precipitated at a pH lowered to 4–5. The protein produced through this method is then filtered and dried to yield a concentrate exceeding 80% (Mäkinen et al., 2017; Brückner-Gühmann et al., 2019). However, this production process entails substantial water and energy consumption. Fortunately, oat grains are rich in β -glucan, and the industrial production of β -glucan results in the generation of oat protein isolate as a by-product, offering a sustainable option for utilization in the food industry. Therefore,

* Corresponding author.

E-mail address: marcin_kurek@sggw.edu.pl (M.A. Kurek).

<https://doi.org/10.1016/j.fbp.2024.04.001>

Received 21 February 2024; Received in revised form 9 April 2024; Accepted 9 April 2024

Available online 11 April 2024

0960-3085/© 2024 The Author(s). Published by Elsevier Ltd on behalf of Institution of Chemical Engineers. This is an open access article under the CC BY license (<http://creativecommons.org/licenses/by/4.0/>).

Table 1
Amino acid composition of oat, wheat and rice proteins.

	Amino acid [g/ 16 g of N]	Oat protein	Wheat protein	Rice protein
Essential amino acids	Arginine	6.93–9.78	2.10–3.35	9.0–11
	Isoleucine	3.48–4.41	2.74–3.77	4.3–4.7
	Leucine	7.07–9.17	6.31–9.30	7.3–9.3
	Threonine	2.65–4.30	0.94–1.96	2.8–5.1
	Valine	4.77–6.01	0.82–3.52	6.3–6.9
	Lysine	3.46–3.79	1.27–3.61	2.7–4.5
	Phenylalanine	5.23–5.56	2.83–5.56	5.4–6.0
	Histidine	2.13–3.68	0.82–1.86	2.6–2.7
	Methionine	1.55–1.73	0.57–2.88	2.0–3.1
	Non-essential amino acids	Glycine	3.75–5.83	4.31–7.11
Alanine		4.08–5.43	5.62–8.70	5.6–5.9
Cysteine		1.77–2.78	0.68–4.32	1.2–1.8
Aspartic acid		6.10–8.36	3.28–6.76	10.0–11.0
Glutamic acid		21.45–24.21	30.53–36.84	19.0–21.0
Tyrosine		3.37–3.61	3.03–4.10	5.3–5.5
Serine		5.12–5.26	4.17–5.18	4.5–6.2
Proline		4.08–7.08	3.32–14.98	4.9–6.2
Protein content [%]		12–20	11–15	7–10

Based on Sterna et al., 2016; Siddiqi et al., 2020; Boukid, 2021; Kumar et al., 2021, own elaboration

exploring applications for this protein aligns with trends related to the circular economy and the sustainable development of the food industry, contributing to the increasing of its popularity. An interesting application of this protein in food may be microencapsulation of essential oils using the complex coacervation method.

Complex coacervation is a process that takes place in solutions of proteins and polysaccharides below the isoelectric point. The alteration in pH induces a decrease in the free electrostatic energy of the reaction system, stemming from the interaction between oppositely charged ions (Napiórkowska and Kurek, 2022). This allows the active substance to be enclosed in the space of microcapsules formed as a result of these interactions. The advantage of this process is that it does not require the use of high temperature, so it can be successfully used for microencapsulation of thermolabile ingredients (Amalraj et al., 2019; Verri et al., 2012).

Juniper essential oil is a valuable extract obtained primarily from juniper berries (*Juniperus communis*). It boasts an intense, fresh scent with distinct woody and citrus notes, making it a sought-after ingredient in various industries, including the food industry, where it serves as a seasoning for meats or flavoring agent for beverages. Beyond its aromatic qualities, juniper essential oil is known for its potent antioxidant and antimicrobial properties, demonstrating efficacy against a range of pathogens including *Salmonella enterica*, *Pseudomonas aeruginosa*, *Escherichia coli*, *Staphylococcus aureus*, and *Bacillus cereus* (Kalaba et al., 2020). The ingredients responsible for this effect of the juniper essential oil are phenolic compounds such as flavonoids, chlorogenic acid, and catechin, alongside terpenes α -pinene, limonene, β -pinene, and β -laurene, and other bioactive substances known for their antibacterial, and antioxidant properties (Feng et al., 2020; Wu et al., 2022; Zheljzakov et al., 2017).

The aim of the study was to fabricate microcapsules based on oat protein and gum Arabic encapsulating wheat germ oil and juniper essential oil. The complex coacervation method was employed due to the volatile nature of the essential oils. Another objective was to optimize the microcapsule production process to increase encapsulation efficiency and solubility while reducing the particle size distribution (PDI) value. To achieve this, the Response Surface Methodology (RSM) method was employed. RSM serves as a potent tool within the food industry, facilitating the optimization of production processes and enhancement of food product quality. This sophisticated statistical approach enables the analysis of intricate relationships among diverse process variables and the characteristics of final products. In our study,

Table 2
Plan of the experiment – sample coding for both factors.

Run	pH [A]	OP% [B]	OP:GA [%]	Sample code
1	4	50	1:1	CS1
2	2.6	29	1:2.33	S1
3	2	50	1:1	S2
4	5.4	71	2.33:1	S3
5	4	80	4:1	S4
6	5.4	29	1:2.33	S5
7	4	20	1:4	S6
8	4	50	1:1	CS2
9	4	50	1:1	CS3
10	4	50	1:1	CS4
11	4	50	1:1	CS5
12	6	50	1:1	S7
13	2.6	71	2.33:1	S8

we employed the RSM method to optimize the microcapsule production process, a detailed account of which is provided later in this article (Kurek et al., 2016). Furthermore, the study aimed to evaluate the physicochemical parameters of the obtained microcapsules, including density, solubility, water content, and hygroscopicity.

2. Materials and methods

2.1. Materials

Soluble fraction of oat protein obtained from Oat Protein Isolate (Helhetshälsa AB, Borghamn, Sweden) and gum Arabic (Warchem, Warsaw, Poland) were used as wall materials. Juniper berry (*Juniperus communis*) essential oil (Ancient Wisdom, Sheffield, Great Britain) was firstly dissolved in wheat germ oil (Zielony Klub, Kielce, Poland) and used as core material. Essential oils were dissolved in oil at a concentration of 1 % v/v to reduce the risk of their evaporation during the freeze-drying process.

2.2. Extraction of an oat protein soluble fraction

A 5% solution of oat protein isolate was prepared. To increase the solubility of the proteins, the pH of the solution was changed to 8 with 1 M NaOH and allowed to stand for 2 h. After this time, the solution was centrifuged (10 min, 9000 rpm). 1 M HCl was added (pH=4) to the collected supernatant to precipitate the remaining insoluble proteins and centrifuged again. The solution of soluble oat protein fractions prepared in this way was frozen and freeze-dried.

2.3. Design of experiments

The combinations of different pH values (A), and content of oat protein (B) were considered to be independent variables using a fractional design with two entry variables, one block and twelve assays. The one additional center point was added to each block using Design Expert software v. 11 (Stat-Ease, Inc., USA) which conducted the experiments to 13 assays (Table 2). The ranges of the A were 2–6 and of the B were 20–80 %.

2.4. Preparation of coacervates

As a wall material, 5 % solution of soluble oat protein fraction (OP) with 5% gum Arabic (GA) solution was used. The solutions were mixed in different mixing ratios according to the RSM analysis results: 29:71, 71:29, 50:50, 80:20 and 20:80 (Table 2). The values given by the program were converted into the mixing ratio of OP and GA – 1:2.33, 2.33:1, 1:1, 4:1, and 1:4, respectively (Table 2). The mass of each system was 300 g. After mixing the solutions together, they were subjected to high shear homogenization using Ultra turrax (IKA T18 basic, Germany) for 10 min at 15,000 rpm/min at room temperature. During

homogenization, each variant was supplemented with juniper essential oil (JEO) dissolved in wheat germ oil (WGO) in a 1:1 ratio, which constituted a total of 5 % of the entire system volume. After emulsification, the pH was adjusted according to the RSM results to: 2.0, 2.6, 4.0, 5.4, and 6.0 (under and above the isoelectric point) using 1 mol HCl (Table 2). All emulsions were stored at 4 °C for 24 h, freeze and freeze-dried. The lyophilizates were screened on a laboratory sieve with a mesh size of 710 μm, then vacuum packed and stored at 4 °C for further determinations.

2.5. Solid yield, and encapsulation efficiency

Solid yield which is freeze-drying losses (SY) were assessed and expressed as the ratio of the mass of the obtained powder (DC) to the mass of liquid coacervates before drying (LC) (Eq. 1) (Rojas-Moreno et al., 2018). All measurements were done in triplicates.

$$SY = \frac{DC}{LC} * 100\% \quad (1)$$

Encapsulation efficiency (EE) was expressed as the ratio of total oil (TO) and surface oil (SO) (Eq. 2) (Mu et al., 2022). All measurements were done in triplicates.

$$EE = \frac{T_o - S_o}{T_o} * 100\% \quad (2)$$

To determine SO content, 1 g of the sample was dissolved in 30 mL of n-hexane under constant stirring (60 rpm) for 15 minutes. The resulting oil-solvent mixture was then filtered into a pre-weighed 25 mL round-bottom flask and evaporated using a Büchi R-100 rotary evaporator (Switzerland). To ensure complete removal of n-hexane, the flasks were heated at 105 °C for 30 minutes in a Binder FP 115 drying oven (Tuttlingen, Germany), and then allowed to cool in a desiccator. The final weight of the round-bottom flasks was recorded, and the solvent oil content was calculated (Eq. 3):

$$SO = OM_1 - OM_2 \quad (3)$$

Where:

OM₁ – oil mass after extraction and evaporation of the solvent

OM₂ – the theoretical weight of oil from the sample

To determine TO content in the samples, 1.5 g of powder were mixed with 4 mL of KCl, 4 mL of acetone, and 8 mL of chloroform under stirring (60 rpm) for 15 minutes. The resulting mixture was then centrifuged at 10,000 rpm for 10 minutes to separate the layers. The chloroform layer containing the extracted oil was filtered into pre-weighed 25 mL round-bottom flasks. This process was repeated with 4 mL of double-distilled water instead of KCl for a second extraction. The solvent was then evaporated using a Büchi R-100 rotary evaporator (Switzerland) followed by heating at 105 °C for 30 minutes in a Binder FP 115 drying oven (Tuttlingen, Germany). The flasks were cooled in a desiccator, weighed, and the total oil content (TO) was calculated (Eq. 4):

$$TO = OM_1 - OM_2 \quad (4)$$

2.6. Bulk and tapped density, Carr index (CI), and Hausner ratio (HR)

Bulk density (ρ_{bulk}) was determined by loosely pouring 1 g of the sample into a 10 mL graduated cylinder and reading the volume it occupied. Then tapping manually the cylinder under its own weight for one minute the tapped density (ρ_{tap}) was determined. Based on the obtained results powder's flowability and tendency to compress were expressed by Carr Index (CI) and Hausner Ratio (HR) (Eqs. 5 and 6) (Bajac et al., 2020; Xin et al., 2022). Determinations were made in triplicate.

$$CI = \frac{\rho_{tap} - \rho_{bulk}}{\rho_{tap}} * 100\% \quad (5)$$

$$HR = \frac{\rho_{tap}}{\rho_{bulk}} \quad (6)$$

2.7. Solubility, hygroscopicity, and moisture content

To assess powder solubility, 0.5 g of the sample was dispersed in 50 mL of double-distilled water. The mixture was then agitated for 30 minutes at 60 rpm before being centrifuged at 10,000 rpm for 5 minutes. After centrifugation, 25 mL of the supernatant was carefully transferred to a pre-weighed petri dish and dried at 105 °C for 6 hours using a Binder FP 115 drying oven (Tuttlingen, Germany). Solubility (%) was calculated as the percentage of dried supernatant relative to the initially added powder amount (De Melo Ramos et al., 2019). Triplicate measurements were conducted for each determination.

To assess the hygroscopicity of the obtained powders, 0.2 g of the sample was placed in a pre-weighed petri dish. The dish was then stored in a desiccator containing a saturated Na₂SO₄ solution for one week. Hygroscopicity was quantified as the g of water absorbed per 100 g of sample (%) (Tavares and Noreña, 2020). Triplicate determinations were conducted for each sample.

To determine the moisture content of the obtained powders, 0.2 g of each sample was placed in a pre-weighed petri dish. The dish with the sample was then dried at 70 °C for 24 hours using a Binder FP 115 drying oven (Tuttlingen, Germany). After drying, the samples were allowed to cool in a desiccator before being re-weighed. The moisture content was calculated by subtracting the initial weight from the final weight after drying, expressed as a percentage of the initial weight (Tavares and Noreña, 2020). Triplicate determinations were performed for each sample.

2.8. Color measurement

The color of the microcapsules was evaluated using a Minolta CR-400 colorimeter (Konica Minolta Inc., Japan). Measurements were conducted under D65 illuminant conditions, utilizing an 8 mm measuring surface and adhering to the standard 2° observer protocol. Data were recorded within the CIELab color space (according to International Commission on Lighting's system (Commission Internationale de L'Éclairage)). Parameters assessed included L* (where L = 0 represents black and L = 100 represents white), a* (where negative a values denote green and positive a values denote red), and b* (where negative b values signify blue and positive b values signify yellow) (Otálora et al., 2023). These determinations were conducted in triplicate immediately following the production process.

2.9. Particle size distribution

The measurement was carried out with the Morphologi® G3SE apparatus (Malvern Instruments Ltd., Malvern, UK) equipped with a dispersion unit for dry samples. The particle size distribution was calculated as the relative volume of molecules in the band shown as size distribution curves (Malvern Microsoft ware v.5.40, Malvern Instruments Ltd.). The examined parameters of the size distribution contained the largest particle size (D₉₀), mean particle volume (D₅₀), and the smallest particle size (D₁₀). The particle size distribution (Span index – SI) was estimated using the following formula (Eq. 7) (De Melo Ramos et al., 2019; Fernandes et al., 2014):

$$SI = \frac{D_{90} - D_{10}}{D_{50}} \quad (7)$$

Table 3

Solid yield (SY), encapsulation efficiency (EE), bulk density (BD), tapped density (TD), Carr index (CI), and Hausner ratio (HR) for all tested samples with the results of statistical tests of fitting the equations of the response surfaces to the values obtained experimentally.

Run	Sample	SY [%]	EE [%]	BD [g/cm ³]	TD [g/cm ³]	CI [%]	HR
1	CS1	9.27 ^f ±0.002	25.65 ^a ±0.280	0.11 ^e ±0.001	0.20 ^e ±0.002	44.68 ^{ab} ±0.000	1.81 ^{bc} ±0.000
2	1 S	8.89 ^c ±0.023	25.07 ^a ±5.650	0.13 ^d ±0.000	0.25 ^d ±0.001	46.34 ^b ±0.000	1.86 ^c ±0.000
3	2 S	9.01 ^d ±0.002	26.30 ^a ±1.960	0.17 ^{ab} ±0.006	0.28 ^{ab} ±0.007	36.92 ^a ±3.100	1.59 ^a ±0.080
4	3 S	8.64 ^a ±0.023	26.46 ^a ±5.520	0.17 ^{abc} ±0.013	0.27 ^{ab} ±0.014	38.90 ^{ab} ±2.030	1.64 ^{ab} ±0.050
5	4 S	9.31 ^f ±0.002	23.46 ^a ±0.230	0.15 ^c ±0.005	0.25 ^{cd} ±0.004	38.46 ^{ab} ±4.220	1.63 ^{ab} ±0.040
6	5 S	9.04 ^d ±0.007	24.58 ^a ±0.800	0.14 ^d ±0.015	0.24 ^d ±0.007	42.83 ^{ab} ±4.970	1.76 ^{abc} ±0.150
7	6 S	9.17 ^e ±0.023	23.39 ^a ±0.960	0.16 ^{bc} ±0.014	0.25 ^{cd} ±0.003	37.96 ^a ±6.120	1.62 ^{ab} ±0.160
8	CS2	9.42 ^f ±0.003	25.69 ^a ±0.140	0.10 ^e ±0.001	0.18 ^e ±0.002	44.44 ^{ab} ±0.000	1.80 ^{bc} ±0.000
9	CS3	9.31 ^f ±0.072	25.71 ^a ±0.310	0.11 ^e ±0.001	0.19 ^d ±0.004	42.10 ^{ab} ±0.000	1.73 ^{bc} ±0.000
10	CS4	9.36 ^e ±0.008	26.05 ^a ±0.420	0.12 ^e ±0.001	0.20 ^d ±0.011	40.00 ^{ab} ±0.000	1.66 ^{bc} ±0.000
11	CS5	9.59 ^e ±0.001	25.13 ^a ±0.232	0.11 ^e ±0.001	0.20 ^d ±0.002	45.00 ^{ab} ±0.000	1.82 ^{bc} ±0.000
12	7 S	8.91 ^c ±0.009	25.91 ^a ±4.160	0.16 ^{bc} ±0.010	0.26 ^{bc} ±0.010	40.57 ^{ab} ±2.310	1.68 ^{abc} ±0.070
13	8 S	8.69 ^b ±0.012	25.43 ^a ±3.760	0.17 ^a ±0.008	0.28 ^a ±0.004	38.16 ^a ±3.190	1.62 ^{ab} ±0.080
Regression coefficients							
	Intercept	9.23	25.62**	0.108	0.1953***	44.68	1.81
	A – pH	-0.0057	-0.001	-0.0031	-0.0037	0.2987	0.0061
	B – oat protein content	-0.0514	0.2919	0.008	0.0074	-1.43	-0.0449
	AB	-0.05	0.3772	-0.0033	-0.001	1.06	0.031
	A ²	-0.2046*	0.3977*	0.0268***	0.0373***	-2.2	-0.0634
	B ²	-0.0662	-0.9436***	0.0215***	0.0276***	-2.47*	-0.0695*
	R ²	0.995	0.997	0.992	0.992	0.987	0.99
	Lack of fit	0.787	0.206	1.414	1.692	0.104	0.46

2.10. Differential Scanning Calorimetry (DSC)

The thermal properties of the samples were evaluated using Differential Scanning Calorimetry (DSC 1) from Mettler Toledo (Schwerzenbach) under an argon atmosphere at a flow rate of 100 cm³/min. The instrument was calibrated with pure indium and zinc. Each sample (5.0 ± 0.1 mg) was placed in a standard 40 µl aluminum crucible (ME-51119870) and covered with a lid (ME-51119871) using the Mettler Toledo Crucible Sealing Press. DSC scans were recorded from 10 °C to 230 °C at a rate of 10 °C/min (β). The thermograms were analyzed using STARE software (v. 9.30) to determine the onset (T_{on}), peak (T_{max}), and endset (T_{end}) temperatures, as well as the areas under the peaks (ΔH) (Napiórkowska et al., 2023).

2.11. Fourier Transform Infrared Spectroscopy (FT-IR)

FT-IR spectra were recorded without any sample preparation on a Nicolet™ iS™ 5 FTIR Spectrometer (Thermo Scientific, Waltham, MA, USA), with horizontal device for attenuated reflectance and diamond crystal, on a spectral window ranging from 4000 to 400 cm⁻¹ (with 16 scans), at a spectral resolution of 2 cm⁻¹. Obtained spectra were processed with the OMNIC program (Thermo Scientific, Waltham, MA, USA) (Napiórkowska et al., 2023).

2.12. Smell pattern – e-nose analysis

For smell pattern analysis the Heracles II electronic nose (Alpha M.O. S., Toulouse, France) was used. Following the methodology we used in our previous study (Napiórkowska et al., 2023) 10% solution of each sample was placed in 20 mL headspace vial sealed with a Teflon-faced silicon rubber cap. Vials were incubated at 35 °C for 900 s under an agitation speed of 8.33 Hz. Hydrogen was used as the carrying gas at a constant flow rate of 1 mL/min. The injector temperature was set at 200 °C, with an injected volume of 3500 µL and an injection speed of 125 mL s⁻¹. The analytes were collected in the trap at 15 °C and subsequently divided and simultaneously transferred into the two columns. The carrying gas was maintained at a constant pressure of 80 kPa, with a split flow rate of 10 mL min⁻¹ at the column heads. The temperature program in the oven was as follows: 60 °C for 2 s, a ramp of 3 °C s⁻¹ to 270 °C, held for 20 s, and FID1/FID2 at 280 °C. Smell pattern data was presented through principal component analysis (PCA) using AlphaSoft

software (v. 8.0.). All samples were analyzed in triplicate.

2.13. Optimization of coacervates production (statistical analysis)

The responses obtained from the assays were analyzed using the Central Composite Rotational Design (CCRD) to investigate the effects of the independent variables – A and B. The Design Expert software v. 11 (Stat-Ease, Inc., USA) was employed for this analysis. The dependent variables, or responses, encompassed various coacervates quality characteristics such as yield, encapsulation efficiency, density, flowability, solubility, hygroscopicity, moisture content, and color. In order to explain how the factors influenced the responses, the CCD modelling was complied with the following quadratic (Eq. 8):

$$y = \beta_0 + \beta_1 X_1 + \beta_2 X_2 + \beta_{11} X_1^2 + \beta_{22} X_2^2 + \beta_{12} X_1 X_2 \quad (8)$$

where

y - is the predicted response;

X₁ and X₂ are the coded factors (independent variables) that influence the response y;

β₀ - is the intercept term;

β₁ and β₂ - are the linear coefficients;

β₁₁ and β₂₂ - are the quadratic coefficients;

β₁₂ is the interaction coefficient between X₁ and X₂.

The significant terms in the model were identified using one-way analysis of variance (ANOVA, p ≤ 0.05) for each response variable, along with assessing the lack of fit and coefficients of determination (R²) to ensure model accuracy. The 3-D surface plots were created using Design Expert software v. 11 (Stat-Ease, Inc., USA).

In addition to elucidating variable behavior through surface plots, the models established in this study can be employed for process optimization utilizing the desirability function. This involves transforming each response variable into a desirability function (di) ranging from 0 to 1. The objective is to identify factor levels that correspond to maximum or minimum values of the response variables, setting di = 1 for high values and di = 0 for low values. Encapsulation efficiency and solubility were designated as "maximally desirable," while the polydispersity index was designated as "minimally desirable." The desirability function functions as a penalty function, guiding the algorithm towards regions where desired response variable values can be found. Factor levels associated with maximum or minimum response variables are referred to as "optimum points" (Kurek et al., 2016).

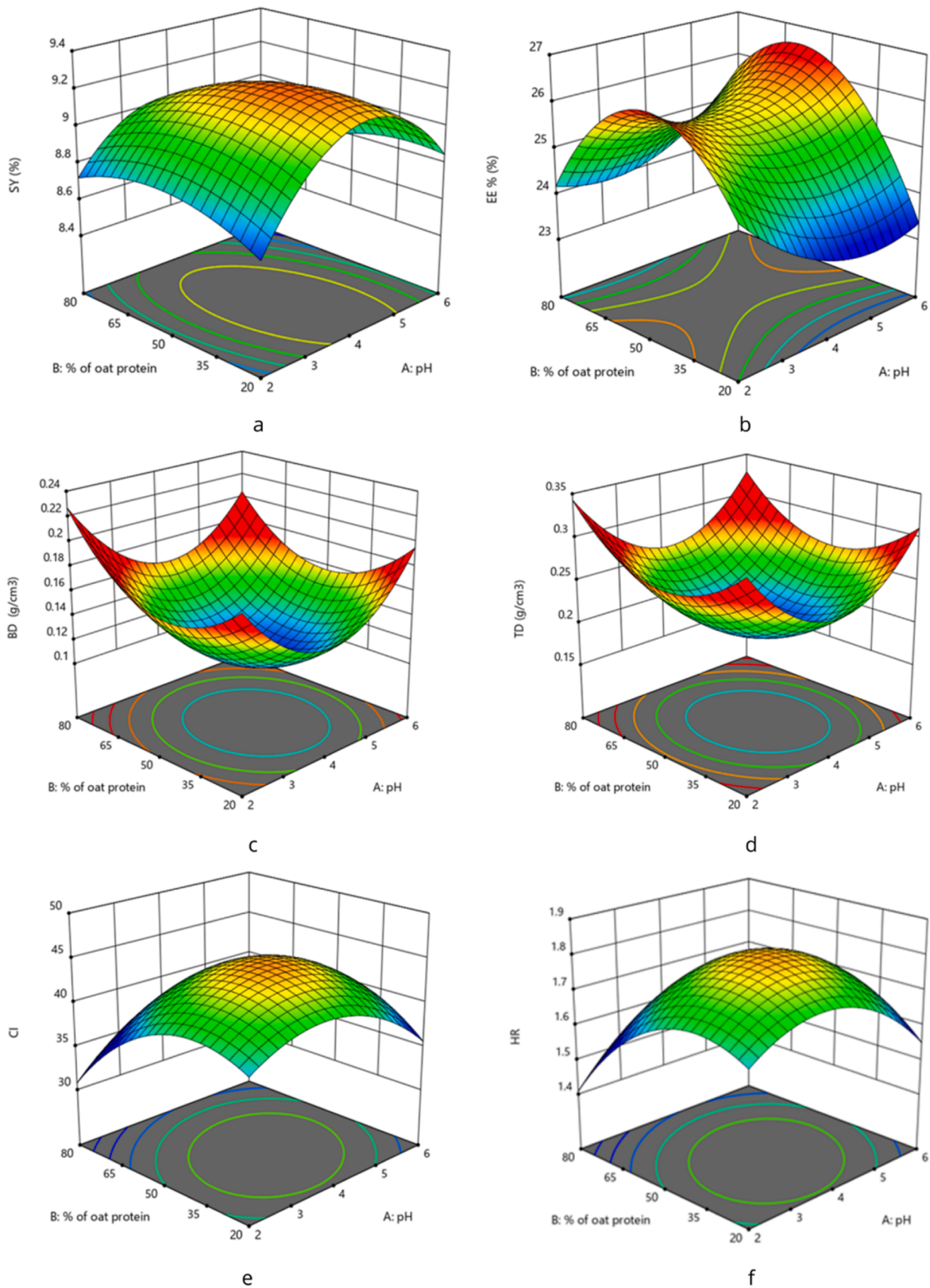


Fig. 1. : Response Surface of: (a) solid yield (SY), (b) encapsulation efficiency (EE), (c) bulk density (BD), (d) tapped density (TD), (e) Carr index (CI), and (f) Hausner ratio (HR) depending on the pH (factor A) and oat protein content (factor B).

Table 4

Solubility (SOL), hygroscopicity (HIG), moisture content (MOIST), color parameters L*, a* and b*, and particle size distribution (PDI) for all tested samples with the results of statistical tests of fitting the equations of the response surfaces to the values obtained experimentally.

Run	Sample	SOL [%]	MOIST [%]	HIG [%]	L*	a*	b*	PDI
1	CS1	83.68 ^{bc} ±0.010	0.37 ^{ab} ±0.003	22.77 ^{ab} ±0.020	80.24 ^{bcd} ±0.770	2.59 ^b ±0.180	29.24 ^{bc} ±1.520	0.77 ⁱ ±0.000
2	1 S	83.16 ^c ±0.000	0.93 ^c ±0.000	35.26 ^a ±0.010	82.02 ^d ±0.480	2.02 ^a ±0.070	27.69 ^{abc} ±0.320	0.69 ^e ±0.000
3	2 S	84.91 ^{bc} ±0.010	0.07 ^a ±0.001	15.03 ^a ±0.000	79.26 ^{abc} ±0.950	3.01 ^c ±0.090	27.86 ^{abc} ±0.310	0.70 ^f ±0.000
4	3 S	82.34 ^{bc} ±0.000	0.85 ^b ±0.001	15.39 ^a ±0.000	77.85 ^a ±0.940	3.63 ^{dc} ±0.130	26.00 ^a ±0.680	0.67 ^d ±0.001
5	4 S	81.60 ^{bc} ±0.000	0.78 ^b ±0.000	15.64 ^{ab} ±0.000	78.65 ^{abc} ±0.180	3.89 ^e ±0.100	27.50 ^{abc} ±0.360	0.65 ^b ±0.000
6	5 S	86.54 ^c ±0.010	0.74 ^b ±0.001	12.35 ^a ±0.000	80.65 ^{cd} ±0.360	2.01 ^a ±0.040	26.30 ^{ab} ±0.270	0.75 ^h ±0.001
7	6 S	85.10 ^c ±0.000	0.71 ^b ±0.001	12.80 ^a ±0.000	81.70 ^d ±0.450	1.64 ^a ±0.130	27.04 ^c ±0.430	0.71 ^g ±0.000
8	CS2	82.99 ^{bc} ±0.010	0.40 ^{ab} ±0.003	22.49 ^{ab} ±0.020	80.47 ^{bcd} ±0.640	2.61 ^b ±0.172	29.32 ^{bc} ±1.571	0.76 ^{ij} ±0.000
9	CS3	83.41 ^{bc} ±0.010	0.36 ^{ab} ±0.004	23.12 ^{ab} ±0.021	81.12 ^{bcd} ±0.791	2.66 ^b ±0.186	30.87 ^{bc} ±0.200	0.77 ^j ±0.001
10	CS4	83.28 ^{bc} ±0.010	0.36 ^{ab} ±0.002	23.09 ^{ab} ±0.010	80.88 ^{bcd} ±0.801	2.43 ^b ±0.103	29.14 ^{bc} ±1.301	0.75 ^{ij} ±0.000
11	CS5	83.16 ^{bc} ±0.011	0.37 ^{ab} ±0.003	22.17 ^{ab} ±0.020	80.28 ^{bcd} ±0.781	2.51 ^b ±0.093	28.94 ^{bc} ±0.687	0.76 ^{ij} ±0.001
12	7 S	84.67 ^b ±0.010	0.91 ^c ±0.001	31.09 ^b ±0.000	77.37 ^a ±1.020	3.16 ^c ±0.140	29.29 ^{bc} ±1.440	0.66 ^c ±0.000
13	8 S	82.47 ^a ±0.010	1.06 ^c ±0.001	53.87 ^c ±0.010	78.31 ^{ab} ±0.710	3.31 ^c ±0.020	29.36 ^{bc} ±0.420	0.60 ^a ±0.000
Regression coefficients								
Intercept		84.08	0.00367	22.1	78.47933	3.43133	27.36733	0.7638**
A – pH		0.3641	0.00099	-2.34	-0.56537	0.18645	-0.09594	0.0094
B – oat protein content		-1.23***	0.00042	5.71	0.12932	0.05201	0.25757	-0.0307**
AB		-0.875	-0.00007	-8.89	1.23250*	-0.60167	0.45917	0.0017
A ²		0.2452	0.00129*	1.87	0.86658*	-0.30046	0.07008	-0.0443*
B ²		-0.4714	0.00259	-2.55	0.79242	-0.30796	-0.14075	-0.0429*
R ²		0.99	0.99	0.991	0.995	0.994	0.99	0.986
Lack of fit		1.667	0.968	0.874	1.097	1.198	0.763	0.329

Following optimization and production of the optimized microcapsules, the selected parameters were measured as before. The obtained results were subjected to one-way analysis of variance (ANOVA, $p \leq 0.05$) using Statistica v. 13.3. The parameters obtained in the DSC analysis were not subject to optimization.

3. Results and discussion

3.1. Solid yield, and encapsulation efficiency

The solid yield was in the range of 8.64–9.29 % and was significantly influenced by pH in quadratic terms reducing the SY values. Encapsulation efficiency was in the range of 23.39–26.46 % and was significantly influenced by the content of OP in quadratic terms, reducing the encapsulation efficiency. The highest EE was obtained for sample 4 (71:29, pH=5.4), and the lowest was for sample 7 (20:80, pH=4) (Table 3, Fig. 1).

The solid yield and encapsulation efficiency were low, possibly attributed to the limited interactions between OP and GA. Coacervate networks are formed when the attractive protein–polysaccharide interactions are favorable (Napiórkowska and Kurek, 2022; Nieto-Nieto et al., 2015; Nieto Nieto et al., 2016). The complexation of protein polysaccharide is significantly influenced by the pH and mixing ratio of biopolymers. pH plays a crucial role in controlling the degree of ionization of functional groups such as -NH₂ and -COOH which are present in used wall materials. It also regulates the strength of electrostatic interactions within the complex. On the other hand, the mixing proportions of biopolymers affect the distribution of electric charges, influencing the charge balance and electrostatic interactions (Naderi et al., 2020). Another factor influencing encapsulation efficiency is the choice of encapsulating material and the type of core material, including the specific essential oil utilized. Published studies have reported encapsulation efficiencies ranging from 0 to over 99 %. Alvarez-Henao et al. (2018) compared the encapsulation efficiency of lutein using maltodextrin, gum Arabic, and modified starch separately or in various combinations. They found that using maltodextrin and modified starch alone resulted in EE values of 6.03 % and 2.38 %, respectively. However, combining them with gum Arabic significantly increased EE, although it remained relatively low (38.82 % and 36.77 %). Additionally, microencapsulation of mandarin essential oil with gum Arabic and maltodextrin achieved an EE of up to 99.6 % (Bringas-Lantigua et al.,

2011). Other studies suggest that employing gum Arabic and maltodextrin for the microencapsulation of JEO can yield an EE of 70.07 %, lower than in studies conducted by Bringas-Lantigua et al. (2011) but higher than in our study (Bajac et al., 2022).

3.2. Bulk (BD) and tapped (TD) densities, Carr index (CI), and Hausner ratio (HR)

Bulk density was in the range of 0.11–0.17 g/cm³. The lowest value was obtained for CS2 and the highest for samples 2 S, 3 S, and 8 S. BD was significantly influenced by both pH and OP in quadratic terms increasing the BD values. Tapped density was two times higher than BD and was in the range of 0.18 – 0.28 g/cm³. TD was also influenced by both pH and OP in quadratic terms increasing its values (Table 3, Fig. 1). Upon analyzing the results, CI and HR were computed, both exceeding 20% and 1.25, respectively (Table 3, Fig. 1). These values indicate that the powders obtained exhibited significant cohesion and poor flow characteristics. This was most likely due to the fact that GA itself is characterized by CI > 30 % and HR > 35, and the formation of the coacervate network did not significantly affect the powder flow (Pudziulevityte et al., 2020).

3.3. Solubility, hygroscopicity, and moisture content

Obtained microcapsules were characterized by a good solubility in the range of 81.6–86.54 % (Table 4, Fig. 2). SOL was influenced by OP content, reducing the solubility. The water content in the samples varied from 0.07 % to 1.06 % (Table 4, Fig. 2). Notably, samples 4 S and 6 S exhibited similar MOIST values at 0.78 % and 0.71 %, respectively. Despite sharing the same coacervation pH, these samples differed in the OP/GA ratio (80:20 and 20:80, respectively). A rise in pH corresponded to an increase in the MOIST value, evident in the comparison of sample 3 S with 0.85 % water and sample 7 S with 0.91 %. This example underscores the positive influence of pH on the MOIST value. The water content directly affected sample hygroscopicity, indicated by higher MOIST values correlating with elevated HIG values (Juarez-Enriquez et al., 2017). This relationship arises from non-covalent interactions between microcapsule components and water molecules in the environment, such as hydrogen bonds or van der Waals bonds (Newman et al., 2008). Functional groups identified through FT-IR analysis (3.7), including -OH, -C=O, -COOH, or -NH₂, can electrostatically interact

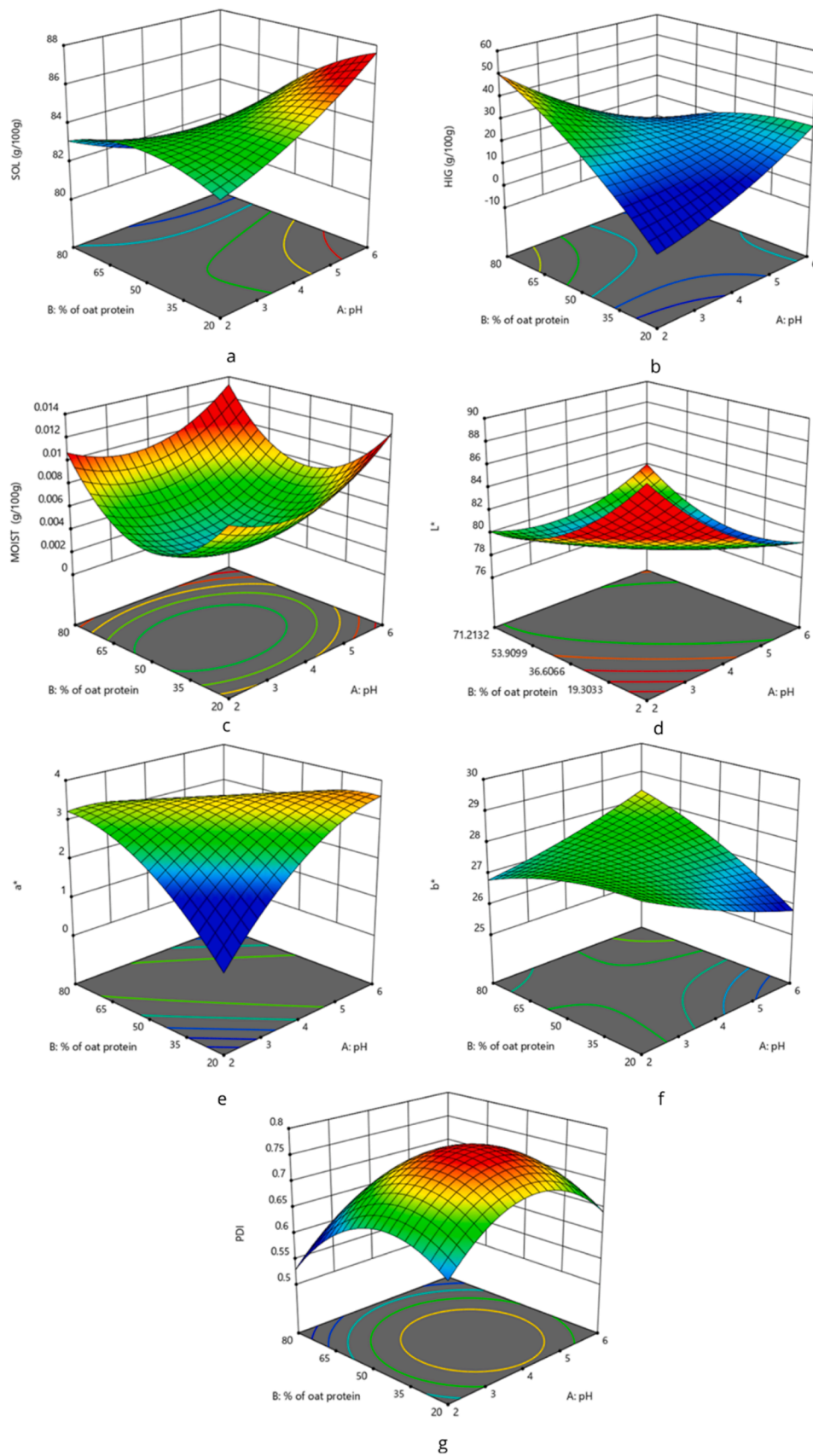


Fig. 2. : Response Surface of: (a) solubility (SOL), (b) hygroscopicity (HIG), (c) moisture content (MOIST), (d) L* parameter, (e) a* parameter, and (f) b* parameter, and (g) particle size distribution (PDI) depending on the pH (factor A) and oat protein content (factor B).

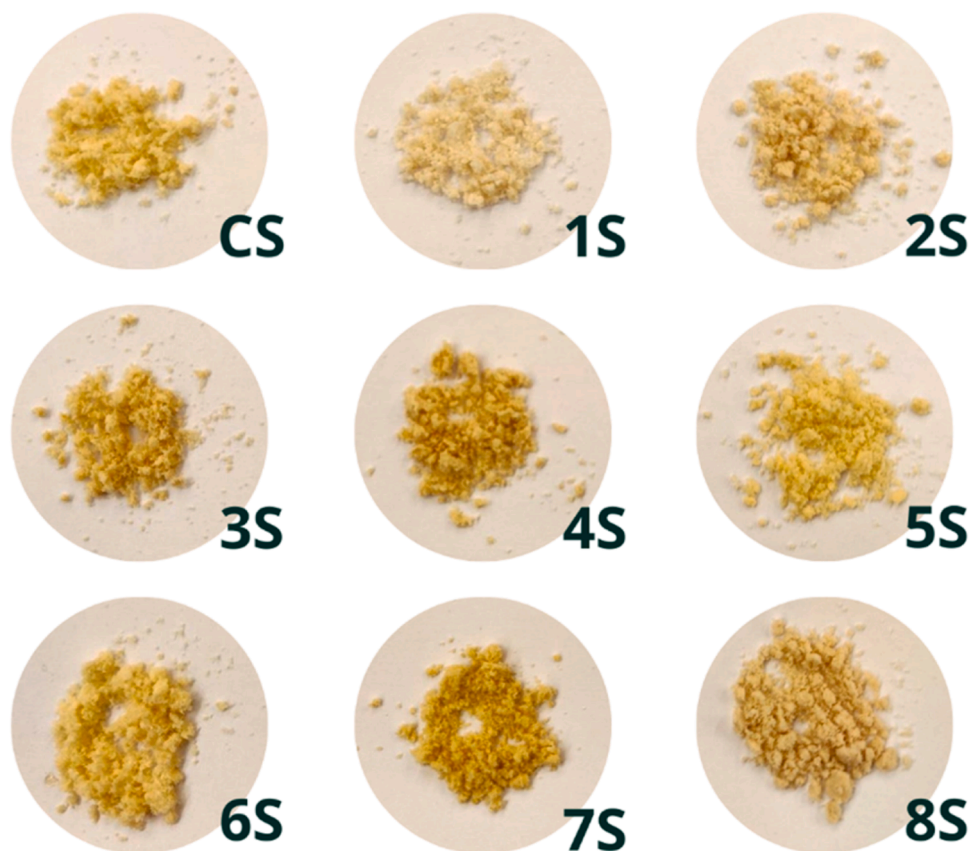


Fig. 3. : Obtained powders. The sample CS is a central point sample corresponding to the samples CS1-5.

with water molecules. Samples ²S–⁶S displayed relatively similar hygroscopicity within the range of 12.35–15.64%, while samples CS1–5, 7 S, and 8 S deviated significantly with hygroscopicity values of 22.77%, 22.49 %, 23.12 %, 23.09 %, 22.17 %, 35.26 %, 31.09 %, and 53.87 %, respectively (Table 4, Fig. 2).

3.4. Color measurement

The samples differed in color due to the different mixing ratios of GA and OP (Fig. 2, Fig. 3). The value of parameter L* ranged from 77.37 to 82.02, the value of parameter a* from 1.64 to 3.31, and the value of parameter b* from 27.04 to 29.36. However, the differences between a* and b* parameters were not statistically significant, differences between L* were influenced by the interaction between pH and OP, as well as by pH in quadratic terms (Table 4).

3.5. Particle size distribution

The PDI observed in the range of 0.60–0.77 (Table 4, Fig. 2) was primarily affected by pH and oat protein (OP) in quadratic terms. Additionally, the linear contribution of OP also played a role in reducing the PDI value. When the PDI value approaches 1.0, it signifies a broad particle size distribution with multiple populations. A PDI > 0.7 is considered to indicate a highly polydisperse sample (Danaei et al., 2018). Although not all samples exceeded this threshold, the differences observed were marginal. Therefore, it can be concluded that the obtained powders lacked homogeneity in terms of particle size.

3.6. Differential Scanning Calorimetry (DSC)

Differential Scanning Calorimetry (DSC) analysis was conducted to assess the thermal stability of the microcapsules obtained, with

Table 5
DSC analysis results for all obtained samples.

Run	Sample	T _{on} [°C]	T _{max} [°C]	T _{end} [°C]	Enthalpy [mJ]
1	CS1	56.53	114.23	155.16	-450.9
2	1 S	47.64	92.58	131.67	-451.55
3	2 S	179.20	180.15	182.37	-721.91
4	3 S	126.98	148.91	162.19	-425.14
5	4 S	176.54	177.98	183.23	-145.92
6	5 S	63.58	117.22	163.71	-605.24
7	6 S	119.98	136.21	165.78	-504.56
8	CS2	56.55	114.74	155.18	-451.94
9	CS3	56.69	115.00	154.86	-444.17
10	CS4	56.61	114.23	155.20	-450.30
11	CS5	56.51	114.23	155.60	-452.19
12	7 S	163.87	164.84	168.20	-134.17
13	8 S	147.10	148.08	148.92	-320.51

individual measurements performed for each material used in their production (Table 5, available in supplementary materials).

The oat protein exhibited an endothermic transformation commencing at 98.43 °C, characterized by T_{max}=110.27±0.01 °C, T_{end}=115.34±0.01 °C, and ΔH=-421.59±0.01 mJ. Similarly, gum Arabic displayed a glass transition starting at 137.93 °C, with T_{max}=139.98±0.01 °C, T_{end}=157.54±0.01 °C, and ΔH=-696.52±0.01 mJ.

Wheat germ oil underwent a two-step thermal process. The initial exothermic reaction, generating primary auto-oxidation products, occurred at 123.92±0.01 °C, with T_{max}=131.12±0.01 °C, T_{end}=135.87±0.01 °C, and ΔH=143.52±0.01 mJ. The subsequent reaction, involving further oxidation and decomposition of oxidation products, commenced at 158.32±0.01 °C, characterized by T_{max}=162.42±0.01 °C, T_{end}=167.34±0.01 °C, and ΔH=248.66±0.01 mJ.

Juniper essential oil exhibited similar thermal behaviors. The first

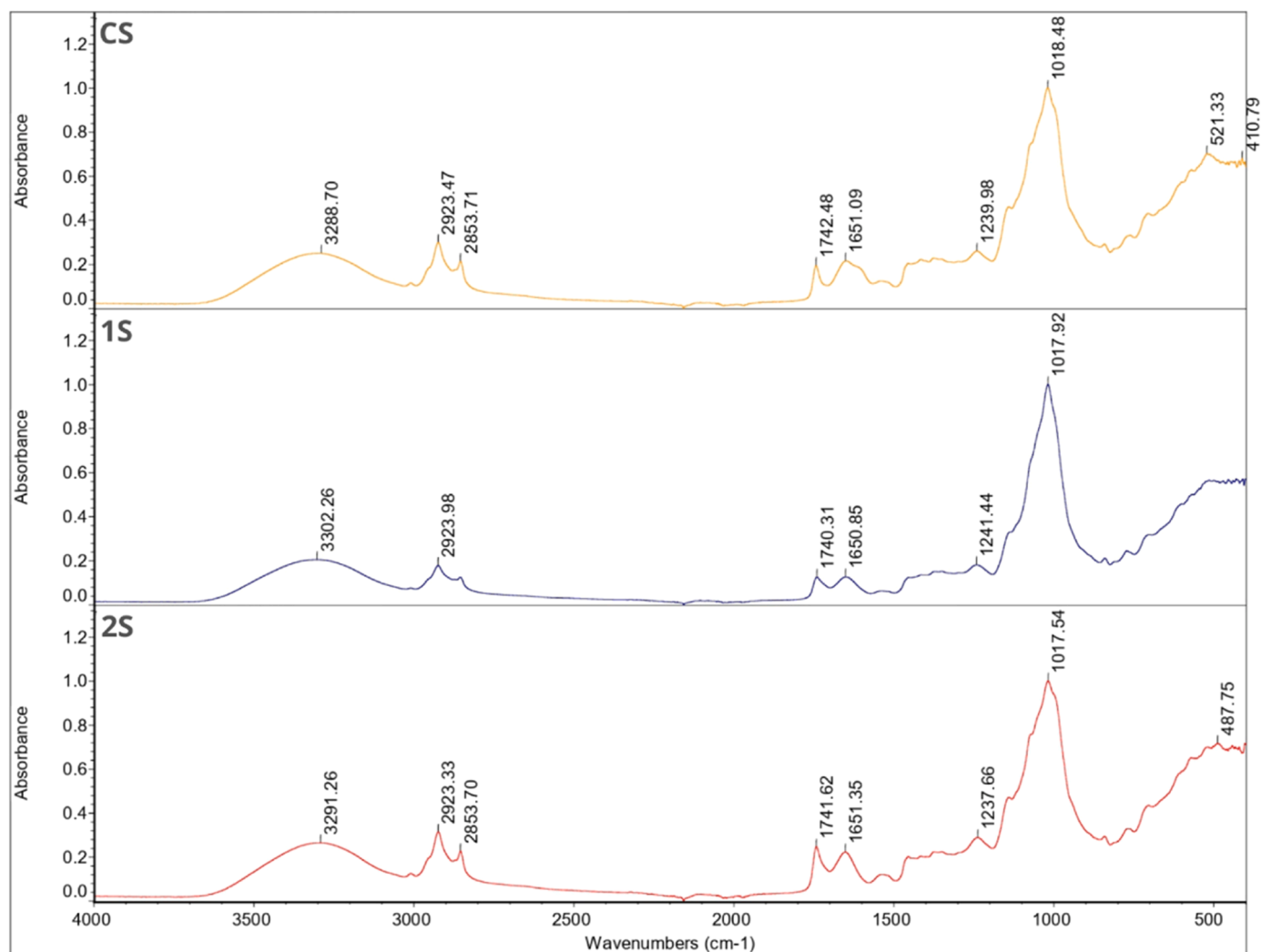


Fig. 4. : FT-IR spectra for sample CS, 1S, and 2S.

endothermic reaction initiated at 24.71 ± 0.01 °C, with $T_{\max} = 89.17 \pm 0.01$ °C, $T_{\text{end}} = 140.95 \pm 0.01$ °C, and $\Delta H = -80.00 \pm 0.01$ mJ, linked to the release of residual water. The subsequent reaction started at 150.43 ± 0.01 °C, with $T_{\max} = 152.17 \pm 0.01$ °C, $T_{\text{end}} = 161.20 \pm 0.01$ °C, and $\Delta H = -350.87 \pm 0.01$ mJ, indicating JEO decomposition.

The final ingredient scrutinized was the emulsifier, Tween 80, displaying an exothermic reaction associated with a flash point ($T_{\text{on}} = 116.40$ °C). $T_{\max} = 138.82 \pm 0.001$ °C, $T_{\text{end}} = 154.42$ °C, and $\Delta H = 58.61$ mJ characterized this reaction (data not presented).

All examined samples displayed a single endothermic reaction (Table 5, available in supplementary materials), indicating a heat absorption process during the heating phase. Notably, CS1–5, 1 S, and 5 S were identified as the most temperature-sensitive among the tested samples, featuring T_{on} temperatures of 56.51 – 56.69 °C, 47.64 °C, and 63.58 °C, respectively. An interesting observation is that samples 1 S and 5 S shared an identical OP/GA ratio (29:71) but had different pH values (2.6 and 5.4). In contrast, the remaining samples exhibited resilience to temperatures surpassing 115 °C.

Sample 2 S (OP/GA = 50:50, pH = 2) emerged as particularly noteworthy due to its superior thermal stability. The recorded parameters were $T_{\text{on}} = 179.20$ °C, $T_{\max} = 180.15$ °C, $T_{\text{end}} = 182.37$ °C, and $\Delta H = -721.91$ mJ. Notably, despite sharing an identical OP/GA ratio with the CS1–5 samples, the latter exhibited significantly lower thermal stability, with $T_{\text{on}} = 56.53$ °C. This discrepancy underscores the pronounced influence of pH, highlighting its pivotal role in shaping the properties of

the final product.

In summary, the results clearly indicate the presence of interactions among the microcapsule components, contributing to a substantial enhancement in thermal resistance compared to individual ingredients. The marked differences between samples, particularly in terms of pH, underscore the critical role of this parameter in determining the properties of the final microcapsules. This emphasizes the significance of considering pH in the design and production of microcapsules to achieve desired properties.

3.7. Fourier Transform Infrared Spectroscopy (FT-IR)

FT-IR analysis was conducted individually for each component of the acquired microcapsules, as well as for all the prepared samples collectively. In the results interpretation, the term "single bond area/region" denotes waves within the wavelength range of 2500 – 4000 cm^{-1} , the "triple bond area/region" pertains to waves falling within the range of 2000 – 2500 cm^{-1} , the "double band area/region" encompasses waves within the range of 1500 – 2000 cm^{-1} , and within the wavelength range of 1500 – 600 cm^{-1} indicates "finger print area/region".

Four distinct peaks were observed in the spectrum of gum Arabic, affirming its organic composition (data not presented). Within the single bond area, a broad absorption band detected at 3300.05 cm^{-1} suggests the presence of a hydrogen bond, specifically indicating the existence of a hydroxyl group (-OH). Furthermore, a narrow absorption band at

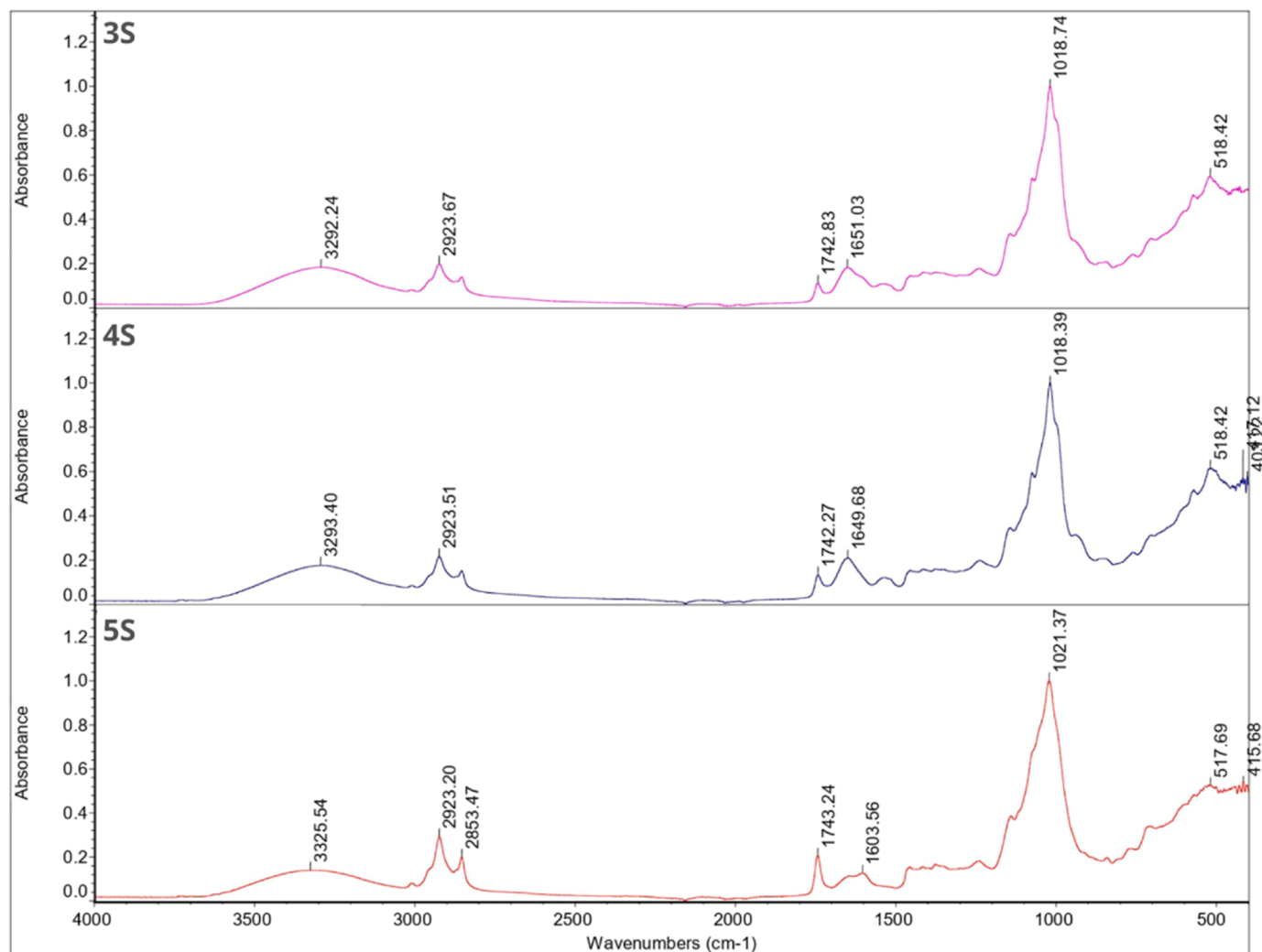


Fig. 5. : FT-IR spectra for sample 3S, 4S, and 5S.

2893.28 cm^{-1} indicates C-H stretching associated with long-chain linear aliphatic compounds, followed by a peak at 1413.05 cm^{-1} linked to -OH and -CH vibrations, as reported by [Tavares and Noreña, 2020](#). No discernible peaks were noted in the triple bond region. In the double bond region, a distinct peak at 1596.88 cm^{-1} is suggestive of carbonyl compounds (C=C). Importantly, the peaks at 1413.05 cm^{-1} and 1596.88 cm^{-1} corroborate the presence of the hydroxyl group identified in the single bond area based on studies by [Cui et al. \(2007\)](#), [Nandiyanto et al. \(2019\)](#), and [Napiórkowska et al. \(2023\)](#).

For oat protein, the analysis revealed 9 peaks, underscoring the molecular complexity of this compound (data not presented). Similar to gum Arabic, a broad absorption peak at 3289.01 cm^{-1} indicated the presence of a hydrogen bond. Peaks in the range of 1600–1300 cm^{-1} suggested hydroxyl and amino groups from amino acids. Additionally, a peak at 2923.65 cm^{-1} indicated the -CH₃ group, characteristic of methionine in oat protein. Notably, no peaks were observed in the triple bond area, while in the double bond region, peak at 1649.48 cm^{-1} hinted at the presence of a carbonyl group (C=O), often associated with carboxylic acid groups in amino acid side chains or within the protein structure itself ([Choudhary et al., 2009](#), [Nandiyanto et al. 2019](#)). Six peaks were discerned in the fingerprint region. The presence of C-N bonds, likely originating from amino groups, is suggested by the peak at a wavelength of 1147.96 cm^{-1} . Following are the peaks at 1075.75 cm^{-1} and 1018.34 cm^{-1} , indicating the presence of ester bonds. The peak at 854.76 cm^{-1} suggests the existence of C-H bonds,

characteristic of CH₃ and CH₂ groups. Additionally, the peak at 519.95 cm^{-1} points to the presence of C-S bonds, likely arising from sulfide groups characteristic of sulfur-containing amino acids (cysteine, methionine). The final identified peak at 409.53 cm^{-1} signifies the presence of C-N bonds ([Nandiyanto et al., 2019](#)).

FT-IR spectra for JEO was reported in our previous work ([Napiórkowska et al., 2023](#)). In summary, the analysis of JEO revealed distinctive peaks at 2917.56 cm^{-1} , 2878.29 cm^{-1} , and 2833.70 cm^{-1} indicating the presence of long-chain linear aliphatic compounds (C-H stretch). Additionally, a subsequent peak at 1446.07 cm^{-1} corresponds to C-OH bend. Nevertheless, the FT-IR spectrum was dominated by terpenoid components present in JEO, such as α -pinene, limonene, and myrcene ([Agatonovic-Kustrin et al. 2020](#)). Peaks observed at 1328.55 cm^{-1} , 1264.26 cm^{-1} , 1164.67 cm^{-1} , 1124.97 cm^{-1} , 1063.07 cm^{-1} , 1014.59 cm^{-1} , 952.06 cm^{-1} , 887.14 cm^{-1} , 786.52 cm^{-1} , 618.60 cm^{-1} , 456.64 cm^{-1} , and 418.96 cm^{-1} are suggestive of the presence of different aromatic rings (C-H stretch in ortho, meta and para positions) ([Bastos et al., 2019](#); [Nandiyanto et al., 2019](#)).

FT-IR analysis of wheat germ oil revealed 8 peaks (data not presented). The broad absorption band at 3279.22 cm^{-1} suggests the presence of hydrogen bonds, which is somewhat unusual for oils. However, in the case of wheat germ oil, this may be attributed to its richness in tocopherols ([Arslan et al., 2020](#)). Another peak at 2924.25 cm^{-1} in the single bond area indicates the existence of CH₃ and CH₂ groups. No spectrum was identified in the triple bond area.

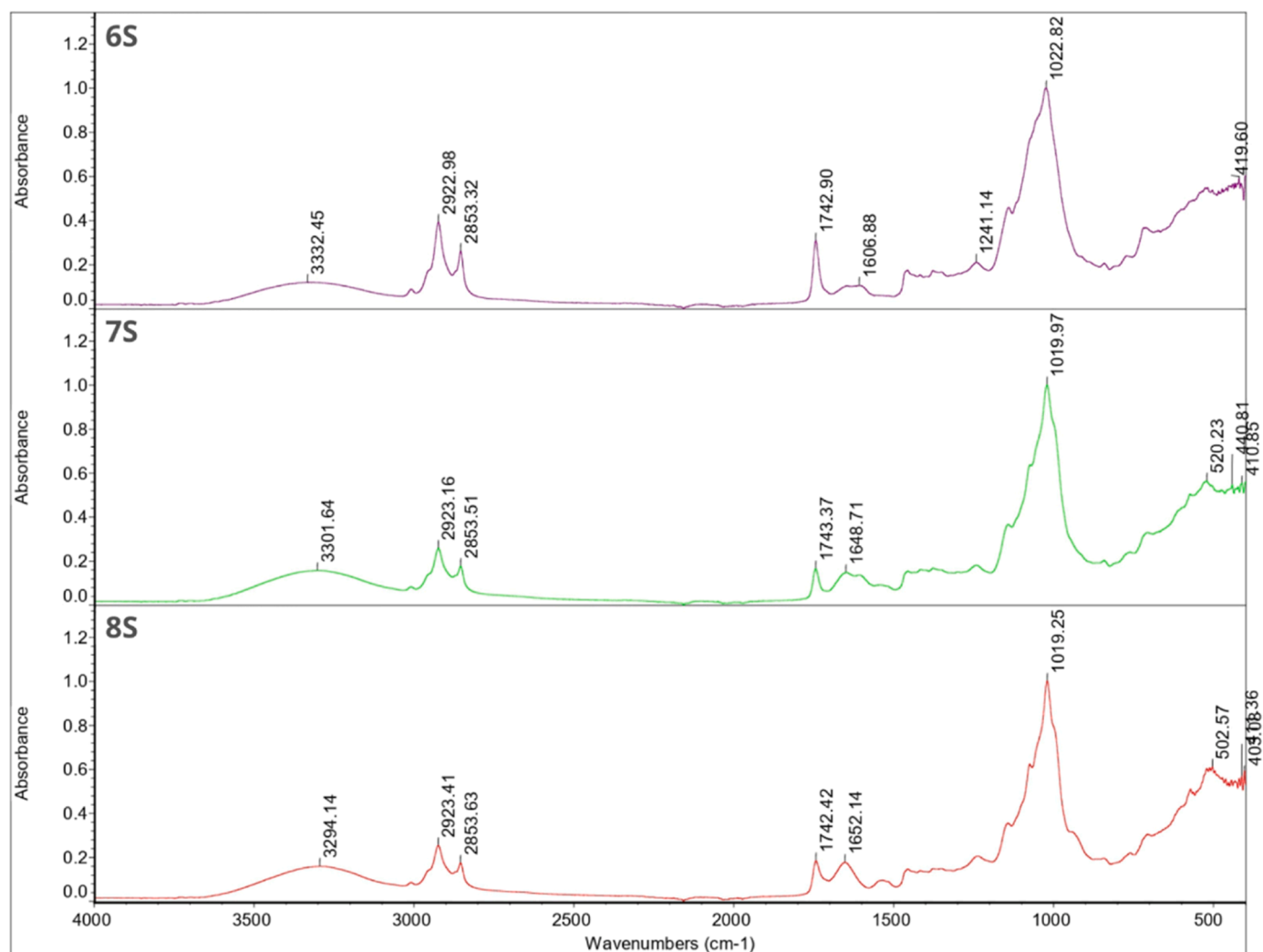


Fig. 6. : FT-IR spectra for sample 6S, 7S, and 8S.

Successive peaks at 1649.11 cm^{-1} and 1148.11 cm^{-1} imply the presence of C=O and C-O-C bonds, characteristic of oils and associated with ester bonds. The remaining peaks in the fingerprint region (1075.78 cm^{-1} , 523.95 cm^{-1} , 442.00 cm^{-1}) indicate the presence of the -CH group, confirming the unsaturated nature of wheat germ oil (Nandiyanto et al., 2019).

The investigation into the Tween 80 emulsifier, as we reported before (Napiórkowska et al., 2023) revealed ten distinctive peaks. The initial peak observed at 2855.75 cm^{-1} could indicate the C-H bend. Its narrow appearance, along with the identification of peaks in the $1470\text{--}720\text{ cm}^{-1}$ range, suggests alignment with long-chain linear aliphatic compounds and -OH bend, consistent with the recognized chemical structure of Tween 80. The subsequent peak at 1734.71 cm^{-1} might correspond to aromatic bands. No indications of triple bonds were noted. The majority of peaks were located in the fingerprint region (1456.94 cm^{-1} , 1348.54 cm^{-1} , 1296.36 cm^{-1} , 1247.46 cm^{-1} , 1096.21 cm^{-1} , 946.67 cm^{-1} , 846.64 cm^{-1} , and 510.58 cm^{-1}), confirming the presence of aromatic rings and double bonds (data not presented) (Nair et al., 2003; Nandiyanto et al., 2019; Pramod et al., 2015).

The Figs. 4–6 shows the FT-IR analysis of microcapsules. Due to the identification of peaks in the same places, the central samples are presented as one curve (CS1–5, Fig. 4). Regarding the number of peaks, there are more than five peaks in every curve, informing that the analyzed samples are not simple chemicals. For all samples, a peak

within the range of $3288.70\text{--}3332.45\text{ cm}^{-1}$, with varying intensity, was detected. The peak's height was influenced by the OP/GA ratio and pH, signifying interactions during complex coacervation. Two subsequent peaks within the ranges of $2922.98\text{--}2923.98\text{ cm}^{-1}$ and $2853.32\text{--}2853.71\text{ cm}^{-1}$ (except for samples 1 S, 3 S, 4 S) were attributed to the presence of OP, GA, and WGO. These peaks exhibited greater intensity than those in individual components, suggesting interaction with JEO, which also displayed peaks in a similar wavelength range. Across all microcapsules, a peak in the range of $1740.31\text{--}1743.37\text{ cm}^{-1}$ was consistently observed, not identifiable in individual components, further confirming chemical interactions between ingredients, indicating the generation of some new chemical bonds (Yang et al., 2014). The subsequent peak (unidentified in samples 5 S and 6 S) within the range of $1648.71\text{--}1652.14\text{ cm}^{-1}$ corresponds to peaks found in OP and WGO. Conversely, samples 5 S and 6 S exhibited peaks at 1603.56 cm^{-1} and 1606.88 cm^{-1} , respectively. The peak shift indicates interactions among the microcapsule components. Despite similar OP/GA ratios in samples 5 S and 6 S (29:71 and 20:80, respectively), the varying pH levels (5.4 and 4) resulted in distinctive peak positions. Additionally, in samples CS1–5, 1 S, 2 S, and 6 S, peaks of varying intensities were identified in the range of $1237.66\text{--}1241.44\text{ cm}^{-1}$, corresponding to aromatic rings present in JEO. A consistent peak within the range of $1017.54\text{--}1022.82\text{ cm}^{-1}$ was observed in all microcapsules, signifying the presence of OP and WGO. The remaining peaks in the sample spectrum align with the presence of JEO, affirming the effective

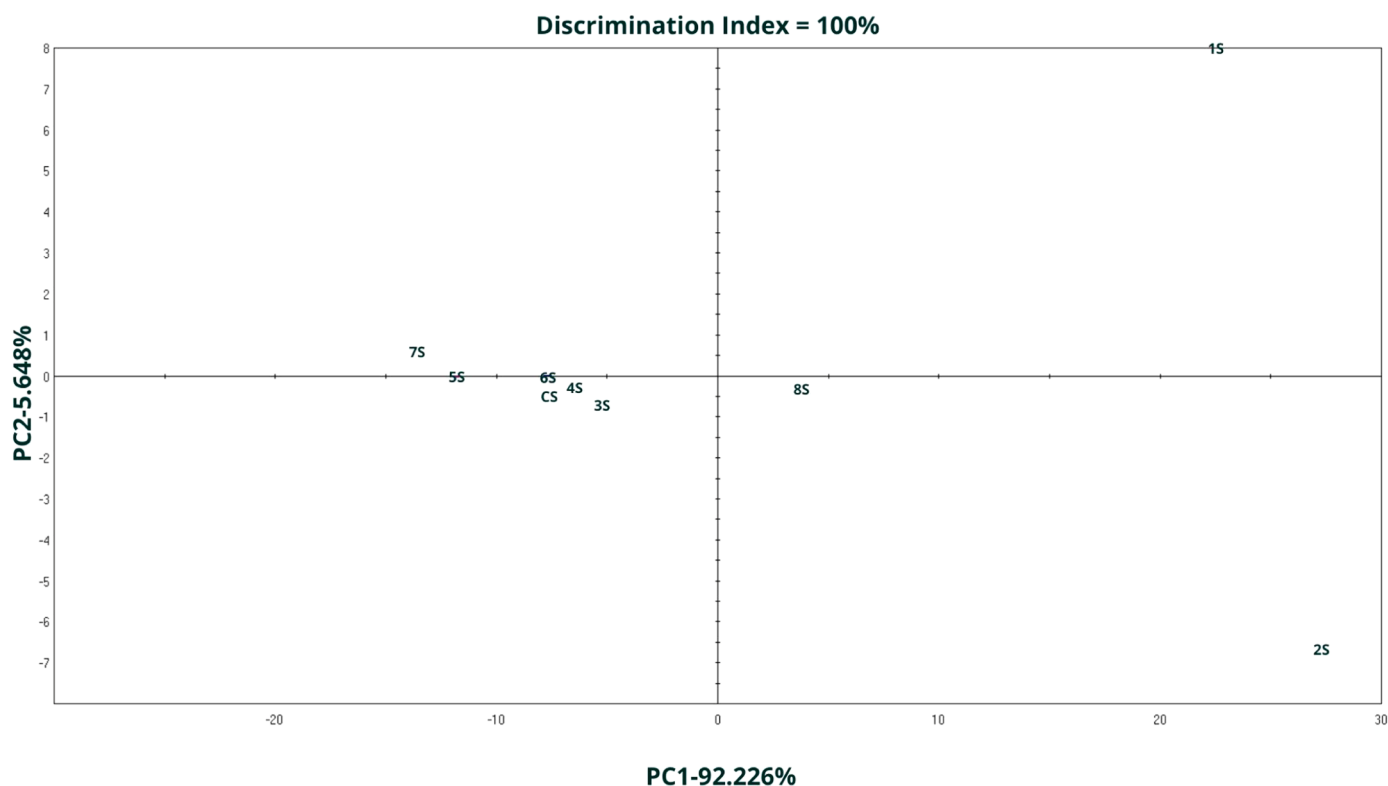


Fig. 7. : Principal Component Analysis (PCA) of all samples.

encapsulation of essential oil within the microcapsule structure (Yang et al., 2014). FT-IR spectra showed that both chemical and physical interactions occurred between the components of the microcapsules (Nandiyanto et al., 2019).

3.8. Smell pattern – e-nose analysis

The Fig. 7 presents the classification of scent profiles in relation to their experimental groups. Samples are represented in a two-dimensional plane with reference to selected components: principal component 1 (PC1) and principal component 2 (PC2). The total contribution variances of PC1 and PC2 for direct electronic nose measurements were 92.226 % and 5.64 % respectively. Differentiation index (DI) was 100 % and the position of different samples was far, indicating that the electronic nose could determine the difference among the samples clearly. There is no overlap area, which means that the difference among these samples was significant.

An interesting observation is that samples 1 S, 2 S, and 8 S deviate from the rest of the samples by appearing on the right side of the graph. A shared characteristic among these samples is the utilization of relatively low pH levels during coacervation: samples 1 S and 8 S were at pH=2.6, while sample 2 S was at pH=2. This observation underscores the substantial influence of pH on the properties of the resulting microcapsules, particularly on shaping the sensory attributes of microcapsules containing essential oils. This influence could be attributed to potential chemical reactions occurring between the components of essential oils and hydrogen ions. Juniper essential oil predominantly comprises α -pinene, limonene, and myrcene, categorized as terpene compounds (Hojjati et al., 2019; Ghorbanzadeh et al., 2021). These compounds are known to react in an acidic environment, particularly with hydrogen ions, leading to the formation of terpenoid-derived products (Li et al., 2010; Liu et al. 2008), which significantly influence the odor profile.

Table 6

Comparison of selected parameters of optimized microcapsules using predicted and experimental values for optimized pH and oat protein content for complex coacervation process.

	Predicted values	Experimental values
EE [%]	25.69	26.61
SOL [%]	83.62	83.64
PDI	0.68	0.66

3.9. Optimization of coacervates production

The optimization of encapsulation efficiency (EE), solubility (SOL), and polydispersity index (PDI) parameters was conducted through multiple response optimization. The culmination of this optimization process indicated that the optimal pH should be set at 2.59, with oat protein content at 61.61%. Subsequently, microcapsules were produced based on the model-derived conditions. Remarkably, the conditions obtained from the model were successfully utilized to produce microcapsules, and upon analysis, these conditions were found to not exhibit statistically significant differences in the measured variables compared to those predicted (Table 6).

4. Conclusion

The utilization of oat protein alongside gum Arabic as microcapsule wall materials primarily ensures their commendable thermal stability, a crucial attribute for encapsulating substances like essential oils. FT-IR analysis revealed that the interactions between oat protein and gum Arabic during complex coacervation involved both chemical and physical bonding, which contributed to the improvement of thermal stability of the complexes compared to the individual components. The research results indicate that the combination of OP with GA can be successfully utilized for stabilizing EO and protecting them from the external environment. Obtained microcapsules exhibited favorable solubility

(>80%), potentially broadening their applicability in the food industry. Nonetheless, the encapsulation efficiency in the study was found to be low, not exceeding 27%. This could be attributed to both the choice of wall materials (gum Arabic, oat protein) and their mixing ratio, as well as the pH employed during the process. Further optimization of these parameters may be necessary to enhance the encapsulation efficiency and overall effectiveness of the microencapsulation process.

While complex coacervation is relatively well-known, its application for microencapsulation of essential oils remains rare or poorly documented in the literature. The innovative aspect of our study lies in utilizing oat protein as an encapsulating material within complex coacervation, a research area that has yet to be extensively explored. By delving into the potential of oat protein for microencapsulation of essential oils, our study enters a new research frontier, paving the way for novel advancements in this field.

CRedit authorship contribution statement

Marcin Andrzej Kurek: Investigation, Methodology, Supervision, Writing – review & editing. **Elżbieta Górka-Horczyzak:** Investigation, Methodology. **Arkadiusz Szpiczer:** Investigation, Methodology. **Havva Aktaş:** Formal analysis, Investigation. **Alicja Napiórkowska:** Conceptualization, Data curation, Formal analysis, Investigation, Methodology, Writing – original draft.

Declaration of Competing Interest

The authors declare that they have no known competing financial interests or personal relationships that could have appeared to influence the work reported in this paper.

References

- Agatonovic-Kustrin, S., Ristivojevic, P., Gegeckhori, V., Litvinova, T.M., Morton, W.D., 2020. Essential oil quality and purity evaluation via FT-IR spectroscopy and pattern recognition techniques. *Appl. Sci.* 10 (20), 7294. <https://doi.org/10.3390/app10207294>.
- Alvarez-Henao, M.V., Saavedra, N., Medina, S., Jiménez Cartagena, C., Alzate, L.M., Londoño-Londoño, J., 2018. Microencapsulation of lutein by spray-drying: characterization and stability analyses to promote its use as a functional ingredient. *Food Chem.* 256, 181–187. <https://doi.org/10.1016/j.foodchem.2018.02.059>.
- Amalraj, A., Jude, S., Sukumaran, N.P., Gopi, S., 2019. Nanomaterials in nutraceutical and phytonutrient industries. *Ind. Appl. Nanomater.* 441–474. <https://doi.org/10.1016/b978-0-12-815749-7.00016-5>.
- Arslan, D., Demir, M.K., Acar, A., Arslan, F.N., 2020. Investigation of wheat germ and oil characteristics with regard to different stabilization techniques. *Food Technol. Biotechnol.* 58 (3), 348–355. <https://doi.org/10.17113/ftb.58.03.20.6638>. PMID: 33281490; PMCID: PMC7709457.
- Bajac, J., Nikolovski, B., Loncarević, I., Petrović, J., Bajac, B., Đurović, S., Petrović, L., 2022. Microencapsulation of juniper berry essential oil (*Juniperus communis* L.) by spray drying: microcapsule characterization and release kinetics of the oil. *Food Hydrocoll.*
- Boukid, F., 2021. Oat proteins as emerging ingredients for food formulation: where we stand? *Eur. Food Res Technol.* 247, 535–544. <https://doi.org/10.1007/s00217-020-03661-2>.
- Bringas-Lantigua, M., Expósito Molina, I., Reineccius, G.A., López-Hernández, O., Pino, J.A., 2011. Influence of spray-dryer air temperatures on encapsulated mandarin oil. *Dry. Technol.* 29 (5), 520–526. <https://doi.org/10.1080/07373937.2010.513780>.
- Brückner-Gühmann, M., Benthin, A., Drusch, S., 2019. Enrichment of yoghurt with oat protein fractions: structure formation, textural properties and sensory evaluation. *Food Hydrocoll.* 86, 146–153. <https://doi.org/10.1016/j.foodhyd.2018.03.019>.
- Chang, Y.-W., Alli, I., Konishi, Y., Ziomek, E., 2011. Characterization of protein fractions from chickpea (*Cicer arietinum* L.) and oat (*Avena sativa* L.) seeds using proteomic techniques. *Food Res. Int.* 44 (9), 3094–3104. <https://doi.org/10.1016/j.foodres.2011.08.001>.
- Choudhary, A., Gandla, D., Krow, G.R., Raines, R.T., 2009. *J. Am. Chem. Soc.* 131 (21), 7244–7246. <https://doi.org/10.1021/ja901188y>.
- Cui, S.W., Phillips, G.O., Blackwell, B., Nikiforuk, J., 2007. Characterisation and properties of *Acacia senegal* (L.) Willd. var. *senegal* with enhanced properties (*Acacia* (sen) SUPERGUM™): part 4. Spectroscopic characterisation of *Acacia senegal* var. *senegal* and *Acacia* (sen) SUPERGUM™ arabic. *Food Hydrocoll.* 21 (3), 347–352. <https://doi.org/10.1016/j.foodhyd.2006.05.009>.
- Danaei, M., Dehghankhold, M., Ataei, S., Hasanzadeh Davarani, F., Javanmard, R., Dokhani, A., Mozafari, M.R., 2018. Impact of particle size and polydispersity index on the clinical applications of lipidic nanocarrier systems. *Pharmaceutics* 10 (2), 57. <https://doi.org/10.3390/pharmaceutics10020057>.
- De Melo Ramos, F., Silveira Júnior, V., Prata, A.S., 2019. Assessing the vacuum spray drying effects on the properties of orange essential oil microparticles. *Food Bioprocess Technol.* 12 (11), 1917–1927. <https://doi.org/10.1007/s11947-019-02355-2>.
- Feng, X., Liu, J., Zhang, Y., Wu, W., Pan, Y., Wang, D., et al., 2020. Podophyllotoxin profiles combined with SRAP molecular markers in *Juniperus rigida*: A promising alternative source of podophyllotoxin. *Ind. Crops Prod.* 153, 112547. <https://doi.org/10.1016/j.indcrop.2020.112547>.
- Fernandes, R.V. d B., Borges, S.V., Botrel, D.A., Oliveira, C., 2014. Physical and chemical properties of encapsulated rosemary essential oil by spray drying using whey protein–inulin blends as carriers. *Int. J. Food Sci.* 49, 1–8.
- Ghorbanzadeh, A., Ghasemnezhad, A., Sarmast, M.K., Ebrahimi, S.N., 2021. An analysis of variations in morphological characteristics, essential oil content, and genetic sequencing among and within major Iranian Juniper (*Juniperus* spp.) populations. *Phytochem* 186, 1–10.
- Hojjati, F., Serešhti, H., Hojjati, M., 2019. Leaf essential oils and their application in systematics of *Juniperus excelsa* complex in Iran. *Biochem. Syst. Ecol.* 84, 29–34.
- Jing, X., Yang, C., Zhang, L., 2016. Characterization and analysis of protein structures in oat bran. *J. Food Sci.* 81 (10), C2337–C2343. <https://doi.org/10.1111/1750-3841.13445>.
- Juarez-Enriquez, E., Olivas, G.I., Zamudio-Flores, P.B., Ortega-Rivas, E., Perez-Vega, S., Sepulveda, D.R., 2017. Effect of water content on the flowability of hygroscopic powders. *J. Food Eng.* 205, 12–17. <https://doi.org/10.1016/j.jfoodeng.2017.02.020>.
- Kalaba, V., Marjanović-Balaban, Ž., Kalaba, D., Lazić, D., Cvjetković, V.G., 2020. Antibacterial activity of essential oil of *Juniperus communis* L. *Qual. Life (Banja Luka)*-Apeiron 18 (1-2). <https://doi.org/10.7251/QOL2001018K>.
- Kumar, L., Sehrawat, R., Kong, Y., 2021. Oat proteins: a perspective on functional properties. *LWT* 152, 112307. <https://doi.org/10.1016/j.lwt.2021.112307>.
- Kurek, M., Wyrwiz, J., Piwińska, M., Wierzbicka, A., 2016. Application of the response surface methodology in optimizing oat fiber particle size and flour replacement in wheat bread rolls. *CyTA - J. Food* 14 (1), 18–26. <https://doi.org/10.1080/19476337.2015.1036309>.
- Li, Y.J., Cheong, G.Y.L., Lau, A.P.S., Chan, C.K., 2010. Acid-catalyzed condensed-phase reactions of limonene and terpineol and their impacts on gas-to-particle partitioning in the formation of organic aerosols. *Environ. Sci. Technol.* 44 (14), 5483–5489. <https://doi.org/10.1021/es101231m>.
- Liu, S.-W., Yu, S.-T., Liu, F.-S., Xie, C.-X., Li, L., Ji, K.-H., 2008. Reactions of α -pinene using acidic ionic liquids as catalysts. *J. Mol. Catal. A: Chem.* 279 (2), 177–181. <https://doi.org/10.1016/j.molcata.2007.06.026>.
- Mäkinen, O.E., Sozer, N., Ercili-Cura, D., Poutanen, K., 2017. Protein from oat: structure, processes, functionality, and nutrition. *Sustainable protein sources*. Academic Press, pp. 105–119.
- Mu, H., Song, Z., Wang, X., Wang, D., Zheng, X., Li, X., 2022. Microencapsulation of algae oil by complex coacervation of chitosan and modified starch: characterization and oxidative stability. *Int. J. Biol. Macromol.* 194, 66–73. <https://doi.org/10.1016/j.jbiomac.2021.11.168>.
- Naderi, B., Keramat, J., Nasirpour, A., Aminifar, M., 2020. Complex coacervation between oak protein isolate and gum Arabic: optimization & functional characterization. *Int. J. Food Prop.* 23 (1), 1854–1873. <https://doi.org/10.1080/10942912.2020.1825484>.
- Nair, L.M., Stephens, N.V., Vincent, S., Raghavan, N., Sand, P.J., 2003. Determination of polysorbate 80 in parenteral formulations by high-performance liquid chromatography and evaporative light scattering detection. *J. Chromatogr. A* 1012 (1), 81–86. [https://doi.org/10.1016/s0021-9673\(03\)01105-1](https://doi.org/10.1016/s0021-9673(03)01105-1).
- Napiórkowska, A., Kurek, M., 2022. Coacervation as a Novel Method of Microencapsulation of Essential Oils—A Review. *Molecules* 27, 5142. <https://doi.org/10.3390/molecules27165142>.
- Napiórkowska, A., Szpiczer, A., Wojtasik-Kalinowska, I., Perez, M.D.T., González, H.D., Kurek, M.A., 2023. Microencapsulation of Juniper and Black Pepper Essential Oil Using the Coacervation Method and Its Properties after Freeze-Drying. *Foods* 12 (23), 4345. <https://doi.org/10.3390/foods12234345>.
- Newman, A.W., Reutzel-Edens, S.M., Zograf, G., 2008. Characterization of the "hygroscopic" properties of active pharmaceutical ingredients. *J. Pharm. Sci.* 97 (3), 1047–1059. <https://doi.org/10.1002/jps.21033>.
- Nieto Nieto, T.V., Wang, Y., Ozimek, L., Chen, L., 2016. Improved thermal gelation of oat protein with the formation of controlled phase-separated networks using dextrin and carrageenan polysaccharides. *Food Res. Int.* 82, 95–103.
- Nieto-Nieto, T.V., Wang, Y.X., Ozimek, L., Chen, L., 2015. Inulin at low concentrations significantly improves the gelling properties of oat protein – a molecular mechanism study. *Food Hydrocoll.* 50, 116–127.
- Otálora, M.C., Wilches-Torres, A., Gómez Castaño, J.A., 2023. Spray-drying microencapsulation of andean blueberry (*Vaccinium meridionale* sw.) anthocyanins using prickly pear (*Opuntia ficus indica* L.) peel mucilage or gum arabic: a comparative study. *Foods* 12, 1811. <https://doi.org/10.3390/foods12091811>.
- Pramod, K., Suneesh, C.V., Shanavas, S., Ansari, S.H., Ali, J., 2015. Unveiling the compatibility of eugenol with formulation excipients by systematic drug-excipient compatibility studies. *J. Anal. Sci. Technol.* 6 (1), 1–14. <https://doi.org/10.1186/s40543-015-0046-2>.
- Pudziuleyte, L., Marksa, M., Sosnowska, K., Winnicka, K., Morkuniene, R., Bernatoniene, J., 2020. Freeze-drying technique for microencapsulation of elsholtzia ciliata ethanolic extract using different coating materials. *Molecules* 25 (9), 2237. <https://doi.org/10.3390/molecules25092237>.
- Siddiqi, R.A., Singh, T.P., Rani, M., Sogi, D.S., Bhat, M.A., 2020. Diversity in grain, flour, amino acid composition, protein profiling, and proportion of total flour proteins of different wheat cultivars of North India. *Front. Nutr.* 7 (September) <https://doi.org/10.3389/fnut.2020.00141>.

- Sterna, V., Zute, S., Brunava, L., 2016. Oat grain composition and its nutrition benefice. *Agric. Agric. Sci. Procedia* 8, 252–256. <https://doi.org/10.1016/j.aaspro.2016.02.100>.
- Tavares, L., Noreña, C.P.Z., 2020. Encapsulation of ginger essential oil using complex coacervation method: coacervate formation, rheological property, and physicochemical characterization. *Food Bioprocess Technol.* <https://doi.org/10.1007/s11947-020-02480-3>.
- Verri, W.A., Vicentini, F.T.M.C., Baracat, M.M., Georgetti, S.R., Cardoso, R.D.R., Cunha, T.M., Casagrande, R., 2012. Flavonoids as anti-inflammatory and analgesic drugs: mechanisms of action and perspectives in the development of pharmaceutical forms. *Stud. Nat. Prod. Chem.* 297–330. <https://doi.org/10.1016/b978-0-444-53836-9.00026-8>.
- Wu, Y.X., Zhang, Y.D., Li, N., Wu, D.D., Li, Q.M., Chen, Y.Z., Yang, J., 2022. Inhibitory effect and mechanism of action of juniper essential oil on gray mold in cherry tomatoes. *Front. Microbiol.* 13, 1000526 <https://doi.org/10.3389/fmicb.2022.1000526>.
- Xin, X., Essien, S., Dell, K., Woo, M.W., Baroutian, S., 2022. Effects of spray-drying and freeze-drying on bioactive and volatile compounds of smoke powder food flavouring. *Food Bioprocess Technol.* 15, 785–794.
- Yang, Z., Peng, Z., Li, J., Li, S., Kong, L., Li, P., Wang, Q., 2014. Development and evaluation of novel flavour microcapsules containing vanilla oil using complex coacervation approach. *Food Chem.* 145, 272–277. <https://doi.org/10.1016/j.foodchem.2013.08.074>.
- Zheljazkov, V.D., Semerdjieva, I.B., Dincheva, I., Kacaniova, M., Astatkie, T., Radoukova, T., et al., 2017. Antimicrobial and antioxidant activity of Juniper galbuli essential oil constituents eluted at different times. *Ind. Crops Prod.* 109, 529–537. <https://doi.org/10.1016/j.indcrop.2017.08.057>.

Warszawa, 8/10/2024

Alicja Kizildag
alicjakizildag@gmail.com

**Rada Dyscypliny Technologia
Żywności i Żywnienia
Szkoły Głównej Gospodarstwa
Wiejskiego w Warszawie**

Oświadczenie o współautorstwie

Niniejszym oświadczam, że w pracy: *Napiórkowska A, Aktaş A, Szpicer A, Górska-Horzyczak E, Kurek MA. Optimization of oat protein and gum Arabic microcapsules containing juniper essential oil using Response Surface Methodology, Food and Bioprocess Technology, 2024, 145,203-216* mój indywidualny udział w jej powstaniu polegał na opracowaniu metodyki badań, wykonaniu części badawczej, przygotowaniu treści manuskryptu oraz jego korekcie po procesie recenzji.

Podpis



Warszawa, 8/10/2024

Havva Aktas
havva_aktas@sggw.edu.pl

**Rada Dyscypliny Technologia
Żywności i Żywienia
Szkoły Głównej Gospodarstwa
Wiejskiego w Warszawie**

Oświadczenie o współautorstwie

Niniejszym oświadczam, że w pracy: *Napiórkowska A, Aktas A, Szpicer A, Górską-Horzyczak E, Kurek MA. Optimization of oat protein and gum Arabic microcapsules containing juniper essential oil using Response Surface Methodology, Food and Bioprocess Technology, 2024, 145, 203-216* mój indywidualny udział w jej powstaniu polegał na wykonaniu części badawczej w zakresie przygotowania emulsji i koacerwatów.

Podpis



Warszawa, 8/10/2024

Arkadiusz Szpicer
arkadiusz_szpicer@sggw.edu.pl

**Rada Dyscypliny Technologia
Żywności i Żywienia
Szkoly Głównej Gospodarstwa
Wiejskiego w Warszawie**

Oświadczenie o współautorstwie

Niniejszym oświadczam, że w pracy: *Napiórkowska A, Aktaś A, Szpicer A, Górska-Horczyzak E, Kurek MA. Optimization of oat protein and gum Arabic microcapsules containing juniper essential oil using Response Surface Methodology, Food and Bioprocess Technology, 2024, 145,203-216* mój indywidualny udział w jej powstaniu polegał na wykonaniu analizy Skaningowej Kalorymetrii Różnicowej, opracowaniu wyników oraz ostatecznej korekcie treści manuskryptu w tym zakresie.

Podpis



Warszawa, 8/10/2024

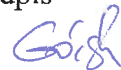
Elżbieta Górską-Horczyzak
elzbieta_gorska-horczyzak@sggw.edu.pl

**Rada Dyscypliny Technologia
Żywności i Żywnienia
Szkoły Głównej Gospodarstwa
Wiejskiego w Warszawie**

Oświadczenie o współautorstwie

Niniejszym oświadczam, że w pracy: *Napiórkowska A, Aktaş A, Szpicer A, Górską-Horczyzak E, Kurek MA. Optimization of oat protein and gum Arabic microcapsules containing juniper essential oil using Response Surface Methodology, Food and Bioproducts Processing, 2024, 145,203-216* mój indywidualny udział w jej powstaniu polegał na przeprowadzeniu analizy ultra-szybkiej chromatografii gazowej „c-nos” oraz ostatecznej korekcie tekstu manuskryptu w tym zakresie.

Podpis



Warszawa, 8/10/2024

Marcin Andrzej Kurek
marcin_kurek@sggw.edu.pl

**Rada Dyscypliny Technologia
Żywności i Żywnienia
Szkoły Głównej Gospodarstwa
Wiejskiego w Warszawie**

Oświadczenie o współautorstwie

Niniejszym oświadczam, że w pracy: *Napiórkowska A, Aktaş A, Szpicer A, Górska-Horzyczak E, Kurek MA. Optimization of oat protein and gum Arabic microcapsules containing juniper essential oil using Response Surface Methodology, Food and Bioprocess Technology, 2024, 145,203-216* mój indywidualny udział w jej powstaniu polegał na nadzorze nad realizacją badań, ocenie zastosowanych metod, konsultacjach merytorycznych oraz wsparciu w analizie wyników i redagowaniu wybranych części publikacji.

Podpis



Article

Microencapsulation of Essential Oils Using Faba Bean Protein and Chia Seed Polysaccharides via Complex Coacervation Method

Alicja Napiórkowska , Arkadiusz Szpicer , Elżbieta Górńska-Horczyzak  and Marcin Andrzej Kurek 

Department of Technique and Food Development, Warsaw University of Life Sciences, 02-787 Warsaw, Poland; arkadiusz_szpicer@sggw.edu.pl (A.S.)

* Correspondence: alicja_napiorkowska@sggw.edu.pl (A.N.); marcin_kurek@sggw.edu.pl (M.A.K.); Tel.: +48-225937078 (M.A.K.)

Abstract: The aim of this study was to develop microcapsules containing juniper or black pepper essential oils, using a combination of faba bean protein and chia seed polysaccharides (in ratios of 1:1, 1:2, 2:1). By synergizing these two polymers, our goal was to enhance the efficiency of essential oil microencapsulation, opening up various applications in the food industry. Additionally, we aimed to investigate the influence of different polymer mixing ratios on the properties of the resulting microcapsules and the course of the complex coacervation process. To dissolve the essential oils and limit their evaporation, soybean and rapeseed oils were used. The powders resulting from the freeze-drying of coacervates underwent testing to assess microencapsulation efficiency (65.64–87.85%), density, flowability, water content, solubility, and hygroscopicity. Additionally, FT-IR and DSC analyses were conducted. FT-IR analysis confirmed the interactions between the components of the microcapsules, and these interactions were reflected in their high thermal resistance, especially at a protein-to-polysaccharide ratio of 2:1 (177.2 °C). The water content in the obtained powders was low (3.72–7.65%), but it contributed to their hygroscopicity (40.40–76.98%).

Keywords: essential oil; faba bean; chia mucilage; complex coacervation

Citation: Napiórkowska, A.; Szpicer, A.; Górńska-Horczyzak, E.; Kurek, M.A. Microencapsulation of Essential Oils Using Faba Bean Protein and Chia Seed Polysaccharides via Complex Coacervation Method. *Molecules* **2024**, *29*, 2019. <https://doi.org/10.3390/molecules29092019>

Academic Editors: Natasa Poklar Ulrih and Ilja Gasan Osojnik Črnivec

Received: 27 March 2024

Revised: 19 April 2024

Accepted: 23 April 2024

Published: 27 April 2024



Copyright: © 2024 by the authors. Licensee MDPI, Basel, Switzerland. This article is an open access article distributed under the terms and conditions of the Creative Commons Attribution (CC BY) license (<https://creativecommons.org/licenses/by/4.0/>).

1. Introduction

Complex coacervation is a method of creating microcapsules in which a homogeneous colloidal solution of protein and polysaccharide is utilized to form a shell around active substances. This process occurs below the isoelectric point characteristic of the given protein. Under such pH conditions, the protein is positively charged, while the polysaccharides remain negatively charged, leading to molecular associative phase separation into coacervate and supernatant phases [1,2]. Various types of proteins are used in the process of complex coacervation, most commonly gelatin [3,4], milk proteins [5,6], soy protein [7,8], or pea protein [9,10]. However, broad bean protein is less popular. To our knowledge, no attempt has been made to use this protein in complex coacervation so far.

Broad beans (*Vicia faba* var. major), also referred to as vetch broad beans, faba beans, or fava beans, are an annual legume plant belonging to the *Fabaceae* family [11]. The popularity of this plant is on the rise, largely due to its high protein content in the seeds, approximately 32.2% [12], and even higher protein content in isolates, approximately 71.6% [13]. Faba bean protein exhibits good solubility in water and the ability to form stable emulsions [14]. Moreover, a broad bean protein isolate requires the lowest concentration to form a gel when compared to other plant-based proteins [15]. These attributes position it as a promising wall material in microcapsules produced through complex coacervation. Additionally, chia seed (*Salvia hispanica* L., *Lamiaceae* family) polysaccharides have emerged as another key component in complex coacervation. Mucus extracted from chia seeds is a complex anionic heteropolysaccharide resulting from the contact of the seeds with water. Even in low concentrations, this mucus increases the viscosity of the solution and has thickening,

emulsifying, or stabilizing properties [16,17]. The combination of broad bean protein and chia seed polysaccharides seems to be promising in the context of microencapsulation of essential oils.

Essential oils are garnering growing attention in the food industry for their antimicrobial properties, which offer the potential for food preservation. However, their application is often restricted by their intense taste and aroma. Being volatile compounds, highly sensitive to environmental factors like light, temperature, and pH, which can induce changes in their chemical composition, essential oils present a challenge related to storage. Consequently, there is a quest for preservation methods, and microencapsulation using complex coacervation emerges as a promising approach [18,19].

The aim of this study was to fabricate microcapsules containing essential oil from juniper or black pepper, utilizing a combination of faba bean protein and chia seed polysaccharides. By synergizing those two polymers, our objective was to enhance the efficiency of microencapsulation of essential oils, thereby paving the way for diverse applications in the food industry. We used soybean and rapeseed oils as core materials to dissolve essential oils to limit their evaporation during the preparation of coacervates and microcapsules. Black pepper and juniper essential oils were selected for their potential health and aromatic properties. Black pepper oil is known for its antibacterial, anti-inflammatory, and stimulating properties. In turn, juniper oil is valued for its disinfecting, anti-inflammatory, and antiseptic properties. Their use in microcapsules may enable easier and more effective use of these beneficial properties in various applications, such as the pharmaceutical, cosmetics, and food industries. Additionally, we aimed to investigate the impact of different polymer mixing ratios on the properties of the resulting microcapsules and the course of the complex coacervation process.

2. Results and Discussion

The study examined twelve distinct samples, categorized into four groups based on three factors: the type of oil (soybean or rapeseed), the type of essential oil (juniper or black pepper), and the mixing ratio of broad bean protein with chia polysaccharides (1:1, 1:2, and 2:1). Comparisons were conducted within each of these four groups, facilitating an assessment of how individual components influenced the ultimate characteristics of the microcapsules.

2.1. Microcapsule Yield and Encapsulation Efficiency

Across all variants, the microcapsule yield remained consistent, ranging from 48.64% to 49.31% (Table 1). Specifically, the RB1 sample exhibited the lowest MY, while the RB2 sample demonstrated the highest value. Statistical analysis showed that all factors and interactions between them significantly influenced the obtained MY values ($p \leq 0.001$) (Table 1).

The encapsulation efficiency ranged from 65.64% to 87.85% (Table 1). Notably, the RB2 sample exhibited the highest EE value, coinciding with its superior efficiency in microcapsule production. Across all instances, samples with an FB/CHP ratio of 1:2 consistently demonstrated higher EE compared to those with other mixing ratios. Factorial ANOVA showed that MR and the EO content in the microcapsules had a statistically significant impact on EE ($p \leq 0.05$) (Table 1).

The mixing ratio of biopolymers plays a crucial role in determining the distribution of electric charges and subsequently influences the balance of charges and electrostatic interactions during the coacervation process [20]. Surprisingly, in this study, the analysis revealed that the mixing ratio did not exert a statistically significant effect on the outcome. This suggests that other factors related to the coacervation process (pH, temperature) itself may have overshadowed the impact of the biopolymer ratio.

2.2. Density, Carr Index, and Hausner Ratio

The bulk density of the samples ranged from 0.11 to 0.16 g/cm³ (Table 1), with RB3 and SJ1 exhibiting the highest density and RB2 and SJ2 showing the lowest. Statistical analysis revealed that all factors and their interactions had a statistically significant impact on the ρ_{bulk} values obtained ($p \leq 0.001$) (Table 2). Tapped density was in the range of 0.20 to 0.30 g/cm³ (Table 1), approximately twice as high as the initial ρ_{bulk} [21]. All factors significantly influenced the values, albeit to different extents. Specifically, the content of oil, essential oil, and the interactions between oil content and MR, as well as oil content and EO, exhibited a greater impact ($p \leq 0.001$) compared to the interactions between MR and EO and all factors concurrently ($p \leq 0.05$) (Table 1). These findings indicate that the complex coacervation process led to a significant reduction in bulk density compared to the individual components. Faba bean protein typically has a ρ_{bulk} of around 0.95 g/cm³ [22], while CHP ranges between 0.472 and 0.567 g/cm³ [23]. Therefore, the observed decrease in bulk density suggests successful microcapsule formation, with the coacervation process effectively reducing the density of the resulting samples. The decrease in bulk density, while indicative of successful microcapsule formation, may have a negative impact from a storage perspective. Lower density results in increased volume for a given mass, potentially posing challenges in storage and transportation due to the larger space requirements [24]. An increase in tapped density compared to bulk density is a common occurrence, typically resulting in roughly a two-fold increase. This happens due to a more ordered arrangement of material particles during the tapping process, reducing the space between them. In the microcapsules we acquired, this difference was approximately two-fold, likely due to their low water content (3.3%, Table 1) [21]. However, the disparity between tapped and bulk densities can vary, depending on factors like water content, particle size, and the type of wall material. In a study by Airouyuwa and Kaewmanee [25], the bulk and shaken densities of microcapsules that were based on pea protein and contained moringa leaf extract were 0.35 and 0.40 g/cm³, respectively. Despite the water content in these microcapsules being similar to that obtained in our tests (ranging from 5.21% to 7.40%), the difference in density values was small. Ultimately, comprehending these differences necessitates considering various process factors and material properties.

The Carr Index ranged from 45.81% to 48.01% (Table 1), while the Hausner ratio spanned from 1.82 to 1.92 (Table 1). In both cases, individual factors and their interactions, as well as the interaction between MR and EO, significantly influenced the CI and HR values ($p \leq 0.001$). However, the interaction between oil content and MR did not show statistical significance. Conversely, the interaction between oil and EO content was statistically significant only concerning the CI values ($p \leq 0.05$) (Table 1). The SJ2 sample exhibited the lowest values for CI and HR, while the SB2 sample showed the highest values. According to the interpretation of CI and HR values, all microcapsules obtained exhibited very poor or virtually no flow characteristics [26]. This aligns with the typical attributes of microcapsules produced via complex coacervation and freeze-drying methods [27,28]. Based on the obtained results, it cannot be concluded that any specific mixing ratio is superior in terms of the resulting CI and HR values. Further optimization of the coacervation process may be required to enhance the flow properties of the microcapsules and facilitate their handling and processing in practical applications.

2.3. Solubility, Moisture Content, and Hygroscopicity

The solubility of the microcapsules in water was found to be low and exhibited a strong dependency on the FB/CHP ratio, ranging from 8.53% to 38.38% (Table 1). Samples with a 1:1 ratio (RJ1, RB1, SJ1, and SB1) displayed the lowest solubility, with values ranging from 8.53% to 13.51%, while those with a 1:2 ratio (RJ2, RB2, SJ2, and SB2) demonstrated higher solubility, ranging from 28.88% to 38.38% (Table 1). Factorial ANOVA showed that the oil content and the interaction between oil and essential oil content had the greatest impact on the solubility of microcapsules ($p \leq 0.001$). The EO content also influenced the solubility but to a lesser extent ($p \leq 0.05$). The remaining factors and the interactions between them were

not statistically significant (Table 1). The moisture content in the samples was generally low, ranging from 3.72% to 7.65%. However, three samples (RB2, SJ2, and SB3) exhibited higher MC, exceeding 5%, with values of 7.65%, 5.02%, and 7.46%, respectively. There was no statistically significant impact of any of the tested parameters on the MC value (Table 1). Interestingly, the water content showed a correlation with density, with density decreasing as moisture content increased (Figure 1). These findings suggest that the observed changes in bulk and tapped densities with increasing moisture content indicate the presence of strong inter-particle liquid bridges and interlocking forces between particles, as reported in previous studies [21]. The hygroscopicity of the samples ranged from 40.40% to 76.98% (Table 1), with the RB3 sample exhibiting the lowest value and the RB2 sample the highest. This parameter showed a direct correlation with water content, increasing with higher moisture content [29]. Such a relationship is likely due to non-covalent interactions between the microcapsule components and water molecules in the environment, including hydrogen bonds or van der Waals forces [30]. The FT-IR analysis revealed the presence of functional groups (-OH, -C=O, -COOH, -NH₂) capable of electrostatically interacting with water molecules, which may explain this observed correlation. Nevertheless, factorial ANOVA showed a statistically significant impact ($p \leq 0.001$) of the oil content in the sample on the H value.

2.4. Color Measurement

Based on the findings, it can be inferred that the microcapsules exhibited a hue akin to that of the wall components, indicating that their color primarily relied on the concentration of these constituents within the sample (Table 1). Statistical analysis showed that the L* parameter was statistically significantly influenced by oil content, mixing ratio, EO content, and interactions between oil I EO and MR I EO ($p \leq 0.001$). The remaining parameters and interactions were not statistically significant. The L* parameter values for the microcapsules spanned from 87.85 to 95.93, signifying their light complexion. Meanwhile, the a* parameter ranged from 0.90 to 1.56, and the b* parameter from 7.50 to 9.91. The parameter a* was significantly influenced by MR and the interaction between oil content and MR ($p \leq 0.001$). The remaining parameters were not significant (Table 1). In turn, parameter b* was significantly influenced by the content of oil and EO as well as the interaction between the content of oil and MR ($p \leq 0.001$). The mixing ratio had a significant impact on the b* value, but to a lesser extent ($p \leq 0.05$) (Table 1). The remaining parameters were not significant. A comparison of these values with the color parameters for broad bean protein (L = 96.67, a = 0.65, b = 6.02 [22]) and chia polysaccharides (L = 87.23, a = 1.76, b = 10.59 [31]) revealed that the microcapsules were lighter than chia polysaccharides (higher L* value) and exhibited a more yellowish tone (higher b* parameter value) than broad bean protein. Hence, it can be inferred that these ingredients influenced the ultimate hue of the microcapsules, with a greater proportion of broad bean protein resulting in a lighter shade and a higher concentration of chia polysaccharides imparting a more yellowish tint. Additionally, it was observed that the presence of RSO, SBO, JEO, or BPO did not exert a statistically significant influence on the color.

Table 1. Microcapsule yield (MY), encapsulation efficiency (EE), solubility (S), hygroscopicity (H), moisture content (MC), bulk and tapped densities (ρ_{bulk} , ρ_{tap}), Carr Index (CI), Hausner ratio (HR), color parameters (L^* , a^* , b^*), and PDI values.

Sample	MY [%]	EE [%]	S [%]	H [%]	MC [%]	ρ_{bulk} [g/cm ³]	ρ_{tap} [g/cm ³]	CI [%]	HR	L^*	a^*	b^*	SI
RJ1	49.27 ± 0.00 ^a	83.23 ± 6.99 ^{ab}	12.58 ± 0.10 ^a	62.74 ^{± 0.00} _{abcd}	4.78 ± 0.20 ^a	0.13 ± 0.00 ^a	0.24 ± 0.01 ^a	45.83 ± 0.34 ^a	1.85 ± 0.01 ^a	90.91 ± 1.93 ^a	1.53 ± 0.08 ^{ef}	8.91 ± 0.54 ^a	0.47 ± 0.00 ^d
RJ2	48.89 ± 0.02 ^e	84.61 ± 6.68 ^{abc}	28.88 ± 0.10 ^a	61.94 ^{± 0.01} _{bcd}	4.20 ± 0.23 ^a	0.14 ± 0.00 ^b	0.24 ± 0.00 ^e	45.83 ± 0.67 ^h	1.85 ± 0.03 ^h	89.35 ± 0.20 ^e	0.99 ± 0.09 ^{ac}	7.69 ± 0.32 ^{bd}	0.49 ± 0.00 ^a
RJ3	49.01 ± 0.00 ^b	74.39 ± 6.60 ^{ab}	27.21 ± 0.06 ^a	50.05 ^{± 0.00} _{abc}	4.04 ± 0.06 ^a	0.15 ± 0.00 ^{bc}	0.28 ± 0.00 ^{bc}	46.43 ± 1.63 ^e	1.87 ± 0.04 ^e	95.93 ± 0.55 ^b	1.20 ^{± 0.26} _{abd}	8.53 ± 0.29 ^{abc}	0.40 ± 0.01 ⁱ
RB1	48.64 ± 0.02 ^d	76.04 ± 6.35 ^b	12.64 ± 0.15 ^a	66.78 ± 0.00 ^d	4.68 ± 0.17 ^a	0.13 ± 0.00 ^e	0.24 ± 0.01 ^{bc}	45.81 ^{± 1.17} _{cd}	1.86 ± 0.06 ^{cd}	87.85 ^{± 0.94} _{bc}	1.36 ± 0.34 ^{def}	8.35 ± 0.51 ^{abcd}	0.37 ± 0.00 ^c
RB2	49.31 ± 0.00 ^f	87.85 ± 4.71 ^{ac}	31.70 ± 0.08 ^a	76.98 ^{± 0.00} _{ae}	7.65 ± 0.10 ^a	0.11 ± 0.00 ^d	0.21 ± 0.00 ^e	47.62 ^{± 1.05} _{bc}	1.91 ± 0.03 ^{bc}	88.65 ± 0.18 ^d	1.07 ± 0.02 ^{abc}	7.50 ± 0.36 ^d	0.45 ± 0.01 ^f
RB3	49.04 ± 0.01 ^g	77.08 ± 3.21 ^{abc}	22.60 ± 0.06 ^a	40.40 ± 0.00 ^e	3.72 ± 0.05 ^a	0.16 ± 0.00 ^g	0.30 ± 0.00 ^b	46.67 ± 2.54 ^g	1.88 ± 0.03 ^g	91.32 ± 0.87 ^a	1.09 ± 0.08 ^{abc}	7.63 ± 0.31 ^d	0.35 ± 0.00 ^e
SJ1	49.17 ± 0.02 ^c	79.49 ± 7.25 ^{ab}	8.53 ± 0.10 ^a	50.91 ^{± 0.01} _{ae}	3.95 ± 0.06 ^a	0.16 ± 0.01 ^c	0.30 ± 0.01 ^{cd}	46.72 ± 2.95 ^e	1.89 ± 0.12 ^e	91.70 ± 0.45 ^a	1.20 ^{± 0.08} _{abd}	7.93 ± 0.72 ^{ac}	0.41 ± 0.00 ^g
SJ2	49.27 ± 0.00 ^c	85.11 ± 6.92 ^c	33.68 ± 0.13 ^a	74.97 ^{± 0.01} _{ab}	7.46 ± 0.12 ^a	0.11 ± 0.00 ^a	0.20 ± 0.00 ^a	44.28 ± 1.05 ^a	1.82 ± 0.03 ^a	89.57 ± 0.38 ^a	1.56 ± 0.13 ^f	9.91 ± 0.58 ^e	0.44 ± 0.00 ^c
SJ3	49.29 ± 0.01 ^a	74.54 ± 4.28 ^{ab}	14.26 ± 0.15 ^a	61.00 ^{± 0.01} _{cd}	4.20 ± 0.06 ^a	0.14 ± 0.00 ^a	0.26 ± 0.00 ^a	46.17 ± 1.99 ^a	1.88 ± 0.02 ^a	94.91 ^{± 0.84} _{bc}	0.99 ± 0.09 ^{ac}	8.57 ± 1.03 ^{abc}	0.38 ± 0.01 ^h
SB1	49.18 ± 0.02 ^h	65.64 ± 6.45 ^{ab}	18.11 ± 0.06 ^a	54.55 ^{± 0.01} _{abe}	4.13 ± 0.06 ^a	0.14 ± 0.01 ^a	0.26 ± 0.00 ^a	46.15 ± 0.93 ^a	1.86 ± 0.03 ^a	92.24 ^{± 0.96} _{ac}	1.19 ± 0.08 _{abd}	8.91 ± 0.62 ^a	0.45 ± 0.00 ^d
SB2	49.13 ± 0.02 ^a	82.42 ± 7.30 ^{ac}	38.38 ± 0.06 ^a	63.93 ^{± 0.00} _{abc}	4.27 ± 0.11 ^a	0.14 ± 0.00 ^f	0.25 ± 0.01 ^a	48.01 ± 1.05 ^f	1.92 ± 0.03 ^f	91.46 ± 0.19 ^d	1.29 ^{± 0.06} _{bde}	8.57 ± 0.05 ^{abc}	0.47 ± 0.00 ^b
SB3	48.91 ± 0.01 ^b	80.00 ± 4.52 ^{ab}	13.51 ± 0.10 ^a	73.00 ^{± 0.03} _{cd}	5.02 ± 0.06 ^a	0.12 ± 0.00 ^d	0.23 ± 0.00 ^d	47.82 ± 3.66 ^b	1.92 ± 0.09 ^b	95.03 ± 0.49 ^d	0.90 ± 0.07 ^c	7.95 ± 0.35 ^{bcd}	0.37 ± 0.01 ^{ab}
S.E.M	0.00	54.0	0.000014	0.000037	3.44	0.0030	79.2	780.02	135.926	0.7	0.02080	0.281	0.000033
Oil	**	NS	**	**	NS	**	**	**	**	**	NS	**	**
MR	**	*	NS	NS	NS	**	**	**	**	**	**	*	NS
EO	**	NS	*	NS	NS	**	**	**	**	**	NS	**	**
Oil*MR	**	NS	NS	NS	NS	**	**	NS	NS	NS	**	**	**
Oil*EO	**	NS	**	NS	NS	**	**	*	NS	**	NS	NS	**
MR*EO	**	*	NS	NS	NS	**	*	**	**	**	NS	NS	**
Oil*MR*EO	**	NS	NS	NS	NS	**	*	**	**	NS	NS	NS	**

Results in this table are expressed as mean ± standard deviation. Mean values with the same superscript letters within a row are not significantly different at $p \leq 0.05$. S.E.M.—standard error of the mean. * = $p \leq 0.05$; ** = $p \leq 0.001$; NS—non – significant effect = $p > 0.05$.

2.5. Particle Size Distribution

The PDI values ranged from 0.35 to 0.49 across all samples, with a trend of higher values observed in samples with an FB/CHP ratio of 2:1 (Table 1). This suggests that the faba bean protein content had a notable influence on particle size distribution. This observation aligns with the similarity between the PDI values of the microcapsules and those reported for pure broad bean protein (0.30–0.46), indicating the dominant role of this component in determining particle size uniformity [32]. All parameters and interactions between them (except MR) had a statistically significant impact on PDI values ($p \leq 0.001$). Notably, the PDI values fell within the range indicative of relatively uniform particle size distribution, reflecting consistent sizing across the microcapsule samples [33,34]. The relatively uniform particle size distribution indicates the effectiveness of microencapsulation via a complex coacervation process in producing consistent-sized microcapsules, which is crucial for applications requiring standardized product characteristics.

2.6. Thermal Stability

The DSC analysis aimed to investigate the thermal behavior of the obtained microcapsules in the temperature range from 20 °C to 230 °C. The obtained results are presented in Table 2.

Table 2. Differential scanning calorimetry analysis results.

Sample	T _{on} [°C]	T _{max} [°C]	T _{end} [°C]	ΔH [mJ]
RJ1	122.81 ± 0.01	133.79 ± 0.01	156.11	−523.77 ± 0.01
RJ2	154.70 ± 0.01	173.79 ± 0.01	195.12 ± 0.01	−438.73 ± 0.01
RJ3	87.01 ± 0.01	132.08 ± 0.01	157.47 ± 0.02	−361.65 ± 0.01
RB1	156.01 ± 0.01	158.99 ± 0.02	170.42 ± 0.02	−120.11 ± 0.00
RB2	177.52 ± 0.01	177.55 ± 0.02	181.40 ± 0.00	−428.38 ± 0.00
RB3	120.01 ± 0.02	135.35 ± 0.00	151.83 ± 0.01	−376.06 ± 0.01
SJ1	105.23 ± 0.00	133.89 ± 0.00	172.51 ± 0.01	−398.25 ± 0.00
SJ2	145.19 ± 0.00	151.69 ± 0.01	163.82 ± 0.01	−413.72 ± 0.00
SJ3	98.06 ± 0.01	134.72 ± 0.01	159.73 ± 0.01	−369.17 ± 0.01
SB1	128.33 ± 0.01	128.58 ± 0.01	174.08 ± 0.01	−466.23 ± 0.01
SB2	155.01 ± 0.01	165.76 ± 0.00	177.50 ± 0.01	−490.12 ± 0.01
SB3	56.80 ± 0.01	116.90 ± 0.02	155.52 ± 0.01	−392.99 ± 0.00
FB	48.97 ± 0.01	63.60 ± 0.01	76.94 ± 0.02	−37.27 ± 0.01
CHP	129.52 ± 0.02	139.62 ± 0.02	154.18 ± 0.01	−9663.97 ± 0.02
JEO	24.71 ± 0.00	89.17 ± 0.00	140.95 ± 0.01	−80.00 ± 0.01
BPO	26.81 ± 0.01	97.10 ± 0.02	148.11 ± 0.00	−92.36 ± 0.01
RSO	184.61 ± 0.01	199.29 ± 0.02	214.88 ± 0.02	102.75 ± 0.01
SBO	155.34 ± 0.01	174.31 ± 0.00	198.20 ± 0.02	108.87 ± 0.00
T80	116.40 ± 0.00	138.82 ± 0.02	154.42 ± 0.00	58.61 ± 0.00

First, the thermal behavior of all substances used to produce the microcapsules was analyzed individually. Broad bean protein exhibited an endothermic transition likely due to denaturation, commencing at 48.97 °C. This reaction peaked at T_{max} = 63.60 °C and concluded at 76.94 °C (ΔH = −37.27 mJ). In a study by Buhler et al. [35], this reaction began at a significantly higher temperature, reaching its peak at 93.2 °C. The researchers noted that the initiation temperature of the reaction decreased with higher temperatures during the protein's prior heating, attributed to partial denaturation of the protein during this process.

Such substantial variations in observations may be attributed to the use of a pre-made preparation of broad bean protein in this experiment, which mainly contained soluble fractions. This factor could directly influence the reduction in the starting temperature of the protein denaturation reaction.

Polysaccharides from chia seeds displayed a single endothermic reaction commencing at $T_{\text{on}} = 129.52$ °C, corresponding to the loss of water and the decomposition of gums present in the mucus. This finding aligns with results reported by other researchers [36,37].

The endothermic reaction for juniper essential oil commenced at a temperature of $T_{\text{on}} = 24.17$ °C, with a peak at $T_{\text{max}} = 89.17$ °C, and concluded at $T_{\text{end}} = 140.95$ °C, with an enthalpy change of $\Delta H = -80.00$ mJ. Similarly, for black pepper essential oil, the endothermic peak was observed at $T_{\text{on}} = 26.81$ °C, and the endothermic reaction reached $T_{\text{max}} = 97.10$ °C and concluded at $T_{\text{end}} = 148.11$ °C, with an enthalpy change of $\Delta H = -92.36$ mJ. In both cases, this reaction can be attributed to the decomposition of EOs [38].

Both oils exhibited a single exothermic transformation, with RSO having a T_{on} of 184.61 °C and SBO having a T_{on} of 155.34 °C, corresponding to the formation of peroxides [39].

The emulsifier (T80) underwent a characteristic reaction with a flash point, characterized by $T_{\text{on}} = 116.40$ °C, $T_{\text{max}} = 138.82$ °C, $T_{\text{end}} = 154.42$ °C, and $\Delta H = 58.61$ mJ [40,41].

Analysis of the obtained results reveals a clear influence of the mixing ratio on the thermal resistance of the produced microcapsules. Across all variants, it is evident that the initiation temperature of the reaction was lowest when FP/CHP = 2:1 and highest when FP/CHP = 1:2. Among all samples, RB2 demonstrated the highest thermal stability ($T_{\text{on}} = 177.52$ °C, $T_{\text{max}} = 177.55$ °C, $T_{\text{end}} = 181.40$ °C, $\Delta H = -428.38$ mJ), whereas SB3 exhibited the lowest thermal stability ($T_{\text{on}} = 56.80$ °C, $T_{\text{max}} = 116.90$ °C, $T_{\text{end}} = 155.52$ °C, $\Delta H = -392.99$ mJ). Notably, the initiation temperature of the reaction surpassed that of pure broad bean protein in all cases, while remaining below that of pure CHP for all samples. This underscores the interactions between the microcapsules' wall materials, a phenomenon further supported by FT-IR analysis (Section 2.7.).

In summary, the results suggest that the optimal mixing ratio of faba bean protein and chia seed polysaccharides affects the thermal resistance of microcapsules, which is important for their potential applications in the food industry.

2.7. Fourier Transform Infrared Spectroscopy

FT-IR analysis was performed for individual components of the microcapsules separately and for all 12 samples. The results are shown in Figures 1–4. In the description of the results, the following markings were used for individual wavelength ranges: the single-bond area means waves with a length in the range of 4000–2500 cm^{-1} , the triple-bond area means waves with a length in the range 2500–2000 cm^{-1} , the double-bond area means waves with a length in the range 2000–1500 cm^{-1} , and the fingerprint area means waves with a length in the range of 1500–600 cm^{-1} [42].

Nine characteristic peaks were identified for FB, confirming its complex nature (data not presented). In the region of single bonds, a broad absorption band at 3278.50 cm^{-1} suggests the presence of hydrogen bonds, indicating the existence of symmetric -OH stretching, ammonium, and amino groups. A peak at 2926.67 cm^{-1} is characteristic of the asymmetric stretching of C-H bonds in methylene groups [42]. This is a common feature in the FT-IR spectrum of proteins as methylene groups are found in amino acids such as alanine, leucine, isoleucine, valine, threonine, and methionine [43], which are components of broad bean protein [44]. A characteristic peak at 1633.37 cm^{-1} , belonging to the amide I band (1700–1600 cm^{-1}) [45], appeared, indicating stretching vibrations of C=C and C=O bonds. Additionally, in the amide II band (1510–1580 cm^{-1}) [45], a peak was observed at 1536.95 cm^{-1} , indicating bending in the N-H plane and stretching vibrations of C-N and C-C bonds. Within the fingerprint region, five peaks of varying intensities were identified: 1394.02 cm^{-1} , 1236.99 cm^{-1} , and 1043.14 cm^{-1} , corresponding to bend vibrations of N-H and -NH₂, and 513.95 cm^{-1} and 410.01 cm^{-1} , corresponding to stretching vibrations of

S-S derived from sulfur amino acids involved in disulfide bridge formation [46–48]. These findings are consistent with previous studies conducted by Sofi et al. [22].

Fourteen peaks were identified in the FT-IR spectrum of CHP (data not presented). A broad absorption band at 3472.39 cm^{-1} indicates the presence of hydrogen bonds, suggesting symmetric -OH stretching and thus indicating the water content in the sample [31,36]. Peaks at 2927.61 cm^{-1} and 2355.77 cm^{-1} indicate C-H stretching. Peaks at 1629.67 cm^{-1} and 1537.45 cm^{-1} belong to amide I, corresponding to C=C and C=O bonds. Peaks at 1449.60 cm^{-1} and 1399.72 cm^{-1} are attributed to symmetrical -COO-link vibrations associated with uronic acids present in CHP [49]. Peaks at 1237.04 cm^{-1} and 1156.27 cm^{-1} indicate O-C-O asymmetric stretching, potentially associated with xyloglucan presence [36,50]. Peaks at 1063.49 cm^{-1} and 1029.91 cm^{-1} are related to the C-O bond, bend vibrations of N-H and -NH₂, and large aromatic rings [42]. Subsequent peaks at 856.07 cm^{-1} and 801.47 cm^{-1} correspond to anomeric configurations, such as CH oscillations of α and β conformers and glycosidic linkages, attributed to α -D-galactopyranose units and β -D-mannopyranose units, respectively [36,50]. The last peak, identified at 661.10 cm^{-1} , may be attributed to CH₂ bonds originating from chains containing more than seven carbon atoms [49].

The FT-IR spectra of JEO exhibit distinctive peaks indicative of its chemical composition (data not presented). A prominent peak at 3387.94 cm^{-1} signifies the presence of phenolic -OH groups. Peaks at 2917.56 cm^{-1} (the most intense peak), 2878.29 cm^{-1} , and 2833.70 cm^{-1} suggest the presence of long-chain linear aliphatic compounds (C-H stretching) [42]. The peak at 1748.55 cm^{-1} corresponds to C=O bonds, while the peak at 1644.81 cm^{-1} corresponds to C=C bonds. Peaks at 1594.93 cm^{-1} and 1515.09 cm^{-1} are associated with C=C bonds from aromatic rings [42,51]. The fingerprint region shows peaks of varying intensity, including those at 1446.07 cm^{-1} , 1364.69 cm^{-1} , and 1328.55 cm^{-1} , corresponding to C-OH bending vibrations and methyl C-H symmetrical and asymmetrical bends [51,52]. The peak at 1264.26 cm^{-1} is attributed to C-C-O and C-O stretching vibrations of phenolics, while peaks at 1164.67 cm^{-1} , 1124.97 cm^{-1} , and 1101.48 cm^{-1} result from C-O and C-OH bond deformation vibrations [51–53]. Peaks at 1063.07 cm^{-1} and 1014.59 cm^{-1} can be assigned to hydroxyl group vibrations and methylene vibrations, while peaks at 989.83 cm^{-1} and 952.06 cm^{-1} represent C-H bending vibration absorptions. Peaks at 887.14 cm^{-1} (the third most intense), 814.45 cm^{-1} , 786.52 cm^{-1} (the second most intense), 618.60 cm^{-1} , and 418.96 cm^{-1} suggest the presence of aromatic rings [3,42].

For BPO, peaks in the single-bond area at 2954.86 cm^{-1} , 2922.95 cm^{-1} (the most intense peak), and 2867.06 cm^{-1} indicate C-H stretching in long-chain linear aliphatic compounds. The peak at 1643.05 cm^{-1} may relate to H-O-H bending, while another peak at 1446.24 cm^{-1} corresponds to C-OH bending [54]. Peaks at 1381.29 cm^{-1} and 1366.31 cm^{-1} are associated with symmetrical deformation of CH₃ [42,55]. The peak at 1276.14 cm^{-1} represents skeletal C-C vibrations. Peaks at 1181.19 cm^{-1} and 1023.33 cm^{-1} may be attributed to stretching vibrations of terpenoid components, while 986.94 cm^{-1} may be related to the asymmetric stretching of the C-O bond [54]. Peaks at 885.83 cm^{-1} (the second most intense) and 875.20 cm^{-1} (the third most intense) suggest the presence of C-H stretching vibrations of aromatics [56]. The peak at 786.32 cm^{-1} is associated with S-C absorption. Finally, peaks at 543.65 cm^{-1} , 421.49 cm^{-1} , and 442.11 cm^{-1} suggest the presence of aromatic rings [3,42] (data not presented).

Triacylglycerols are the primary constituents of oils; hence, they dominate the spectrum in the FT-IR analysis of rapeseed and soybean oil. Peaks identified for RSO include 3076.53 cm^{-1} corresponding to the C-H stretching of cis double bonds, 2923.53 cm^{-1} and 2853.29 cm^{-1} corresponding to the methylene C-H asymmetrical stretching, 1743.07 cm^{-1} corresponding to the ester C=O stretching, a prominent peak at 1629.91 cm^{-1} assigned to the cis C=C stretching, 1530.48 cm^{-1} , 1454.27 cm^{-1} , and 1401.01 cm^{-1} corresponding to the H-C-H and =C-H (-cis) bending, and peaks at 1235.43 cm^{-1} , 1156.58 cm^{-1} , and 1045.80 cm^{-1} assigned to the ester C-O stretching. These findings are in line with previous research findings [42,57]. For SBO, peaks at similar wavelengths were observed, corresponding to the same bonds as in the case of RSO: 3008.58 cm^{-1} , 2922.40 cm^{-1} , 2852.54 cm^{-1} ,

and 1742.92 cm^{-1} . Additionally, peaks at 1456.95 cm^{-1} and 1377.02 cm^{-1} are attributed to the $-\text{CH}_2$ bending of cis $\text{C}=\text{C}$ bonds, while peaks at 1159.01 cm^{-1} and 1097.76 cm^{-1} are attributed to $\text{C}-\text{O}$ stretching vibrations. Furthermore, a peak at 720.99 cm^{-1} , attributed to the $-\text{CH}_2$ rocking, was identified [42,58].

The analysis of the Tween 80 emulsifier revealed an initial peak at 2855.75 cm^{-1} that may signify $\text{C}-\text{H}$ bending. Peaks in the $1470\text{--}720\text{ cm}^{-1}$ range suggest alignment with long-chain linear aliphatic compounds and $-\text{OH}$ bending. The subsequent peak at 1734.71 cm^{-1} may correspond to aromatic bands. No indications of triple bonds were observed. Peaks in the fingerprint region (1456.94 cm^{-1} , 1348.54 cm^{-1} , 1296.36 cm^{-1} , 1247.46 cm^{-1} , 1096.21 cm^{-1} , 946.67 cm^{-1} , 846.64 cm^{-1} , and 510.58 cm^{-1}) confirmed the presence of aromatic rings and double bonds (data not presented). The obtained results are consistent with previous studies [41,42,59].

Figures 1–4 illustrate the FT-IR spectra for all obtained microcapsules. The absence of characteristic peaks for RSO, SBO, JEO, and BPO in the spectra suggests successful microencapsulation, corroborated by EE test results (Section 2.1., Table 1). The spectra closely resemble those of FB, consistent with their composition, with the FB concentration being the highest in all cases. Variations in peak intensity were observed, notably with higher intensity at specific wavelengths for certain mixing ratios. Notably, a peak characteristic of RSO and SBO appeared in all samples except RB2, which exhibited the highest EE (87.85 ± 4.71). This indicates a correlation between microcapsule composition, peak intensity, and encapsulation efficiency.

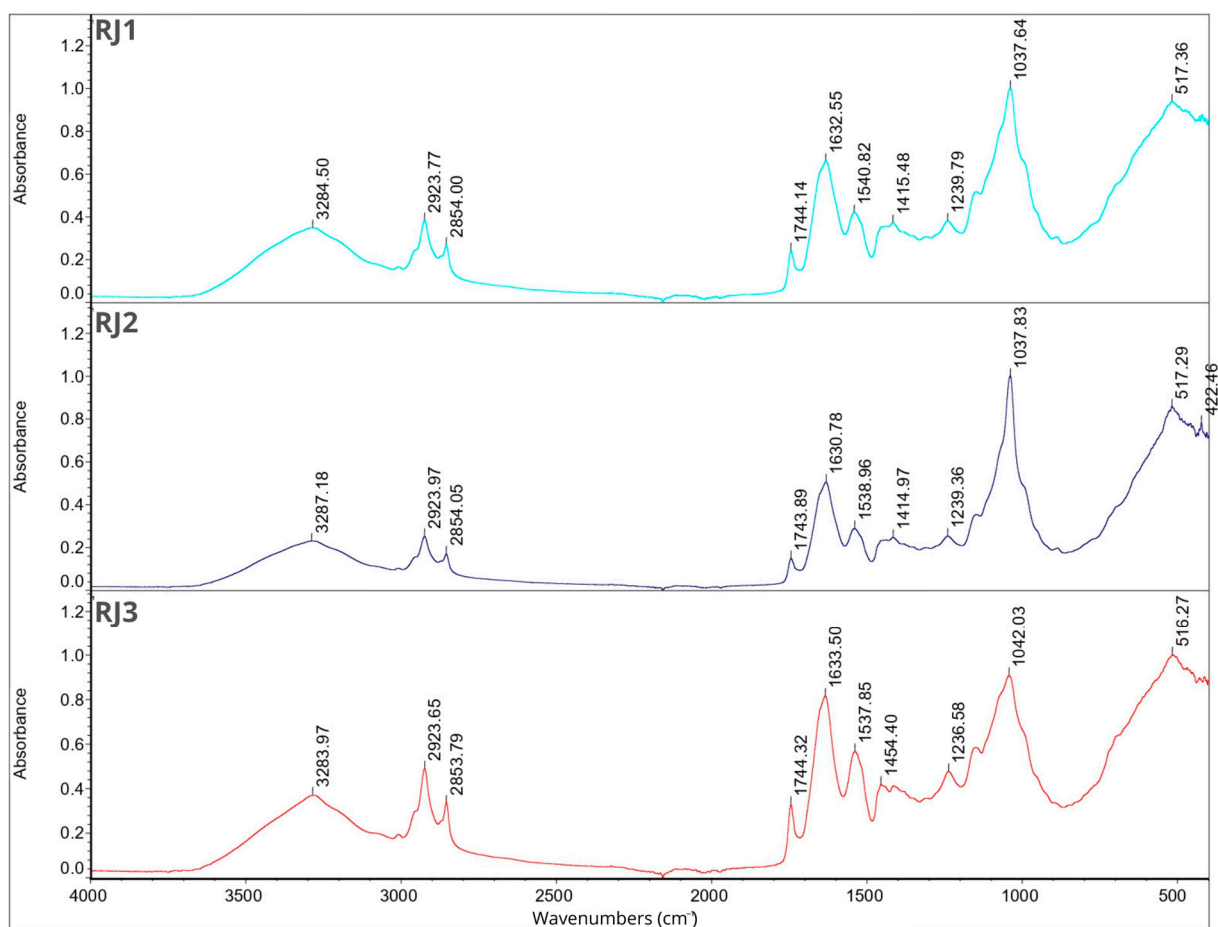


Figure 1. FT-IR spectra for samples RJ1, RJ2, RJ3.

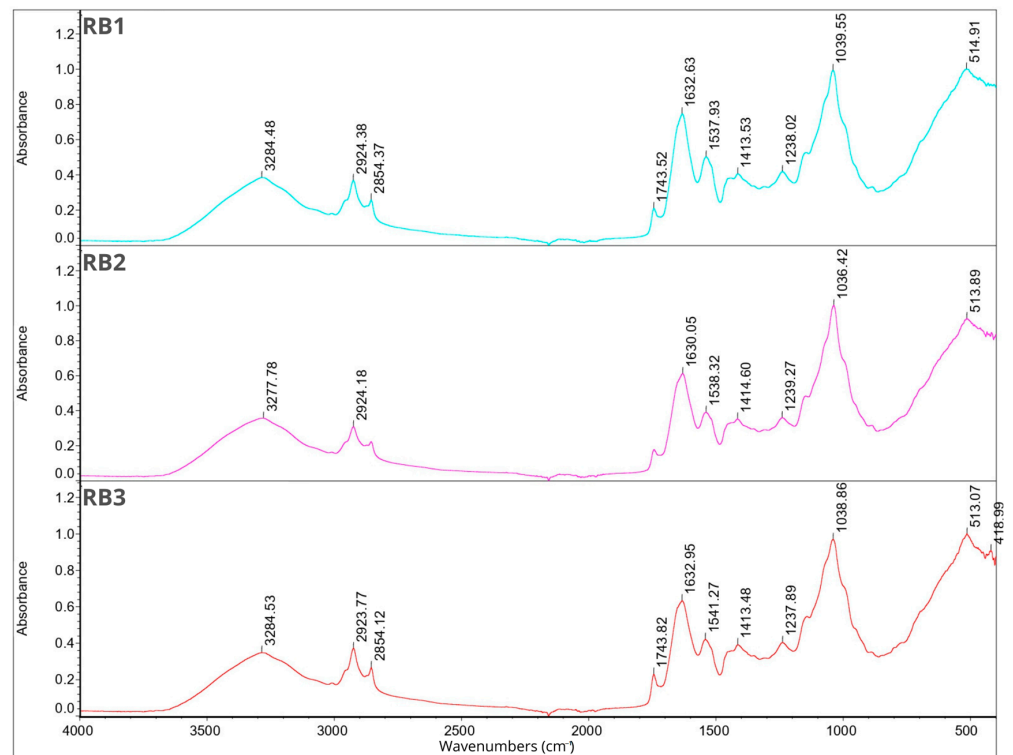


Figure 2. FT-IR spectra for samples RB1, RB2, RB3.

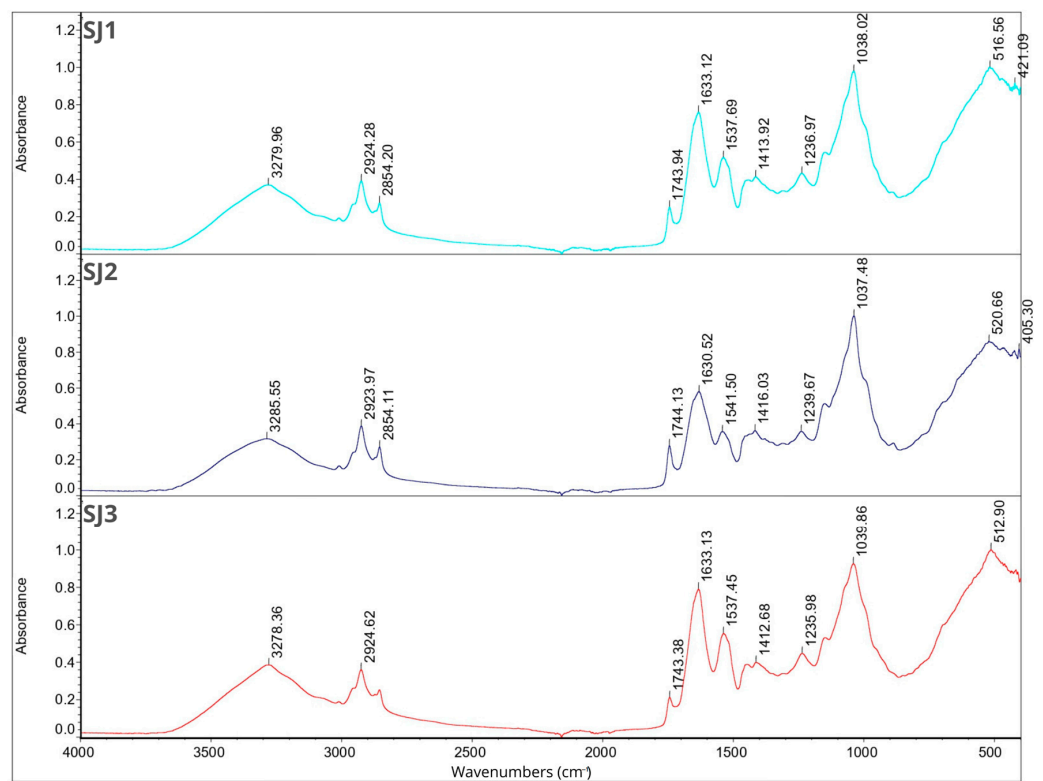


Figure 3. FT-IR spectra for samples SJ1, SJ2, SJ3.

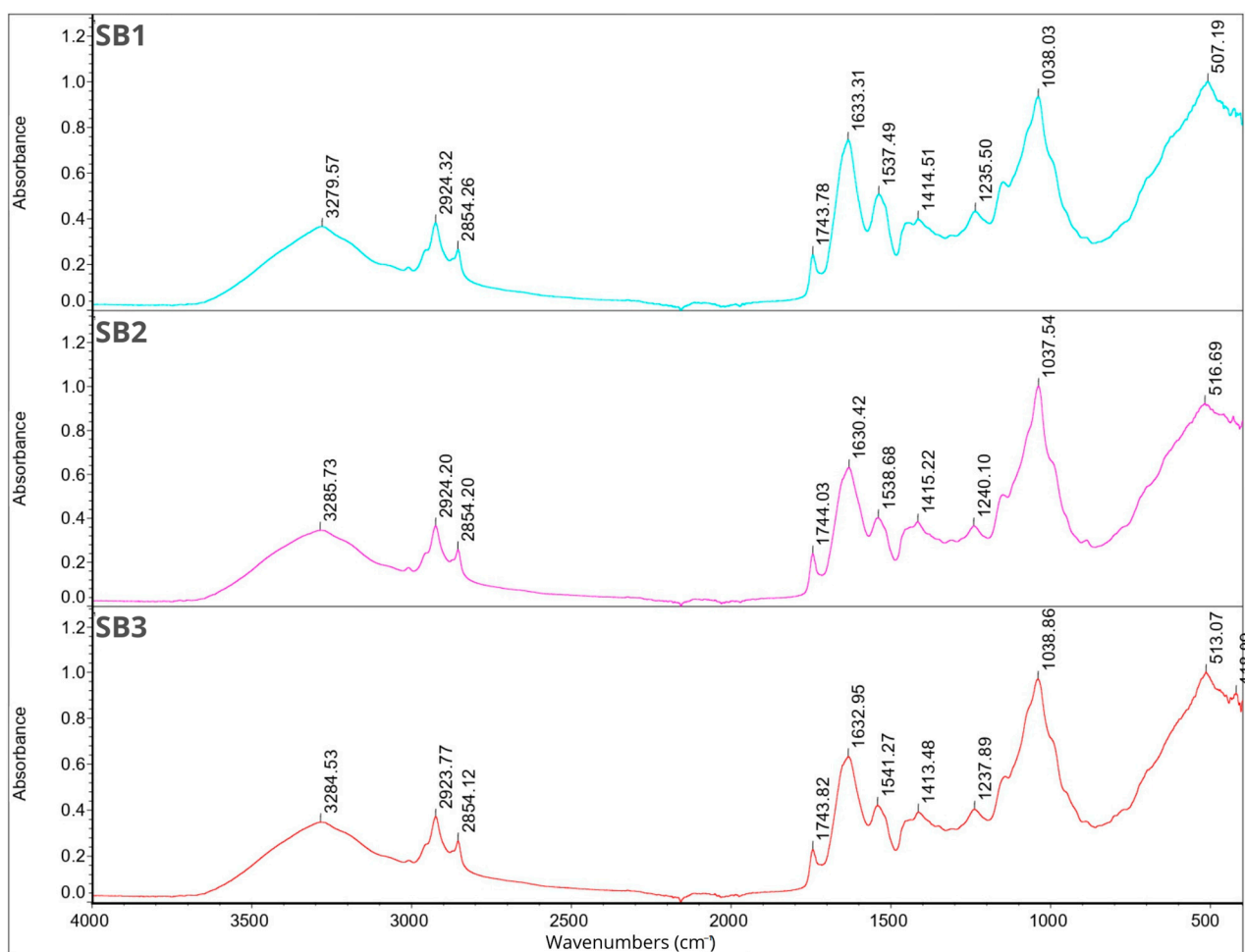


Figure 4. FT-IR spectra for samples SB1, SB2, SB3.

2.8. Smell Pattern

Figure 5 illustrates the classification of scent profiles relative to their respective experimental groups. The samples are depicted in a two-dimensional plane based on principal component 1 (PC1) and principal component 2 (PC2). The total contribution variances of PC1 and PC2 from direct electronic nose measurements were 98.574% and 1.082%, respectively. The differentiation index (DI) was 100%, indicating clear discrimination among the samples. Notably, the samples were well separated with no overlapping areas, underscoring significant differences among them. Interestingly, samples containing black pepper essential oil were predominantly positioned on the left side of the chart, while those with juniper essential oil were primarily located on the right side. Additionally, samples containing RSO tended to cluster in the upper part of the graph, whereas those with SBO were mainly situated in the lower part. Each group exhibited distinct separation from one another, as indicated by the color markings on the chart. The distinct separation of scent profiles based on experimental groups suggests that the electronic nose technique effectively discriminates between different sample compositions. The observed clustering patterns could be attributed to the unique chemical compositions of the essential oils and carrier oils used in each sample, highlighting the potential influence of these components on scent profiles.

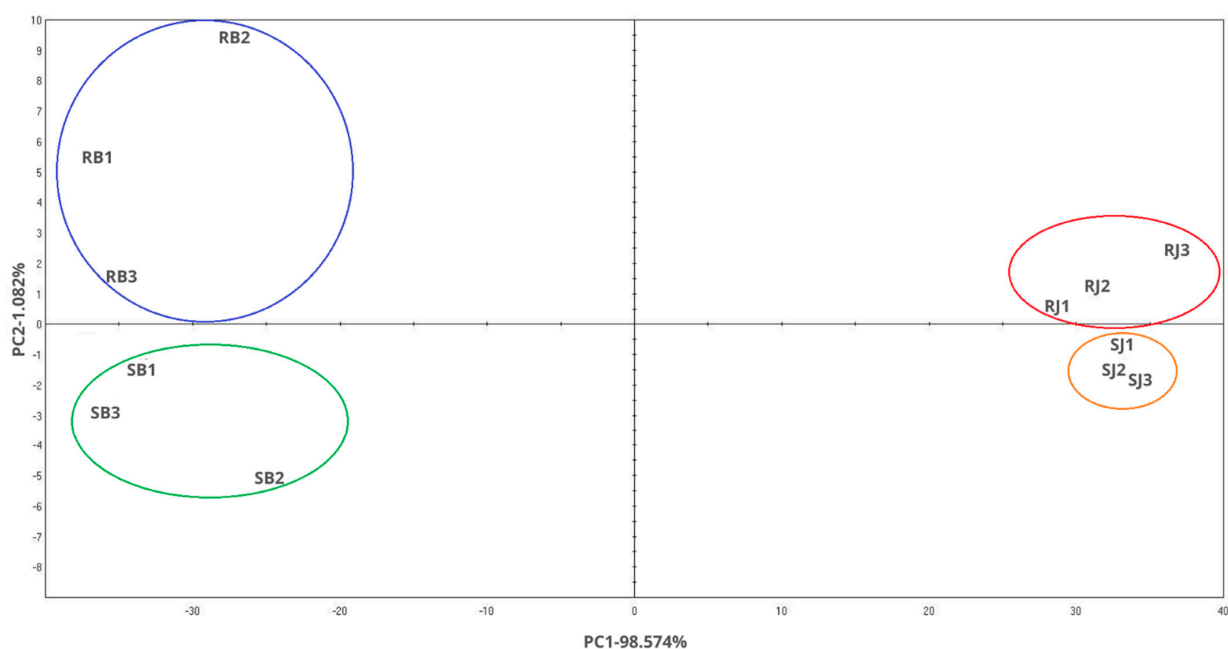


Figure 5. Smell pattern chart.

3. Materials and Methods

3.1. Materials

Faba bean protein (Hortimex, Konin, Poland) and polysaccharides extracted from chia seeds (Agnex, Białystok, Poland) were employed as wall materials in this study. Juniper berry essential oil (*Juniperus communis*) and black peppercorn essential oil (*Piper nigrum*) (Ancient Wisdom, Sheffield, United Kingdom) were initially dissolved in soybean oil (Dary Natury, Koryciny, Poland) or rapeseed oil (Olwita, Marcinowice, Poland) and utilized as core materials. Samples were prepared with the addition of the emulsifier Tween 80 (Sigma Aldrich, Saint Louis, MO, USA).

3.2. Chia Polysaccharide Extraction

Chia seeds were combined with distilled water at room temperature, using a ratio of 5 g of seeds per 100 g of water. Polysaccharide extraction took place at room temperature over a 4 h period, with constant stirring. Following extraction, the polysaccharides were filtered through cheesecloth, subjected to centrifugation at 10,000 rpm for 5 min, and then freeze-dried for 72 h. The resulting mucilage, prepared using a slightly modified version of the methodology outlined by Silva et al. [31], was promptly employed for the subsequent coacervation process (Section 3.3.).

3.3. Preparation of Coacervates

A 5% solution of faba bean protein (FB) was mixed with a 2% solution of chia seed polysaccharides (CHP) (*w/v* in double distilled water) in various mass ratios (1:1; 1:2, and 2:1) to obtain 300 g of solution. The mixture of wall materials prepared in this way with 0.5% Tween 80 was mixed on a magnetic mixer for 10 min until the solutions were completely combined with the emulsifier. After this time, a mixture of soybean (SBO) or rapeseed (RPO) oil with juniper (JEO) or black pepper (BPO) essential oil was added in an amount of 5% of the total sample weight. Each sample contained 2.5% oil and 2.5% essential oil. After initial mixing on a magnetic stirrer, the samples were subjected to high shear homogenization using an Ultra Turrax (IKA T18 basic, IKA, Staufen, Germany) for 10 min at 15,000 rpm/min at room temperature. After emulsification, the pH was adjusted to 4.0 (below the isoelectric point) using 1 M HCl. Subsequently, all emulsions were stored at 4 °C for 24 h, followed by transfer to −20 °C for an additional 24 h, and then transferred again to −60 °C for another 24 h. The frozen samples were then subjected to lyophilization for

72 h at $-80\text{ }^{\circ}\text{C}$. Following lyophilization, the lyophilizates were sieved using a laboratory sieve with a mesh size of $710\text{ }\mu\text{m}$, vacuum packed, and stored at $4\text{ }^{\circ}\text{C}$ for further analyses (Table 3).

Table 3. Coding of samples.

Oil	Essential Oil	FP/CHP	Code
Rapeseed	Juniper	1:1	RJ1
		1:2	RJ2
		2:1	RJ3
	Black pepper	1:1	RB1
		1:2	RB2
		2:1	RB3
Soybean	Juniper	1:1	SJ1
		1:2	SJ2
		2:1	SJ3
	Black pepper	1:1	SB1
		1:2	SB2
		2:1	SB3

3.4. Microcapsule Yield and Encapsulation Efficiency

Using the mass of liquid (LC) and dried (DC) coacervates, we calculated the actual yield of microcapsules (MY). All measurements were performed in triplicates.

$$\text{MY} = \frac{\text{DC}}{\text{LC}} * 100\%$$

To determine the encapsulation efficiency (EE), we used the methodology from our previous study [60]. Briefly, the encapsulation efficiency was determined as the ratio of internal oil to the total oil content of the samples. Total oil (TO) and surface oil (SO) were measured in triplicate for each sample.

$$\text{EE} = \frac{\text{TO} - \text{SO}}{\text{TO}} * 100\%$$

To calculate SO, the sample was dissolved in 30 mL of n-hexane, filtered, and evaporated (R-100, Büchi, Flawil, Switzerland). The remaining oil mass after evaporation was subtracted from the theoretical weight of oil from the sample. For determining TO, the sample (1.5 g) was mixed (60 rpm, 15 min) with 4 mL of KCl, 8 mL of acetone, and 8 mL of chloroform. After centrifugation (10,000 rpm, 10 min), the chloroform layer containing the extracted oil was filtered and evaporated. The remaining oil mass after evaporation was then measured.

3.5. Density, Carr Index, and Hausner Ratio

Bulk density (ρ_{bulk}) was assessed by pouring 1 g of the sample into a 10 mL graduated cylinder and measuring the volume it occupied. Tapped density (ρ_{tap}) was determined by manually tapping the cylinder repeatedly for one minute at a vertical distance of $14 \pm 2\text{ mm}$. Both measurements were conducted in triplicate, and densities were expressed in g/cm^3 . The Compressibility Index (CI) and Hausner ratio (HR) were calculated from the obtained results to evaluate the powder's flowability and compressibility [28].

$$\text{CI} = \frac{\rho_{\text{tap}} - \rho_{\text{bulk}}}{\rho_{\text{tap}}} * 100\%$$

$$HR = \frac{\rho_{\text{tap}}}{\rho_{\text{bulk}}}$$

3.6. Solubility, Moisture Content, and Hygroscopicity

The solubility of the powders was evaluated using a method involving the dispersion of 0.5 g of the sample in 50 mL of double-distilled water. The mixture was then agitated for 30 min at 60 rpm before undergoing centrifugation at 10,000 rpm for 5 min. After centrifugation, 25 mL of the supernatant was carefully transferred onto a pre-weighed Petri dish and dried at 105 °C for 6 h using a Binder FP 115 drying oven from Tuttlingen, Germany. The solubility (%) was calculated as the percentage of dried supernatant relative to the initially added amount of powder, following the procedure outlined by De Melo Ramos et al. [61]. All measurements were performed in triplicate to ensure the accuracy and consistency of results.

The moisture content of the obtained powders was determined by placing 0.2 g of the sample in a pre-weighed Petri dish. The dish with the sample was then dried at 70 °C for 24 h (Binder FP 115 drying oven, Tuttlingen, Germany). Subsequently, the dried samples were transferred to a desiccator to cool completely before being re-weighed. The moisture content was calculated based on the observed difference in weight before and after the drying process (%) [62]. Determinations were performed in triplicate.

The hygroscopicity of the obtained powders was determined by placing 0.2 g of the sample in a pre-weighed Petri dish. The dish was then stored in a desiccator containing a saturated Na₂SO₄ solution for a duration of one week. Hygroscopicity was expressed as g of water absorbed per 100 g sample (%) [62]. Determinations were performed in triplicate.

3.7. Color Measurement

The color of the microcapsules was assessed using a Minolta CR-400 colorimeter manufactured by Konica Minolta Inc., Tokyo, Japan. The measurements were conducted under D65 illuminant conditions, with an 8 mm measuring surface and following the standard 2° observer protocol. The recorded data were expressed in accordance with the International Commission on Lighting's (Commission Internationale de L'Eclairage) system within the CIELab color space.

The parameters analyzed and evaluated included L* (where L = 0 represents black and L = 100 represents white), a* (where −a signifies green and +a signifies red), and b* (where −b represents blue and +b represents yellow) [63]. These determinations were performed in triplicate immediately after the production process to ensure accuracy and consistency.

3.8. Particle Size Distribution

The particle size analysis was carried out using the Morphologi[®] G3SE instrument from Malvern Instruments Ltd., headquartered in Malvern, UK. The instrument was outfitted with a dispersion unit tailored for dry samples. Particle size distribution was determined by assessing the relative volume of particles within predefined size ranges, as illustrated in the size distribution curves. Data analysis was conducted using Malvern Microsoftware v.5.40, proprietary software provided by Malvern Instruments Ltd. Additionally, the particle size distribution (span index—SI) was estimated using the formula outlined by Hernandez-Nava et al. [64]:

$$SI = \frac{D_{90} - D_{10}}{D_{50}}$$

where D₉₀, D₅₀, and D₁₀ are the equivalent volume diameters at 90%, 50%, and 10% cumulative volume, respectively.

3.9. Thermal Stability

The thermal properties of the samples were evaluated using a differential scanning calorimetry instrument (DSC 1) from Mettler Toledo 820 (Schwerzenbach, Switzerland)

under a nitrogen atmosphere at a flow rate of 100 cm³/min, as per the method described [21] with some modifications. The instrument was calibrated with pure indium and zinc. Each sample (5.0 ± 0.1 mg) was placed in an aluminum crucible (ME-51119870) and covered with a lid (ME-51119871) using the Mettler Toledo Crucible Sealing Press. DSC scans were recorded from 10 °C to 230 °C at a rate of 10 °C/min. The thermograms were analyzed using STARe Software (Version 9.30) to determine the start (T_{on}), maximum (T_{max}), and end (T_{end}) temperatures, as well as the areas under the peaks (ΔH).

3.10. Fourier Transform Infrared Spectroscopy (FT-IR)

FT-IR spectra were recorded on a Nicolet™ iS™ 5 FTIR Spectrometer (Thermo Scientific, Waltham, MA, USA), with a horizontal device for attenuated reflectance and diamond crystal, on a spectral window ranging from 4000 to 400 cm⁻¹, at a spectral resolution of 2 cm⁻¹. Spectra were recorded without any sample preparation and were processed with the OMNIC program (Thermo Scientific, Waltham, MA, USA).

3.11. Smell Pattern

The volatile compounds within the microcapsules were extracted using the Heracles II electronic nose (Alpha M.O.S., Toulouse, France), which utilizes ultra-fast gas chromatography with headspace. The system features a detection system comprising two metal columns of varying polarities (nonpolar MXT-5 and slightly polar MXT1701, diameter = 180 μm, length = 10 m) and two flame ionization detectors (FIDs).

For the analysis, 10% solutions (0.25 g in 5 g) of each sample were placed in standard headspace vials sealed with a Teflon-faced silicon rubber cap. Incubation was performed at 35 °C for 900 s under an agitation speed of 8.33 Hz. The carrying gas was hydrogen (flow rate 1 mL/min). The injector temperature was set at 200 °C, with an injected volume of 3500 μL and speed of 125 mL s⁻¹. The analytes were collected in the trap at 15 °C and subsequently divided and simultaneously transferred into the two columns. The carrying gas was maintained at a constant pressure of 80 kPa, with a split flow rate of 10 mL/min at the column heads. The temperature program in the oven was as follows: 60 °C for 2 s, a ramp of 3 °C s⁻¹ to 270 °C, held for 20 s, and FID1/FID2 at 280 °C.

The volatile compounds identified in the samples were presented in the form of a table with Kovats indices. All samples were analyzed in triplicate. Kovats indices were established using alkane standards (n-butane to n-hexadecane) (Restek Centre County, PA) measured under the same conditions as the samples [65,66].

3.12. Statistical Analysis

For statistical analysis, STATISTICA (v. 13.3) software was used. To check the impact of the mixing ratio, oil, and essential oil content on obtained results and significant differences between them, factorial ANOVA and Fisher LSD test (*p*-value < 0.05, α = 95%) were used.

4. Conclusions

In this study, microcapsules containing essential oils were developed using broad bean protein and chia seed polysaccharides at various ratios (1:1, 1:2, or 2:1). The results revealed that the encapsulation efficiency of the microcapsules ranged from 65.64% to 87.85%, indicating their potential for industrial applications. Particularly noteworthy was the highest encapsulation efficiency observed in samples with a protein-to-polysaccharide ratio of 1:2. Another significant finding was the impact of water content on the density and hygroscopicity of the microcapsules, where an increase in water content resulted in decreased density and increased hygroscopicity. This observation was corroborated by FT-IR analysis. Additionally, the microcapsules exhibited varying degrees of temperature resistance, with the most thermally stable ones observed at a protein-to-polysaccharide ratio of 1:2. These findings underscore the importance of the ratio of broad bean protein to chia seed polysaccharides in determining encapsulation efficiency, with the 1:2 ratio being optimal. Moreover, this ratio facilitated the production of microcapsules with enhanced

thermal stability, a crucial factor considering the presence of volatile compounds like essential oils. Lastly, the influence of water content on microcapsule properties emphasizes the necessity of considering this factor during the production process design.

Author Contributions: Conceptualization, methodology, investigation, writing—original draft preparation: A.N.; investigation (DSC): A.S.; investigation (smell pattern): E.G.-H.; supervision, methodology, writing—review and editing: M.A.K. All authors have read and agreed to the published version of the manuscript.

Funding: This research received no external funding.

Institutional Review Board Statement: Not applicable.

Informed Consent Statement: Not applicable.

Data Availability Statement: The raw data supporting the conclusions of this article will be made available by the authors on request.

Conflicts of Interest: The authors declare no conflicts of interest.

References

1. Sing, C.E.; Perry, S.L. Recent Progress in the Science of Complex Coacervation. *Soft Matter* **2020**, *16*, 2885–2914. [[CrossRef](#)] [[PubMed](#)]
2. Zhou, L.; Shi, H.; Li, Z.; He, C. Recent Advances in Complex Coacervation Design from Macromolecular Assemblies and Emerging Applications. *Macromol. Rapid Commun.* **2020**, *41*, e2000149. [[CrossRef](#)] [[PubMed](#)]
3. Bastos, L.P.H.; Vicente, J.; dos Santos, C.H.C.; de Carvalho, M.G.; Garcia-Rojas, E.E. Encapsulation of black pepper (*Piper nigrum* L.) essential oil with gelatin and sodium alginate by complex coacervation. *Food Hydrocoll.* **2020**, *102*, 105605. [[CrossRef](#)]
4. Shaddel, R.; Hesari, J.; Azadmard-Damirchi, S.; Hamishehkar, H.; Fathi-Achachlouei, B.; Huang, Q. Use of gelatin and gum Arabic for encapsulation of black raspberry anthocyanins by complex coacervation. *Int. J. Biol. Macromol.* **2018**, *107*, 1800–1810. [[CrossRef](#)] [[PubMed](#)]
5. Ghorbani Gorji, E.; Waheed, A.; Ludwig, R.; Toca-Herrera, J.L.; Schleinig, G.; Ghorbani Gorji, S. Complex coacervation of milk proteins with sodium alginate. *J. Agric. Food Chem.* **2018**, *66*, 3210–3220. [[CrossRef](#)] [[PubMed](#)]
6. Hasanvand, E.; Razavi, S.M.A. Fabrication and characterisation of milk proteins-chitosan complex coacervates. *Int. Dairy J.* **2023**, *145*, 105716. [[CrossRef](#)]
7. Jun-xia, X.; Hai-yan, Y.; Jian, Y. Microencapsulation of sweet orange oil by complex coacervation with soybean protein isolate/gum Arabic. *Food Chem.* **2011**, *125*, 1267–1272. [[CrossRef](#)]
8. Li, G.Y.; Chen, Q.H.; Su, C.R.; Wang, H.; He, S.; Liu, J.; Nag, A.; Yuan, Y. Soy protein-polysaccharide complex coacervate under physical treatment: Effects of pH, ionic strength and polysaccharide type. *Innov. Food Sci. Emerg. Technol.* **2021**, *68*, 102612. [[CrossRef](#)]
9. Carpentier, J.; Conforto, E.; Chaigneau, C.; Vendeville, J.E.; Maugard, T. Complex coacervation of pea protein isolate and tragacanth gum: Comparative study with commercial polysaccharides. *Innov. Food Sci. Emerg. Technol.* **2021**, *69*, 102641. [[CrossRef](#)]
10. Lan, Y.; Ohm, J.B.; Chen, B.; Rao, J. Phase behavior and complex coacervation of concentrated pea protein isolate-beet pectin solution. *Food Chem.* **2020**, *307*, 125536. [[CrossRef](#)] [[PubMed](#)]
11. Dhull, S.B.; Kidwai, M.K.; Siddiq, M.; Sidhu, J.S. Faba (broad) bean production, processing, and nutritional profile. In *Dry Beans and Pulses: Production, Processing, and Nutrition*; Wiley: Hoboken, NJ, USA, 2022; pp. 359–381.
12. Bartóg, P.; Grzebisz, W.; Łukowiak, R. The Effect of Potassium and Sulfur Fertilization on Seed Quality of Faba Bean (*Vicia faba* L.). *Agronomy* **2019**, *9*, 209. [[CrossRef](#)]
13. Arogundade, L.A.; Tshay, M.; Shumey, D.; Manazie, S. Effect of ionic strength and/or pH on Extractability and physico-functional characterization of broad bean (*Vicia faba* L.) Protein concentrate. *Food Hydrocoll.* **2006**, *20*, 1124–1134. [[CrossRef](#)]
14. Karaca, A.C.; Low, N.; Nickerson, M. Emulsifying properties of chickpea, faba bean, lentil and pea proteins produced by isoelectric precipitation and salt extraction. *Food Res. Int.* **2011**, *44*, 2742–2750. [[CrossRef](#)]
15. Makri, E.; Papalamprou, E.; Doxastakis, G. Study of functional properties of seed storage proteins from indigenous European legume crops (lupin, pea, broad bean) in admixture with polysaccharides. *Food Hydrocoll.* **2005**, *19*, 583–594. [[CrossRef](#)]
16. Capitani, M.I.; Corzo-Rios, L.J.; Chel-Guerrero, L.A.; Betancur-Ancona, D.A.; Nolasco, S.M.; Tomás, M.C. Rheological properties of aqueous dispersions of chia (*Salvia hispanica* L.) mucilage. *J. Food Eng.* **2015**, *149*, 70–77. [[CrossRef](#)]
17. Hernández-Nava, R.; López-Malo, A.; Palou, E.; Ramírez-Corona, N.; Jiménez-Munguía, M.T. Complex Coacervation Between Gelatin and Chia Mucilage as an Alternative of Encapsulating Agents. *J. Food Sci.* **2019**, *84*, 1281–1287. [[CrossRef](#)] [[PubMed](#)]
18. Bakry, A.M.; Abbas, S.; Ali, B.; Majeed, H.; Abouelwafa, M.Y.; Mousa, A.H.; Liang, L. Microencapsulation of Oils: A Comprehensive Review of Benefits, Techniques, and Applications. *Compr. Rev. Food Sci.* **2016**, *15*, 143–182. [[CrossRef](#)]

19. Napiórkowska, A.; Kurek, M. Coacervation as a Novel Method of Microencapsulation of Essential Oils—A Review. *Molecules* **2022**, *27*, 5142. [[CrossRef](#)] [[PubMed](#)]
20. Naderi, B.; Keramat, J.; Nasirpour, A.; Aminifar, M. Complex coacervation between oak protein isolate and gum Arabic: Optimization & functional characterization. *Int. J. Food Prop.* **2020**, *23*, 1854–1873. [[CrossRef](#)]
21. Mitra, H.; Pushpadass, H.A.; Franklin, M.E.E.; Ambrose, R.P.K.; Ghoroi, C.; Battula, S.N. Influence of moisture content on the flow properties of basundi mix. *Powder Technol.* **2017**, *312*, 133–143. [[CrossRef](#)]
22. Sofi, B.A.; Wani, I.A.; Masoodi, F.A.; Saba, I.; Muzaffar, S. Effect of gamma irradiation on physicochemical properties of broad bean (*Vicia faba* L.) starch. *LWT—Food Sci. Technol.* **2013**, *54*, 63–72. [[CrossRef](#)]
23. dos Santos, F.S.; de Figueirêdo, R.M.F.; Queiroz, A.J.d.M.; Paiva, Y.F.; Moura, H.V.; Silva, E.T.d.V.; Ferreira, J.P.d.L.; de Melo, B.A.; Carvalho, A.J.d.B.A.; Lima, M.d.S.; et al. Influence of Dehydration Temperature on Obtaining Chia and Okra Powder Mucilage. *Foods* **2023**, *12*, 569. [[CrossRef](#)]
24. Akseli, I.; Hilden, J.; Katz, J.M.; Kelly, R.C.; Kramer, T.T.; Mao, C.; Osei-Yeboah, F.; Strong, J.C. Reproducibility of the measurement of bulk/tapped density of pharmaceutical powders between pharmaceutical laboratories. *J. Pharm. Sci.* **2018**, *108*, 1081–1084. [[CrossRef](#)] [[PubMed](#)]
25. Airouyuwa, J.O.; Kaewmanee, T. Microencapsulation of *Moringa oleifera* leaf extracts with vegetable protein as wall materials. *Food Sci. Technol. Int.* **2019**, *25*, 533–543. [[CrossRef](#)] [[PubMed](#)]
26. Reddy, R.S.; Ramachandra, C.T.; Hiregoudar, S.; Nidoni, U.; Ram, J.; Kammar, M. Influence of processing conditions on functional and reconstitution properties of milk powder made from Osmanabadi goat milk by spray drying. *Small Rumin. Res.* **2014**, *119*, 130–137. [[CrossRef](#)]
27. Bordón, M.G.; Paredes, A.J.; Camacho, N.M.; Penci, M.C.; González, A.; Palma, S.D.; Ribotta, P.D.; Martinez, M.L. Formulation, spray-drying and physicochemical characterization of functional powders loaded with chia seed oil and prepared by complex coacervation. *Powder Technol.* **2021**, *391*, 479–493. [[CrossRef](#)]
28. Xin, X.; Essien, S.; Dell, K.; Woo, M.W.; Baroutian, S. Effects of Spray-Drying and Freeze-Drying on Bioactive and Volatile Compounds of Smoke Powder Food Flavouring. *Food Bioprocess Technol.* **2022**, *15*, 785–794. [[CrossRef](#)]
29. Juárez-Enriquez, E.; Olivas, G.I.; Zamudio-Flores, P.B.; Ortega-Rivas, E.; Perez-Vega, S.; Sepulveda, D.R. Effect of water content on the flowability of hygroscopic powders. *J. Food Eng.* **2017**, *205*, 12–17. [[CrossRef](#)]
30. Newman, A.W.; Reutzel-Edens, S.M.; Zografi, G. Characterization of the "hygroscopic" properties of active pharmaceutical ingredients. *J. Pharm. Sci.* **2008**, *97*, 1047–1059. [[CrossRef](#)]
31. Silva, L.A.; Sinnecker, P.; Cavalari, A.A.; Sato, A.C.K.; Perrechil, F.A. Extraction of chia seed mucilage: Effect of ultrasound application. *Food Chem. Adv.* **2022**, *1*, 100024. [[CrossRef](#)]
32. Martínez-Velasco, A.; Lobato-Calleros, C.; Hernández-Rodríguez, B.E.; Román-Guerrero, A.; Alvarez-Ramirez, J.; Vernon-Carter, E.J. High intensity ultrasound treatment of faba bean (*Vicia faba* L.) protein: Effect on surface properties, foaming ability and structural changes. *Ultrason. Sonochem.* **2018**, *44*, 97–105. [[CrossRef](#)] [[PubMed](#)]
33. Danaei, M.; Dehghankhold, M.; Ataei, S.; Hasanzadeh Davarani, F.; Javanmard, R.; Dokhani, A.; Khorasani, S.; Mozafari, M.R. Impact of Particle Size and Polydispersity Index on the Clinical Applications of Lipidic Nanocarrier Systems. *Pharmaceutics* **2018**, *10*, 57. [[CrossRef](#)] [[PubMed](#)]
34. Hoseini, B.; Jaafari, M.R.; Golabpour, A.; Momtazi-Borojeni, A.A.; Karimi, M.; Eslami, S. Application of ensemble machine learning approach to assess the factors affecting size and polydispersity index of liposomal nanoparticles. *Sci. Rep.* **2023**, *13*, 18012. [[CrossRef](#)]
35. Bühler, J.M.; Dekkers, B.L.; Bruins, M.E.; van der Goot, A.J. Modifying Faba Bean Protein Concentrate Using Dry Heat to Increase Water Holding Capacity. *Foods* **2020**, *9*, 1077. [[CrossRef](#)] [[PubMed](#)]
36. Punia, S.; Dhull, S.B. Chia seed (*Salvia hispanica* L.) mucilage (a heteropolysaccharide): Thermal, pasting, rheological behaviour and its utilization. *Int. J. Biol. Macromol.* **2019**, *140*, 1054–1063. [[CrossRef](#)] [[PubMed](#)]
37. Muñoz, L.A.; Vera, C.N.; Zúñiga-López, M.C.; Moncada, M.; Haros, C.M. Physicochemical and functional properties of soluble fiber extracted from two phenotypes of chia (*Salvia hispanica* L.) seeds. *J. Food Compos. Anal.* **2021**, *104*, 104138. [[CrossRef](#)]
38. Mehran, M.; Masoum, S.; Memarzadeh, M. Microencapsulation of *Mentha spicata* essential oil by spray drying: Optimization, characterization, release kinetics of essential oil from microcapsules in food models. *Ind. Crop. Prod.* **2020**, *154*, 112694. [[CrossRef](#)]
39. Kozłowska, M.; Gruczyńska, E. Comparison of the oxidative stability of soybean and sunflower oils enriched with herbal plant extracts. *Chem. Pap.* **2018**, *72*, 2607–2615.
40. Shiko, G.; Gladden, L.; Sederman, A.; Connolly, P.; Butler, J. Degradation of polysorbates 20 and 80: Studies on thermal autoxidation and hydrolysis. *J. Pharm. Sci.* **2011**, *100*, 721–731. [[CrossRef](#)] [[PubMed](#)]
41. Pramod, K.; Suneesh, C.V.; Shanavas, S.; Ansari, S.H.; Ali, J. Unveiling the compatibility of eugenol with formulation excipients by systematic drug-excipient compatibility studies. *J. Anal. Sci. Technol.* **2015**, *6*, 34. [[CrossRef](#)]
42. Nandiyanto, A.B.D.; Oktiani, R.; Ragadhita, R. How to read and interpret FTIR spectroscopy of organic material. *Indones. J. Sci. Technol.* **2019**, *4*, 97–118.
43. Barchi, J.J., Jr.; Strain, C.N. The effect of a methyl group on structure and function: Serine vs. threonine glycosylation and phosphorylation. *Front. Mol. Biosci.* **2023**, *10*, 1117850. [[CrossRef](#)]
44. Martineau-Côté, D.; Achouri, A.; Karboune, S.; L'hocine, L. Faba Bean: An Untapped Source of Quality Plant Proteins and Bioactives. *Nutrients* **2022**, *14*, 1541. [[CrossRef](#)] [[PubMed](#)]

45. Grdadolnik, J. Saturation effects in FTIR spectroscopy: Intensity of amide I and amide II bands in protein spectra. *Acta Chim. Slov.* **2003**, *50*, 777–788.
46. Babault, N.; Paizis, C.; Deley, G.; Guérin-Deremaux, L.; Saniez, M.H.; Lefranc-Millot, C.; Allaert, F.A. Pea proteins oral supplementation promotes muscle thickness gains during resistance training: A double-blind, randomized, Placebo-controlled clinical trial vs. Whey protein. *J. Int. Soc. Sports Nutr.* **2015**, *12*, 3. [[CrossRef](#)] [[PubMed](#)]
47. Shanthakumar, P.; Klepacka, J.; Bains, A.; Chawla, P.; Dhull, S.B.; Najda, A. The Current Situation of Pea Protein and Its Application in the Food Industry. *Molecules* **2022**, *27*, 5354. [[CrossRef](#)] [[PubMed](#)]
48. Sokolowska, I.; Wetie, A.G.N.; Woods, A.G.; Darie, C.C. Automatic Determination of Disulfide Bridges in Proteins. *J. Lab. Autom.* **2012**, *17*, 408–416. [[CrossRef](#)] [[PubMed](#)]
49. Darwish, A.M.; Khalifa, R.E.; El Sohaimy, S.A. Functional properties of chia seed mucilage supplemented in low fat yoghurt. *Alex. Sci. Exch. J.* **2018**, *39*, 450–459. [[CrossRef](#)]
50. Chiang, J.H.; Ong, D.S.M.; Ng, F.S.K.; Hua, X.Y.; Tay, W.L.W.; Henry, C.J. Application of chia (*Salvia hispanica*) mucilage as an ingredient replacer in foods. *Trends Food Sci. Technol.* **2021**, *115*, 105–116. [[CrossRef](#)]
51. Cebi, N.; Arici, M.; Sagdic, O. The famous Turkish rose essential oil: Characterization and authenticity monitoring by FTIR, Raman and GC–MS techniques combined with chemometrics. *Food Chem.* **2021**, *354*, 129495. [[CrossRef](#)] [[PubMed](#)]
52. Li, Y.; Kong, D.; Wu, H. Analysis and evaluation of essential oil components of cinnamon barks using GC–MS and FTIR spectroscopy. *Ind. Crop. Prod.* **2013**, *41*, 269–278. [[CrossRef](#)]
53. Maeh, R.K.; Jaaffar, A.I.; Al-Azawi, K.F. Preparation of Juniperus extract and detection of its antimicrobial and antioxidant activity. *Iraqi J. Agric. Sci.* **2019**, *50*, 1153–1161.
54. Bhatia, S.; Shah, Y.A.; Al-Harrasi, A.; Jawad, M.; Koca, E.; Aydemir, L.Y. Novel applications of black pepper essential oil as an antioxidant agent in sodium caseinate and chitosan based active edible films. *Int. J. Biol. Macromol.* **2024**, *254*, 128045. [[CrossRef](#)]
55. Amalraj, A.; Haponiuk, J.T.; Thomas, S.; Gopi, S. Preparation, characterization and antimicrobial activity of polyvinyl alcohol/gum arabic/chitosan composite films incorporated with black pepper essential oil and ginger essential oil. *Int. J. Biol. Macromol.* **2020**, *151*, 366–375. [[CrossRef](#)]
56. Cebi, N.; Taylan, O.; Abusurrah, M.; Sagdic, O. Detection of orange essential oil, isopropyl myristate, and benzyl alcohol in lemon essential oil by FTIR spectroscopy combined with chemometrics. *Foods* **2020**, *10*, 27. [[CrossRef](#)] [[PubMed](#)]
57. Lu, Y.; Du, C.; Shao, Y.; Zhou, J. Characterization of rapeseed oil using FTIR-ATR spectroscopy. *J. Food Sci. Eng.* **2014**, *4*, 244–249.
58. Rohman, A.; Ariani, R. Authentication of Nigella sativa seed oil in binary and ternary mixtures with corn oil and soybean oil using FTIR spectroscopy coupled with partial least square. *Sci. World J.* **2013**, *2013*, 740142. [[CrossRef](#)]
59. Nair, L.M.; Stephens, N.V.; Vincent, S.; Raghavan, N.; Sand, P.J. Determination of polysorbate 80 in parenteral formulations by high-performance liquid chromatography and evaporative light scattering detection. *J. Chromatogr. A* **2003**, *1012*, 81–86. [[CrossRef](#)] [[PubMed](#)]
60. Napiórkowska, A.; Szpicier, A.; Wojtasik-Kalinowska, I.; Perez, M.D.T.; González, H.D.; Kurek, M.A. Microencapsulation of Juniper and Black Pepper Essential Oil Using the Coacervation Method and Its Properties after Freeze-Drying. *Foods* **2023**, *12*, 4345. [[CrossRef](#)] [[PubMed](#)]
61. De Melo Ramos, F.; Silveira Júnior, V.; Prata, A.S. Assessing the Vacuum Spray Drying Effects on the Properties of Orange Essential Oil Microparticles. *Food Bioprocess Technol.* **2019**, *12*, 1917–1927. [[CrossRef](#)]
62. Fernandes, R.V.d.B.; Borges, S.V.; Botrel, D.A.; de Oliveira, C.R. Physical and chemical properties of encapsulated rosemary essential oil by spray drying using whey protein-inulin blends as carriers. *Int. J. Food Sci. Technol.* **2013**, *49*, 1522–1529. [[CrossRef](#)]
63. Otálora, M.C.; Wilches-Torres, A.; Gómez Castaño, J.A. Spray-Drying Microencapsulation of Andean Blueberry (*Vaccinium meridionale* Sw.) Anthocyanins Using Prickly Pear (*Opuntia ficus indica* L.) Peel Mucilage or Gum Arabic: A Comparative Study. *Foods* **2023**, *12*, 1811. [[CrossRef](#)] [[PubMed](#)]
64. Hernández-Nava, R.; López-Malo, A.; Palou, E.; Ramírez-Corona, N.; Jiménez-Munguía, M.T. Encapsulation of oregano essential oil (*Origanum vulgare*) by complex coacervation between gelatin and chia mucilage and its properties after spray drying. *Food Hydrocoll.* **2020**, *109*, 106077. [[CrossRef](#)]
65. Górska-Horczyk, E.; Wojtasik-Kalinowska, I.; Guzek, D.; Sun, D.W.; Wierzbicka, A. Differentiation of chill-stored and frozen pork necks using electronic nose with ultra-fast gas chromatography. *J. Food Process Eng.* **2017**, *40*, e12540. [[CrossRef](#)]
66. Wojtasik-Kalinowska, I.; Guzek, D.; Górska-Horczyk, E.; Brodowska, M.; Sun, D.W.; Wierzbicka, A. Diet with linseed oil and organic selenium yields low n-6/n-3 ratio pork Semimembranosus meat with unchanged volatile compound profiles. *Int. J. Food Sci.* **2018**, *53*, 1838–1846. [[CrossRef](#)]

Disclaimer/Publisher’s Note: The statements, opinions and data contained in all publications are solely those of the individual author(s) and contributor(s) and not of MDPI and/or the editor(s). MDPI and/or the editor(s) disclaim responsibility for any injury to people or property resulting from any ideas, methods, instructions or products referred to in the content.

Warszawa, 8/10/2024

Alicja Kizildag
alicjakizildag@gmail.com

**Rada Dyscypliny Technologia
Żywności i Żywienia
Szkoły Głównej Gospodarstwa
Wiejskiego w Warszawie**

Oświadczenie o współautorstwie

Niniejszym oświadczam, że w pracy: *Napiórkowska A, Szpicer A, Górską-Horczyczak E, Kurek MA. Microencapsulation of Essential Oils Using Faba Bean Protein and Chia Seed Polysaccharides via Complex Coacervation Method. Molecules. 2024; 29(9):2019* mój indywidualny udział w jej powstaniu polegał na opracowaniu metodologii i przeprowadzeniu badań, napisaniu manuskryptu oraz jego korekcie po otrzymaniu recenzji.

Podpis



Warszawa, 8/10/2024

Arkadiusz Szpicer
arkadiusz_szpicer@sggw.edu.pl

**Rada Dyscypliny Technologia
Żywności i Żywienia
Szkoły Głównej Gospodarstwa
Wiejskiego w Warszawie**

Oświadczenie o współautorstwie

Niniejszym oświadczam, że w pracy: *Napiórkowska A, Szpicer A, Górską-Horzyczak E, Kurek MA. Microencapsulation of Essential Oils Using Faba Bean Protein and Chia Seed Polysaccharides via Complex Coacervation Method. Molecules. 2024; 29(9):2019* mój indywidualny udział w jej powstaniu polegał na nadzorowaniu analizy Skaningowej Kalorymetrii Różnicowej, wsparciu merytorycznym przy analizie i interpretacji otrzymanych wyników oraz ostatecznej korekcie treści manuskryptu w tym zakresie.

Podpis



Warszawa, 8/10/2024

Elżbieta Górską-Horczyzak
elzbieta_gorska-horczyzak@sggw.edu.pl

**Rada Dyscypliny Technologia
Żywności i Żywienia**

**Szkoły Głównej Gospodarstwa
Wiejskiego w Warszawie**

Oświadczenie o współautorstwie

Niniejszym oświadczam, że w pracy: *Napiórkowska A, Szpicer A, Górską-Horczyzak E, Kurek MA. Microencapsulation of Essential Oils Using Faba Bean Protein and Chia Seed Polysaccharides via Complex Coacervation Method. Molecules. 2024; 29(9):2019* mój indywidualny udział w jej powstaniu polegał na przeprowadzeniu analizy ultra-szybkiej chromatografii gazowej „e-nos”, opracowaniu wyników i pomocy w ich analizie.

Podpis



Warszawa, 8/10/2024

Marcin Andrzej Kurek
marcin_kurek@sggw.edu.pl

**Rada Dyscypliny Technologia
Żywności i Żywienia
Szkoły Głównej Gospodarstwa
Wiejskiego w Warszawie**

Oświadczenie o współautorstwie

Niniejszym oświadczam, że w pracy: *Napiórkowska A, Szpicer A, Górską-Horczyzak E, Kurek MA. Microencapsulation of Essential Oils Using Faba Bean Protein and Chia Seed Polysaccharides via Complex Coacervation Method. Molecules. 2024; 29(9):2019* mój indywidualny udział w jej powstaniu polegał na nadzorowaniu badań, weryfikacji metod, konsultacjach merytorycznych oraz pomocy przy interpretacji wyników i redakcji wybranych sekcji artykułu.

Podpis





Szkoła Główna Gospodarstwa Wiejskiego
w Warszawie
Instytut Nauk o Żywieniu Człowieka

mgr inż. Alicja Kizildag

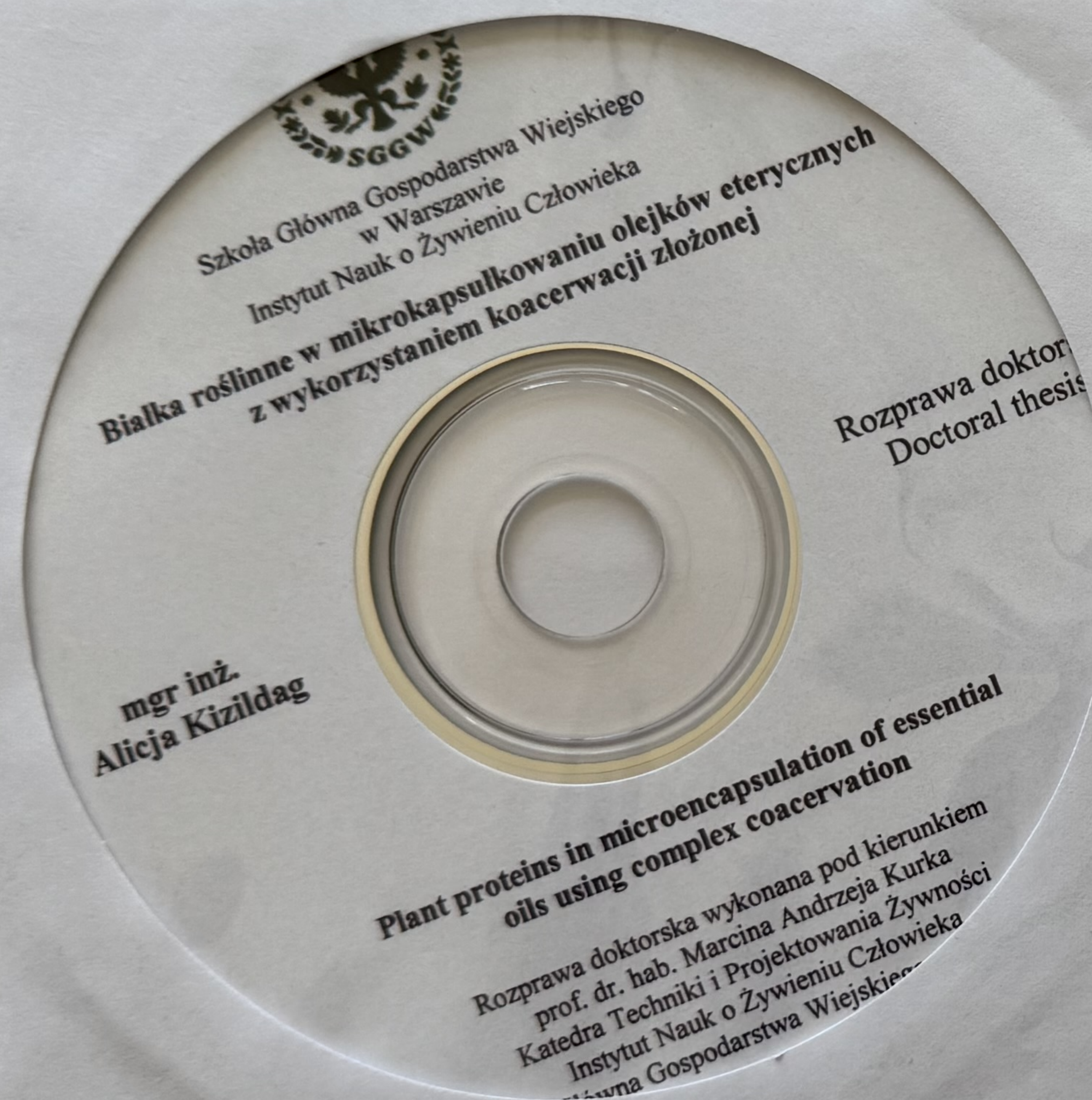
Białka roślinne w mikrokapsułkowaniu olejków eterycznych z wykorzystaniem koacerwacji złożonej

Plant proteins in microencapsulation of essential oils using complex
coacervation

Rozprawa doktorska
Doctoral thesis

Rozprawa doktorska wykonana pod kierunkiem
prof. dr. hab. Marcina Andrzeja Kurka
Katedra Techniki i Projektowania Żywności
Instytut Nauk o Żywieniu Człowieka
Szkoła Główna Gospodarstwa Wiejskiego w Warszawie

Warszawa, 2024



WPLYNĘŁO DNIA

1 Noce-168/2024
2024-10-10

Instytut Nauk o Żywieniu Człowieka
Sekretariat *[Signature]*